RUB

Doctoral Thesis

ELECTROCOAGULATION IN THE SEPARATION PROCESS OF

USED BENTONITE SUSPENSIONS

submitted in fulfilment of the requirements for the degree of Doctor of Engineering
(Dr.-Ing.) to the Department of Civil and Environmental Engineering of the
Ruhr University Bochum

BY

IVAN POPOVIC, M.SC.

Electrocoagulation in the separation process of used bentonite suspensions

Doctoral Thesis

submitted in fulfilment of the requirements for the degree of Doctor of Engineering (Dr.-Ing.) to the Department of Civil and Environmental Engineering of the Ruhr University Bochum

BY

IVAN POPOVIC, M.SC.

Reviewers: Prof. Dr.-Ing. M. Thewes, Ruhr University Bochum

Institute for Tunnelling and Construction Management

Prof. Dr.-Ing. habil. M. Wichern, Ruhr University Bochum

Institute of Urban Water Management and Environmental Engineering

Date of submission: 03.03.2020

Date of oral examination: 17.06.2020

Preface

The present study was developed in my time as research assistant at the Institute for Tunnelling and Construction Management ("TLB") of the Ruhr University Bochum.

My special thanks goes first to Prof. Dr.-Ing. Markus Thewes for his guidance of this thesis. The mutual exchange of ideas and many discussions had a very positive impact on the thesis. Moreover, his support on my way from a non-German speaking intern on the Institute to a research assistant teaching on German was of great importance. Additionally, I would like to thank Dr.-Ing. Britta Schößer for her support, input and guidance of the project, in frame of which this thesis was developed. To Prof. Dr.-Ing. habil. Marc Wichern I would like to thank for his interest in this subject, for our informative discussions and his willingness to be my reviewer. Furthermore, I would like to thank Prof. Dr.-Ing. Annette Hafner for taking the task of a non-specialist examiner.

Big thanks goes to my colleagues for the friendly atmosphere they created at the Institute, in which it was pleasure to work. Their support during research and while writing this thesis was very important to me. I could always rely on each and every one of them, but I would like to mention Anna-Lena Hammer, Annika Jodehl and Peter Hoffmann in particular.

During the experimental part of this research several master theses were written, which I supervised. The obtained experimental data were analysed in depth in this dissertation. For this, many thanks to my former master students Wenyu Jian, Sergey Vishnyakov and Stanislav Bezhenov. Also my former student assistants Marco Schürmanns, Ardit Bektashi and Frederik Klask, including students in summer internships, spent many hours in the laboratory. I am very grateful for their help.

Big thanks goes also on Daniel Lehmann, who was always ready to handle any small malfunction of the experimental equipment. Moreover, he brought the idea to automatically record electricity data and installed the necessary hardware and software. This saved a lot of time and improved the quality of data acquisition by the mid-scale experiments.

Last but not the least; I would like to thank the people from my private life. My parents have always supported me in my desire to either travel around as a tourist or to do internships abroad. The last internship I went to, to the TLB in Bochum, changed my life completely. Here, I also met my girlfriend Yvonne. She deserves special thanks for her support and motivation during the whole time I was writing this thesis.

Herne, in February 2020

Ivan Popovic

Acknowledgements

Abstract

The separation of fines and the disposal of used bentonite suspensions are important eco-nomic and ecological factors in hydroshield tunnelling and the construction of diaphragm walls. To support the separation process of the slurry and to reduce separation time and costs, chemicals like metal salts and polymers are added to the slurry prior to its treatment in a chamber filter press or a centrifuge. However, most of those chemicals are classified as water hazardous substances. If they are not dosed correctly, they end up not only in the dewatered fines but also in the separated water that needs to be disposed. Moreover, addi-tion of polymer solutions to the suspension increases water consumption on the construction site and the total volume of the suspension to be treated.

The thesis presents an alternative support method for fine separation processes by means of electrocoagulation. This electrochemical process causes coagulation and destabilisation of the suspension by applying an electrical current. It has a similar effect on the subsequent fine separation as the addition of chemicals, but offers the advantage that no water hazard-ous substances are required and the water consumption on the construction site decreases.

In order to determine the extent to which electrocoagulation can support the separation of used slurries, a standard for a used suspension was defined, which was subjected to para-metric studies. First studies were performed with laboratory-size electrocoagulation cells which had a volume of 2 to 4 l. Based on the results, the technology was scaled up to a mid-scale cell with a volume of 320 l. This equipment, together with a laboratory chamber filter press, enabled a practice-oriented investigation of the influence of the electrocoagulation treatment on the separation of fines. The results were validated with a used suspension from a tunnelling construction site.

The studies have shown that electrocoagulation could reduce the required filter press ca-pacity by up to 20 % and could save at least 0.2 m³ water per 1 m³ of used slurry.

An ecological comparison between electrocoagulation and conventional conditioning showed that the electrocoagulation is ecologically beneficial. An economical comparison has shown for electricity prices in Germany that the costs were in the same order of magni-tude. However, it is important to note that the operational cost of EC depends to a great extent on electricity price at the site, which differs significantly between countries. Therefore, electrocoagulation could be more economically beneficial in countries with lower electricity prices than Germany.

The thesis includes design recommendations for a real-scale prototype as well as ideas for further research. The experimental procedure and analysis developed in this thesis allow the investigation of any given used suspension. The next steps should be the investigation

of further used suspensions from construction sites and determining the electricity consumption during electrocoagulation depending on the used suspension properties.

.

Index

List of Figures

List of Tables

List of Abbreviations

%	Percent
$(Al_2(SO_4)_3)$	Aluminium sulfate
AbfAblV	Abfallablagerungsverordnung (• Waste Disposal Ordinance)
AC	Alternating current
AG	Aktien Gesellschaft
Al	Aluminium
$Al(OH)_3$	Aluminium hydroxide
$Al(OH)_4^-$	Tetrahydroxoaluminat-ion
approx..	Approximately
ASTM	American Society for Testing and Materials
AwSV	Verordnung über Anlagen zum Umgang mit wassergefährdenden Stoffen (Ordinance on facilities for handling substances that are hazardous to water)
BP	Bipolar electrodes
CA	Conditioning agents
ccc	Critical coagulation concentration
CFP	Chamber filter press
Cl	Chlor
cm	Centimetre
Cr	Chromium
DC	Direct current
DepV	Verordnung über Deponien und Langzeitlager (Deponieverordnung), Deponierverordnung (• Landfill Ordinance)
DIN	Deutsches Institut für Normungen (German Institute for Standardization
DK	Deposition class
DLVO	Derjaguin-Landau-Verwey-Overbeek-Theorie
e.g	For example
EC	Electrocoagulation
Eq	Equation
exp	Experiment
Fe	Iron
$Fe(OH)_2$	Iron (II)-hydroxid
$Fe(OH)_3$	Iron (III)-hydroxide
$FeCl_3$	Ferric chloride
FW	Filtrate water
GmbH	Gesellschaft mit beschränkter Haftung (Company with limited liability)
i.e.	lat. id est, meaning
IEP	Isoelectric point
kg	Kilogram

LAGA	Länderarbeitsgemeinschaft Abfall, Bund/Länder-Arbeitsgemeinschaft Abfall (Federal / State Working Group on Waste)
LCFP	Laboratory chamber filter press
LEL	Lower explosive limit
Li	Lithium
Mg	Magnesium
mm	Millimetre
MP-P	Monopolar electrodes in parallel connection
MP-S	Monopolar electrodes in serial
NaCl	Sodium chloride
pH	potentia hydrogenii
prEN	European standard - draft
PZC	Point of zero charge
PZD	Negative logarithm of the Fe(x) concentration, Predominance-zone diagram
SUS	Standard used suspension
t	Time
TDS	Total dissolved solids
TOT layer	Tetrahedral-octahedral-tetrahedral layer
UEL	Upper explosive limit
VwVwS	Verwaltungsvorschrift wassergefährdende Stoffe (Administrative Regulation on Water-Polluting Substances)
WGK	Water hazard class
WHG	Wasserhaushaltsgesetz (Water Resources Act)
Zn	Zinc

List of Symbols

ΔFt_{EC}	[-]	Change of filtration time after EC
ΔFV_{EC}	[-]	Change of filtration volume after EC
ΔFW	[%]	Increase of the filtrate water release
$\Delta \rho$	[%]	Decrease of the remaining suspension density
A	[cm²]	Electrode surface area
A	[m²]	Cross section area
B	[g]	Dry weight of coagulated bentonite
B_0	[g]	Dry weight of bentonite particles in suspension
B_{kt}	[%]	Percentage of coagulated bentonite
C_e	[%]	Current efficiency
c_{el}	[nM]	Concentration of electrolytes
F	[As/mol]	Faraday constant = 96485
F%	[-]	Time ratio of a filtration process in one filtration cycle
FV	[-]	Factor for decrease of filtration volume due to EC
FW_o	[ml]	Filter water release of the suspension before EC treatment (obtained using the API filter press)
FW_r	[ml]	Filter water release of the remaining suspension (obtained using the API filter press)
FW_{rel}	[l]	Filtrate water release at the end of the filtration (obtained using the laboratory chamber filter press)
I	[A]	Electrical current
K	[W^{-1}m^{-1}]	Specific electricial conductivity
L	[m]	Length
M	[g/mol]	Molar mass
$m_{d,cm}$	[kg]	Dry weight of coagulated material
$m_{d,cm}$	[kg]	Dry weight of filter cakes
$m_{w,cm}$	[kg]	Wet weight of coagulated material
$m_{w,cm}$	[kg]	Wet weight of filter cakes
P	[kWh]	Power consumption
P_{cfp}	[-]	Factor for change of productivity of chamber filter press with EC
P_{sep}	[-]	Factor for productivity of separation process when replacing CA with EC
R	[Jmol-1K-1]	Ideal gas constant = 8.314
R	[Ω]	Resistance
R_{cfp}	[-]	Factor for calculation of required chamber filter press capacity when replacing CA with EC
RM_{cm}	[-]	Residual moisture of coagulated material
RM_{fc}	[-]	Residual moisture of the filter cake
T	[K]	Absolute temperature of the produced gas
t	[h]	Time
$t_{FW,CA}$	[h]	Filtration time after CA
$t_{FW,EC}$	[h]	Filtration time after EC
U	[V]	Voltage

V	[l]	Volume of the produced gas
V_a	[J]	Van der Waals attractive energy
V_b	[J]	Barrier to redispersion
V_{CA}	[m³]	Volume of CA added to used suspension prior to filtration (per m³ used suspension)
V_{cfp}	[m³]	Volume of chamber filter press
V_{CM}	[m³]	Volume of coagulated material
$V_{FW,CA}$	[m³]	Filtrate water discharge with CA
$V_{FW,EC}$	[m³]	Filtrate water discharge after EC
V_m	[J]	Maximal energy barrier
V_r	[J]	Interparticle double layer repulsion energy
$V_{S,CM}$	[m³]	Volume of soil in coagulated material
V_t	[J]	Total interaction energy
$V_{W,CM}$	[m³]	Volume of water in coagulated material per m³ suspension
Z	[-]	Valence of ions of the substance
δ_S	[t/m³]	Grain density
δ_{SUS}	[t/m³]	Suspension density
Z	[mV]	Zeta potential
μm	[1µm]	Micrometre
ρ_o	[g/cm³]	Density of suspension before the EC treatment
ρ_r	[g/cm³]	Remaining suspension density
ρ_w	[g/cm³]	Water density

1 Introduction

1.1 Problem statement and motivation

Bentonite suspensions are stable mixtures of water and bentonite particles, which are used as a supporting, lubricating and conveying medium in civil engineering. In the construction of diaphragm walls, bentonite suspensions support the trench. In hydroshield tunnelling, they support the tunnel face during excavation and convey the excavated soil material to the separation plant. There, soil particles larger than approx. 0.02 mm are removed from the suspension, which is afterwards circulated back to the tunnel face. However, fine particles such as clay and silt (<0.02 mm) remain in the suspension, which leads to a constant increase in density. As a result, the bentonite suspension loses its properties and must be replaced with a fresh suspension. The discarded suspension, so-called "used suspension", needs to be disposed.

Prior to disposal, the used suspension is dewatered in a fine separation process. The fine separation, or dewatering, is a cost-intensive process that takes place in chamber filter presses and centrifuges. To accelerate the process and reduce the costs, fine separation is supported with the addition of chemicals called conditioning agents (CA). They are mixed with water and added to the suspension prior to the fine separation. Therefore, the usage of CA increases the water consumption on the construction site and the volume of the suspension to be dewatered. Moreover, most of those chemicals, such as metal salts and polymers, are classified as water hazardous substances. If they are not correctly dosed, they end up not only in the dewatered soil material but also in the separated water that needs to be disposed.

This thesis investigates electrocoagulation (EC) as an alternative supporting method for the fine separation process. EC has already been used as a wastewater purification method and is regarded as eco- friendly and cost-effective. This electrochemical process works by applying direct current via electrodes (cathodes and anodes) into the suspension. This causes soil particles from the suspension to coagulate on the anode. Furthermore, it destabilises the suspension, causing a similar effect on the filtration as the addition of CA. However, EC does not require the usage of water hazardous substances and additional amounts of water to achieve destabilisation.

1.2 Goals and methodological approach

Previous research at the Institute for Tunnelling and Construction Management has established that EC can be used as a separation and destabilisation method for fresh bentonite suspensions in a laboratory scale (Paya, 2016). This thesis intends to determine the extent

to which EC can be used in a larger scale and for used bentonite suspensions. The approach was empirical since EC is still not a standardised method with a defined optimal cell design and best combination of operational parameters.

In order to perform parametric studies, a standard used suspension (SUS) was developed by loading the bentonite suspensions with fine soil particles. This suspension was put through series of tests in laboratory scale. Parameters were developed to evaluate the experimental results, with a special emphasis on effectiveness of separation and destabilisation through EC. Based on laboratory results with 2 l-EC cells, a larger 320 l-EC-cell was designed. A laboratory chamber filter press was acquired in order to enable a practice-oriented evaluation of the impact of EC on fine separation. The results were validated with one used suspension from a construction site.

Following, a calculation model was developed to analyse the impacts of replacing CA with EC on separation and disposal of used suspensions on construction sites. This was performed by evaluating the filtration time and volume, residual moisture of separated material, as well as analysing the residuals of CA and electrodes in the separated material.

An objective of this study was to give recommendations for a real-scale prototype for construction sites. This was done based on the knowledge gained from the laboratory and mid-scale experiments.

1.3 Structure of the dissertation

The overall structure of this dissertation takes the form of eleven chapters, divided into three blocks: fundamentals, experiments and relevance of the experimental results for practice.

Fundamentals

Chapter two describes the basics of the bentonite, bentonite suspensions and the conventional separation of used bentonite suspensions on construction sites. In the first part, special attention is given to the reasons for the stability of bentonite suspensions. Moreover, the electrokinetic behaviour of soil particles that can be found in a used bentonite suspension is explained. In the second part, applications of bentonite suspensions and their separation at tunnelling construction sites is explained, with a special focus on the fine separation of used bentonite suspensions.

The third chapter describes the basics of EC. First, the electrochemical processes behind EC are explained. In the second part, the factors affecting the separation and destabilisation efficiency of EC are discussed.

Chapter four gives a summary of previously undertaken research on EC of bentonite suspensions at the Institute for Tunnelling and Construction Management.

Experiments

The fifth chapter presents the laboratory experiments with a standardised used suspension. First, the standard used suspension is defined. This suspension was used in a series of EC experiments in the laboratory scale. The goal of the experimental series was to investigate the operating parameters of the EC process and find the best-fitting combination of parameters.. The findings from the laboratory series were used as basis for the scale-up to a larger scale EC prototype.

Chapter six comprises the description of the EC prototype and the analysis of experiments performed with it. First, the EC prototype and the laboratory chamber filter press are described. Secondly, the evaluation parameters for the experiments with the EC prototype are defined. Afterwards, eight experimental series with a total of 50 EC experiments and 109 filtration experiments were performed. The experiments with standard used suspension were validated with a suspension from a tunnelling construction site.

Relevance of the experimental results for the practice

The seventh chapter is concerned with the impact of EC on fine separation and disposal. Based on the results gained in the experimental phase, the influence of EC on the filtration process and on overall fine separation capacity is evaluated. Moreover, the effects that EC could have on disposal of soil and water are analysed.

Chapter eight contains the suggestions for improvement of the current prototype and recommendations for the real-scale prototype. The improvement ideas arose from the knowledge and experience gained in the experimental phase.

The ninth chapter compares the conventional conditioning and the EC in ecological terms. Here, the eco-friendly aspect of EC is discussed.

Chapter ten evaluates EC from construction management aspects. The analysis includes a cost comparison between EC and conventional conditioning.

In the last chapter, a summary and outlook are given.

2 Bentonite suspensions

2.1 Structure of bentonite particle

The term bentonite was first proposed in 1898 by W. C. Knight for the plastic, clay stone found near Rock River in Wyoming. The name originated from Benton Shale, the geological formation in which this clay was thought to occur at the time (Hosterman & Patterson, 1992). In the majority of cases, bentonites are formed through hydrothermal alternation of volcanic ash and rocks (Jasmund & Lagaly, 1993: 200; Imerys, 2018).

Bentonite is characterised by a high chemical stability, a low permeability, and furthermore by high adsorption properties. Therefore, it is often used as an impermeable barrier for land-fills and even as an isolator for nuclear waste disposal (Leroy et al., 2015). Mixed with water, bentonite creates stable colloidal suspensions with high importance in special civil engineering and tunnelling. In this field of application, it is used to support the trench during the diaphragm wall excavation and as a supporting, lubricating and conveying media in tunnelling. Besides civil engineering, bentonite is also applied in the pharmaceutical, cosmetic, agriculture, and beverage industry.

In this thesis, the tendency of bentonite to create stable colloidal suspensions is of high interest, and ways of destabilising this suspension are investigated. Therefore, the focus of this chapter is the colloidal properties of bentonite.

Colloidal fractions (< 2 µm) of bentonite clays are dominantly made up of clay minerals. The structure of clay minerals is composed of aluminium octahedral sheets and silica tetrahedral sheets joined together and stacked on top of each other. The combination of one octahedral sheet and one or two tetrahedral sheets is called a unit layer or a platelet. The structure of a unit layer repeats itself in a lateral direction. The combination of more layers stacked together is called a crystal lattice or a particle (Luckham & Rossi, 1999, Leroy et al., 2015).

The prevailing clay mineral in bentonite (60 – 80 % of the mass) is a platelet-formed mineral called montmorillonite (Praetorius & Schößer, 2016), which belongs to the smectite mineral group. Smectites consist of swellable three-sheet minerals with electrostatic charged layer surfaces. Besides smectite, bentonite also consists of common mica, hydrous mica, cristo-balite, and zeolite (Jasmund & Lagaly, 1993: 200).

Montmorillonite is the clay mineral that mainly defines the characteristics of a bentonite clay. Figure 1 shows the composition of a montmorillonite platelet and crystal lattice. The structure of a montmorillonite platelet consists of one AlO_6-octahedral sheet between two SiO_4-tetra-hedral sheets. (Jasmund & Lagaly, 1993: 46; van Olphen, 1963: 64). A unit layer with such combination of sheets is referred to as a TOT layer (tetrahedral-octahedral-tetrahedral layer).

Electrostatic charges on layer surfaces result from isomorphous substitution: tetravalent Si in the tetrahedral sheet is partly replaced by trivalent Al or Fe and Al in the octahedral sheet may be replaced by divalent Mg or, more rarely, by Fe, Cr, Zn, Li. Since the atoms of lower positive valence replace those of higher positive valence, a lack of positive charge and an excess of negative charge occurs. Due to this structure, the basal surface of a platelet carries a negative surface charge (van Olphen, 1963: 64). The negative electrostatic surface charge is counterbalanced by Ca^{2+}, Mg^{2+} or Na^+ cations in the interlayer space (space between the two unit layers), which causes the individual platelets to stack together.

The electrostatic charge on the edge surface, however, is dependent on the pH value and can be negative or positive (Tombacz & Szerekes, 2004; Stein, 2007: 15; Baik & Lee, 2010; Leroy et al., 2015). According to Leroy et al. (2015), the specific surface area of a perfectly dispersed montmorillonite is around 700-800 m^2g^{-1}, wherefrom the edge surface has about 10-30 m^2g^{-1} and the basal surface has about 750-770 m^2g^{-1}. This input and the thickness of the platelet and crystal lattice from Figure 1 are to be considered as correct in order of magnitude, since the size of clay minerals may differ by other authors. A sketch of one montmorillonite particle with negative charged basal surface and positive charged edges is shown in Figure 2.
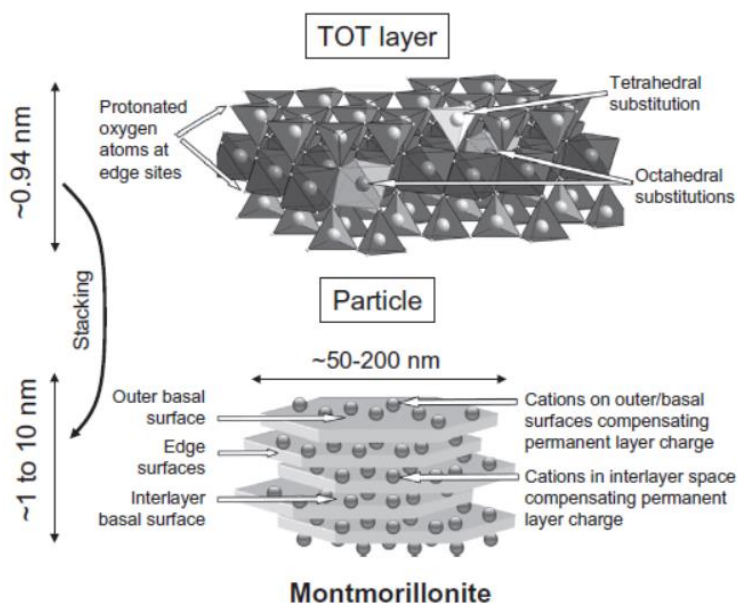
Figure 1: Montmorillonite: TOT layer (above) and a particle (below) (Leroy et al., 2015, modified from Tournassat et al., 2011.)
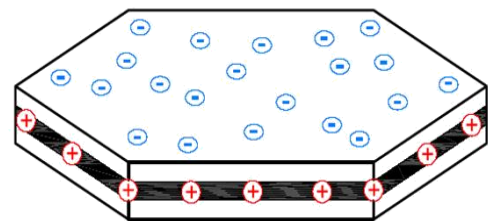
Figure 2: Sketch of a bentonite particle with a negative charged basal surface and positive charged edge surface (Praetorius & Schößer, 2016: 13)

Fifteen to twenty exchangeable cations interconnect platelets to build one montmorillonite particle (Stein 2003: 513). In the presence of water, interlayer cations can be replaced by

other cations available in the solution. Therefore, they are called "exchangeable cations". They can also be replaced with water molecules, even if only in contact with water vapour. (van Olphen, 1963: 65; Luckham & Rossi, 1999).

Bentonite products that are available on the market can be divided in four main groups. Two of those that can be found in nature are named after the type of exchangeable cations. If Na^+ cations represent a majority of cations between the platelets, bentonite is referred to as sodium bentonite. When Ca^{2+} or Mg^{2+} bind the platelets together, the bentonite is referred to as calcium bentonite. Calcium bentonite is often used to fabricate sodium bentonite since sodium bentonite is less common and more expensive than calcium bentonite. Specifically, Ca^{2+} is replaced with Na^+ cations through the activation process. This is done by adding a soda to a wet bentonite or through a technical process (Stein, 2007: 14; Praetorius & Schößer, 2016: 19). Bentonite produced this way is also known as active bentonite and represents the third group. The fourth group is presented by polymer-modified bentonite (Praetorius & Schößer, 2016: 20).

One of the most important properties of bentonite is its ability to swell in contact with water. The swelling, or hydration process, is normally induced by the adsorption of water molecules between the elementary layers of montmorillonite crystal lattices, which widens the interlayer space. Sodium bentonite has a bigger adsorption capacity (600-700%) than calcium bentonite (200-300%), meaning that bentonite can "expand" its dry volume in water several times. Ultimately, the width of the interlayer space can become so big that the connection between the platelets is lost and the crystal lattices decompose into individual platelets (Praetorius & Schößer, 2016: 10).

2.2 Stability of bentonite suspensions

2.2.1 Introduction to stability

Bentonite correctly dispersed in water creates a colloidal suspension, otherwise known as a slurry. The main characteristic of colloidal suspension is its stability, defined as the property of either not segregating or segregating as little as possible over a long period of time.

Colloidal suspension stability is a result of permanent Brownian motion of water molecules (Lettermann, 1999) and repulsive forces between the bentonite platelets (van Olphen, 1963: 63). Brownian motion was discovered by Brown in 19th century but first explained by Einstein in 1905. Since the water molecules are in continuous chaotic thermal motion, they collide with the colloidal particles. At any point in time, a colloidal particle is struck from various directions, giving it a "kick" in one direction. However, the direction can change at the next instant. This causes a constant random movement of particles in water. (Gregory, 2006: 22.) However, bentonite platelets repel each other upon approach due to the same sign charge

on their surface, or more precisely, due to the overlapping of their double layers (chapter 2.2.2 - 2.2.4). The combination of constant random motion and repelling forces is a cause for stability and equal distribution of bentonite particles in the water.

Stability of bentonite suspension is of great significance during tunnel excavation but causes difficulties in the process of dewatering used suspensions. Stable suspensions require longer handling times and the addition of chemicals which destabilise the suspension to improve the dewatering process. Stability and destabilisation emerge from the interaction forces between dispersed bentonite particles in a suspension, which are explained in the following sections.

2.2.2 Electrical double layer

For a better understanding of interaction forces between bentonite particles, an explanation of the electrical double layer developed around colloidal particles in a solution like water is needed (Figure 3). The double layer consists of the particle surface charge and an equivalent amount of ionic opposite charge, which are accumulated in the liquid near the particle surface (van Olphen, 1963: 29). The first layer is close to the particle surface and consists only of ions of opposite sign, known as counter-ions. This layer is called the Stern layer and it is considered to be always bounded to the particle surface.

The second layer in the electrical double layer is referred to as the diffuse or Gouy-Chapman layer. There is an excess of counter-ions and a deficit of co-ions in this layer, which compensates the remaining surface charge of the particle (Gregory, 2006: 54). While being electrostatically attracted by opposite charged particle surface, counter-ions also tend to diffuse away from the particle surface, where their concentration is highest, to the bulk solution, where their concentration is lower. This results in an equilibrium distribution of counter-ions, where their concentration gradually decreases with increasing distance from the surface (van Olphen, 1963: 30). Similar to counter-ions, co-ions are also under influence of electrostatic forces and diffusion: the particle surface repels them but they simultaneously tend to diffuse to the electrical double layer where their concentration is low (van Olphen, 1963: 30). At a certain distance from the particle, the diffuse layer ends and the counter-ions and co-ions are again in balance (Gregory, 2006: 54).

Figure 3 shows the diffuse electric double layer model or Stern-Gouy-Chapman model. For simplicity, only the excess of counter-ions is shown. The thickness of the Stern layer is usually in the order of the radius of a hydrated ion. (Gregory, 2006: 53-55).
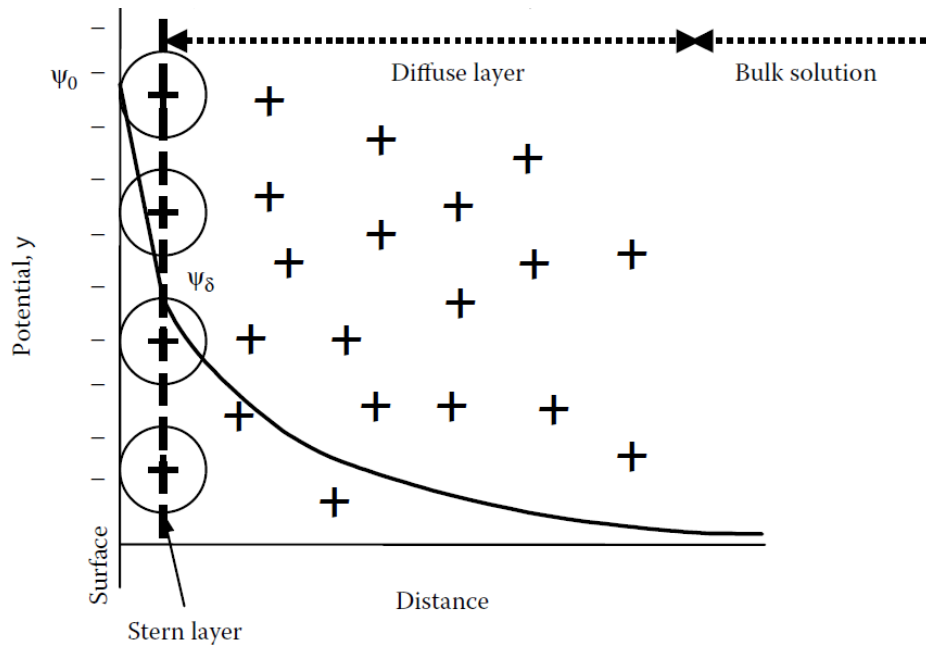
Figure 3: The Stern-Gouy-Chapman model of the electrical double layer adjacent to a negatively charged surface (Gregory, 2006: 54)

2.2.3 Particle interaction forces

Prior to dealing with the interaction of colloidal particles in water, two features must be addressed. First, these interactions occur only at distances smaller than the particles size. Secondly, interactions are dependent on particle size. While the strength of interaction between two particles increases to the first power of the particle size, gravity increases with mass and thus increases to the third power of particle size (for constant density of the particles). In other words, interaction forces between the particles lose their significance with increasing particles size because they become weak in comparison to the gravitational force. (Gregory, 2006: 63-64). Therefore, only the interaction forces between colloidal or smaller particles are able to compete with gravitational forces.

There are both attractive and repulsive interactions between the colloidal particles in a solution. London-van der Waals forces represent the most important attractive interaction. They arise from the attraction between dipoles of two molecules. (Gregory, 2006: 67). London-van der Waals forces between two particles of the same material embedded in a fluid are always attractive.

Even though this force is usually weak, it is additive. When analysing the two bentonite particles, the total sum of attractive forces between them is the sum of all attractive forces between all the atoms in both particles. This theory was developed by Hamaker (1937). Moreover, for larger particles, the attractive force decays less rapidly with increasing distance. According to van Olphen (1963), the van der Waals force between two atoms is inversely proportional to the seventh power of distance, but for two particles, it is inversely

proportional to the third power of distance between the particle surfaces (van Olphen, 1963: 36). Hence, van der Waals forces between small particles at shorter distances are considerable and able to compete with the repulsive forces between the particles.

On the other hand, the repulsive forces are of electrical nature – electrostatic repulsive forces between particles with same sign charge. When two same-sign particles approach, the diffuse parts of their double layers overlap and cause the increase in counter-ion concentration between the particles. This causes a rise in a repulsive force (Fisher et al., 2001, van Olphen, 1963: 35; Gregory, 2006: 75).

The distance at which particles become strongly repulsive depends of the thickness of their double layers (Fisher, 2001). This can be influenced by adding electrolytes or manipulating the pH-value of the solution, as described in chapter 2.2.5. The term electrolyte represents all ions in the dispersion medium (Paya, 2016: 14).

2.2.4 **Total interaction energy**

By assuming that attractive and repulsive forces between the particles are additive, it is possible to quantify their interaction (Gregory, 2006: 78). The interaction between the particles is determined by a combination of the interparticle double layer repulsion energy (V_r), describing the amount of work needed to bring the particles from infinite separation to a given distance, and the van der Waals attractive energy (V_a), describing the amount of work required to bring the particles from given distance to infinite separation. This theory was developed by Deryaguin and Landaau (1941) and Verwey and Overbeek (1948) and it is referred as DLVO theory. The total interaction energy (V_t) is calculated by simply adding the attractive (V_a) and repulsive energy (V_r) at each particle distance. In doing so, two additional short-range repulsion force repulsions were taken into account. The first one resists the interpenetration of the extruding lattice points or regions. The second one is caused by adsorbed water on a particle surface. It represents the amount of energy that would have to be invested to desorb the adsorbed water layer on the particle surface in order to bring the particles closer together (van Olphen, 1963: 39, Luckham & Rossi 1999). Due to these two short-range repulsion forces, the particles can never come in true contact (Gregory, 2006: 80). Instead, they stay in primary minimum at very small distance The results of these additions are so called net interaction curves shown in Figure 4.

Two additional terms are shown in Figure 4: the maximal energy barrier (V_m) that particles need to overcome in order to fall into primary minimum and coagulate, and V_b, which represents the barrier to redispersion. The height of V_m, which depends on temperature and pH of the solution and on concentration and valence of the electrolyte, and determines the sta-

bility of the suspension (Luckham & Rossi, 1999). Because of the depth of the primary minimum, the redispersion energy V_b, is often multiple times larger than the energy needed to coagulate the particles.
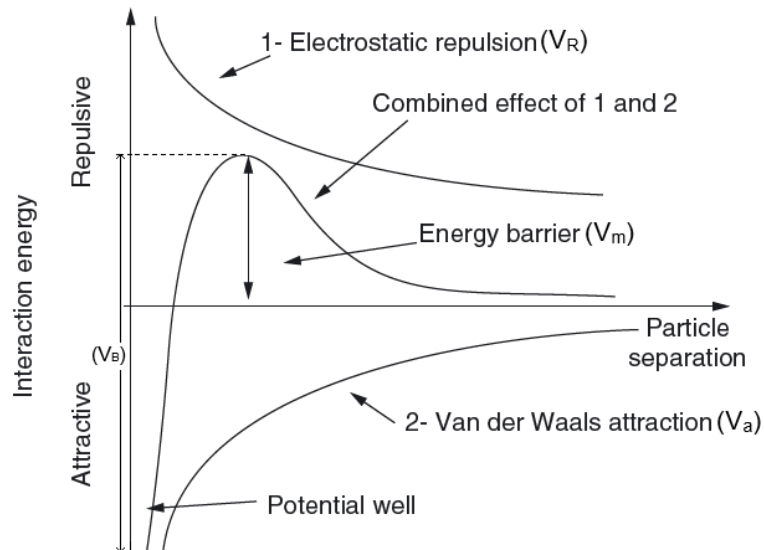
Figure 4: Repulsive, attractive and total interaction energy as a function of particle separation at intermediate electrolyte concentrations (after Thomas et al., 1999)

2.2.5 Influence of ionic strength of electrolyte and pH value of the solution on the total interaction energy

Influence of the ionic strength (concentration and valence) of electrolyte

The thickness of the electric double layer is dependent on the ionic strength (concentration and valence) of the electrolyte in the solution. The higher the concentration and valence of the ions with opposite sign in the solution, the thinner the double layer is (van Olphen, 1963: 36). This effect, known as double-layer compression, is shown schematically in Figure 5. At low ionic strength, the diffuse layer around the particle is large and the repulsive force between two particles, arising from the overlapping of two diffuse layers, acts on bigger distances and prevents the particles from coming closer to each other. At increased electrolyte concentration, the diffuse layers become thinner and particles can approach each other more closely before their diffuse layers overlap. (Gregory, 2006: 80).
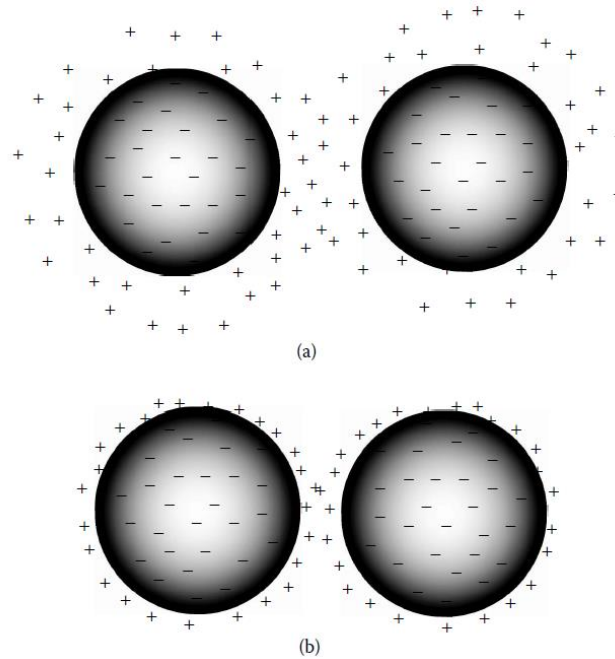
Figure 5: Effect of the ionic strength on the double layer thickness and the range of double-layer repulsion in low (a) and high (b) concentration of electrolytes (Gregory, 2006: 81)

Double layer compression reduces repulsive energy between the particles, while having no effect on attractive London - van der Waals forces (van Olphen, 1963: 36). This phenomenon has a significant influence on the balance of repulsive and attractive forces, as shown in Figure 6 and Figure 7. Figure 6 displays repulsive and attractive forces for three different electrolyte concentrations and Figure 7 displays the total interaction energy for these cases, starting from low concentration in 7a to high concentration in 7c. As displayed in the Figure 7, gradual increase of electrolyte concentration decreases the total interaction energy between the particles. If the particle can approach very close before repulsion is felt, the attractive van der Walls forces may outweigh the repulsion forces. In Figure 7c (high concentration of electrolytes), the total interaction energy is negative all the way up to the very small distance between the particles, where short-range repulsion forces become active. In other words, the resultant force along the whole approach-way is attractive and the particles coagulate upon each collision. The suspension under these conditions is described as unstable.
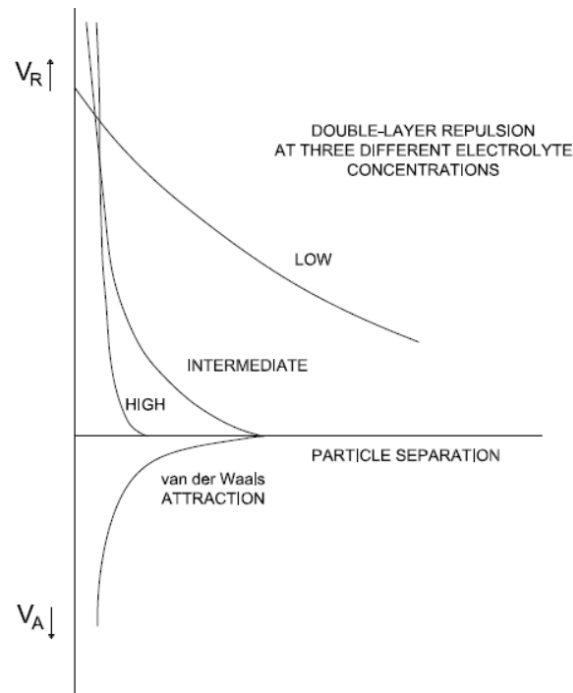
Figure 6: (a) Repulsive (V$_r$) and attractive (V$_a$) energy as a function of particle separation distance at three concentrations electrolytes with the same valence (after van Olphen, 1963: 37)
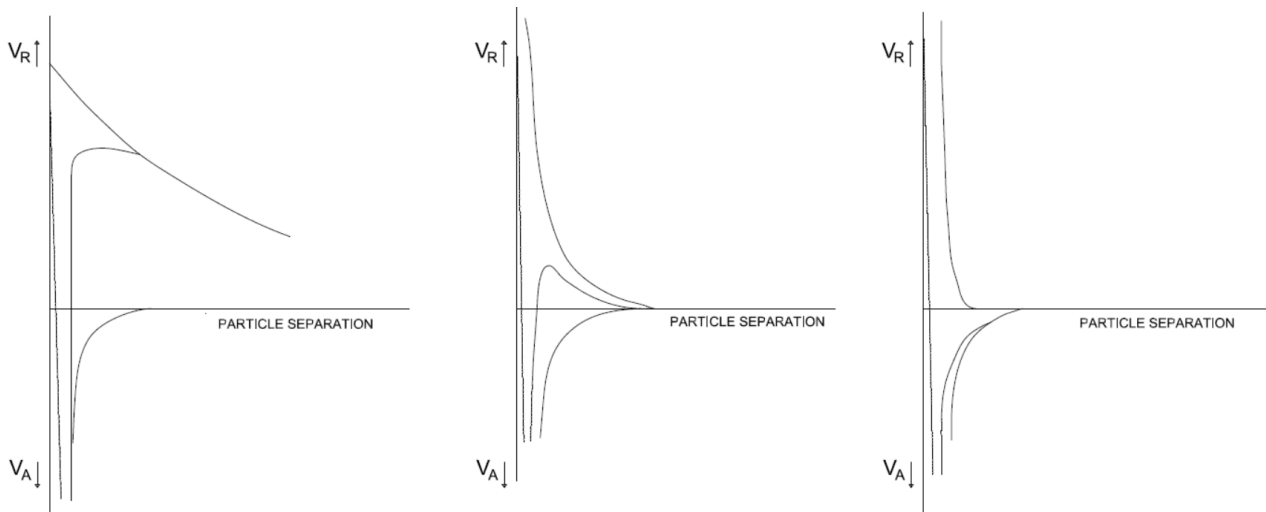
Figure 7: Total interaction energy (V$_t$) as a function of particle separation distance at three electrolyte concentrations: a) low, b) intermediate, c) high (after van Olphen, 1963: 38-40)

The smallest electrolyte concentration at which the suspension is completely destabilised (V$_m$ = 0) is called the critical coagulation concentration (ccc). At this concentration, the co-agulation becomes very fast and is only controlled only by Brownian motion. (Morbidelli & Arosio, 2016: 88). However, not only the electrolyte concentration, but also the valence has a major influence on repulsive forces between the particles. In fact, the influence of the valence is much stronger than the influence of the concentration. According to Shulze-Hardy

rule, the ccc depends on an ion's valence with a ratio of $1/z^6$, where z represents the electrolytes' valence. That means, ccc for a trivalent, divalent, and monovalent ion has a ratio of $1^{-6} : 2^{-6} : 3^{-6} = 1 : 0.016 : 0.0014$. If the valence is the same, the type of electrolytes play a minor role (Morbidelli & Arosio, 2016: 90). In other words, an Al^{3+} ion destabilises a suspension approximately 11 times stronger than an Fe^{2+} ion and 730 times stronger than an Na^+ ion. However, these are only theoretical considerations with some assumptions and simplifications. Experimentally, a dependence nearer to $1/z^3$ is found in many cases (Gregory, 2006: 82).

Influence of the pH value of the solution

As already mentioned before, bentonite particles possess negative charges on the surface and pH-dependent charges on the edges. Since pH determines the charge on the edges, it influences the stability of the suspension in general. Tombacz et al. (1990) researched the total interaction energy as a function of pH with a constant concentration of monovalent electrolytes (Figure 8). They calculated the total interaction energy after DLVO and experimentally verified the decrease of montmorillonite suspension stability with decreasing pH values. Suspensions at pH 2, 4 and 8 coagulated upon addition of 0.1, 0.2 - 0.25 and 0.35 - 0.4 mmol dm^{-3} NaCl, respectively. That means, for lower pH values, less electrolytes were needed to destabilise the suspension.
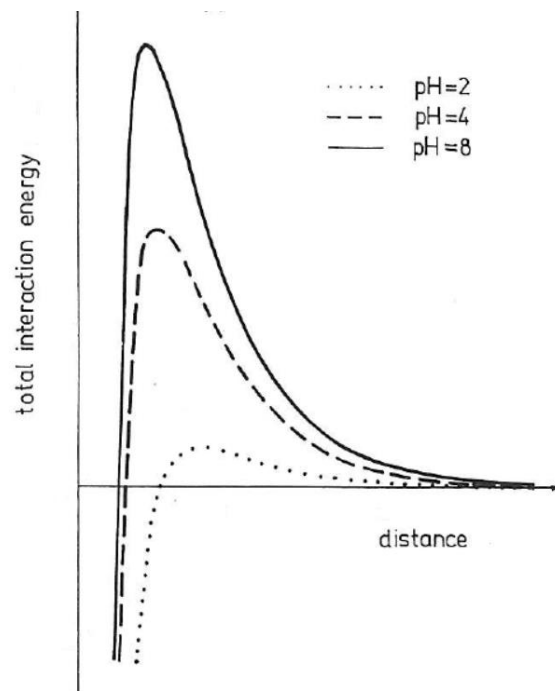
Figure 8: Total interaction energy (V_t) as a function of particle separation distance at three pH values and constant electrolyte concentration Tombacz et al. (1990)

In another major study, Tombacz and Szekeres (2004) researched the mutual interaction of pH and electrolyte concentration on a double layer of bentonite particles and consequently on the stability of bentonite suspensions. They found that the edges of bentonite particles are positively charged for a pH < 6.5 and negatively charged for a pH > 6.5. They also claim that, even if the charge on the edges is positive, negatively charged edge double could be hidden in a "cloud" of a positively charged basal double layer that spills over it. The edge double layer could emerge only by the reduction of double layer thickness of the basal surface caused by a high concentration of electrolytes (c_{el}) in a suspension (Figure 9).
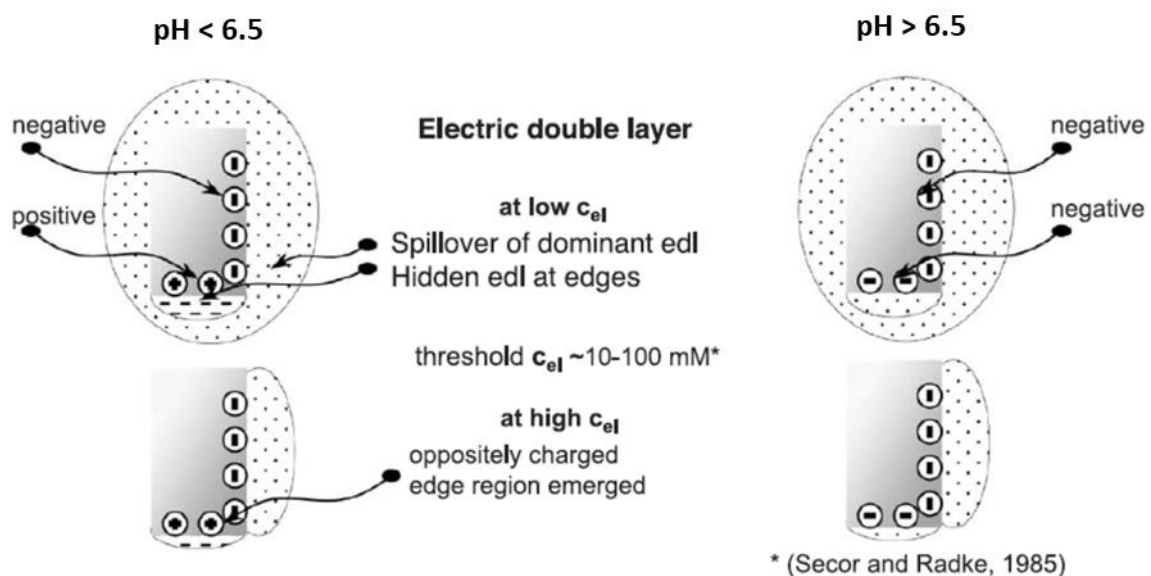
Figure 9: Basal and edge electric double layer at different pH and electrolyte concentrations (after Tombacz & Szekeres, 2004)

Summary

The pH value and the electrolyte ionic strength have a significant influence on the total interaction energy between the bentonite particles and consequently on the stability of bentonite suspensions. Increased electrolyte concentration reduces the thickness of the double layer, allowing the particles to come closer to each other. By adding a certain amount of electrolytes, the repulsive energy between the particles can be overcome and the particles will coagulate upon collision.

The influence of the pH value is not as significant as the influence of the electrolyte concentration. When bentonite particles disperse in a solution with acidic pH value, the edges of the particles will be positively charged, reducing the overall negative charge of the particle and consequently reducing the repulsive energy between the particles and the stability of the suspension. However, the repulsive energy between the particles cannot be completely overcome just by lowering the pH value of the solution (Figure 9).

There is a method in colloidal electrochemistry that can be used to validate this double layer theory and indirectly measure the charge of colloidal particles. This method is called zeta potential and it is explained in the next subchapter.

2.2.6 **Zeta potential**

The electrochemical properties and the surface charge of colloidal particles cannot be directly measured. Therefore, models had to be developed to estimate these properties (Leroy et al., 2015). A considerable amount of literature has been published on one of the most used models, the zeta potential. The term zeta potential (ζ potential) is defined as the electric potential in the double layer on the shear plane between the envelope of water that moves with a particle and the rest of the solution (Ghernaouth et al., 2015) This envelope of water consists of a Stern layer and a part of a diffuse layer. The zeta potential of any colloid particle in a solution is a measurable value and can therefore be used as an indirect measurement of the surface charge of a particle. Since the zeta potential is the electric potential a certain distance from the surface of the particle, it is not equal to but rather lower than the actual surface charge of a particle. The exact position of the shear plane and the distance to this plane from the particle surface cannot be determined (Shang, 1997).
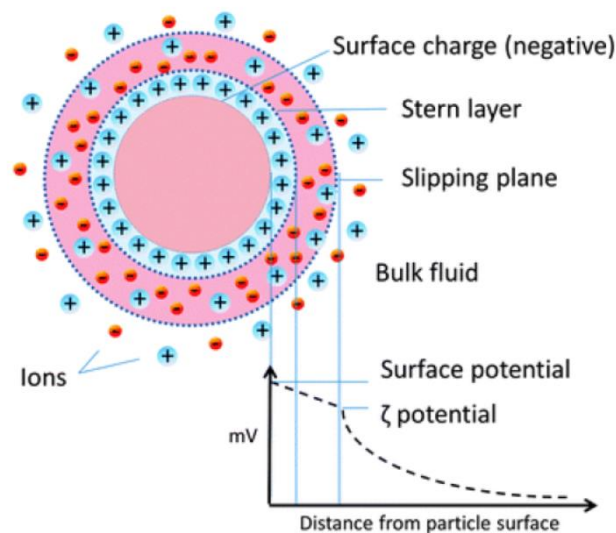
Figure 10:   Electrical double layer configuration (Marriaga-Cabralesa & Machuca-Martinez, 2014)

The zeta potential has been often used as an indicator for the stability of colloidal systems (ASTM Standard, 1985). According to DLVO theory, the larger the absolute value of zeta potential, the stronger the repulsive forces between the particles are and thus the suspension is more stable (Sincero & Sincero, 2003; Baldo & Junior, 2014) As the zeta potential approaches zero, suspensions become unstable (Baik & Lee, 2010). Because the zeta potential indicates the charge of the double layer, it is dependent on the pH value of the solution and even more dependent on the electrolyte valence and its concentration in the solution.

In terms of this dissertation, the zeta potential is not only important as an approximation of a surface charge of the particles but also as an indicator for a suspension stability. Additionally, the zeta potential also explains the electrokinetic behaviour of the particles in used bentonite suspension during EC.

As already mentioned in the introduction, bentonite suspensions can reach a density of up to 1,25 t/m^3 during excavation, before being replace with newly mixed, fresh bentonite suspension. When considered that the density of fresh bentonite suspensions is around 1.02 – 1.05 t/m^3, it becomes clear that the amount of non-bentonite particles in a used suspension exceeds the amount of bentonite particles multiple times. Therefore, it is important to know how all of these particles react on the separation treatment presented in this thesis. Their behaviour during the electrocoagulation and filtration can be explained by looking at their zeta potential. Therefore, the zeta potential of the bentonite particles and of the other particles from the suspension used in parametric studies (chapter 5.1) need to be overviewed.

For further discussion about zeta potential, the term point of zero charge (PZC), or isoelectric point (IEP), needs to be introduced. It is defined as a pH-value at which a particle shows no electrostatic charge, or rather, it is a pH-value at which the total amount of negative and positive charges are equal (Tunc & Duman, 2008).

Zeta potential - bentonite

The charge on the bentonite particle's surface is the result of isomorphous substitution that causes a negative charge on the basal surface and a pH-dependent charge on the edge surface. Even though the edge surface can be positively charged, it does not have significant influence on the overall charge of the particle. As already mentioned in chapter 2.1, the edge surface has about 10 – 30 m²g^{-1} and the basal surface has about 750 – 770 m²g^{-1} (Leroy et al., 2015). This view was supported by Duc et al. (2005) who reported that the negative charge accounts for 90 – 95 % of the total particle charge. Moreover, as mentioned in chapter 2.2.5, the positively charged edge double layer could be hidden in the negatively charged basal double layer (Tombacz & Szekeres, 2004). Therefore, it is no surprise that most researchers, such as Tunc & Duman (2008), Au & Leong (2013) and Huang et al. (2016), reported negative zeta potentials of fresh bentonite suspensions on the whole pH-range that they tested, in cases of low or medium electrolyte concentration (Table 1). Together, these studies indicate that the change of the pH value does not influence the overall particle charge in such a magnitude to overcome the negative charge and to change the zeta potential from negative to neutral or even positive.

Table 1: Zeta potential of bentonite particles in dependence of pH

	Maximum		Minimum		Reference
IEP	pH	Zeta potential (mV)	pH	Zeta potential (mV)	
-	11.7	-32	1.8	-8	Tunc & Duman, 2008
-	12	-35	2	-30	Au & Leong, 2013
-	12.3	-35.0	2.5	-12.8	Huang et al., 2016

Baik & Lee (2010) studied the effects of electrolyte concentration and pH value on the zeta potentials of calcium bentonite suspensions. $NaClO_4$ was used as an electrolyte. They have reported a negative zeta potential spreading from -20 to -40 mV at the electrolyte concentration of 0.001 M and 0.01 M, for the whole pH range tested (3-11). However, with an electrolyte concentration of 0.1 M, the zeta potential was increased to values between 0 - 10 mV for the whole pH range tested (Table 2).

Similar findings were reported by Zbik et al. (2014). Instead of increasing the concentration of electrolytes and measuring the zeta potential like Baik & Lee (2010), they increased the electrolytes' valence while keeping a constant concentration. This resulted in a drop of zeta potential from - 61.4 mV in deionized water to – 43.5 mV in 0.1 M of NaCl (M=mol/l) and further to – 12.3 mV in $CaCl_2$ (Table 2). Moreover, they measured the repulsive force between the particles with an atomic force microscope and found that the repulsive force between the particles on any chosen distance was smaller in a bentonite suspension treated with 0,1M $CaCl_2$ in comparison to a bentonite suspension treated with 0,1M NaCl.

Table 2: Zeta potential of bentonite particles in dependence of electrolyte concentration and valence

Electrolyte	Average zeta potential (mV)	Reference
0.001 M $NaClO_4$	-32	
0.01 M $NaClO_4$	-28	Baik & Lee (2010)
0.1 M $NaClO_4$-	5	
Deionized water	-61.4	
0.1 M NaCl	-43.5	Zbik et al. (2014)
0.1 M $CaCl_2$	-12.3	

These findings are in agreement with the DLVO theory and thus strongly support the idea of using the zeta potential as an indicator for the stability of colloidal suspensions.

Zeta potential - kaolin

For the parametric studies presented in this dissertation, a standard suspension was created in order to represent a commonly used bentonite suspension from a construction site (chapter 5.1). Since it was created by adding kaolin and silica flour into the bentonite suspension, the surface charge of these particles in water is of great significance for understanding of the ongoing processes during the electrocoagulation and filtration of such a suspension.

Kaolin is largely composed of the clay mineral called kaolinite. The kaolinite is a layered clay mineral consisting of one AlO_6-octahedral sheet and one SiO_4-tetrahedral sheet, thus one tetrahedral sheet less than montmorillonite. Typical kaolinite particles are disk or plate-like in shape, with a diameter of 0.5-1 µm and a thickness of 0.1 µm (Greenwood et al., 2006). Similar to montmorillonite, kaolinite also has a negative charged basal surface, arising from isomorphic substitution of Al^{3+} for Si^{4+} in the tetrahedral sheet of the mineral (Yukselen & Kaya, 2003), a pH-dependent edge surface charge and a high ratio of basal surface area to edge surface area. The IEP of the edge charge is around a pH 7.

At the pH< 7, the edge charge is positive and at pH> 7, it is negative (Greenwood et al., 2006). Due to the relatively small edge surface, some of the researchers found that a kaolin particle has a negative zeta potential overall tested pH range (Table 3). Similar to bentonite, the zeta potential of kaolin becomes more negative at higher pH values and decreases by adding electrolytes (Yukselen & Kaya, 2003), as shown in Table 3 and Table 4.

Table 3: Zeta potential of kaolin particles in dependence of pH (after Yukselen & Kaya, 2003)

| IEP/PZC | Maximum | | Minimum | | Reference |
	pH	Zeta potential (mV)	pH	Zeta potential (mV)	
4	11	-40	3.5	≈ 7	Lorenz, 1969
-	11	-30	3.5	5.5	Williams & Willams, 1977
2.2	10	-40	0	2.2	Smith & Narimatsu, 1993
6	12	-40	2	10	Dzenitis, 1997
2 < pH <3	10	-54	2	0.7	Vane & Zang, 1997
4.5	11	-85	3	≈ 8	Hotta et al., 1999
-	9.5	-65	3	$\approx$-3	Hotta et al., 1999
< 3	12	-32	3	Small values	West & Stewart, 2000
-	7 and 11	-25	3	-8	Stephan & Chase, 2001
-	11	-43	3	-25	Stephane & Chase, 2001
-	11	-42	3	-25	Yukselen & Kaya ,2003
-	10	-60	3.25	-5	Greenwwod et al., 2005
-	12	-35 / -52	2	-13 / -17	Au & Leong, 2013
2	12	-31	2	0	Ersoy et al., 2014

Table 4: Zeta potential of kaolin particles in dependence of electrolyte concentration and valence

Electrolyte concentration	Average Zeta potential (mV)	Reference
0.01 M NaCl	-35	
0.01 M CaCl$_2$	-8	Yukselen & Kaya (2003)
0.0001 M CaCl$_2$	-14	

Zeta potential – silica flour

Besides bentonite particles and kaolin where surface charge arises as a result of isomorphic substitution, most of the other particles also acquire a surface electrical charge when suspended in water (Leroy et al., 2015). In other words, all materials either possess surface charge or acquire it when suspended in a fluid. The surface charge arises in general from the four principal mechanisms: direct dissociation or ionisation of surface groups, lattice imperfections on the solid surface, isomorphic replacements within the lattice, and preferential

adsorption from ions in the solution (Stumm & Morgan, 1996; Delgado, 2002). The most common reason for a particle to acquire charge in water is that the particle's surface has chemical groups that ionize in water, leaving a residual charge on the surface (Gregory, 2006, p 47). Unless the pH value of the solution is very acidic, the charge that a particle acquires is usually negative (Kim & Lawler, 2005).

Acidic materials, such as silica, lose protons on the surface and acquire a negative surface charge charged over most of the pH range. (Gregory, 2006: 50). Kobayashi et al. (2005) called this reaction a deprotonation of silanol groups, written as $SiOH \longleftrightarrow SiO^- + H^+$. As for bentonite and kaolin particles, the negative electric surface charge of silica flour particles can be reduced by decreasing pH value or by adding electrolytes (Table 5 & Table 6).

Table 5: Zeta potential of silica particles in dependence of pH

	Maximum		Minimum		Reference
IEP	pH	Zeta potential (mV)	pH	Zeta potential (mV)	
2	9	-60	1	10	Fischer et al. (2001)
-	10	-65	2	-10	Kim & Lawler (2005)
-	≈ 9	≈ -40	≈ 4	≈ -3	Metin et al. (2011)
≈ 2	14	-30 / -90	0.5	25 / 80	Junior & Baldo (2014)

Table 6: Zeta potential of silica particles in dependence of electrolyte concentration

Electrolyte concentration	Zeta potential (mV)	Reference
0.01 mg/l $Al_2(SO_4)_3$	-70	
0.6 mg/l $Al_2(SO_4)_3$	0	Kim & Lawler (2010)
5 mg/l $Al_2(SO_4)_3$-	67	

2.2.7 Stability of bentonite suspensions - summary

The purpose of this section was to provide an explanation for the stability of bentonite suspensions. Understanding the reasons for stability is fundamental to understanding how the suspensions can be destabilised.

The suspensions are stable because all colloid particles possess the electrical charge of the same sign, which causes the particles to repel each other. The DLVO theory and measurements of zeta potential have shown that the repelling forces are dependent on the electrolyte ionic strength (concentration and valence) and the pH-value of the solution. Addition of electrolytes reduces the zeta potential and destabilises the suspension. That is exactly what happens during EC.

Moreover, the negative charge that colloid particles either possess or acquire in water explains their electrokinetic behaviour during EC, more precisely why all particles in the suspension are attracted to the anode (positively charged electrode).

2.3   Destabilization and coagulation of bentonite suspensions

Brownian motion causes dispersed particles to collide frequently in the suspension. If the collision energy is not great enough to overcome the repulsion energy at close distances, the particles will not coagulate and the suspension can be described as stable. The higher the electrolyte concentration is, the less energy particles need to overcome. In the case of high electrolyte concentration, electrical double layer is so compressed that the energy barrier V_m decreases to zero and the particles coagulate rapidly upon every collision. The suspension can be described as unstable or destabilised.

These essential steps of coagulation, the destabilisation of particles and the aggregation, are schematically shown in Figure 11.
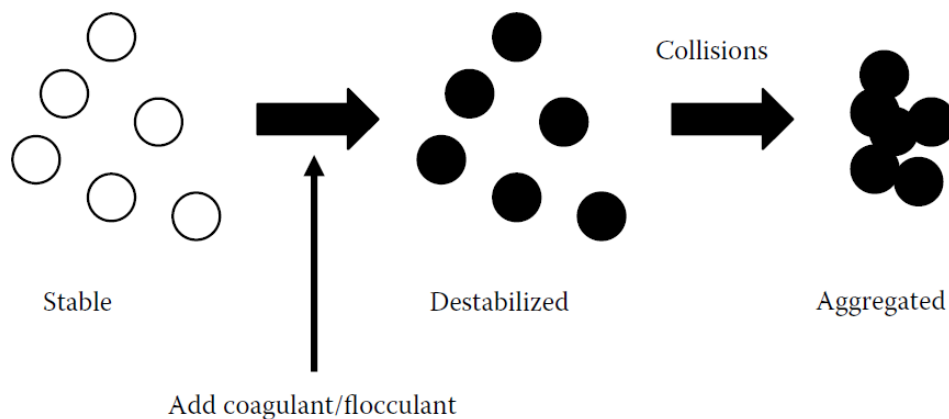
Figure 11:   Destabilization and aggregation (coagulation) of particles (Gregory, 2006: 112)

Those are the basics of the destabilisation and the coagulation of colloidal suspension. The specific mechanisms that occur during EC are discussed in chapter 3.2.2.

2.4   Slurries in tunnelling and underground engineering

The unique properties of bentonite suspensions (slurries) like viscosity, stability, and the ability to form filter cake favour their application in special civil engineering and tunnel construction practices (Büttner, 1993; Paya, 2016: 18). Bentonite suspensions can serve as lubricants in pipe jacking or as a conveying medium for vertical drilling. However, the largest application of bentonite suspensions is their use as a supporting and conveying medium in special civil engineering and tunnel construction, especially for diaphragm walls and in the mechanized tunnelling with hydroshields. (Paya, 2016: 18). In colloid science, the mixture of bentonite and water is referred to as bentonite suspension. However, in a civil engineering practice it is usually referred to as a slurry.

The hydroshields are tunnelling machines that use pressurised fluid to support the tunnel face during excavation (Maidl et al., 2012). The pressurised fluid is usually a bentonite suspension. It is prepared on the construction site and pumped through the slurry feed pipe in the excavation chamber of the shield, shown in Figure 12. There, it is pressurised by an air cushion to counteract the earth and water pressure and in doing so to support the tunnel face during excavation (Figure 13). Depending on the soil permeability and the bentonite content in the suspension, the tunnel face support is realised through a membrane model or a penetration model. In a case of low permeability and sufficient bentonite content, an impermeable membrane called filter cake will be formed at the tunnel face, through which the pressure from the suspension can be transferred onto the soil grains. In more permeable soils, even with a higher bentonite content, a filter cake cannot always be formed. In this case, the suspension penetrates through the tunnel face into the ground, transferring the shear forces onto the grain skeleton and keeping the tunnel face stable (Maidl et al., 2012: 29).
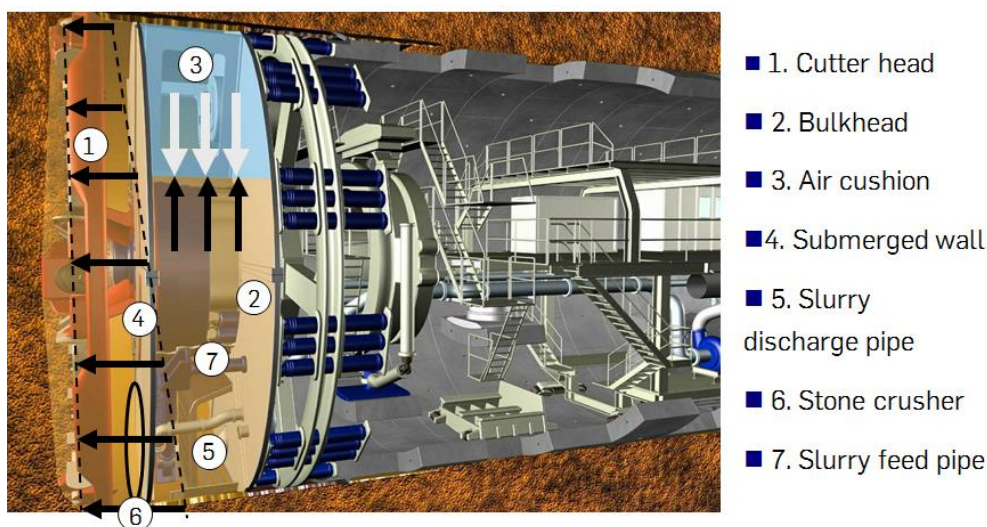
Figure 12:   Excavation chamber of a hydroshild (Zizka, 2019: 9, after Herrenknecht AG)
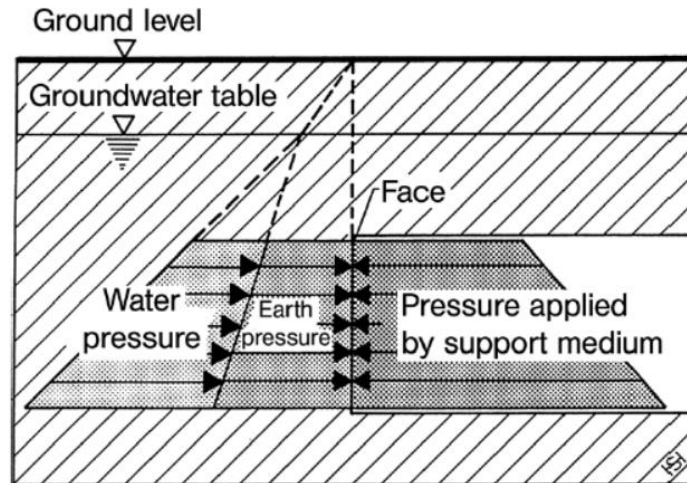
Figure 13: Principle of slurry support (Maidl et al., 2012: 28)

At the same time, the suspension with excavated soil is hydraulically conveyed from the excavation chamber through the slurry discharge pipes to the separation plant on the construction site. Hydraulic conveying is achieved by counteracting the gravitational forces that cause the soil particles to deposit on the bottom of the pipe with high flow velocity and the rheological properties of the suspension. (Büttner, 1993; Paya, 2016: 20). In the separation plant, suspension is regenerated - most of the excavated soil is separated from the suspension, which allows the suspension to be reused. The regenerated suspension is pumped back into the excavation chamber. This is known as a slurry circuit. The hydroshield technology can therefore be viewed as a combination of a tunnelling machine in the ground and a separation plant on the surface. While the tunnelling machine is responsible for the soil excavation, the plant is used to separate the excavated soil from the slurry (Zizka, 2019: 9).

A layout of a typical separation plant is shown in Figure 14. The suspension loaded with soil particles is transported from the excavation chamber of the tunnelling machine to the separation plant. There, it is first fed through the coarse screen (1). The purpose of coarse screen is to separate coarse material gravel. Afterwards, suspension is fed into hydrocyclones. There, the soil particles are separated from suspension with centrifugal energy. Due to gravity, they concentrate in the tailwater (the opening at the bottom of the hydrocyclone), and the cleaned suspension comes through the headwater. There are usually two cyclone stages: coarse (2) and fine cyclones (3). Fine cyclones have a smaller diameter, which makes higher radial acceleration possible. Depending on the type, coarse cyclones separate soil particles up to a threshold of 70 to 150 μm, while fine cyclone separate up to 35 μm or less. (Maidl et al., 2012: 111-112) The headwater of the fine cyclone is pumped to the travelling basin (4), from where it can be pumped back to the excavation face (5).

However, the regenerated suspension still contains fine soil particles like clay and silt parti-cles, which originate from the dispersion of clay lumps during the transportation of the sus-pension from the excavation chamber to the separation plant (Paya, 2016). Since these particles cannot be separated hydrocyclones, they remain in the regenerated suspension and cause a constant increase of suspension's density by repeated reuse of regenerated suspension. This increases clogging potential (Hollmann & Thewes, 2013), as well as wear potential, pipe resistance, and pressure loss (Seidenfuß, 2007, Paya, 2016: 22).

After successive loading of the suspension with fine particles, a critical point occurs at which the regenerated suspension no longer meets the requirement to be reused and must be replaced with a new, fresh suspension. The regenerated suspension is no longer recircu-lated into the slurry circuit, but stored in a tank (6). This suspension is labelled as used suspension. Prior to deposition, it is dewatered in chamber filter presses or centrifuges in a so-called fine separation process. Here, the used suspension is separated into fine particles (e.g. clay, silt, bentonite, etc.) and water (Paya, 2016: 22). The bottom right corner of Figure 14 shows the fine separation area. The volume of discharged suspension is replaced with a fresh suspension, mixed in the bentonite mixing plant.
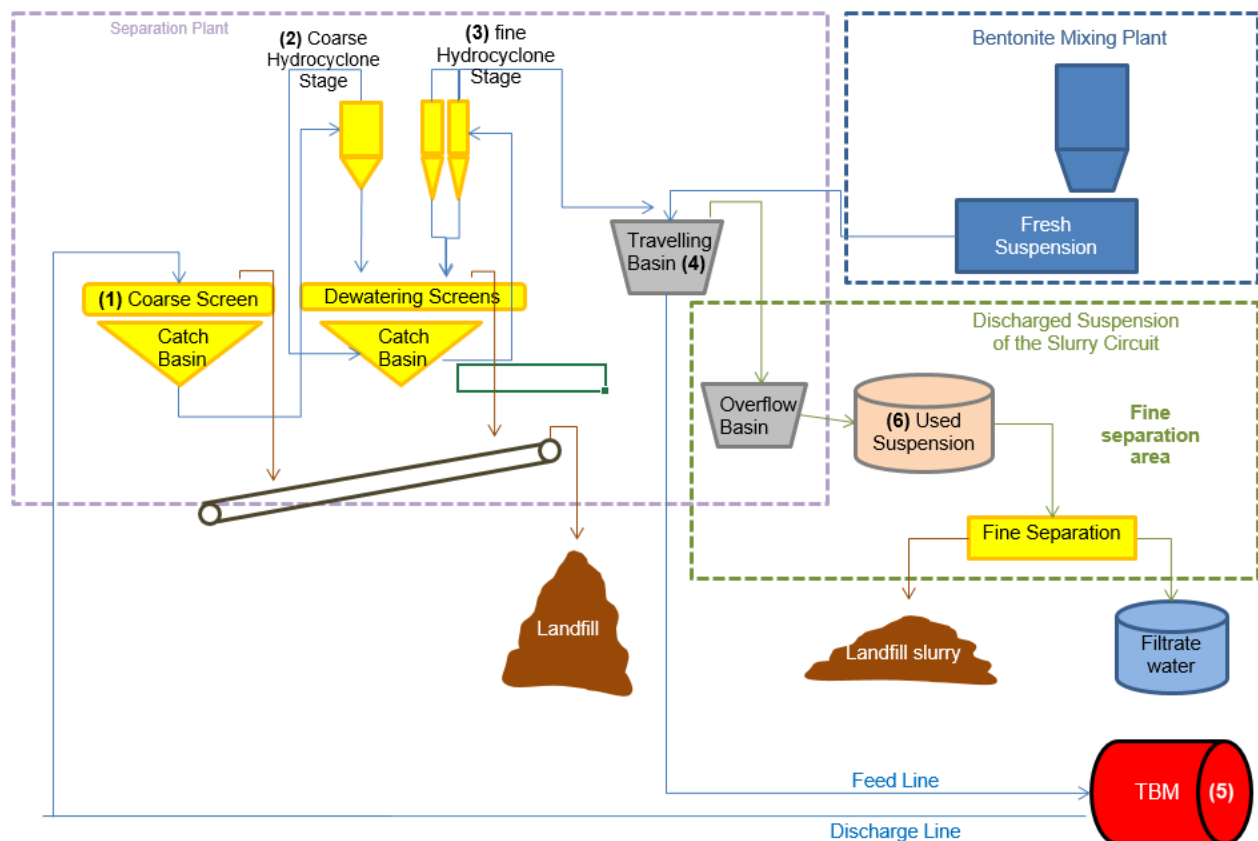
Figure 14:   Sketch of a separation plant (after Lipka, 2009)

2.5 Fine separation of used suspensions

In most cases, used suspensions are not directly disposed, but dewatered first. The aim is to transform the suspension into a landfillable soil material and water. On construction sites, dewatering is performed with chamber filter presses and centrifuges, where the used suspension is conditioned by adding chemicals that support the dewatering process (Paya, 2016: 30). The products of the dewatering are called filter cakes and filtrate water for chamber filter press or sludge and centrate water for centrifuges.

2.5.1 Conditioning of the used suspension

Before entering the chamber filter press or centrifuge, the used suspension is conditioned by adding inorganic additives, coagulants, and flocculants (Conrad, 1984; Anger, 2004). The inorganic additives are used to maintain the pH value of the used suspension on an optimum level for further conditioning with coagulants and flocculants. For this purpose, sulphuric acid (H_2SO_4) and alkalis such as soda (Na_2CO_3) are used. Coagulants and flocculants chemically support the dewatering in the chamber filter press or centrifuge. Coagulants are inorganic, soluble metal salts such as Al and Fe salts (Schumann, H. & Friedrich, C, 1997). They neutralize the surface charges of the colloid particles and form "primary flakes," according to the DLVO theory. Flocculants or polyelectrolytes are organic compounds that differ in charge (anionic, cationic or non-ionic) and molecular weight (low or high) (Anger, 2004). The most frequently used flocculants are organic anionic high-molecular polymers (Schumann, H. & Friedrich, C; 1997). They bridge the primary flakes together, which leads to bridging and formation of larger "secondary flakes" (Loll & Melsa, 1992; Anger, 2004). (Paya, 2016: 31)

Coagulants and flocculants are usually supplied as powders or emulsions. The dosage depends on their properties, the soil properties and the soil amount in the suspension. It is measured in tonnes of powder per tonne of dry matter of the suspension or litres of solution per m^3 of suspension. The higher the dry matter content, the higher the requirement for conditioning agents (CA). According to practical experience, the dosage for fresh suspensions can be up to 2 kg flocculant powder/tonne dry matter and for old suspensions between 0.3 and 1.3 kg flocculant powder/tonne dry matter. The dosage of the coagulants can be between 1 and 2 kg/tonne dry matter (Paya, 2016: 32).

2.5.2 Separation with filter presses

Filter presses dewater the flushing from the fine cyclone stage by applying pressure on it. Depending on the design of the filter element, a distinction is made between frame, chamber and membrane filter presses. Filter presses used on construction sites are almost exclusively chamber filter presses (Maidl et al., 2012: 113). They consist of filter plates, filter cloths and inlet/outlet channels . The flushing is fed into the space between filter plates with filter

cloths. Upon filling all the chambers, flushing is pressurised and the solid phase is separated from the liquid phase over the filter cloth. A filter cake forms on the filter cloth by the accumulation of soil particles (solid phase) on the surface of the filter cloth. Upon forming of the first layer of the filter cake, further filtration occurs over the cake, in which even the finest particles are retained. The liquid phase flows off as filtrate water. The performance of the chamber filter press, e.g. the thickness of the filter cake and its solid content, is determined by the filtration pressure and duration, the filter fabric, suspension density and the conditioning (Feifel & Oechsle, 2000, Maidl et al., 2012: 114). The inside an the outside view of an chamber filter press are shown in Figure 15 and Figure 16.
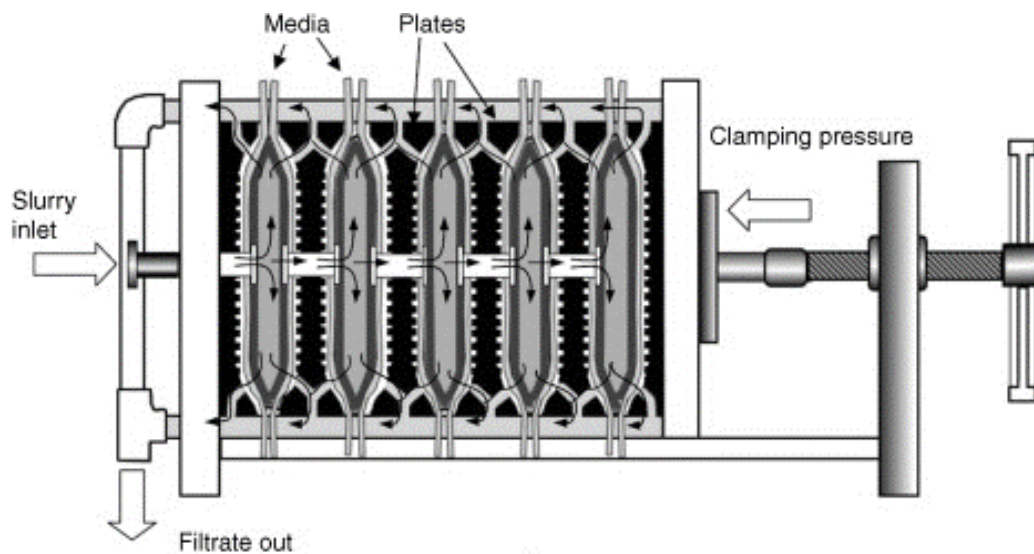
Figure 15:   Chamber filter press: inside view (Gupta & Yan, 2016)
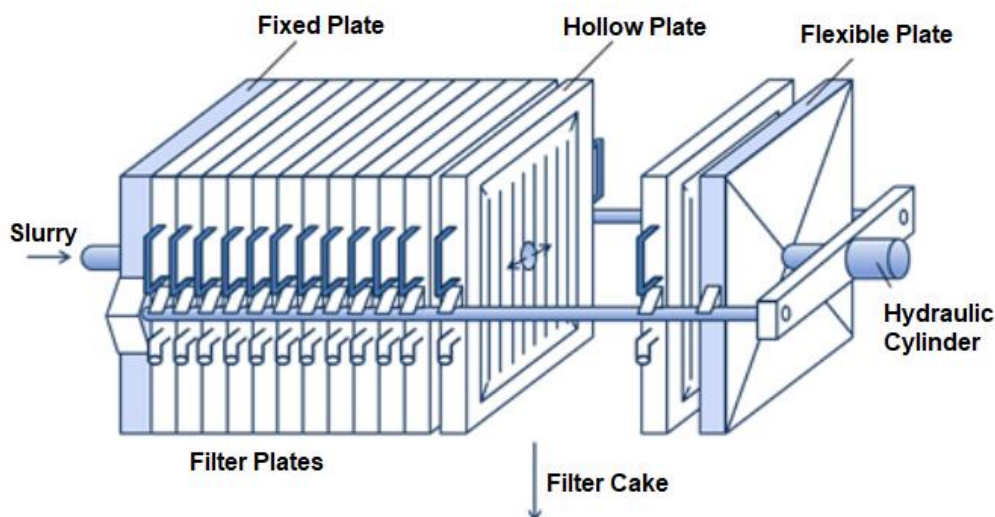
Figure 16:   Chamber filter press: outside view (Trevi, 2019)

Low filtration volumes, which is advantageous for the support function of the suspension, is disadvantageous for the filtration performance in the chamber filter press (Maidl et al., 2012:

114). Therefore, the old suspension is conditioned with coagulants and flocculants (metal salts or polymers) as well as additional substances (e.g. lime, chalk) prior to dewatering in chamber filter presses. The aim is to increase the compressibility of the filter cake and reduce its residual moisture (Luckert, 2004). However, the dosage of CA s is problematic: both too low dosage and overdosage lead to difficulties in the operating procedure. A low dosage causes insufficient flocculation formation. The filter cake has a paste-like consistency and then adheres firmly to the filter cloth. Overdosing leads to an obstruction of the filtration flow due to the deposition of polymers that not bound to the solids on the filter cloth. Therefore, the addition of lime is necessary to increase the compressibility of the filter cake and the filtration flow through the filter cloth (Paya, 2016: 34).

The filter cycle ends as soon as the flow rate of the membrane pump drops by approx. 80 %. The time required for a filter cycle is approximately one hour. After each filter cycle, the plates are pulled apart. For automated operation, it is optimal if the filter cake loosens itself and is then disposed of via a container or conveyor belt. According to practical experience, however, this is an exception. For this reason, this last step requires monitoring by operating personnel. A vibrating or stripping device can be used to automatically empty the plates (Feifel & Oechsle, 2000; Paya, 2016: 34).

In comparison to centrifuges, the performance of chamber filter presses is slightly lower (5 to 7 t/h), but the residual moisture of the cake is much lower than the moisture of the solid phase from centrifuge. (Maidl et al., 2012: 114). Another disadvantage is the discontinuity of the filtration process and the necessary degree of supervision by the operating personnel. (Paya, 2016: 36).

2.5.3 Separation with a centrifuge

The centrifuges used in tunnel construction are generally horizontally rotors, which continuously separate the solids from the liquid phase. Centrifuges work as an accelerated sedimentation process, in which solid particles do not settle slowly under gravity but are pressed into the outside of a drum under centrifugal force of 2,500 g to 4,000 g caused by high revolutions of the drum (in operation: 1,500 min^{-1} to maximum 2,500 min^{-1}). The solid particles are deposited on the outside and the liquid phase, called the centrate, is collected in the diameter of the drum. The centrate is discharged over an adjustable overflow weir. The addition of CA is unavoidable to achieve the discharge performance required from a centrifuge nowadays (11 t/h). (Maidl et al., 2012: 115). It is worth mentioning that the dewatering of used suspensions with a centrifuge was not a part of experimental studies in this dissertation.
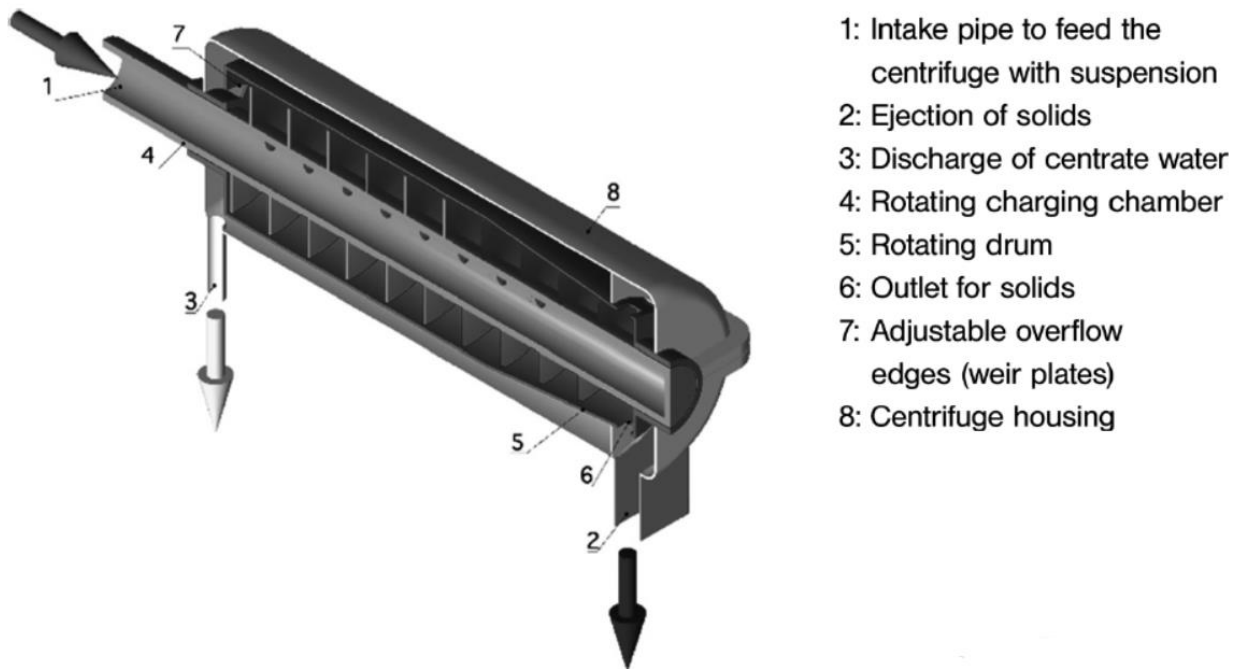
Figure 17:   Basic principle of a centrifuge (Maidl et al., 2012: 114)

2.5.4 Disposal of products of fine separation process

Sludge

The sludge (solid phase) from the fine separation consists of soil particles, bentonite and residual water. Bentonite as a natural mineral can be classified as soil (Paya, 2016: 36). There are three way to deposit the sludge:

- on agricultural area,
- in gravel pit and
- on landfill (Biermann, 2010).

The first two options are rarely used nowadays and the deposition on the landfill has become the standard procedure for deposing a sludge Thus, there are regulations that have to be considered.

In Germany, these include:

- Landfill Ordinance (Deponieverordnung - DepV),
- Waste Disposal Ordinance (Abfallablagerungsverordnung - AbfAblV),
- and LAGA Guidelines (Bund/Länder-Arbeitsgemeinschaft Abfall (LAGA)-Richtlinien).

According to DepV and AbfAblV, the sludge has to be tested on pollutants like chromium, cooper, zinc, nickel and properties like compression strength, axial deformation but also on

pH-value and electrical conductivity of its eluate. Depending on the results, sludge is categorised in classes O, I II or III, whereby a higher class is equating for more pollution and higher deposition costs. LAGA Guidelines prescribe the soil properties and maximal pollutant content required for reuse of sludge, for example as filling material or in roads construction.

The disposal costs depend significantly on the position of the construction site, since the deposition regulation differs internationally, or even locally from region to region. There has been a steady increase in deposition costs since the last years because the ecological restrictions are getting harsher and the demand for the new landfills is higher than the supply.

Water

Not only sludge, but also filtrate/centrate water need to be deposited. Deposition of filtrate or centrate water regulated with Water Resources Act (Wasserhaushaltgesetz - WHG) and local wastewater regulations. In principle, there are two ways do dispose filtrate/centrate water:

- convey to waste water system or
- to inshore waters.

Depending on the water regulations and properties of filtrate/centrate water, a conditioning of the filtrate/centrate water is necessary in order to meet the requirements in regulations, such as pH-value, temperature and pollutants content.

2.5.5 Issues concerning conventional dewatering technology

The challenges concerning conventional dewatering technology can be observed from ecological and economical point of view.

From the ecological point of view, the usage of CA and their ecological impact is disputable. Bidder (1997) analysed the wastewater treatment and searched for traces of coagulants based on Fe and Al in the wastewater treatment. The results showed that these coagulants have "only a minor influence" on the heavy metal concentrations in the centrate or filtrate water and in the sewage sludge (Paya, 2016: 37).

However, the ecological impact of flocculants have not been sufficiently researched. They are released into the environment through the sludge and in some cases even through centrate or filtrate water (Stowa, 1995). The dosage of flocculants depends on the density and charge of the used suspension. The fact that used suspension varies due to the change of subsoil along the tunnel makes the optimal dosing of flocculants difficult. So far, there is no evidence of an environmental impact from the disposal of sludge to which organic polymers

are attached. Nevertheless, the fact remains that flocculants are generally difficult to biode-grade (Schumann & Friedrich, 1997; Imerys, 2014; Paya, 2016: 38).

At an optimum dosage, the entire flocculant is bound to the sludge and disposed with it. However, practice and laboratory tests show that traces of flocculants get into the filtrate water if the sludge is overdosed or even if it is insufficiently dosed. This can be recognised by white colour and viscosity of the filtrate water, caused by polymer residue (Stowa, 1995; Paya, 2016: 38).

To protect water bodies from substances that are hazardous to water it is required that sub-stances and mixtures released into environment are classified for their water-hazardous properties. In Germany, classification is carried out on the basis of the Ordinance on facilities for handling substances that are hazardous to water (Verordnung über Anlagen zum Um-gang mit wassergefährdenden Stoffen - AwSV, 2017): There are three water hazard classes (WGK):

- slightly hazardous to water (WGK 1)

- obviously hazardous to water (WGK 2)

- highly hazardous to water (WGK 3)

Furthermore, substances can be classified as non-hazardous to water or are deemed haz-ardous to water in general. Substances that are currently not published with a WGK classi-fication are regarded as not classified and have to be regarded as highly hazardous to water (WGK 3) for reasons of precaution. Facility operators are obliged to self-classify these sub-stances according to Annex 1 of AwSV and to submit the WGK documentation to the Ger-man Environment Agency (Umweltbundesamt) (Umweltbundesamt, 2018).

In the Administrative Regulation on Water-Polluting Substances (Verwaltungsvorschrift was-sergefährdende Stoffe – VwVwS), cationic polyacrylamides are classified in WGK 2 to 3 depending on their ionic strength. Anionic and non-ionic polyacrylamides are classified in WGK 2.

From an economical point of view, conventional dewatering technology has high investment and operational costs. The current price of a new modern centrifuge can amount up to ap-prox. 600.000 EUR and of one chamber filter press 400.000 EUR (Paya, 2016: 39). The need for operating personnel is another critical aspect. The centrifuge can operate with a small number of operating personnel - the operating personnel from the separation plant also operates the centrifuge. In contrast, a chamber filter press sometimes requires addi-tional operating personnel for emptying and cleaning the filter cloths. Power consumption, for both machines is almost identical (Paya, 2016: 40).

The costs of the CA must also be considered. According to construction site data, the prices of flocculants can reach up to 6,000 €/t. (Paya, 2016: 39). The conditioning costs are very variable as they depend on the varying properties of used suspension.

An additional challenge with fine separation technology relates to the separation performance and the dimensioning of the chamber filter press and centrifuge. While centrifuges operate continuously with a higher throughput than chamber filter presses (1.5 chamber filter presses can balance the throughput of a centrifuge), chamber filter presses achieve a higher separation efficiency than centrifuge. The sludge from the chamber filter press (filter cake) has a lower water content than that from the centrifuge. The quality of the filtrate water is usually also better than of the centrate water from centrifuge. (Paya, 2016: 39)

As a conclusion, there is some obvious improvement potential of the current dewatering technology. The electrocoagulation as a new dewatering method could improve the current dewatering technology.

3 Fundamentals of electrocoagulation (EC)

3.1 Introduction to EC

Electrocoagulation (EC) is an electrochemical separation method for removing pollutants from aqueous solutions by applying electrical current. The simplest EC reactor consists of one EC cell with two electrodes and a power source. By connecting the electrodes to the power source, one electrode becomes positively charged (anode) and another becomes negatively charged (cathode). Anodes, usually made of metal elements or metal alloys, take part in the electrochemical reactions by dissolving and thus supplying the solution with metal ions. Therefore, they are called sacrificial anodes. The metal ions generated by electrodissolution of a sacrificial anode form various coagulant species, which destabilise and coagulate the solution.

First patents describing this method date back to late 19th century. At the end of 19th century and the beginning of the 20th century, several plants for purification of waste and canal water were built in England and in the USA. By the 1930s they were abandoned due to high operational costs (Vik et al., 1984).

This idea has recently been rediscovered. The latest research in wastewater treatment using EC has shown that it could be a competitive technology with the conventional coagulation process (Canizares et al., 2007, Elnenay et al., 2016). Smaller scale EC processes are considered as a reliable and effective technology (Holt et al., 2002). Even though the numerous advantages have been reported in the literature, industrial application of EC is not yet considered as an established wastewater technology. This is due to the lack of systematisation, standards and literature on several crucial subjects: standardisation of the EC cell design (Bharath et al., 2018), systematic models for reactor scale-up (Hakizimana et al., 2017), and general detailed technical literature on EC (Holt et al., 2002). Moreover, most of the operational parameters of EC are empirically optimised. Therefore, there is still a need of a systematic holistic approach to understand the fundamentals of EC process and its controlling parameters. This would enable a priori prediction of the treatment of various pollutant types (Holt et al. 2005, Sahu et al., 2014).

Electrochemical reactions in the field of wastewater treatment can also be used to gain energy, e.g. in form of microbial fuel cells for sewage treatment plants. They use the chemical energy from the metabolism of the waste water constituents to convert it directly into usable electrical energy via electrochemical reactions. (Wichern et al., 2012)

3.2   Electrochemical processes during EC

During EC process, there are generally three main processes occurring:

- electrochemical reactions on electrodes and mass transfer
- the formation of coagulants and gases
- the destabilisation and the coagulation of particles

3.2.1 Electrochemical reactions on electrodes and mass transfer

Fundamental electrochemical processes behind the EC are electrochemical reactions at the electrodes surface and mass transfer in the solution between the electrodes. Electrochemical reactions are heterogeneous chemical reactions which occur via a transfer of charge across the interface between the electrode and the solution (Walsch, 1993). The minimum requirements for those reactions are one cell with an aqueous solution, two electrodes (one anode and one cathode) and a power source. (Popovic et al., 2017)

Upon connecting the electrodes to the power source, the electrodes become electrically charged. The negatively charged electrode is called a cathode and it supplies the electrons into the solution, causing reduction processes (see Equation 3-1):

$$E + e^- \rightarrow E^-$$ (Eq. 3-1)

where E represents a species (an atom, ion or a molecule) gaining an electron e-, thus reducing its oxidation state.

The anode is the positively charged electrode. A reverse process to reduction, called oxidation, occurs on its surface. Species E losses an electron e-, thus increasing its oxidation state (see Equation 3-2):

$$E \rightarrow E^+ + e^-$$ (Eq. 3-2)

If the anode is made of metal M, the reaction from Eq. 3-2 describes the electrodissolution of the anode, which creates coagulants in the form of metal cations (Eq. 3-3)

$$M_{(s)} \rightarrow M_{(aq)}^{n+} + ne^-$$ (Eq. 3-3)

The mass transfer represents the transfer of reactants and products to and out of the electrode-solution interface. Together with above-mentioned electrochemical reactions, it is responsible for conduction of electricity through the solution in an EC cell (Hering et al., 2012). Mass transfer occurs through three processes: convection, diffusion and migration. While the convention is led by velocity and diffusion by a concentration gradient, migration is led by a potential gradient and it is thereby responsible for the passage of electrical current through the aqueous solution (Walsch, 1993). (Popovic et al., 2017)

3.2.2 Formation of coagulants and gases

The creation of the coagulant, described in Eq. 3-3, can be controlled by amount of applied electrical current. To explain this, the laws of Ohm and Faraday need to be introduced.

Ohm's law (Equation 3-3) defines the relationship between the electric current I [A], potential difference U [V], and resistance R [Ω].

$$I = \frac{U}{R} \hspace{8cm} \text{(Eq. 3-4)}$$

Faraday's electrolysis laws quantitatively describe the relationship between charge quantity and electrochemical effects. The first law states that the mass of a substance released at the electrode is directly proportional to the amount of current passing through the electrolyte. The second law states that the masses of various substances released by the same amount of electricity are directly proportional to their chemical equivalent masses M/z. (Popovic et al., 2017). Both laws are summarized in Equation 3-5.

$$m = \frac{M \cdot I \cdot t}{z \cdot F} \hspace{8cm} \text{(Eq. 3-5)}$$

with:

m mass of the substance released at the electrode [g]

M molar mass of the substance [g/mol]

I electrical current [A]

t time [s]

z valence number of ions of the substance [-]

F Faraday's constant [96485 As/mol]

Equation 3-5 can be used to estimate the amount of produced electrolysis gases (oxygen and hydrogen) and the mass of dissolved metal ions during the EC process. After inserting the molar mass and the valance in Eq. 3-5, the mass of the created substance is dependent only on amperage and duration of EC experiment.

3.2.3 Coagulation mechanisms during EC

EC can produce similar effects as chemical coagulation. Electrical current dissolves sacrificial anodes, which metal ions act as destabilisation and coagulation agents. Depending on the pH of the solution, these ions can build complex structures with hydroxide ions (Garcia-Segura et al., 2017).

Electrokinetic behaviour of particles

When an electric field is applied to a solution containing small particles, ultramicroscopic observation shows that the particles move toward one of the electrodes. If the polarity of the field is reversed, the particles change direction and move to the other electrode. (van Olphen, 1963). The positive ions get attracted from the cathode while the negative ions move to the anode.

Electrokinetic behaviour of a particle should represent an average of basal surface and edge surface properties. (Greenwood et al., 2006). As explained in chapters 2.2.5 and 2.2.6, clay particles like kaolin and bentonite possess on overall a negative surface charge, since their edge charge does not contribute much to the total charge. The particles that do not possess a surface charge acquire it when in water, and this charge is in most of the cases negative. Therefore, all particles in an used bentonite suspension move to the anode during EC.

Destabilisation of particles

The basics of coagulation of particles in the suspension are explained in chapter 2.3.

According to the DLVO theory, the addition of electrolytes destabilises the colloidal suspension by reducing the repulsive forces between the particles, which makes the coagulation of particles possible. Destabilisation does not influence collision rate of the particles but it improves collision efficiency (Gregory, 2006: 129).

Electrolytes are, in the case of EC, the dissolved ions and its compounds created by electrodissolution of the anode. They reduce the repulsive forces between the particles, allowing the attractive forces to overcome and result in the coagulation of particles upon collision.

Coagulation mechanisms

However, DLVO theory cannot fully explain these complex processes because interactive forces other than electrostatic repulsion (e.g.: hydration, hydrophobic interactions…) also influence colloids stability (Hubbard, 2002; Santo et al.,2012; Garcia-Segura et al., 2017). The exact mechanisms of destabilisation and coagulation during EC are still researched and discussed up to date. There is no mutual consent between the researches as to which mechanisms occur in which situations. Some of the mechanisms which emerge more often in discussions are described in following:

- The compression of the double layer of a colloidal particle or charge neutralisation (DLVO theory): caused by interactions of the particles with the metal cations generated from electrochemical dissolution of the sacrificial electrodes. This is one of the most common mechanisms. The metal cations act as charge shielding and reduce the thickness of the double layer (Hakizimana et al., 2017; Garcia-Segura et al.,

2017). This reduces the repulsive forces between particles, allowing them to come closer and eventually coagulate by collision.

- Adsorption of metal ions onto the surface of charged colloidal particles.

- Sweep coagulation (enmeshment mechanism or colloids entrapment): hydroxide precipitates entrap the colloidal particles that are in water/wastewater. This mechanism requires a significantly high dosage of coagulant in solution (Garcia-Segura et al., 2017.

- In the complexation, pollutant acts as a ligand. It is coordinated to the metallic centre and precipitates within the coagulant floc (Garcia-Segura et al., 2017).

The actual coagulation mechanism depends on the pollutant nature (size, charge, hydrophobicity…), the coagulant type and its dosage, the electrode material and the operating parameters of EC (especially electrical current). Different mechanisms could coexist simultaneously (Hakizimana et al., 2017; Garcia-Segura et al., 2017)
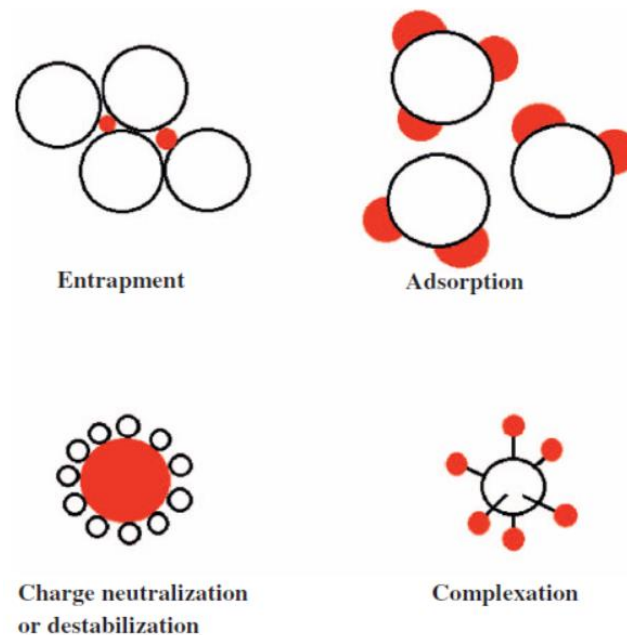
Figure 18:   Pollutant removal mechanisms (Garcia-Segura et al., 2017)

3.3 Factors effecting EC

EC is a complex process with a variety of mechanisms that act synergistically to remove pollutants from water. In the literature, there are many opinions on key mechanisms, control parameters and reactor configurations. Typically, empirical studies on EC are conducted to define major operating parameters for broad classes of water pollutants (Sahu et al., 2014).

There is a wide variety of opinions in the literature about the best cell configuration. Mollah et al. (2001) and Chen (2004) described six typical configurations for industrial EC-cells and

report their respective advantages and disadvantages. However, there is no dominant cell design in use (Holt et al., 2002). The optimal cell design is one of many parameters that are usually empirically determined in every research, since there is a lack of literature explaining the effect of the cell design.

The electrode surface area to volume ratio (A/V) is considered to be a significant scale-up parameter (Sahu et al., 2014). Electrode area influences surface current density and energy consumption. According to Mameri et al. (1998), as the A/V ratio increases, optimal current density decreases. Moreover, parameters such as EC cell operation type (continuous or batch), cell geometry, electrode connection modes and electrode distance have to be optimised to design an efficient EC cell (Sahu et al., 2014).

The parameters described in sections 3.3.1 - 3.3.11 influence the efficiency of an EC process. They can be divided in three groups: design, operational and solution parameters (Table 7). Design parameters are fixed upon the construction of an EC cell and cannot be changed later. During a research and development phase of a new EC cell, it is better to have as few fixed parameters as possible. Operational parameters are those which can vary in parametric studies. Many of the parameters cannot be assigned to just one of these of those two groups, because in some EC reactors they are fixed by design and is others they can be changed between or during the experiments. Solution parameter are specific electrochemical properties of the solution. Many researches adjust some of solution properties, like pH value and electrical conductivity of the solution, in order to reach better results. Therefore, pH value and electrical conductivity can be assigned to both solution and operational parameters. The parameters from Table 7 are explained in following subchapters.

Table 7: Factors effecting EC divided in three groups of parameters

	Electrode material	Current density	Electrode gap	Electrode connection modes	Electrical current type	pH value	Experiment duration
Design parameter	x		x	x	x		
Operational parameter	x	x	x	x	x	x	x
Solution parameter						x	

	Temperature	Electrical conductivity and supporting electrolyte	Flow state of the Solution	Pollutant concentration
Design parameter			x	
Operational parameter		x	x	
Solution parameter	x	x		x

3.3.1 **Electrode material**

The electrodissolution of the anode supplies the suspension with electrolytes. Their type and valence has a major role in destabilization and coagulation of the suspension (chapter 2.2.5).

Ghernaout et al. (2011) summarized the criteria for the selection of the electrode material as follows:

- The material must oxidise electrolytically and dissolve in water. This criterion limits the candidate materials to metals.
- The material should have high utilisation value, which leads to low residual concentrations of the coagulants in the treated solution.
- The material should have high electrical conductivity.
- The material should be inexpensive and easy to acquire.
- The material must not be toxic.

The literature on EC reveals that iron and aluminium are the most used electrode materials. They have been widely used in EC cells because of their low price, availability, non-toxicity and high valence of their ions. (Hakizimana, 2017). The EC systems with those materials have proved to be very effective (Canisarez et al., 2007). Moreover, according to Verma et al. (2012), aluminium and iron chloride salts are the most used coagulants in the conventional chemical coagulation treatment of wastewater. Therefore, the use of iron and aluminium ions to destabilise and coagulate pollutants in water is an established practice both in chemical coagulation treatment and in EC treatment.

Iron electrodes

When iron or steel are used, the anode supplies the suspension with Fe^{2+} and/or Fe^{3+} ions, as follows:

$$Fe \rightarrow Fe^{2+} + 2e^-$$ (Eq. 3-5)

$$Fe \rightarrow Fe^{3+} + 3e^-$$ (Eq. 3-6)

These ions can react with hydroxide ions and create diverse iron species, depending on the pH of the solution. Figure 19 presents the predominance-zone diagrams (PZD) of iron and its hydro-complexes as a function of the pH value of the solution. PZD show which species will be dominant at a certain concentration and pH value. On the ordinate, pFe(x) stands for the negative logarithm of the Fe(x) concentration.

Not all of the species from Figure 19 are equally good as coagulating agents. Among all Fe(II) species, $Fe(OH)_2$ is considered to be the best coagulating agent, and among Fe(III)

species, it is $Fe(OH)_3$. As presented in Figure 19b), $Fe(OH)_3$ is the only Fe(III)-species in solution when the pH is in the range of 6.2 - 9.6. (Garcia-Segura et al., 2017)
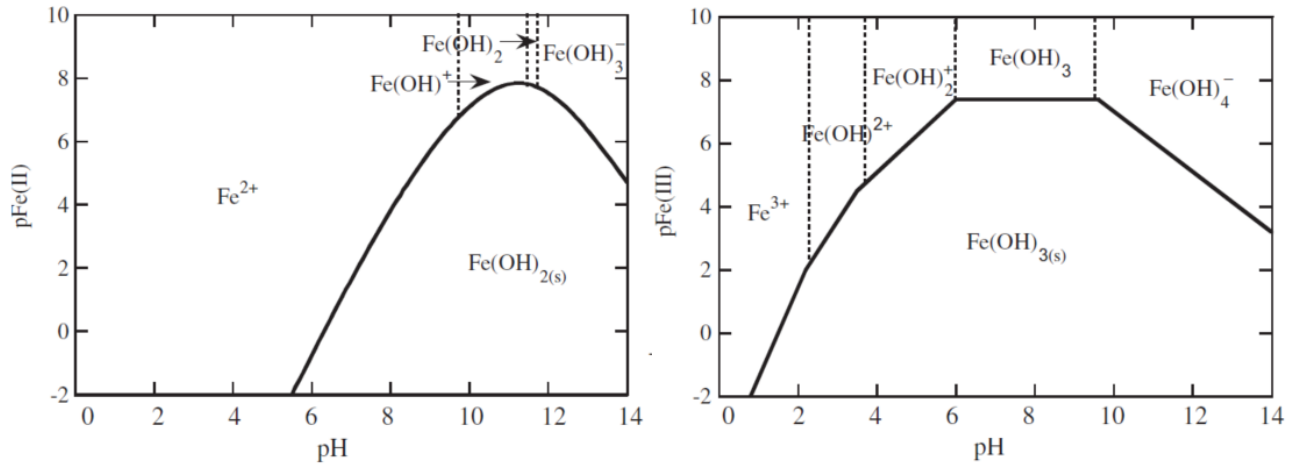
Figure 19: Predominance-zone diagrams for (a) Fe(II) and (b) Fe(III) chemical species in aqueous solution. The straight lines represent the solubility equilibrium for insoluble $Fe(OH)_2$ and $Fe(OH)_3$, respectively, and the dotted lines represent the predominance limits between soluble chemical species (Martinez-Huitle & Brillas, 2009)

Aluminium electrodes

In the case of EC with aluminium anodes, the electrodissolution of the anode produces aluminium cations, as presented in equation 3-7. These cations can form various species in an aqueous medium. Figure 20 presents predominance zones for different aluminium species, with the pH value on the abscissa and the logarithm of Al(III) concentration on the ordinate. In the usual pH-range of bentonite suspensions (pH 6-10), the possible Al(III) species are $Al(OH)_{3(s)}$, $Al(OH)_4^-$ and $Al(OH)_{3(aq)}$. According to Garcia-Segura et al. (2017), $Al(OH)_3$ is considered to be the best coagulation agent among all aluminium species.

$$Al \rightarrow Al^{3+} + 3e^- \qquad\qquad\qquad\qquad\qquad\qquad\qquad\qquad \text{(Eq. 3-7)}$$

For both aluminium and steel (or any other electrode material), water reduction occurs on the cathode, as presented in Eq. 3-8:

$$3H_2O + 3e^- \rightarrow \frac{3}{2}H_2 + 3OH^- \qquad\qquad\qquad\qquad\qquad\qquad \text{(Eq. 3-8)}$$

When electrocoagulation is performed with aluminium electrodes, additional chemical reactions can take place. Several researchers have reported chemical dissolution of aluminium cathode during electrocoagulation (Canizares et al., 2007, Mouedhen et al., 2008) or even after the electricity is turned off (Picard et al, 2000). This occurs at alkali medium due to the chemical reaction of OH⁻ ions produced during reduction of water (Eq 3-8), with the aluminium cathode, as presented in Eq 3-9: This chemical reaction has not been reported for iron cathodes.

$$2Al + 6H_2O + 2OH^- \rightarrow 2Al(OH)_4{}^- + 3H_2 \qquad \text{(Eq. 3-9)}$$

Kobya et al. (2006) claimed that similar chemical reaction can also take place at acidic medium (Eq. 3-10):

$$2Al + 6H^+ \rightarrow 2Al^{3+} + 3H_2 \qquad \text{(Eq. 3-10)}$$

It has to be emphasized that the reactions from Eq 3-9 and 3-10 are chemical reactions of aluminium in alkali or acidic medium. They are not directly caused by electricity flow through the cell and cannot be calculated with Faraday's law.
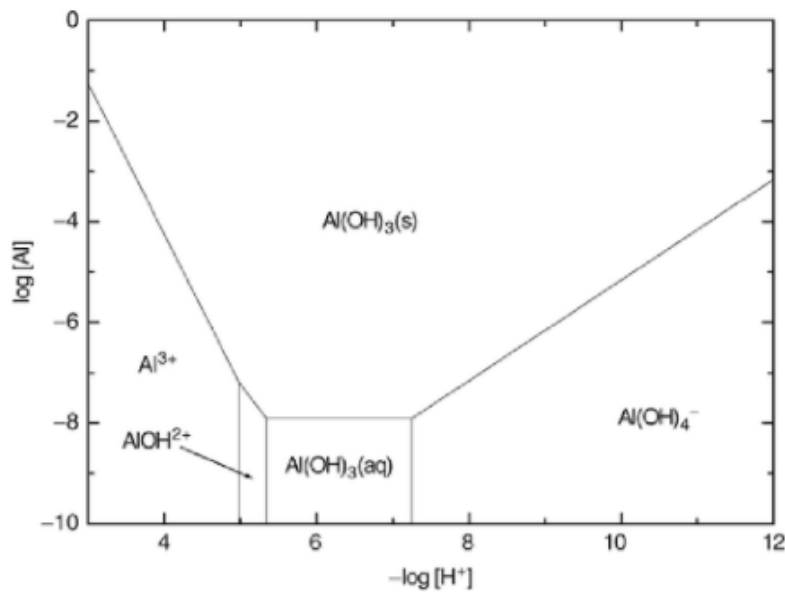
Figure 20:   Predominance-zone diagram of Al(III) ion (Brown & Eckberg, 2016)

Other materials

Besides iron or aluminium electrodes, electrocoagulation can also be performed with other metals. All materials with a specific resistance from 10^{-6} Ωcm to 10^{-4} Ωcm can be used as electrodes (Walsch, 1993). Sacrificial anodes made of arsenic (As), barium (Ba), brass (CuZn), cadmium (Cd), caesium (Cs), calcium (Ca), chromium (Cr), cooper (Cu), magnesium (Mg), platinum (Pt), silicon (Si), silver (Ag), sodium (Na), strontium (Sr), titanium (Ti), and zinc (Zn) can be found in the literature (Kirmaier et al., 1984; Patermarakis et al., 1990; Mickley, 2009, Verma, 2017). However, disadvantages of other materials (besides Al and Fe) are either their high price, low valence or toxicity. As mentioned in chapter 2.2.5, the critical coagulation concentrations (ccc) for monovalent, divalent and trivalent electrolytes are in the ratio of 1 : 0.016 : 0.0014. Considering this ratio, divalent materials like zinc, magnesium or cooper need to have around 11.5 times higher concentration in a solution to produce similar effects as aluminium. In order to produce this concentration, more material is required and higher amounts of electrical energy need to be consumed.

Aluminium or iron?

A great deal of previous research into EC has focused on the effect of electrode material on the EC treatment in terms of pollutant removal efficiency, ecological concerns, and economical aspects. Aluminium and iron are to date the most tested and discussed materials, and a number of authors have compared their advantages and disadvantages. Chen et al. (2000) and Canisares et al. (2007) have reported that iron electrodes can be oxidized easily when the cell is not in use, which leads to problems with corrosion. They suggest the use of aluminium in the processes that are not continuous in time. Moreover, the use of iron as the electrode materials brings additional problem because of the colour of Fe(III) salts (Canisares et al., 2007). Recently, Nariyan (2017) has reported that aluminium electrodes were more efficient than iron electrodes for the removal of metals from mine water.

A combination of iron and aluminium electrodes in the same cell is also possible and has been reported in the literature (Valero et al., 2008; Malakootian & Yousefi, 2009; Nouri et al., 2010, Verma, 2017). For example, a combination of iron cathode and aluminium anode can be used in order to avoid additional chemical dissolution of aluminium cathode in alkali medium and thus to have a better control of the amount of coagulants created. With this combination, the anode would provide the solution with aluminium ions through electrodissolution and the cathode would not dissolve. However, Canisares et al. (2007) recommended the usage of the same materials for all electrodes, since this allows reversing of the polarity in the cell, which helps to reduce the problems arising from a deposition of carbonate layers on the surface of the cathodes and passivation of the anodes.

3.3.2 Electrical current and current density

Various cells with electrodes of different shape and size can be found in the EC literature. Therefore, there are two standardized terms which enable the comparison between electrical current in different research. The first one is the surface current density [A/m^2], defined as the ratio of electrical current to electrode surface area. The second one is the volumetric current density [A/l] defined as the ratio of electrical current to the volume of the treated suspension. In this thesis, the volumetric current density is referred to as current density.

The electrical current is the key operating parameter of the electrocoagulation process. The effect of current is well known – according to Faraday's law (Eq. 3-5), the more electrical current flows through the system, the more metal ions will dissolve from the anode, which decreases the suspension stability and improves the coagulation of the particles. Moreover, more hydrogen will be produced at the cathode.

Sahu et al., 2014 recommended a surface current density to be in the range of 20-25 A/m^2, in order for the EC system to operate with minimum maintenance.

3.3.3 **Electrode gap**

The distance between the electrodes affects the electrical energy consumption and electro-chemical reactions during the process. In an electrocoagulation cell, the solution to be treated acts as an electricity conductor between the electrodes. The resistance of any electrical conductor is proportional to its length l [m] and inversely proportional to its cross-sectional area A [m^2] and K [Ω^{-1}m^{-1}], the specific electrical conductivity of the material (Eq. 3-12).

$$R = \frac{l}{A \cdot K}$$ (Eq 3-12)

An increase of the distance between the electrodes increases the length of the conductor, while the other two parameters do not change. As a result, the resistance increases and higher voltage is required to obtain a certain current density (Ohm's law Eq. 3-4). This increases power consumption, which can be calculated with the following equation:

$$P = I \cdot U \cdot t$$ (Eq 3-13)

with:

P power consumption [kWh]

I electrical current [A]

U voltage [V]

t time [h]

Significate energy savings can be achieved by keeping a small distance between the electrodes. (Sahu et al., 2014). Aswathy et al., 2016 performed a series of test at 1 cm, 3 cm and 5 cm electrode gap and observed a current of 0.62 A, 0.35 A and 0.21 A, respectively. They concluded that the increased current at lesser electrode gaps increased the EC efficiency. However, short distance between the electrodes can cause lower removal efficiency of the pollutants from water (Garcia-Segura et al., 2017), when performing the test with the identical amperage. The optimal distance varies for different solutions and it is therefore often empirically determined.

3.3.4 **Electrode connection modes**

In its simplest form, an electrocoagulation cell consists of one anode and one cathode. However, one electrocoagulation cell can have more than one pair of electrodes. Some researchers even recommend more electrode pairs in order to reach higher pollutant removal efficiency (Szynkarcuk et al., 1994; Chen et al., 2000; Holt, 2002, Kobya et al., 2003; Paya, 2016). When there is more than one electrode pair in the cell, the way the electrodes are

connected affects the removal efficiency and energy consumption of the electrocoagulation process. The most typical connection modes are monopolar electrodes in series (MP-S) or parallel connection (MP-P) and bipolar electrodes (BP) (Kobya et al., 2003, 2007 & 2011; Sahu et al., 2014, Garcia-Segura et al., 2017). In monopolar connection mode, each electrode is either completely positive charged (anode) or completely negative charged (cathode). The difference between the parallel and series connection is shown in Figure 21. In parallel connection mode, electrodes of the same sign are directly connected to each other and to the power source. In series connection mode, the inner electrodes are connected to each other in pairs and only the outer electrodes are connected to the power source. In the bipolar arrangement, the inner electrodes are neither connected to each other nor to the power source. They possess both polarities, one on each side.

Among all these connection modes, there is no clear preference in the literature. However, monopolar electrodes in parallel circuit present generally lower operational costs (Garcia-Segura et al., 2017).
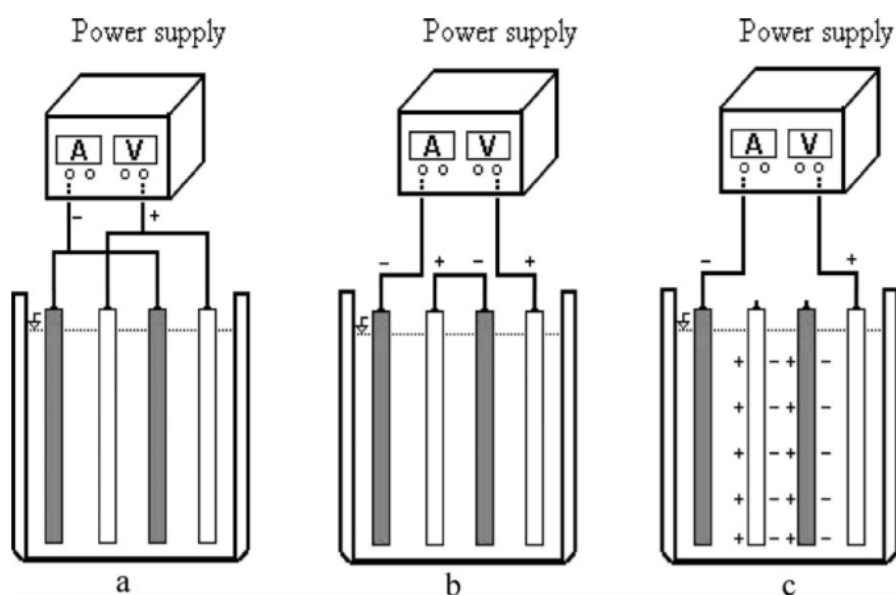
Figure 21: Three most typical electrode connection modes: a) monopolar electrodes in parallel connection (MP-P), b) monopolar electrodes in series connection (MP-S), c) bipolar electrodes (BP-S) (Kobya et al., 2007)

3.3.5 **Electrical current type**

Direct current (DC) is typically used in EC systems. However, there are some reports of alternating current (AC) and DC with polarity reversal modes being used. Vasudevan & Lakshmi (2011) tested AC and observed a similar pollutant removal efficiency and a slightly lower energy consumption in the comparison to DC mode. Some authors like Nikolaev et al. (1982), Chen and Hung (2007) and Eyvaz et al. (2009) recommend polarity reversal during

the process in order to increase efficiency by reducing the passivation of electrodes (Sahu et al., 2014). Passivation of the electrodes is a term used to describe the generation of metal oxides, carbonates and hydroxides on the electrodes surface (Nikolaev et al. 1982, Marriaga-Cabralesa & Machuca-Martinez, 2014). This layer requires a higher voltage at the beginning of the experiment in order to be destroyed (Ostermann, 2007). It increases electrode resistance, cell voltage and thus the operation costs (Mechelhoff et al., 2013), but also the EC efficiency is significantly reduced (Eyvaz et al., 2009).

Paya (2016) has tested polarity reversal during the electrocoagulation treatment of bentonite suspension in order to remove the particles that coagulate on the anode during the process. However, the electrical method of cleaning the anode proved to be less efficient than other methods tested.

3.3.6 **pH value**

The pH value of the solution to be treated is one of the key parameters of EC treatment. Sahu et al. (2014) have summarized that it affects five following parameters:

- total interaction energy between the particles (chapter 2.2.5) – decrease of pH value decreases the repulsive forces between the particles
- zeta potential (chapter 2.2.6) - decrease of pH value decreases the zeta potential and thus the suspension's stability
- Speciation of hydroxides (Figure 19 and Figure 20) - species $Al(OH)_{3(s)}$ for $Al(III)$ and $Fe(OH)_{3(s)}$ $Fe(III)$ are preferred coagulant agents. Therefore, neutral and alkaline media provide the best conditions for EC
- Dissolution of electrodes – acidic and alkali pH values cause a chemical dissolution of aluminium cathode. (Eq. 3-9 & 3-10)
- conductivity of the solution

Moreover, the pH value can vary during the EC treatment, making it a constantly changing parameter.

3.3.7 **Experiment duration**

The effect of the experiment duration can be explained with the Faraday's law (Eq. 3-4). Experiment duration together with electrical current defines the ampere-hours (Ah) invested in production of a coagulating agent through electrodissolution of the anode. Longer experiment duration leads to more coagulating agent produced and consequently to higher removal efficiency of the pollutant from the solution. However, the removal efficiency does not necessarily increase linearly with the experiment duration. Moreover, it is possible to pro-

duce an above-optimum concentration of metal ions, which could even turn the zeta potential of particles in the suspension to positive values. This could re-stabilise the suspension, since the particles would again have same sign charge (this time positive) and the repulsive forces could be dominant again. Holt et al. (2002) reported such a case. They were treating a 1 g/l kaolin clay suspension with EC and found that the zeta potential rose from initial value of ca. -50 mV to +20 mV after approximately 25 minutes of treatment with a constant current of 0.5 A. This can happen also with CA, not only with EC. Kim and Lawler (2005) observed that the zeta potential of silica particles continuously increased with an increase in aluminium sulphate dosage during conventional conditioning, from an initial value of -70 mV to +67 mV at a dose of 5 mg/l. IEP was reported at the aluminium sulphate concentration of approximately 0.6 mg/l. As expected, the best solids removal efficiency was achieved at zeta potential of the particles close to 0 mV.

The duration of the electrocoagulation treatment also affects the pH of the solution (Abdel-Gawad et al., 2012) and can therefore affect the metal species being produced at the anode and the chemical dissolution of the cathode. Moreover, the conductivity of the solution and the amount of the coagulated particles on the anode change with time.

For above-mentioned reasons, an optimal electrocoagulation treatment duration is usually empirically determined for each solution to be treated.

3.3.8 **Temperature**

Research has been inconclusive about the effect of solution temperature on the electro-coagulation process and the removal of the pollutants from the solution. Yilmaz et al. (2008) and Vasudevan et al. (2009) found that an increase in temperature improved the removal rate of the pollutants. However, Kazal & Pahlavanzadeh (2011) and Chen (2004) reported a negative effect of increased temperature on removal efficiency. It is possible that the effect of the temperature depends on the pollutant itself. (Sahu et al., 2014)

By studying the stability of silica suspensions, Metin et al. (2011) reported that increase of the suspension's temperature from 25°C to 70°C decreased ccc. This finding leads to the conclusion that the same amount of coagulating agents produced by electrodissolution of the anode should be more effective at higher temperatures than at lower temperatures. A possible explanation for this discovery is that the increase of kinetic energy of the particles increases the particles collision rate, thus making them coagulate faster when the suspension is destabilised.

3.3.9 **Electrical conductivity and supporting electrolyte**

Electrical conductivity of the solution to be electrocoagulated is inversely proportional to the cell voltage needed to obtain a certain current density. Solutions with higher conductivity therefore allow higher maximal currents for the same voltage. In other words, an intended current can be reached with lower voltage, and thus with lower energy consumption, if the solution has higher electrical conductivity. Therefore, many researchers add NaCl as a supporting electrolyte to the solution to be treated in order to increase the conductivity and lower the cost. The addition of NaCl not only improves the conductivity but can also contribute to water disinfection (Wong et al., 2002) and decreases the zeta potential of the particles (Zbik et al., 2014), thus contributing to the destabilisation of the suspension. Utilising this phenomenon, Elnenay et al. (2016) reported an increase of removal efficiency by an addition on NaCl in the solution in experiments with the same electrical current. With the addition of more NaCl, high removal rates were achieved earlier in the experiment, which means that the addition of NaCl can even shorten the experiment duration. Holt et al. (2005) therefore recommended addition of at least 200 mg/l of NaCl to improve the efficiency of water treatment with EC (Sahu et al., 2014).

Besides chlorides, other electrolytes like sulphates and nitrates can also positively influence EC processes. However, chlorides are preferred due to their corrosive power, which promotes dissolution of the anode and thus the creation of coagulants. The voltage required for the electrodissolution of the anode is lower in the presence of chloride than for sulphate or nitrate electrolytes. However, chlorides cause localised corrosion of the anode, meaning that some parts of the anode stay smooth while others have holes. Conversely, sulphates cause uniform corrosion while nitrates cause crevice corrosion. (Hu et al., 2003, Lin et al., 2010, Garcia-Segura et al., 2017). Chlorides are also advantageous because they can break the passivating layers at the anode through the mechanism of pitting corrosion. (Marriaga-Cabralesa & Machuca-Martinez, 2014).

Also in the area of microbial fuel cell was determined that the increased temperature and electrical conductivity increase the power density of the process (Hiegemann, Wichern, et al., 2016).

3.3.10 **Flow state of the solution**

A solution in the EC cell can be in an idle state or flow state. Movement of the suspension during the EC treatment improves the distribution of the electrolytes in the solution (Walsch, 1993). The flow can be characterized as continuous or discontinuous as well as turbulent or laminar flow. In contrast to laminar flow, turbulent flow can contribute to reducing or avoiding the accumulation of particles at the anode (Donini et al., 1994). (Paya, 2016)

3.3.11 **Pollutant concentration**

The initial pollutant concentration in the solution is another parameter that affects the efficiency of the EC treatment. When increasing the pollutant concentration but keeping the same electrical charge (Ah), the amount of the coagulant generated through electrodissolution of the anode will not change, but there will be more particles which need to be destabilised in order to coagulate. In that case, an increase in the pollutant concentration decreases the pollutant removal efficiency. Therefore, either more electrical current or longer EC duration are necessary to reach the required pollutant removal efficiency by increased pollutant concentrations (Bharath et al., 2018).

3.4   **Comparison between chemical coagulation and electrocoagulation**

EC offers an alternative to usage of chemical coagulants and flocculants like metal salts, polymers or polyelectrolytes (Sahu et al., 2014). Many publications about EC include discussion about the advantages and disadvantages of EC in comparison to chemical coagulation. However, reported pros and cons of EC are often generalized and sometimes even contradictory. In this subchapter, only those advantages and disadvantages that could apply for EC of bentonite suspensions with aluminium or iron electrodes are discussed.

From a technical perspective, conventional chemical coagulation consists of direct dosing of coagulants into the wastewater, which reduce the electrical repulsion forces that prevent the coagulation of particles. Hydrolysing metal salts of Fe^{3+} or Al^{3+} like ferric chloride ($FeCl_3$) and aluminium sulphate ($Al_2(SO_4)_3$) are commonly used as coagulant agents. Metal salts dissociate in solution and leave salt anions like Cl^- as by-products, which acidify the solution. Moreover, chemical conditioning requires flocculants.

By contrast, EC consists of the in situ generation of coagulants by electrodissolution of the anode material (Canizares et al., 2007, Marriaga-Cabralesa & Machuca-Martinez, 2014). Metal cations produced this way do not bring any salt anions with them and the pH of the solution usually stabilises in the alkaline range. (Holt et al. 2002). EC creates oxygen and hydrogen gases as by-products of electrolysis (subchapter 3.1). However, these by-products can be considered useful. Hydrogen is a source of clean energy and thus it could be reused to create energy, reducing the total energy expenditure of the process.

From an economics perspective, Kobya et al. (2007) compared chemical coagulation and EC in terms of pollutant removal and operating costs for the treatment of textile wastewater. Various direct and indirect cost items including electricity, sacrificial electrodes, labour, sludge handling, maintenance and depreciation costs have been considered in the calculation of the total cost. As a result, the EC had lower operational costs than the chemical

coagulation with similar removal efficiency. However, the exact equation of cost calculation has not being published.

From an ecological perspective, chemical coagulation has several disadvantages in comparison to EC. The conventional dewatering of used bentonite suspensions in chamber filter presses and centrifuges requires the use of inorganic additives to regulate the pH value of the suspension as well as coagulants and flocculants to support the separation process. Some of these chemicals might be harmful to the environment (Luckert, 2004). The risk of overdosing is always present, as the dosing of chemicals is difficult to estimate and control. A further disadvantage is the quality of the separated water obtained in the process – it usually does not fulfil the requirements to be disposed of in the sewage water system without further treatment.

EC, on the other hand, significantly reduces the risk of overdosing. The coagulant is produced constantly during the process. Its quantity is controlled by the current and treatment time and is therefore easily adjustable. In addition, Mollah et al. (2001) reported that the sludge produced by EC tends to be easily dewatered.

Some of other commonly reported advantages are:

- Aluminium ions created by electrodissolution of the anode are more effective than aluminium ions introduced by chemical coagulation in the form of aluminium sulphate in the solution. (Ghernaout et al., 2011) Since coagulants are directly electrogenerated, competing anions like chloride or sulfate ions are not introduced in the solution. This fact allows maximum adsorptive removal and improves the pollutant removal (Garcia-Segura et al., 2017). Therefore, a smaller amount of chemicals is required to reach a required removal efficiency. (Marriaga-Cabralesa & Machuca-Martinez, 2014; Garcia-Segura et al., 2017). Moreover, lower metal residuals are obtained (Marriaga-Cabralesa & Machuca-Martinez, 2014);
- EC prevents the formation of chlorides, producing an effluent with a higher quality than chemical coagulation (Mamelkina et al., 2017). Moreover, the amount of residual total dissolved solids (TDS) is lower as compared with chemical treatments. If this water is reused, this contributes to a lower water treatment cost. (Marriaga-Cabralesa & Machuca-Martinez, 2014, Bharath et al., 2018).
- pH control is not necessary, except for extreme values (Marriaga-Cabralesa & Machuca-Martinez, 2014; Garcia-Segura et al., 2017).
- The operating costs are much lower than conventional technologies (Marriaga-Cabralesa & Machuca-Martinez, 2014; Garcia-Segura et al., 2017);
- There are no additional chemicals required in EC process. (Bharath et al., 2018:)
- More environmentally friendly than other methods (Song et al., 2017)

However, there are also several reported disadvantages:

- The possible anode passivation or/and sludge deposition on the electrodes can inhibit the electrolytic process in continuous operation mode (Garcia-Segura et al., 2017). Those processes together with deposition of hydroxides of calcium, magnesium, etc., onto the cathode lead to increased resistance of the electrodes surface and thus to overvoltages, which increase power consumption. However, overvoltages can be reduced by using alternate current (AC) or alternating pulses of direct current (DC), varying the period of polarization (Eyvaz et al., 2009, Garcia-Segura et al., 2017).
- High concentrations of iron and aluminium ions can be present in the effluent, which prohibit its direct release to the environment. (Marriaga-Cabralesa & Machuca-Martinez, 2014) Thus, a post-treatment is required to reduce the concentration of ions after EC treatment in order to meet the environmental regulations (Garcia-Segura et al., 2017)
- The sacrificial anodes are consumed during the EC process and must be replaced periodically. (Garcia-Segura et al., 2017; Bharath et al., 2018)
- High conductivity of the suspension is required for EC treatment. (Marriaga-Cabralesa & Machuca-Martinez, 2014; Bharath et al., 2018) The voltage drop over a suspension caused by its resistance can be minimized if the conductivity of the suspension is increased by using a support electrolyte like NaCl.

3.5 Safety precautions

Two aspects define work safety during EC treatment (Paya, 2016: 58):

- Assessment of the danger from an explosive atmosphere caused by hydrogen
- Electrical safety measures

3.5.1 Hydrogen

Depending on the amount of hydrogen created by the electrocoagulation treatment and the installed ventilation system in the surrounding area, an explosive atmosphere can be generated. Three basic requirements must be met for an explosion to occur: sufficient explosive substance, sufficient oxidizer and ignition source.

Every explosive gas has a lower and upper explosive limit (LEL and UEL), with an explosive range between LEL and UEL. Limits are expressed as volume percentage of gas in air at 25°C and atmospheric pressure. At a concentration lower than the LEL, there is not sufficient explosive substance to cause an explosion. At a concentration higher than the UEL, there is not enough oxidizer (oxygen) to support an explosion. At a concentration between the

LEL and UEL, the atmosphere is considered explosive and the only remaining requirement is an ignition source. Hydrogen has an LEL of 4% and a UEL of 78%. (AGBF, 2008).

European norms EN 1127-1:2011 and prEN 1127-1:2017 specify methods for the identification and assessment of hazardous situations leading to an explosion and general design and construction methods to help achieve explosion safety. Required safety is achieved by risk assessment and risk reduction methods.

The risk assessment shall be carried out for each individual situation in accordance with EN ISO 12100 and EN 15198, with the following steps (prEN 1127-1:2017):

a) Identification of explosion hazards and determination of the likelihood of occurrence of a hazardous explosive atmosphere;

b) Identification of ignition hazards and determination of the likelihood of occurrence of potential ignition sources;

c) Estimation of the possible effects of an explosion in case of ignition;

d) Evaluation of the risk and whether the intended level of protection has been achieved

If the intended level of protection is not achieved, risk must be reduced. Two fundamental principles of risk reduction are prevention and protection. Prevention can be achieved either through avoidance or reduction of explosive atmospheres and/or through avoidance of any possible ignition source. Protection, on the other hand, means accepting that explosion will occur and limiting the range and damage to a sufficient level by protection methods (prEN 1127-1:2017).

One possibility for prevention by avoidance or reduction of explosive atmospheres is adding an inert gas such as nitrogen to dilute the atmosphere. The principle is simple: by raising the concentration of nitrogen, the concentration of oxygen in the atmosphere will fall under the level required to support an explosion. (Figure 22).
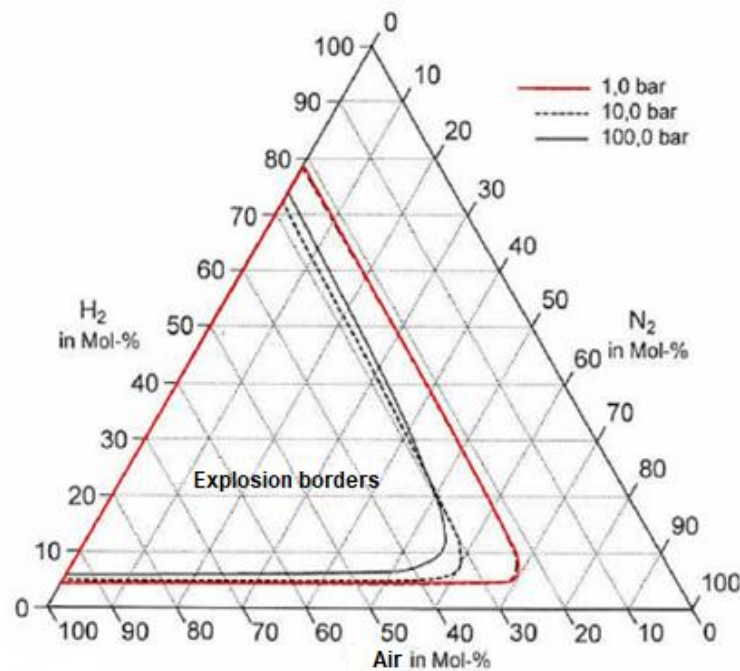
Figure 22:   Explosive range of hydrogen/nitrogen/air mixtures (Schröder, 2002)

However, this method can be very expensive in larger scale EC cells. Sufficient amounts of nitrogen should be always available. Another technical possibility for prevention by avoidance or reduction of explosive atmospheres is installing a sufficient ventilation system, which would assure that the amount of hydrogen never reaches the LEL.

Prevention through avoidance of any possible ignition source could be a complicated task for the EC process. Among all possible ignition sources described in prEN 1127-1:2017, the ones that are possible / conceivable during EC experiments are:

- hot surfaces;
- mechanically generated impact,
- friction and grinding;
- stray electric currents and static electricity.

The norm specifically addresses the use of aluminium as an electrode material: "*If parts of a system able to carry stray currents are disconnected, connected or bridged - even in the case of slight potential differences - an explosive atmosphere can be ignited as a result of electric sparks and/or arcs. Moreover, ignition can also occur due to the heating up of these current paths. When impressed current cathodic corrosion protection is used, the above-mentioned ignition risks are also possible. However, if sacrificial anodes are used, ignition risks due to electric sparks are unlikely, unless the anodes are aluminium or magnesium.*" This had s significant influence on the design of the EC prototype (chapter 6).

Due to Eq. 3-9 and 3-10, it is essential to consider the quantity of gases not only by means of a theoretical calculation using Faraday's law (Eq. 3-4), but also by performing an experimental measurement.

3.5.2 Electricity

The second safety aspect relates to electrical work. Due to the effects of electric current on the human nervous and muscle system, all equipment must provide measures to protect against direct contact with live parts and also against indirect contact (BGI 519, 2009). Due to the fact that EC is usually performed with DC, only safety aspects of working with DC are presented here. Figure 23 shows the effects of DC on the human body, which are dependent on the flow duration t and the current through the body I_B, whereby current path is from the left hand to the feet. From DC-2 onwards, slight involuntary muscle contractions can occur, but will not cause harmful physiological effects. Strong involuntary muscle contractions can occur with increasing current and flow duration (DC-3). In the DC-4 range, the probability of pathophysiological effects on the heart increases. DIN VDE 0100-200 also defines low voltage as the maximum voltage where protection against electric shock is ensured. This is achieved through the use of a permanently permissible contact (Kiefer & Schmolke, 2011). For DC, the low voltage is 120 V (Paya, 2016: 59-60).

Protective measures must be taken during EC. The basic rule of electrical safety is that live parts must not be touchable. This means that the cell and especially the electrodes must be avoided at all times during EC. In addition, insulating gloves and shoes must always be worn as effective protection against dangerous live currents (Paya, 2016: 60).
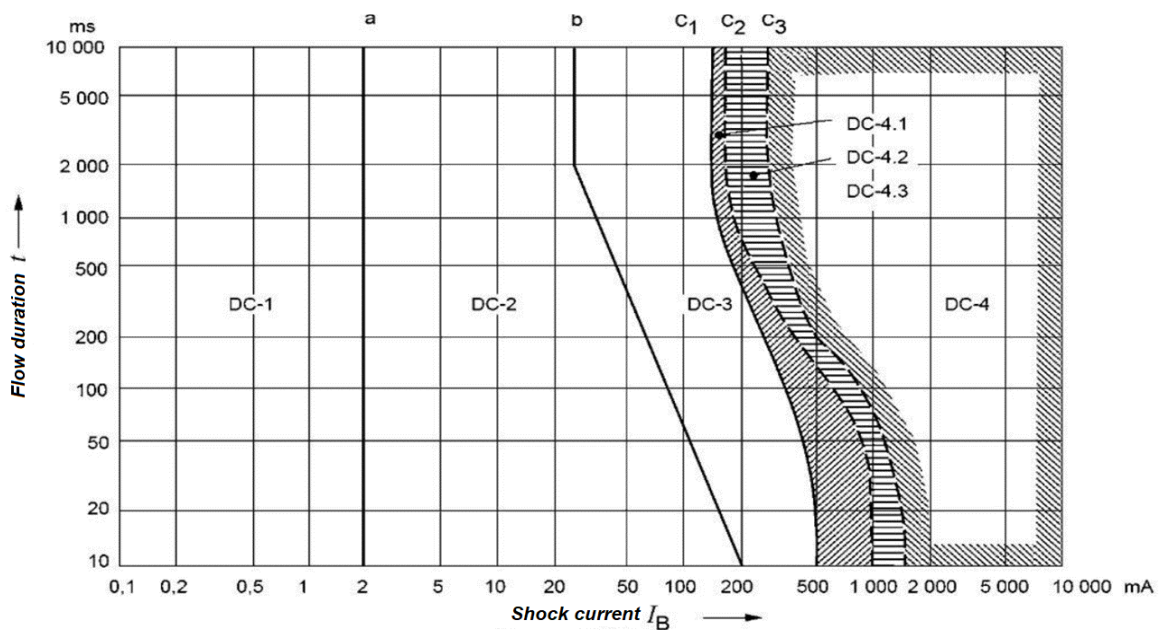
Figure 23:   Effects of direct electrical current on the human body (BGI 519, 2009)

4 Implementation of electrocoagulation as a separation method for bentonite suspensions

As mentioned previously, EC is not a new idea. The first wastewater treatment plants based on EC technology were built more than one hundred years ago, but were shut down due to high energy consumption. However, in recent decades, electrocoagulation has been widely researched again. Several prototypes and pilot plants have arisen from this new research.

Bentonite in small concentration is often used in EC research to simulate suspended matter in wastewater. Concentrations of up to 0.1% were used in some studies like Donini et al., 1994; Holt, 2002; Bebeselea et al., 2006 and Ghernaout et al., 2008 (Paya, 2016). However, from an engineering point of view, these concentrations do not represent a bentonite suspension.

Only a few research studies have focused on dewatering of slurries or similar highly loaded suspensions. Paya (2016) has performed EC experiments with bentonite suspension with 2.5% - 4% concentration of bentonite as well as some tests with loaded suspensions. Also, a similar dewatering method using electrical fields was tested at RWTH Aachen. These studies are discussed in chapters 4.3 and 4.2, respectively.

4.1 Introduction to EC of bentonite suspensions

Fundamentals of EC, described in chapter 3, fully apply to the EC of bentonite suspensions. In particular, there are two main reactions happening during EC of bentonite suspensions:

- electrolysis of water
- electrodissolution of the anode.

Water molecules undergo reduction on the cathode and oxidation on the anode, resulting in a redox reaction. As a result of those reactions, hydrogen is produced at the cathode (Eq. 4-1) and oxygen at the anode (Eq. 4-2):

$$4H_2O_{(l)} + 4e^- \rightarrow 2H_{2(g)} + 4OH^-_{(aq)} \qquad \text{(Eq. 4-1)}$$

$$4OH^-_{(aq)} \rightarrow 2H_2O_{(l)} + 4e^- + O_2 \qquad \text{(Eq. 4-2)}$$

Electrodissolution of the anode, caused by oxidation of the electrode material, creates coagulants in form of metal ions, as already expressed in Eq. 3-3:

$$M_{(s)} \rightarrow M^{n+}_{(aq)} + ne^- \qquad \text{(Eq. 3-3)}$$

where n represents valence of a metal M. As already mentioned in chapter 3.3.1, this metal is usually aluminium or iron. Al and Fe ions in the solution hydrolyse to iron or aluminium

hydroxide, which are excellent coagulants (Mollah et al., 2004). Van Olphen (1963) proposed aluminium ions as coagulants for clay suspensions. He justified this proposal due to affinity of aluminium ions to adsorb on the surface of the clay particles and compress their double layer.

The coagulation process by means of EC is outlined in Figure 24. Initially, bentonite and other fine soil particles in the suspension repel each other, since all of them are negatively charged on the surface. When the current is switched on, these particles are attracted to the positively charged electrode (anode). In the immediate vicinity of the anode, the particles come into contact with metal cations, which destabilise the suspension and cause coagulation. The rate of metal ion production during EC, and therefore the amount of coagulants in the solution, can be controlled according to Faraday's law (Eq-3-5) by adjusting amperage (Popovic et al., 2017). However, chemical dissolution of the aluminium cathode also contributes to the total amount of coagulants in the solution.
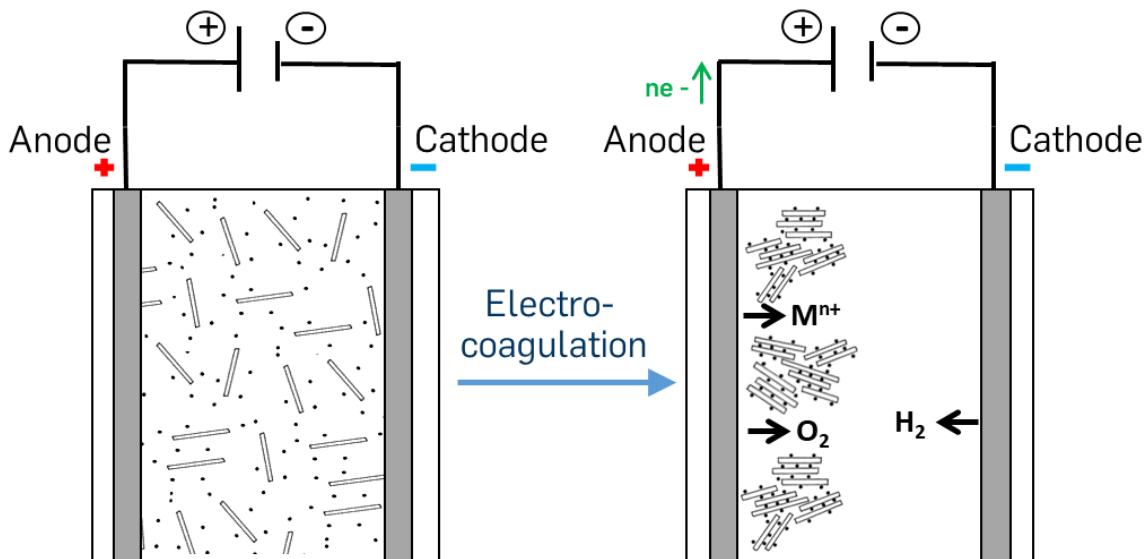
Figure 24:   EC process (Popovic & Schößer, 2019)

Build-up of the particles on the anode's surface leads to an increase of the electrical resistance between the electrodes. This leads to a higher voltage needed to maintain a certain current density and thus to higher energy consumption. However, the electrodes' surfaces can be cleaned during the process. There are two cleaning mechanisms presented in the literature: mechanical and electrical (Holt, 2002).

Mechanical cleaning refers to the continuous or discontinuous cleaning of the coagulated layer from the anode by means of non-conductive scrapers (Heffernan & Rea, 2013). Electrical cleaning of the anode is realized by a reversal of electrodes' polarity (Jiang et al., 2002; Holt, 2002). The time interval between two mechanical cleaning or polarity reversal actions is an additional operating parameter when conduction EC experiments (Paya, 2016).

4.2 Research and implementation of EC or similar methods as a separation method for bentonite suspensions worldwide

There are not many reports about the separation of bentonite suspensions using only EC or using multiphase processes including EC. Those that are known to the author of this dissertation are presented in the following passages.

The company Halliburton from the USA treats wastewater with their CleanWave® technology, which incorporates EC (Halliburton, 2010). They claim that the technology also works on drilling muds. Even though not explicitly stated, those fluids could include bentonite-based slurries. However, no further details or publications were found. Another company, Global Advantech from the UK, combines EC with other technologies as a remediation method for water-based drilling fluids and cleaning of cuttings (Global Advantech, 2012). Similarly, this could include bentonite suspensions, even though they were not specifically mentioned in the found sources.

Research about the dewatering of bentonite suspensions using electrical fields has also been conducted in Germany. Dewatering of bentonite using electroosmosis was researched at RWTH Aachen (Ulke, n.d.). In an electrical field, bentonite particles are attracted to the anode and water particles to the cathode, and this phenomenon was used to speed up the sedimentation process of bentonite suspensions. The vertical and horizontal placement of electrodes was tested as well. Horizontally, an anode were placed 2 cm above the bottom of the experimental tank and a cathode 30 cm above the anode. The experiment duration was usually 24 hours. It was reported sedimentation process was significantly accelerated. The water separated using this method was tested and it met the requirements to be discharged into the sewage system without further treatment. However, it was reported that this separation process does not bring "big economic advantages" at the current market prices for electricity and disposal. Moreover, nothing was mentioned about the residual moisture of the separated bentonite, which has a significant influence on the disposal methods and costs.

4.3 Electrocoagulation of bentonite suspensions at the Institute for Tunnelling and Construction Management - overview of previous research

The research presented in this dissertation is conducted in the scope of the second phase of a research project about electrocoagulation of bentonite suspensions, performed at the Institute for Tunnelling and Construction Management at the Ruhr-University Bochum. Within the scope of the first phase of this research project, Paya (2016) performed extensive laboratory parametric studies. The findings from the first phase were used as a basis for

further research in the second phase. For better understanding of the proceedings in the second phase, the research of Paya (2016) is briefly described on the following pages.

4.3.1 Experimental setup and procedure

The first step in the experimental process was to design and construct EC cells and electrodes (Figure 25). The cells were made of acrylic glass. Cells A and B have slots to place the electrodes parallel to each other at exact distances (Figure 26). When using one pair of electrodes, they could be placed between 0.5 and 6.5 cm apart, with available increments of 1cm. In the EC cell C, the distance between the electrodes was fixed to 6.5 cm.

EC cell A   EC cell B   EC cell C
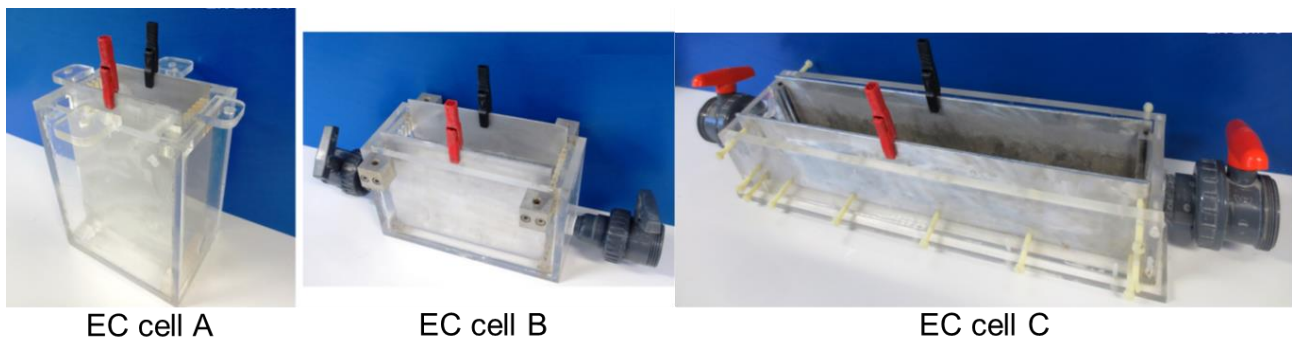
Figure 25:   EC cells used in the research of Paya (Paya, 2016: 63)

Aluminium and iron have been chosen as the materials for the electrodes. Electrodes were designed flat and rectangle-shaped with a thickness ca. 0.4 mm. A direct current source supplied the system with up to 5 A and 65 V. The complete experimental setup with EC cell B (Figure 26) is shown in Figure 27. Parts of the experimental setup from the first phase of the project were used also for the laboratory experiments in the second phase, which are described in chapter 5.

Experiments were performed with DC. After the experiment, coagulated material was separated from the remaining suspension. The term "remaining suspension" defines the suspension that remains after EC, thus without the particles that coagulated on the anode. The dry weight of the coagulated material as well as the density and filtrate water release of the remaining suspension were measured and the corresponding effectivity parameters B_{kt}, $\Delta\rho$ and ΔFW (chapter 4.3.2) were calculated (Popovic et al., 2017).
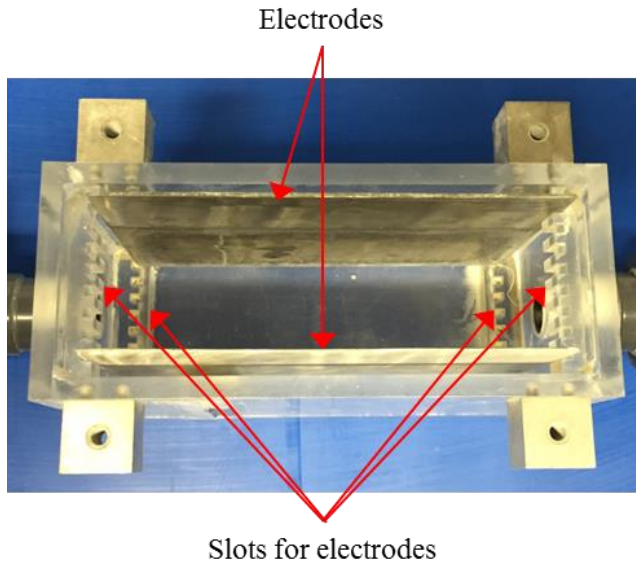
Figure 26:   Electrocoagulation cell B (Popovic et al., 2017)
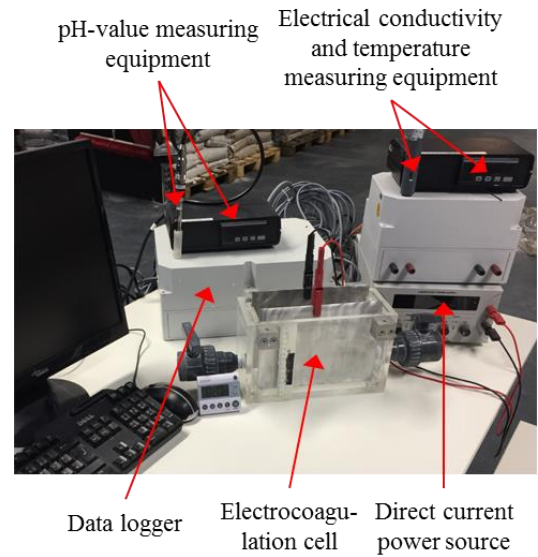
Figure 27:   Experimental setup (Popovic et al., 2017)

4.3.2 Effectivity parameters for the laboratory scale experiments

EC of bentonite suspensions has three main effects: (Popovic et al., 2017):

1. Bentonite particles from the suspension coagulate on the anode surface;

2. The density of remaining suspension is decreased,

3. Remaining suspension is destabilized

Figure 28:   left: coagulated bentonite particles on the anode; right: destabilised remaining suspension (Popovic & Schößer, 2019)

In order to measure those effects and evaluate the performance of each EC experiment, three parameters were defined, which reflect the three above mentioned effects. They were named "effectivity parameters", and were defined by Paya (2016) and Popovic et al. (2017) as the following:

a) Percentage of coagulated soil particles B_{kt} (Eq 4-4) is defined as the dry weight of coagulated soil particles B [g] in relation to the total dry weight of the soil particles in suspension B_0 [g]:

$$B_{kt} \ [\%] = \frac{B}{B_0} \cdot 100 \qquad \text{(Eq 4-4)}$$

b) The decrease of the remaining suspension density $\Delta\rho$ describes the convergence of the remaining suspension density to water density, expressed by the Eq 4-5:

$$\Delta\rho \ [\%] = \frac{\rho_r - \rho_0}{\rho_w - \rho_0} \cdot 100 \qquad \text{(Eq 4-5)}$$

where ρ_r [g/cm3] is the remaining suspension density, ρ_0 [g/cm3] is density of the suspension before the electrocoagulation treatment and ρ_w [g/cm3] is the density of water (1 g/cm^3).

c) The decrease of the remaining suspension stability is defined through parameter ΔFW. It is measured as percentage increase of the filtrate water release after EC. The filtrate water release was obtained using the API filter press and was measured according to DIN 4127:2014-02. The filtration time was 7.5 minutes. This parameter is the only effectivity parameter that can reach values of over 100%. It is expressed in Eq 4-6:

$$\Delta FW \ [\%] = \frac{FW_r - FW_0}{FW_0} \cdot 100 \qquad \text{(Eq 4-6)}$$

where FW_r [ml] is the filter water release of the remaining suspension and FW_0 [ml] is the filter water release of the suspension before the EC treatment (without CA).

4.3.3 Parametric study and results/conclusions

Table 8 provides a complete overview on the parametric study performed by Paya (2016). Except in the experimental series concerning bentonite suspension properties concentration of 2.5% of bentonite type W was used.

Table 8: Overview of the parametric study by Paya (2016)

Influence of cell parameters	Influence of the operational parameters	Influence of bentonite suspension properties	Effect of the EC on the stability of the bentonite suspension
Cell geometry and electrodes surface	Flow condition (Idle state, turbulent and laminar continuous flow)	Concentration of bentonite W	Settling experiments
Electrode material and gap	Dwell time	Charge	
Amount of electrodes and their connection modes	Mechanical and electrical cleaning of the electrodes		
Amperage			

Selected important findings are summarized in the following passages.

Cell geometry and electrodes surface:

Investigations of EC cells A and B (EC cell C was mainly used for flow state experiments) with their corresponding electrode surfaces showed no clear tendencies with regard to the effectivity parameter. However, cell B had a larger electrode surface and thus required a lower voltage than EK cell A to produce the same amperage.

Electrode material

The choice of the electrode material did not have any noticeable influence on the parameters B_{kt} and $\Delta\rho$. However, ΔFW was significantly improved when using aluminium electrodes, which means that aluminium ions destabilised the suspension more effectively than iron ions.

Electrode gap

A larger gap between the electrodes showed in general better results.

Amount of electrodes and their connection modes

The use of four monopolar electrodes resulted in an increase of effectivity parameters compared to the use of two standard electrodes. The MP-P connection mode is preferred as it generally resulted in a higher effectiveness and consumed less energy than the MP-S connection mode.

Amperage

Electrical currents of 1 A and 2 A were tested. Increase of the amperage improved the results concerning all three effectivity parameters (B_{kt}, $\Delta\rho$ and ΔFW).

It is interesting to mention that an increase in amperage improved the results, but the change in size of the electrode surface (and thus the change in current density) did not have a significant effect of the effectivity parameters.

Flow state of the solution

The fluid flow in the EC cell was achieved through the use of stirrers or pumps. The use of pumps also enables a closed circuit flow. The researched flow states are presented in Figure 29.
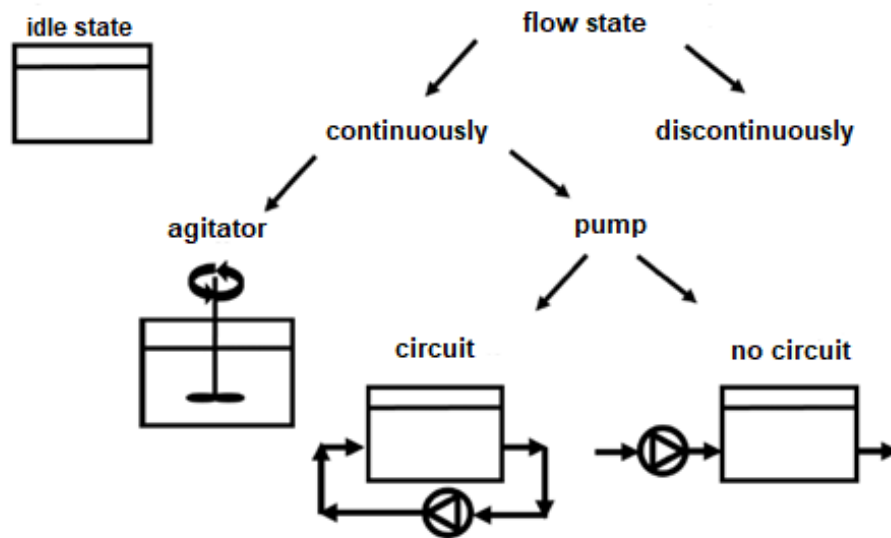
Figure 29:   Flow modes of the solution in the EC cell (Paya, 2016: 56)

One stirrer was placed between the electrodes to mix the suspension during the experiment. In comparison to the idle state, agitation of the suspension during the EC has slightly improved the results for one experimental setup: an electrode gap of 1.5 cm. Otherwise, the results were similar for the agitated and idle states.

For the parametric study concerning flow state using pumps, both laminar and turbulent flows of the suspension were investigated. The laminar flow state resulted in better EC performance than the turbulent flow. Since this requires the use of a larger volume of suspension in order to fill both the pump and the pipes, the results cannot be directly compared with the rest state, at which only 2 litres of the suspension are treated.

Electrode cleaning mechanisms

The integration of mechanical cleaning of the anode during the experiment led to a higher performance of electrocoagulation compared to EC treatment without the cleaning. The cleaning interval of 5 minutes was more effective than 10 minutes. The electrical cleaning method (polarity reversal of the electrodes) was also investigated, but it led to higher energy consumption without any improvement of the results. For this reason, electrical cleaning was not further researched in the second phase.

Duration of the experiment

Experiment durations of 5, 10, 15, 20, 30, 60 and 90 minutes were investigated. It was found that the optimal experiment duration was not the same for all three effectivity parameters. For the parameters B_{kt} and $\Delta\rho$ it was 30 minutes, after which they did not further improve. Interestingly, ΔFW continued to improve with increasing time, all the way to the longest tested duration of 90 minutes.

4.3.4 **Best combination of parameters**

The best reached results were: $B_{kt} = 51\%$; $\Delta\rho = 88,6\%$ $\Delta FW = 188\%$. Paya (2016) concluded that the preferred parameters for EC treatment of bentonite suspensions, which lead to the best results in with regard to the three effectivity parameters, are the following:

- For one electrode pair: Al electrodes, a current strength of 2 A (for 2 litres of suspension) and an electrode spacing of 6.5 cm, with the electrode cleaning interval of 5 minutes

- For two electrode pairs: MP-P connection, Al electrodes, a current strength of 2 A and an electrode spacing of 2.5 cm.

Paya (2016) further assumed, that the combination of both previous point (two pair of monopolar electrodes with an electrode spacing of 6.5 cm) could possibly increase the effectiveness even further.

5 Laboratory experiments with standard used suspension

5.1 Defining a standard used suspension

In the first phase of this research project, parametric studies were mostly performed with a "pure" bentonite suspension. This means bentonite was the only particle in the water. This suspension had a density of up to 1.02 t/m³, which corresponds well to the density of a fresh (newly mixed) suspension on a construction site. However, the suspension that arrives to the fine separation devices (chamber filter presses and centrifuges) on construction sites usually has a density of >1.20 t/m³. As previously mentioned, this large difference arises through the fact that the bentonite suspension gets loaded with soil particles during excavation, some of which cannot be separated in the separation plant. Since the EC would be implemented in the fine separation area, it was necessary to investigate EC with a bentonite suspension loaded with fine particles.

In order to perform extensive EC experimental series with loaded used suspensions, a representative suspension for used suspensions from construction sites was designed. The challenge by this task was that used suspensions from construction sites can have significantly different properties. First of all, the composition of used suspension depends on the composition of the excavated soil. Hence, it can vary not only from one construction site to another, but also within the same tunnel project, if the tunnelling machine is driven through different soil layers during an excavation. The only common property of all used suspensions is a significantly higher density that those of fresh bentonite suspension.

Based on expert opinions, it was decided that the suspensions density should be approx. 1.25 t/m³. The particle size distribution curve was designed to resemble the probe of a used suspension from the construction site in town of Karlsruhe, where a metro line was being built at the time.

To simulate the particle size distribution curve from the Karlsruhe suspension and the chosen density of 1.25 t/m³, a suspension with B1 bentonite loaded with fine particles was created. Fine particles are represented with a type of kaolin clay called kaolin W and silica flour types M500 and M300 (Figure 30). Datasheets of aforementioned products can be found in Appendix A. This "laboratory" created used suspension was named the standard used suspension (SUS). Its composition is shown in Table 9. The particle size distribution curve of the suspension from Karlsruhe as well as SUS and its components are shown in Figure 31.
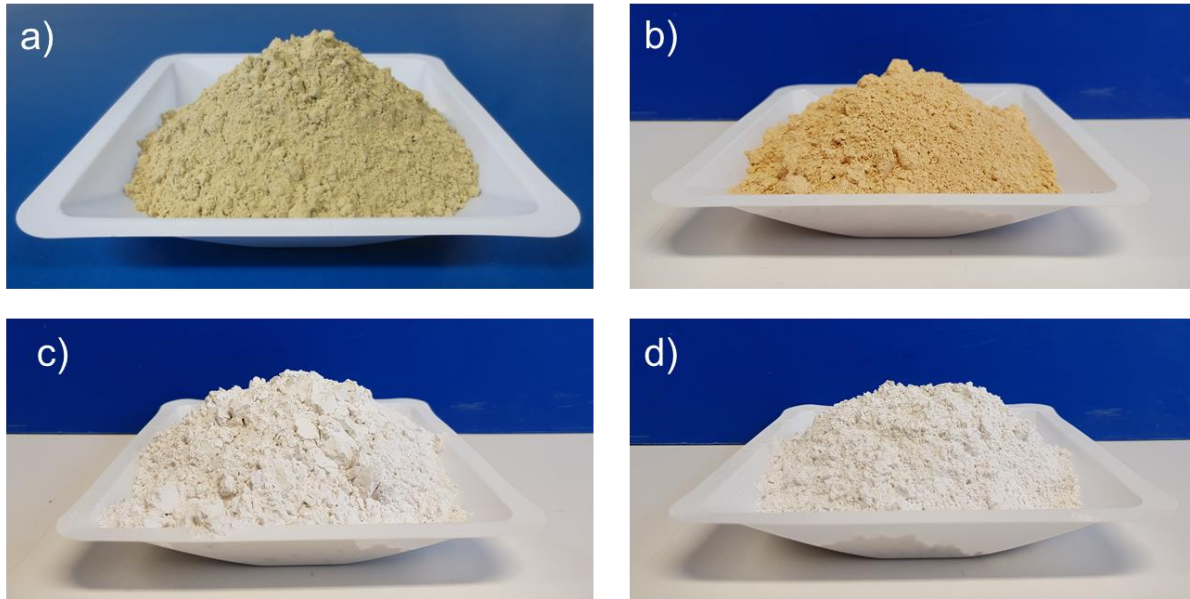
Figure 30:   a) Bentonite B1, b) Kaolin W, c) Silica flour M 300, d) Silica flour M 500

Table 9: Composition of 1 l of the standard used suspension (SUS)

Material	Bentonite B1	Kaolin W	Silica flour M 500	Silica flour M 300	Water	∑ (SUS)
Weight (g/l)	40.0	60.0	200.0	120.0	838.7	1258.7
Volume (cm³/l)	17.4	23.1	75.5	45.3	838.7	1000.0
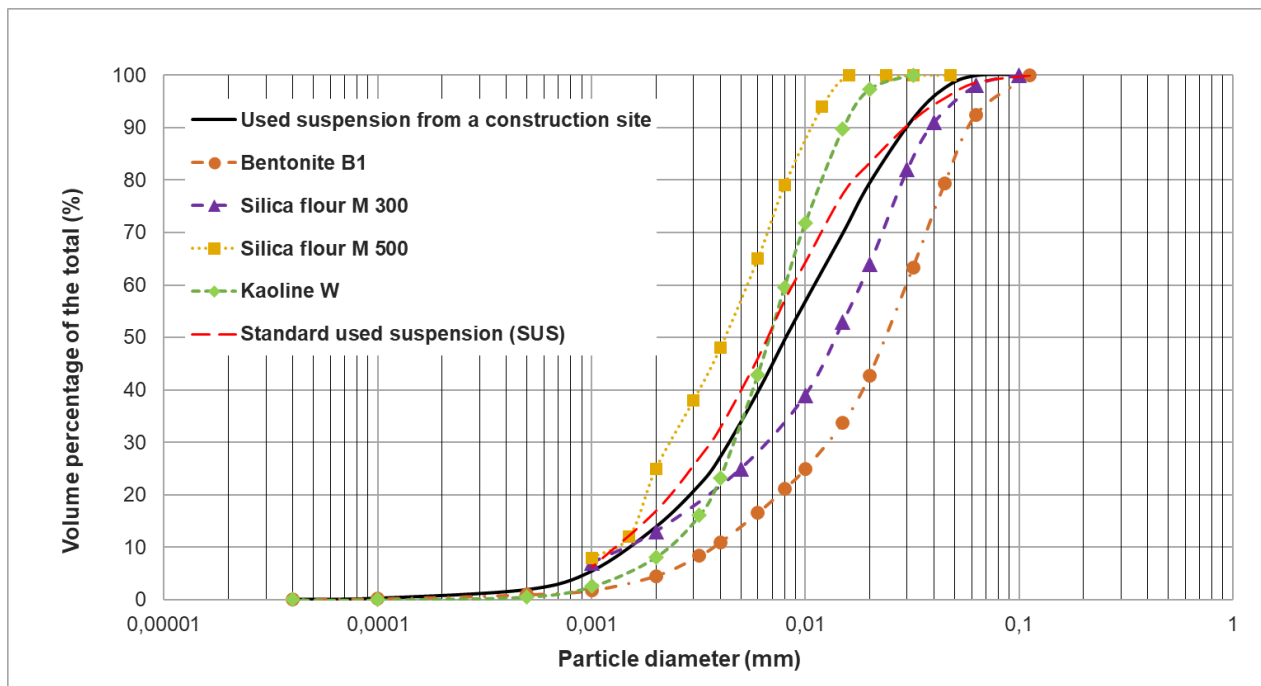
Figure 31:   Particle-size distribution curve of the standard used suspension, its components and the used suspension form a construction site in Karlsruhe (Popovic, 2019)

The way suspension is mixed can also influence its parameters. Therefore, it was always mixed the same way. First, bentonite was mixed with water after DIN 4127 (2014) and it was left to swell for at least 16 hours. Afterwards, the suspension was gradually loaded with kaolin and silica flour, while simultaneously mixing the suspension. This resulted in a well-swelled loaded bentonite suspension with properties as listed in Table 10.

Table 10:   **Properties of the SUS**

Marsh time (s)	Filtrate water release (mg)	Filter cake thickness (mm)	Density (g/cm³)	Conductivity (µS/cm)	pH-value
$t_{m1000} = 35$ $t_{m1500} = 63$	18.4	2.2	1.255	1270	9

5.2 Experimental setup and procedure

The experimental setup and procedure for the laboratory experiments were largely inherited from the previous project phase. One addition to the existing equipment were the new electrodes made of copper, stainless steel, and brass, that were employed in experiments besides already existing aluminium and steel electrodes.

5.2.1 Experimental setup

Experimental setup included EC cells A and B together with corresponding measuring and data logging devices.

EC cell A (Figure 32)

The internal dimensions of cell A are 18 x 13 x 25 cm³ with a volume of 4.6 l. Electrodes' dimensions are 16 cm x 25.2 cm, which makes a surface of 408 cm². Here, the term active electrode surface needs to be introduced. It is the electrode area that is involved in the EC reactions, i.e. the surface of the electrode that is immersed in the suspension. When cell A is filled with 2 litres of suspension, the active electrode surface is 124 cm² (Figure 32)
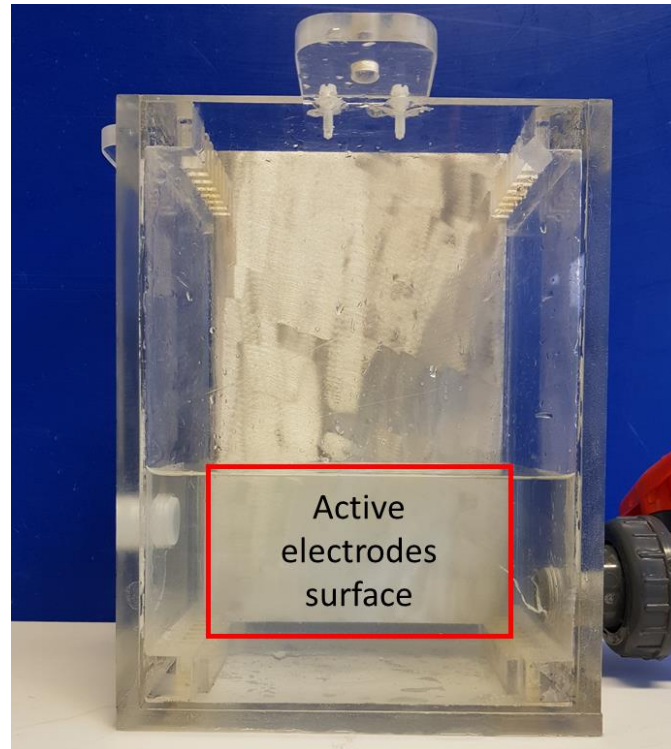
Figure 32: Active electrode surface of the cell A, with 2 l of water

EC cell B (Figure 26**)**

Cell B was the most used cell in parametric studies. Internal dimensions of cell B are 23.5 x 8.5 x 15 cm³ with a total internal volume of 2.8 litres. Electrodes had dimensions of 21 x 15.5 cm, resulting in a total surface of 325.5 cm^2 (Popovic et al., 2017). The active electrode surface of cell B is 212 cm² by the experiments with 2 litres of suspension.

Both cells were designed with slots to place electrodes on distances from 0.5 - 6.5 cm, with a step of 1 cm.

Measuring devices

The DC source and the measuring devices for the pH, electrical conductivity and suspensions temperature were connected to one data logger and computer, on which LabView software was programmed to show and store the measured data.

5.2.2 **Experimental procedure**

Preparation

Upon mixing of SUS and shortly before the experiment, several SUS properties were measured, including density, temperature, pH, electrical conductivity, filter water release, filter case thickness, and residual moisture. Moreover, the electrodes were weighted prior to experiments, in order to determine their loss of weight during EC.

Experiments execution

Electrodes were placed in the cell and the SUS was slowly poured in afterwards. Upon filling the SUS in the cell, electrodes were connected to the DC source and the intended electrical current was selected. Next, the LabView and DC source were turned on.

During EC experiments, only observation and documentation of the process was necessary. An exception was the mechanical cleaning experiments (chapter 5.3.4), in which the anode was being cleaned in certain intervals during the experiment. It was done with following steps:

   i.   Electricity was turned off

   ii.   The coagulated material was scratched away from anodes surface. Three variations of mechanical cleaning were tested

> Variation 1: The anode was removed from the cell and the coagulated material was scratched away from its surface and removed from the cell. The anode was then placed back in the cell and the electricity was turned back on. The total break required to perform one cleaning in this variation was ca. 10 seconds. These experiments were marked as XX_A, whereby *XX* represents the cleaning interval in minutes

> Variation 2: The process from variation 1 was repeated, but the suspension in the cell was additionally screened to remove small flocs from the suspension. The total break was ca. 20 seconds per cleaning. These experiments were marked as XX_B, whereby *XX* represents the cleaning interval in minutes

> Variation 3: In this process, the anode was not removed from the cell but rather lifted up just enough to allow cleaning of its surface when the electricity was turned off. The coagulated material was left in the cell and the suspension was not screened. The reason for this variation was to perform experiments with constant volume in the cell. The total break required for this cleaning variation was approx. 5 seconds. These experiments were marked as XX_C, whereby *XX* represents the cleaning interval in minutes

   iii.   Electricity was turned back on and the experiment continued

Post-experiment procedure and measurements

When the experiment finished, the electricity was turned off. The coagulated material was scratched off the anode and the suspension was screened to remove small flocs. The coagulated material was accumulated in one or more bowls and weighted. Afterwards, it was dried in an oven and weighted again in order to calculate the effectivity parameter B_{kt} (Eq 4-

4) and to calculate the residual moisture of coagulated material. Residual moisture is important for industrial use of EC because it is one of the parameters determining if the coagulated material can be directly disposed of or if the moisture must first be decreased.

Remaining suspension was tested on the same parameters as before the experiment (density, temperature, pH, electrical conductivity, filter water release, filter case thickness, and residual moisture). These measurements were used to calculate effectivity parameters Δρ (Eq 4-5) and ΔFW (Eq 4-6) as well as to determine the influence of EC on temperature, pH and electrical conductivity of the suspension.

5.3 Laboratory experimental series (LES)

Extensive experimental series were designed and performed. The aim of those series was to determine a response of SUS to EC treatment in general and to test several cell and operational parameters of EC.

The following presentation of results is structured in four parts for every experimental series:

- Introduction: The purpose of the particulate set of experiments and EC operational and cell parameters are noted
- Results: The results are presented without further discussion
- Discussion: The results are explained, further analysed, and concluded
- Scale-up recommendation: The findings that are relevant for the design of a bigger scale prototype are summarised. Here, the first ideas about scale-up parameters emerged from the best combination of parameters by Paya (2016) (chapter 4). However, these ideas were reviewed and adjusted based on the results of EC experiments with SUS. Moreover, some challenges like safety issues concerning hydrogen arose during the design of the prototype. Those challenges were solved with the help of laboratory experiments.

Due to different range of results for laboratory experimental series, abscissas in following diagrams do not have identical values. Three different values appear 30, 70 and 160 %.

5.3.1 LES1: Influence of the electrode material and gaps: aluminium and steel electrodes, all gaps

The first experimental series included the investigation of the two most commonly used electrode materials for EC (Al und Fe) and all the possible electrode gaps in the cell B (0.5 – 6.5 cm). The experiment duration was 30 minutes and had a 2 A electrical current. Figure 33 presents the results obtained from this set of experiments. Experiments with electrode gaps of 3.5 – 6.5 cm were performed two times because these gaps were relevant for the

mid-scale prototype (chapter 6). Average values of the effectivity parameters from these experiments are presented.

Results - effect of electrodes gap

Figure 33 shows that the electrode gap of 0.5 cm provided the worst results in regards to all three effectivity parameters. Interestingly, from the gap of 1.5 cm to 6.5 cm, there was no improvement effect of the increasing gap on the results. Actually, *ΔFW* by aluminium electrodes decreased as the distance increased from 2.5 cm to 6.5 cm. Parameters B_{kt} and $\Delta\rho$ were almost constant from gaps 1.5 cm to 6.5 cm.

Results - effect of electrodes material (aluminium and steel)

Concerning the effectivity parameters B_{kt}, a slight effect of electrode material on the parameter was observed. The experiments with aluminium electrodes showed a better performance than those with steel electrodes at all gaps and resulted in 1 – 5 % higher B_{kt}, in absolute values. Interestingly, no effect of electrode material on the parameter $\Delta\rho$ was observed.

What stands out in Figure 33 is the effect of the electrode material on the parameter *ΔFW*. To compare, the *ΔFW* of the steel electrodes (Fe) at gaps of 1.5 cm to 6.5 cm vary from 9 % to 13 % while the *ΔFW* of the aluminium electrodes (Al) vary from 44 % to 61 %.
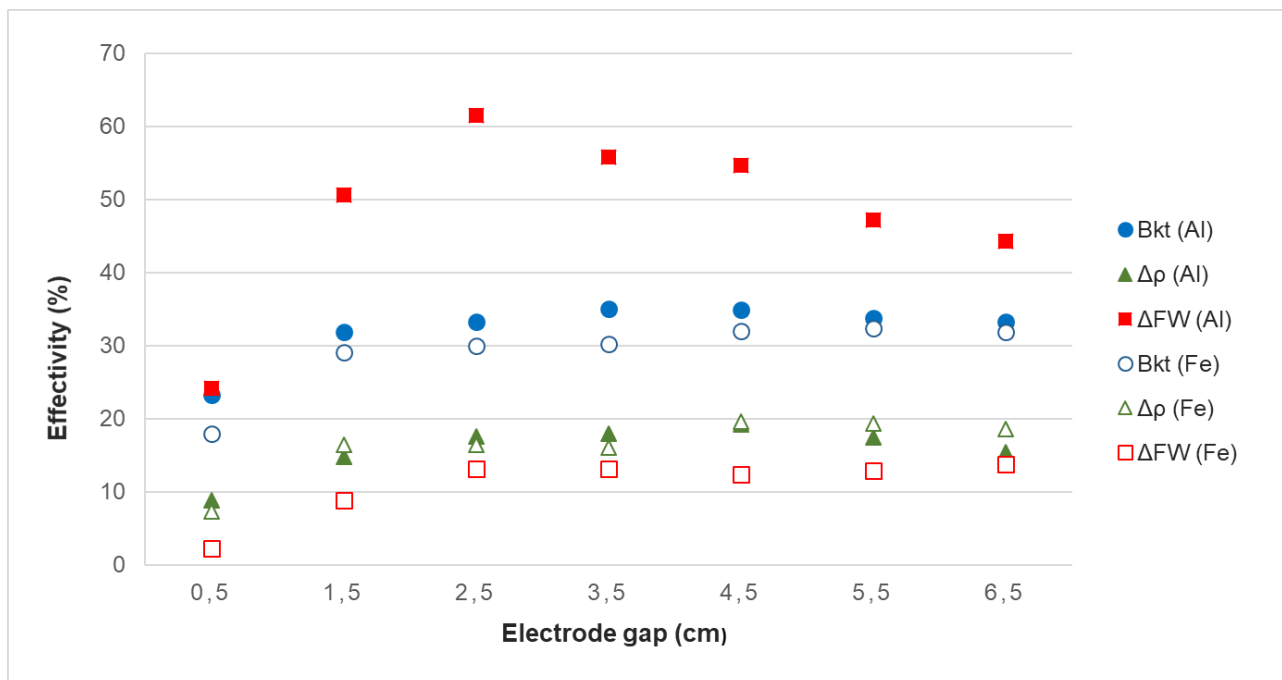
Figure 33:   Comparison of effectivity parameters for aluminium and steel electrodes

Discussion

The first important finding of this set of experiments was that the SUS can be successfully electro-coagulated.

Regarding the electrode gaps, 0.5 cm is not recommended for further experiments (Figure 34). Wider gaps (1.5 cm – 6.5 cm) showed better results regarding all three effectivity parameters. The destabilisation of suspension with aluminium electrodes decreased as the gap increased from 2.5 cm to 6.5 cm. This finding was unexpected, since it contradicts the findings of Paya (2016), who found that a wider electrode gap in general improves the results. However, those results were acquired with a pure bentonite suspension, where SUS has different properties. As mentioned in the literature review, every solution can react differently to an EC treatment, which is why optimal cell and operating parameters are usually empirically determined before building an industrial scale prototype. SUS has much higher density than pure bentonite suspension (1.25 t/m in comparison to 1.02 t/m³) which obviously has significant influence on the EC performance and operational parameters.

The results of this experimental series indicate that the electrode gap for EC of SUS should not be smaller than 1.5 cm but also not increased beyond 6.5 cm. Since a thick layer of the coagulated material on the anode was formed during the experiment, the gaps of 1.5 – 2.5 cm should also be avoided. Otherwise, after a certain EC duration, there could be only coagulated material and no suspension between electrodes.
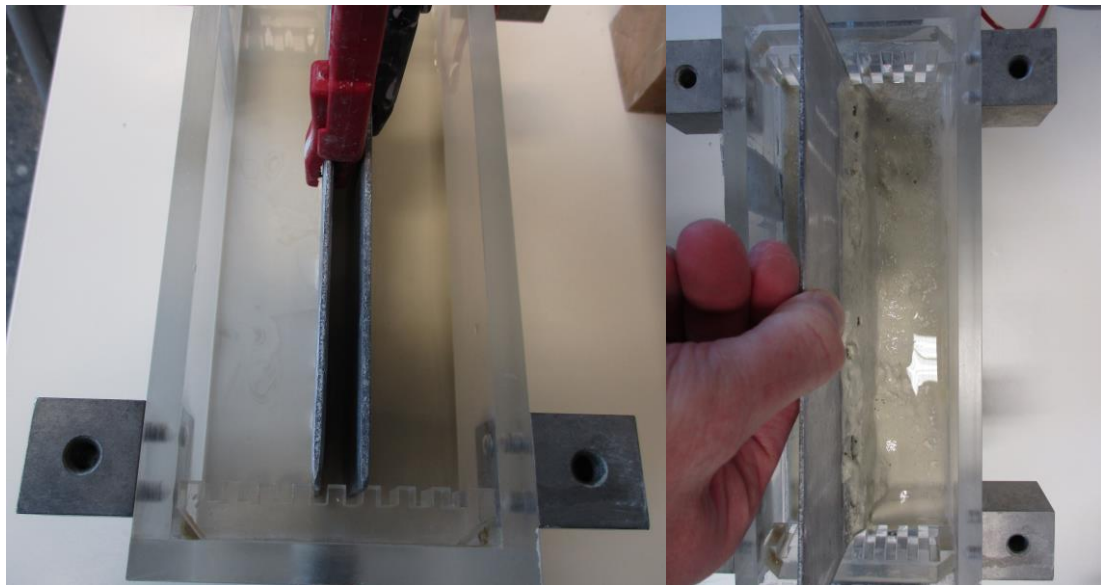
Figure 34:   Experiment with an electrode gap of 0.5 cm.

Concerning the electrode material, aluminium performed much better in terms of destabilisation of the SUS. This could be based on the following two reasons. First, Fe ions can be divalent and trivalent, while Al ions are always trivalent. As mentioned in chapter 2.2.5, ions with higher valence destabilise the suspension much stronger than the lower valence ions. Secondly, aluminium cathodes lost weight (chemical dissolving – Eq 3-9) during EC experiments. This did not occur by experiments with steel cathodes. Therefore, for the same electrical current, the concentration of Al ions in the solution was higher than the concentration

of Fe ions. Higher concentration of metal ions improves the destabilisation of the suspension (chapter 2.2.5).

Scale-up recommendations

The results of this experimental series indicate that aluminium should be used as an electrode material for the mid-scale prototype. Concerning the gap, it should not be smaller than 2.5 cm or larger than 6.5 cm.

5.3.2 LES2: Influence of the cell design and electrical current: cells A and B, 1 A and 2 A

The next set of experiments examined the cell parameters and electrical current as an operational parameter. Experiments were performed in cells A and B with aluminium electrodes, at the currents of 1 A and 2 A. For the current of 2 A and the cell B, the results from the previous experimental series were used. The experiments were performed at electrode gaps of 2.5 – 6.5 cm.

Results

The results are presented in Figure 35.
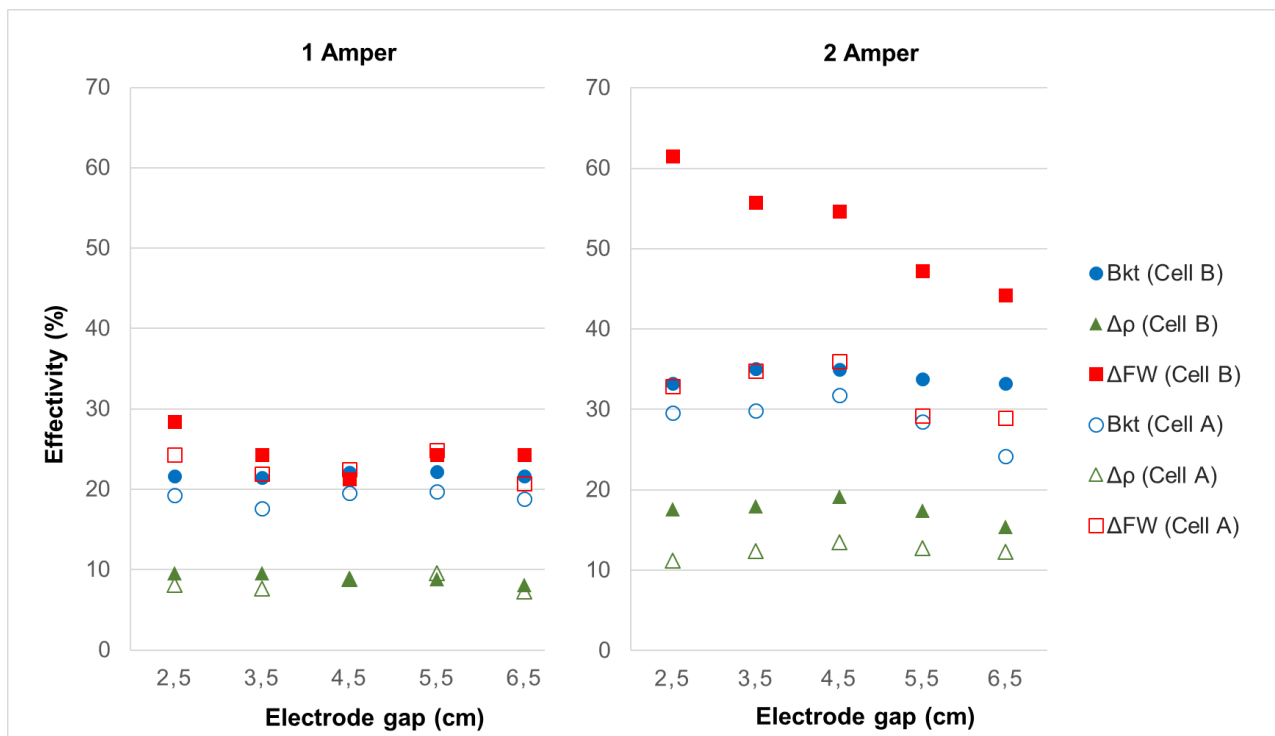
Figure 35:   Comparison of effectivity parameter for the EC cells A and B at 1 A (left) and 2 A (right)

Figure 35 left presents the results of experiments performed at 1 A. On average, in all the tested electrode gaps, all three effectivity parameters reached higher values in cell B than

in cell A. Parameter B_{kt} was 3 % higher than in cell A, parameter $\Delta\rho$ was 1 % higher, and ΔFW 2 % higher, in absolute values.

At an intended current of 2 A (Figure 35 right), the difference in the results from cell A and B was even higher. On average, over all the tested gaps, parameter B_{kt} was 5 % higher in cell B than in cell A, parameter $\Delta\rho$ was also 5 % higher, and ΔFW 20 %, in absolute values. The results were not only better on average, but also at every single gap, for every effectivity parameter. The advantage of the cell B design was clearly visible here. However, such a difference in results between those two cells at the intended electrical current of 2 A could arise from one somewhat unanticipated finding: the experiments in cell A with intended electrical current of 2 A did not obtain this current, because the maximal available voltage of 65 V was reached during the experiments. Therefore, the term "intended" electrical current is used, while the "actual" electrical current is shown in Table 11 and Table 12, along with other electrical parameters.

Table 11: Electrical parameters at different gaps, cell A

Electrode gap (cm)	Average voltage (V)	Average current (A)	Average surface current density (mA/cm²)	Average volumetric current density (A/l)
3.5	63.44	1.83	14.72	0:91
4.5	64.80	1.71	13.82	0.86
5.5	64.95	1.55	12.46	0.77
6.5	64.94	1.37	11.09	0.69

Table 12: Electrical parameters at different gaps, cell B

Electrode gap (cm)	Average voltage (V)	Average current (A)	Average surface current density (mA/cm²)	Average volumetric current density (A/l)
3.5	47.29	1.99	9.40	1.00
4.5	50.95	1.99	9.38	1.00
5.5	50.35	1.98	9.34	0.99
6.5	50.28	1.96	9.25	0.98

Concerning the comparison of the results at electrical currents of 1 A and 2 A in the same cell, it is clear that the more electrical current results in the better EC performance regarding all effectivity parameters. The smaller difference between the parameters in cell A is again caused by the fact that the intended electrical current of 2 A was not obtained.

Discussion

The results show a preference for cell B. At the electrical current of 1 A, the results with cell B were slightly better than those with cell A. This difference grows at a higher intended electrical current, but the largest share of this growth most probably arose due to the fact that the indented current of 2 A does not match the actual current obtained in cell A. However, this finding is also an important result in the search for optimal cell parameters. Since cell A has a smaller active electrode surface than the cell B (124 in comparison to 212 for 2 l of suspension), it needs to obtain higher surface current densities (A/cm²) to reach the intended electrical current. This results in the higher voltage (Eq 3-12: smaller conductor surface leads to higher resistance). However, the voltage in the experimental setup was limited to 65 V due to safety reasons. Whenever maximum voltage was reached, the electrical current automatically dropped. In cell A, a surface current density of 16,1 mA/cm² is required to reach 2 A, in comparison to 9,4 mA/cm² required in cell B. As presented in Table 11, the average surface current densities in cell A were 14.7, 13.8, 12.5, and 11.1 mA/cm² at the gaps of 3.5, 4.5, 5.5, and 6.5 cm, respectively. The greater the gap between the electrodes, the smaller the current densities obtained. This is due to an increase of the conductor resistance through increase of length (Eq 3-12).

Meanwhile, in cell B, the densities of 9.4 mA / cm² required to reach the intended electrical current of 2 A were obtained (Table 12). However, even here, the influence of the gap on the current densities is visible. This occurred due to the fact that a resistance peak arose on the beginning of every experiment. The larger the gap was, the longer was the electrical current under the intended current of 2 A. The same pattern was observable not only by all laboratory experiments, but also by all experiments with the mid-scale prototype (chapter 6). Paya (2016) observed the same in her experiments and explained the resistance peak with a layer of aluminium oxide on the surface of the electrode that needs to be destroyed with overvoltage at the beginning of every experiment.

Scale-up recommendations

Even though the results at the current of 2 A for cells A and B cannot be directly compared, the fact that cell A needs higher voltages to acquire the same amperage means that it requires a higher energy consumption (Eq. 3-13) to reach a similar effectiveness as cell B.

Additionally, even at the same current (1 A), cell A performed worse than cell B. Therefore, the findings of this set of experiments suggest that cell B should be used as scale-up basis for a mid-scale prototype. The electrodes surface at the prototype should be designed in a way that the surface current density stays under 10 A/cm² by a volumetric current density of 1 A/l.

5.3.3 LES3: Influence of the monopolar electrodes connection mode: serial (MP-S) and parallel (MP-P) connection

The next set of experiments was aimed to determine the influence of monopolar electrode connection mode on the EC treatment of SUS. The importance of this experimental series lays in the assumption that a bigger cell needs more electrode pairs. The experiments in this series were conducted with a goal to find the optimal connection mode for the electrodes, when there are more than 2 electrodes in a cell. This is the only laboratory experimental series in which two pairs of electrodes (2 anodes and 2 cathodes) were used.

Moreover, at MP-P mode, the electrical current and electrode gap were varied. Experiments were performed in cell B for a duration of 30 minutes. Since the dimensions of the cell are fixed, placing two electrode pairs in the cell shrank the possible electrode gaps to 1.5 and 2.5 cm.

Results

The results are presented in Figure 36. The results of the "standard" setup with one electrode pair (1P in Figure 36) are compared with the results of the monopolar electrodes.
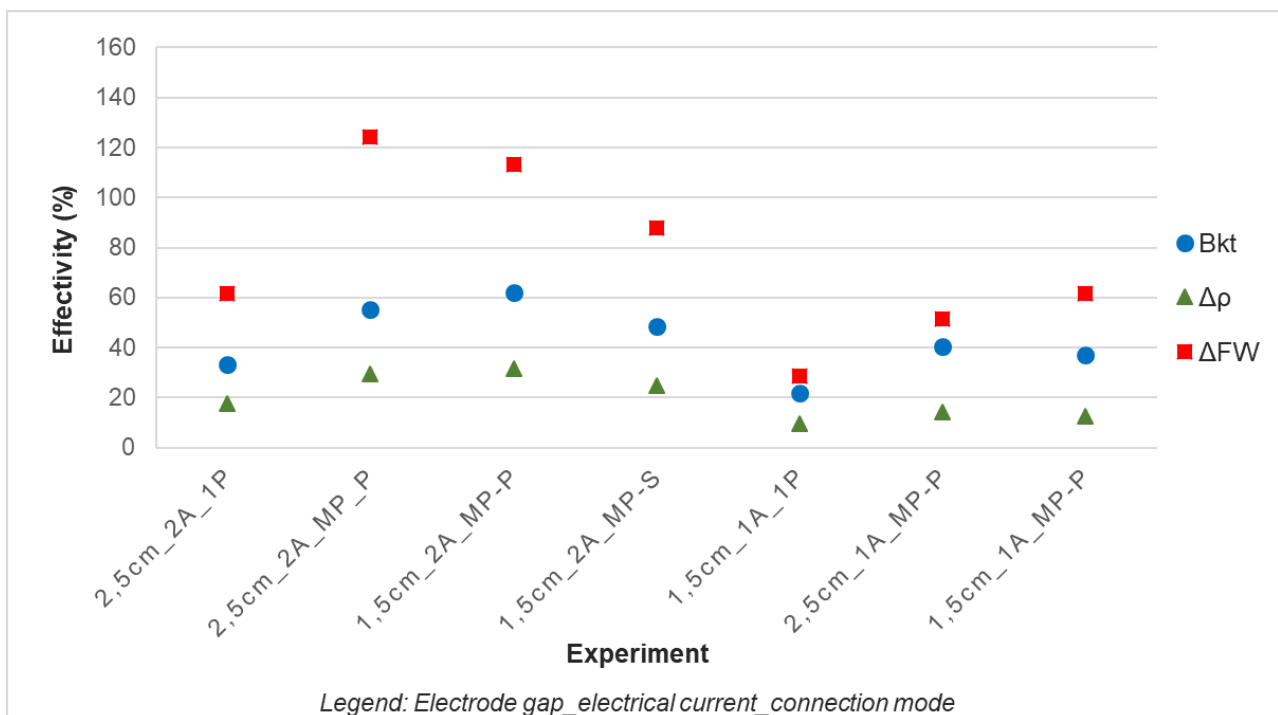
Figure 36: Influence of the monopolar electrode connection mode on the effectivity of the EC experiments

Concerning the serial and parallel connection, Figure 36 shows that the MP-P mode resulted in a higher effectivity of the EC process in all three effectivity parameters, compared with the MP-S mode with the same electrical current. When comparing the results for electrode

gap of 1,5 cm, B_{kt} was 10 % higher (50 % MP-S, 60 % MP-P), $\Delta\rho$ was around 8 % (22 % MP-S, 30 % MP-P), and the *ΔFW was* 26 % *(*88 % MP-S, 114 % MP-P).

Regarding the gap between the electrodes in a pair for MP-P mode, the change of the gap did not show any clear influence on the results. Some differences where measured, however, while looking at the results for all three effectivity parameters from all four experiments, no clear trend or preference can be observed.

The experiments with 1 A produced worse results than the experiments with 2 A, as expected. B_{kt} was 20 % lower (40 % at 1 A, 60 % at 2 A), $\Delta\rho$ *was* 18 % (12 % at 1 A, 30 % at 2 A), and *ΔFW was 60 % (*60 % at 1 A, 120 % at 2 A), when the results from both gaps were averaged.

Discussion

The connection mode MP-P provided better results than MP-S. These results are in agreement with findings of Paya (2016) on electrode connection modes.

The gap between the electrodes in a pair did not shown any significant influence. This is probably due to the fact that only two gaps (1.5 and 2.5 cm) could be tested. ΔFW is a little higher for the gap of 2.5 cm, similar to experiments with one electrode pair.

Influence of electrical current was as expected – doubled electrical current improved all three effectivity parameters, especially the destabilisation of the suspension. This agrees with the literature and all other performed experiments.

Scale-up recommendations

These findings suggest that the MP-P connection mode should be installed in a mid-scale prototype.

5.3.4 **LES4: Influence of the mechanical cleaning and experiment duration**

The next experimental series had two objectives. The first one was to determine the influence of the mechanical cleaning to EC of SUS. The second objective was to investigate if the mechanical cleaning could prolong the optimal EC duration time of 30 minutes, determined in the first research phase.

All experiments were performed with aluminium electrodes at the electrode gap of 6.5 cm. The experiments time durations were 30 and 60 minutes. Three variations of the mechanical cleaning were tested, as described in chapter 5.2.2.

Results

The results are presented in Figure 37 and Figure 38.
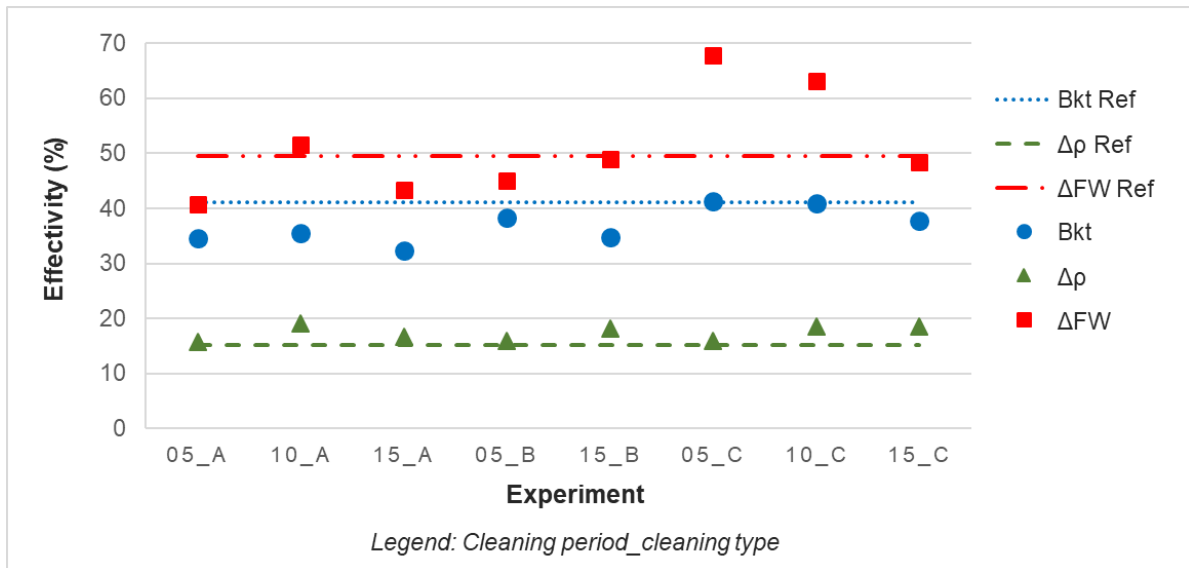
Figure 37:   Influence of the mechanical cleaning on the effectivity of the EC experiments
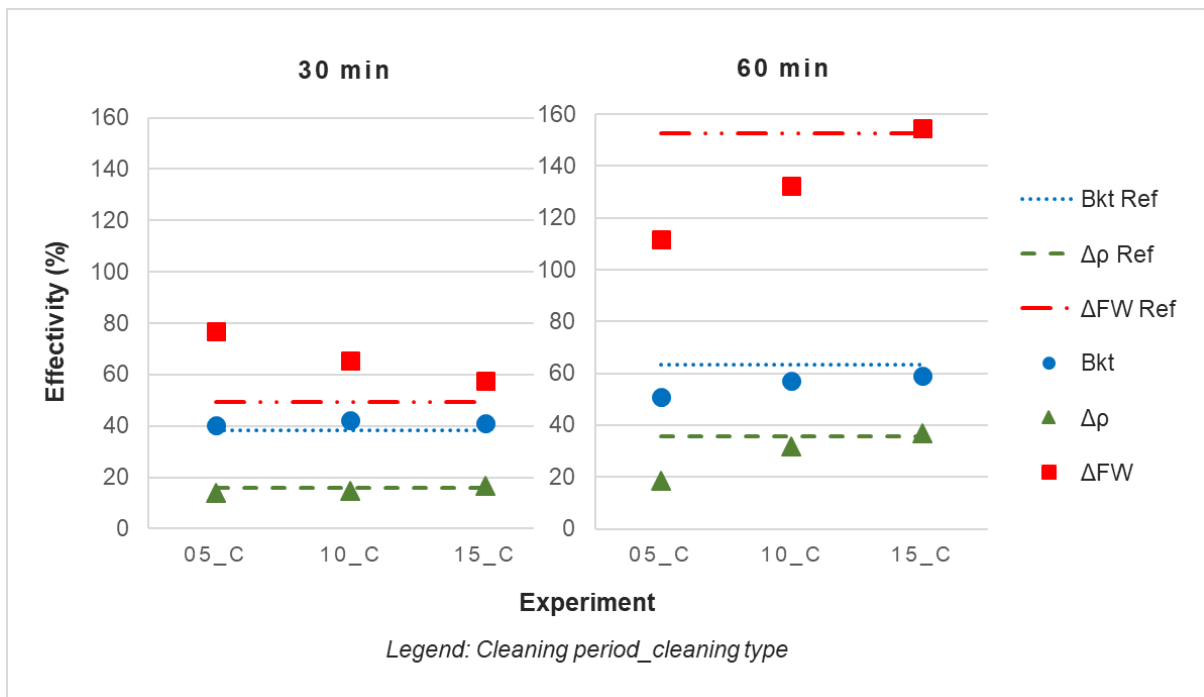
Figure 38:   Influence of the mechanical cleaning and experiment duration on the effectivity of the EC experiments

Figure 37 shows the results of the mechanical cleaning experiments compared with the results of the "standard", or rather, reference experiments without cleaning (presented with lines and marked with Ref). What stands out in this figure is that there was no improvement of the effectivity parameters B_{kt} and $\Delta FW,$ in the experiments, at which coagulated material from the anode was removed from the cell (cleaning type A and B). B_{kt} was on average 35,1%, $\Delta\rho$ was 17.1%, and ΔFW was 46.0%, which is respectively 6.0 % lower, 2.0 %

higher, and 3.5 % lower than the experiment without cleaning, in absolute values. In contrast, in the experiments in which the anodes were cleaned but the coagulated material was left in the cell (it sank to the bottom of the cell), B_{kt} was on average only 1 % lower and ΔFW was 10.3 % higher than in the experiments without cleaning. $\Delta \rho$ was improved for 2.5 %. The experiments at which the coagulated material was left in the cell also showed an increase of ΔFW by shorter cleaning intervals.

Since the experiments at which the coagulated material was left in the cell showed better performance than other mechanical cleaning combinations, the experiments presented in Figure 38 with the duration of 60 minutes were performed in this way. These experiments had a rather interesting outcome. The effect of mechanical cleaning on EC performance by experiments with 60 minutes duration are the opposite of those with 30 minutes duration. Periodical mechanical cleaning did not improve the results with the 60 minutes experiment duration time. On the contrary, the shorter the cleaning intervals were, the larger the negative effect on the results was. Only the cleaning interval of 15 minutes did not result in a negative influence on the effectivity parameters.

The most striking result to emerge from the experiments is that the standard experiment (without cleaning) with duration of 60 minutes delivered much better results than the standard experiment with the duration of 30 minutes, regarding all three effectivity parameters. B_{kt} rose from 38 to 64 %, $\Delta \rho$ rose from 16 to 36 % and ΔFW rose from 49 to 104 %.

Discussion

Experimental series with mechanical cleaning showed quite interesting results. The cleaning variations 1 and 2 (with removal of coagulated material from the cell) showed no improvement in comparison to the standard experiment. This can be traced back to the electricity data. The removal of the coagulated material decreased the suspension level in the cell, causing a decrease in the active electrode surface and an increase in the surface current density over starting 9.4 mA/cm². The experiments in cell A (chapter 5.3.2) showed that the surface current densities higher than approx. 11.1 mA/cm² at the electrode gap of 6.5 cm was not obtainable. Upon reaching the maximal voltage of 65 V, the electrical current decreased from the intended current of 2 A , which negatively influenced the effectivity parameters. The third variation of mechanical cleaning (without removal of coagulated material from the cell) had a positive influence on the results by the experiments with EC duration of 30 minutes.

However, the third variation of mechanical cleaning had an opposite effect on the experiments with the duration of 60 minutes. The best results were achieved when the anodes were not cleaned at all. Moreover, a shorter cleaning interval has positive influence in experiments with 30 minute, but a negative influence in the experiment with 60 minute. There

is no comprehensible/plausible explanation for these rather contradictory results. It would appear that cleaning has positive effect on shorter experiments but a negative effect on longer experiments. The theoretical implications of these findings are unclear.

There was another important finding in this experimental series: in contrast to earlier findings from Paya (2016), the EC duration time of 30 minutes does not seem to be the optimal duration time for EC of SUS. All three effectivity parameters continued rising after 30 minutes. Moreover, it can be roughly stated that doubling the EC duration doubled the value of the effectivity parameters (B_{kt}: 38 % $\rightarrow$ 64 %, $\Delta\rho$: 16 % $\rightarrow$ 36 %, ΔFW: 49 % $\rightarrow$ 104 %), meaning that there was not even a noticeable slow-down of the process after the 30th minute. These results are likely to be related to the amount of soil particles in suspension. The pure bentonite W 2.5% suspension tested by Paya (2016) had 25 g of bentonite particles in 1 l suspension. The SUS on the other hand has 420 g of soil particles in 1 l of suspension, which is 17 times more. Since bentonite and kaolin particles possess a negative surface electric charge and silica flour particles acquire a negative surface charge when in water (chapter 2.2.6), all particle in SUS need to be destabilised in order to coagulate. Therefore, the finding that SUS needs more electrical charge (Ah), or rather, more coagulants, to reach similar EC effects as with pure bentonite suspension seems very plausible.

Scale-up recommendations

It is recommended to build a cleaning system in the mid-scale prototype in order to further test on a larger scale. Regarding the EC duration time, the prototype should be able to perform open-end experiments so that this operational parameter can be optimised.

5.3.5 LES5: Further electrode materials: cooper, brass, stainless steel

Since a security issue with hydrogen and aluminium electrodes occurred during the design of the mid-scale prototype (chapter 3.5.1 - in explosive atmosphere, sacrificial anodes of aluminium present an ignition risks due to electric sparks), other materials have been tested to replace aluminium as an electrode material. Electrodes made of stainless steel (EN 1.4301), brass (CuZn37), and copper have been designed with the same dimensions as aluminium and steel electrodes.

The experiments were performed in cell B for 30 minutes. Since the prototype was already in the design phase and the electrode gaps were already set to 4.5, 5.5, and 6.5 cm, experiments in this series were only performed at these gaps.

Results

The new electrode materials results were compared with the results obtained using aluminium and steel electrodes (LES1, chapter 5.3.1). These results are presented in Figure 39.
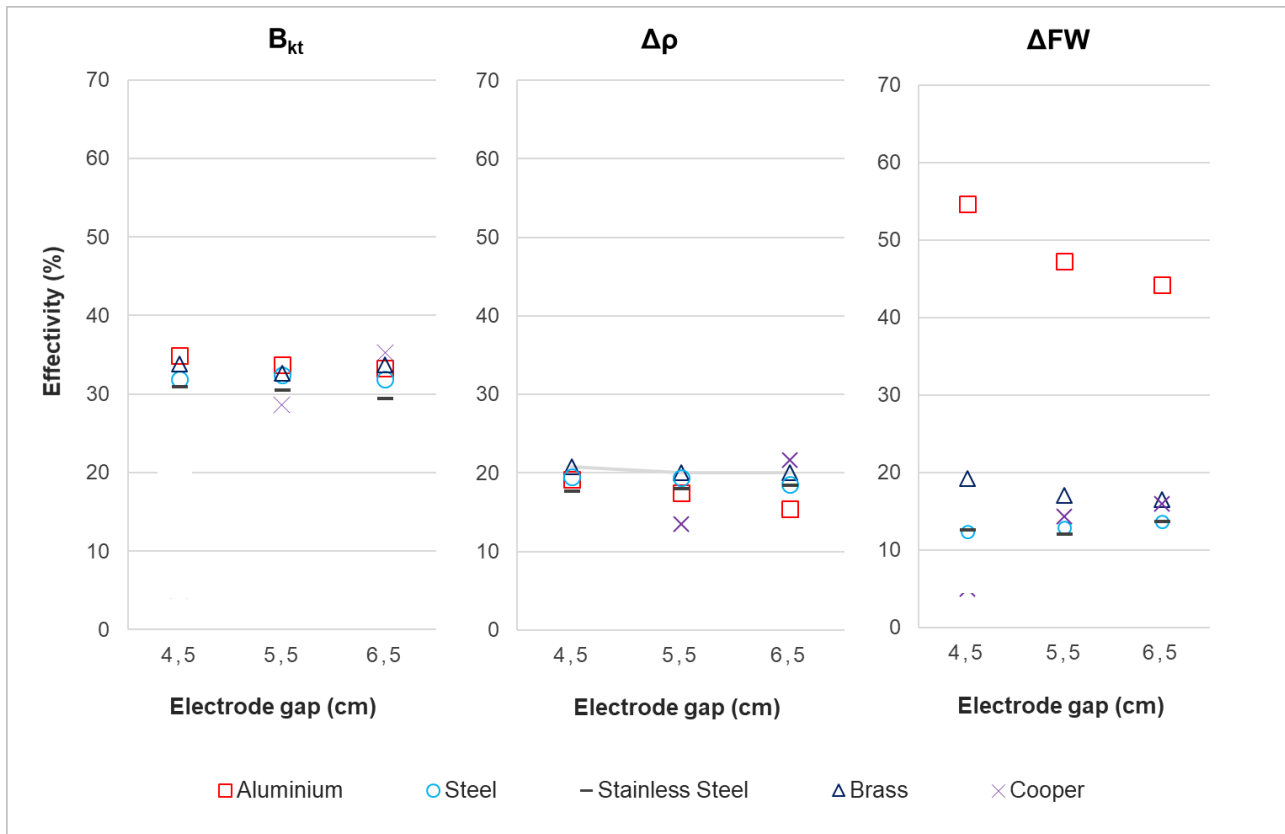
Figure 39: Influence of various electrode materials on the effectivity of the EC with experiments (Popovic, 2019)

Results

The investigated materials showed only a small influence on the parameter B_{kt}. The tests with aluminium electrodes showed on average the best results - average B_{kt} over all three gaps was 34.0%. Brass electrodes followed with an effectiveness of 33.4%.

The influence of the electrode material on the parameter $\Delta\rho$ was also minor. The tests with brass electrodes showed slightly better average results than other materials - the average $\Delta\rho$ over all the gaps was 20.3 %. Steel electrodes followed this with an effectiveness of 19.2 %. Aluminium electrodes performed only at 17.2 %.

The parameter ΔFW is significantly higher in the tests with the aluminium electrodes - the average ΔFW over all three gaps is 48.7 %. The second highest material is brass with an effectiveness of 17.6%.

Overall, the best results were obtained with aluminium electrodes, followed by brass electrodes.

Discussion

The performed experiments provided only a small difference in the amount of the coagulated material and the reduction of density. It seems that the type of metal ion does not play a role

in the electro-osmotic attraction of soil particles to the anode and their coagulation on the anode.

However, the difference in the destabilisation effect was significant. None of the tested materials came close to the destabilisation effect of aluminium. This can be explained through the influence of ions valence and amount on the destabilisation (chapter 2.2.5). Since Cu and Zn ions are divalent, they do not destabilise the suspension in the same magnitude as aluminium ions. The stainless steel used in these experiments consisted of 8 – 10 % of nickel (Ni), 18 - 20 % chromium (Cr), 2 % mangan (Mn) and up to 70 % of iron (Fe). Most often valences of those materials are 2 for Ni; 2, 3, and 6 for Cr; 2, 3, 4, 6, and 7 for Mn and 2 and 3 for Fe. Stainless steel and steel had similar results. A possible explanation for this could be that since stainless steel is still mostly consists of Fe, and the other materials are divalent or can be divalent.

Furthermore, since aluminium cathodes dissolve during EC (Eq. 3-9) and other tested materials it did not dissolve, the concentration of ions in the remaining suspension in the experiments with aluminium electrodes was probably higher than with other materials.

Scale-up recommendations

Since none of the tested materials came close to the performance of aluminium in the destabilisation of the suspension, aluminium remained the choice for the electrode material in the prototype. Potential ignition of the explosive atmosphere trough electrical sparks was solved by installing a sufficient ventilation of the EC mid-scale prototype and by completely covering the electrodes with the suspension during an experiment. In order to calculate the minimum requirement for the ventilation, the gas measurement experiments were performed. They are discussed in the following chapter.

5.3.6 **LES6: Gas measurements**

Gas evolution and metal dissolution during EC should theoretically follow Faraday's law (Eq 3-5). However, several reports in the literature presented different results. Picard et al. (2000) measured an additional amount of hydrogen and mass loss of the cathode which should not be happening according to the Faraday's theory. He assumed that both encountered reactions come from one chemical process involving the dissolution of the cathode and creation of hydrogen as product, according to Eq. 3-9. These findings are supported by Mouedhen et al. (2008) who performed experiments with titanium and aluminium electrodes. They tested three cathode-anode combination:

- both electrodes of aluminium
- aluminium anode – titanium cathode

- titanium anode – aluminium cathode

In a case of two aluminium electrodes, the measured amount of aluminium ions in a solution was higher than the theoretical amount developed through electrodissolution of the anode after Faraday's law. This, however, did not occur as the cathode was made of titanium – the amount of aluminium ions in the solution matched the theoretical values. As the cathode was made of aluminium and the anode was made of titanium, there should have been no increase of aluminium ion concentration in the solution after the EC. However, there was an increase of aluminium concentrate where the measured amount was similar to the additional amount measured in first combination. This lead to the conclusion that the aluminium cathode dissolves during the EC. This dissolution can however not be calculated with Faraday's law. Also, Canisares et al. (2005) supported the chemical dissolution of the cathode and found that it is strongly influenced by the pH value. They stated that this dissolution could be increased by order of magnitude in alkaline media.

Experimental setup and procedure

In order to investigate these findings and measure the amount of hydrogen produced during EC, gas measurement experiments were performed. The electrode gap was 6.5 cm and experiment duration was 15 minutes. However, the measurements continued for the following 5 Minutes after turning the DC source off. Experimental setup is shown in Figure 40.
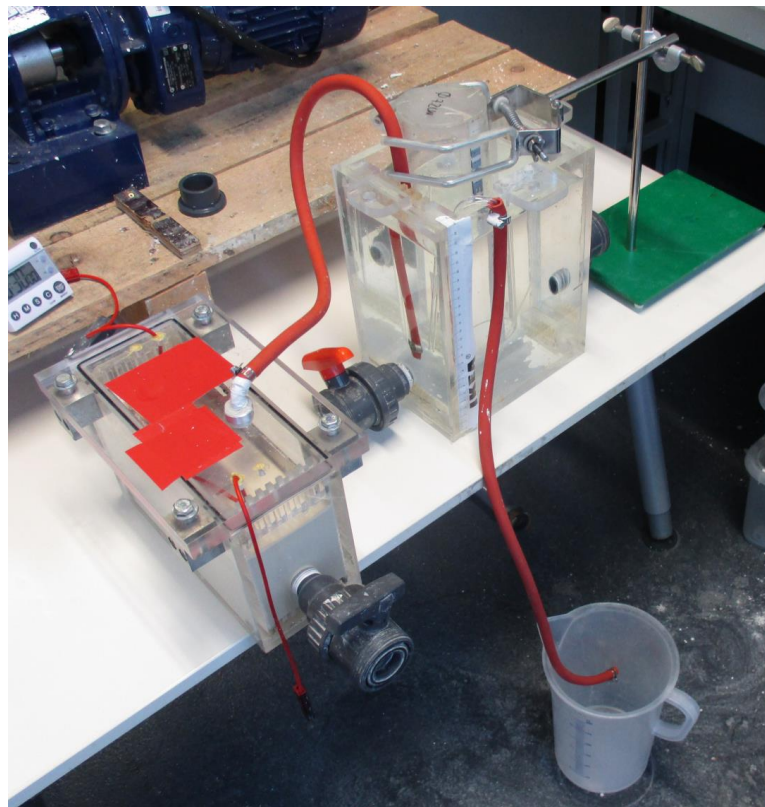
Figure 40:   Experimental setup for gas measurement experiments

The cell can be sealed airtight with a cover specially made for the EC cell B. A measuring cylinder is immersed in a second tank filled with water. A hose is connected to a small opening in the cover of the TLB test cell B, the other end of which ends in the measuring cylinder of the second container. The gases produced during the test can thus pass through the tube into the measuring cylinder. The gases displace the water in the cylinder. In this way, the volume of the resulting gases can be determined. Water pressure was continuously balanced by stepwise removal of water from the cell surrounding the cylinder, in order not to compress the produced gas (Figure 41).
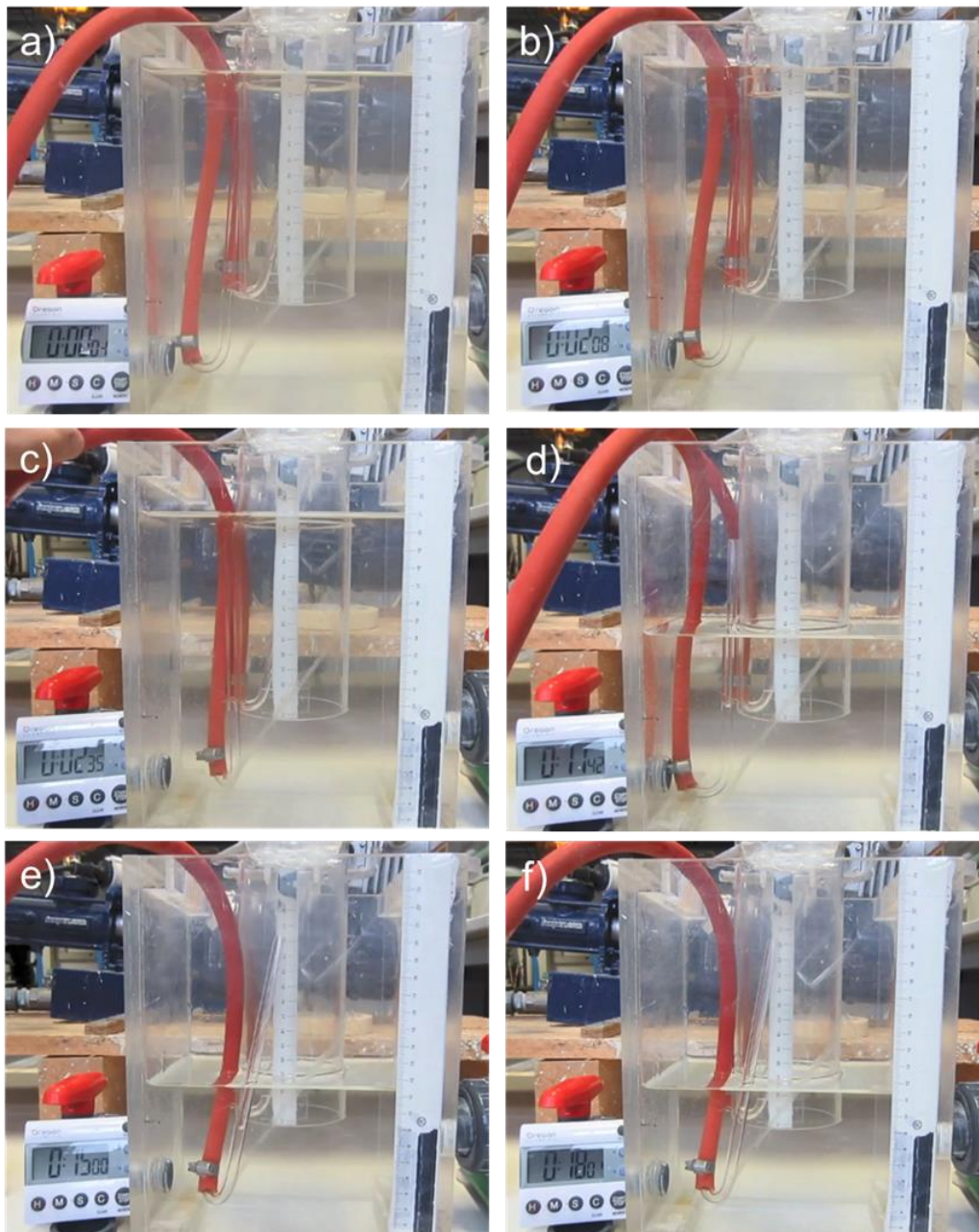
Figure 41:   a) Start of the experiment, b) Gas produced in the cell displaces water in the cylinder, c) Pressure balance, d) Status after 11 minutes, e) Status at 15th minute, at this point the electricity is turned off, e) Status at 18th minute, no additional gas was measured after the electricity was turned off

In order to rule out any leakage of the system, a negative pressure was created in the tank by draining the water before each test. The fact that the water levels remain is an indication that the system is completely leak-proof.

After checking the tightness, the test begins by switching on the current. Every minute the level of the displaced water is recorded in the measuring cylinder. After 15 minutes, the current was switched off and the measurements runs for a further 10 minutes to ensure that no further gases are produced after the current is switched off.

Five gas measurement experiments were performed. Theoretical values for produced hydrogen were calculated by including the measured electrical current values into the combination of Faraday's law (Eq 3-4) and the ideal gas law (Eq 5-1), as shown in the Eq 5-2. Experimental values were documented during the experiment by reading the height of the air column in the measuring cylinder.

$$m = \frac{M \cdot I \cdot t}{z \cdot F} \quad \rightarrow \quad \frac{m}{M} = \frac{I \cdot t}{z \cdot F} \tag{Eq. 3-4}$$

$$pV = \frac{m}{M} \cdot R \cdot T \quad \rightarrow \quad pV = \frac{I \cdot t}{z \cdot F} \cdot R \cdot T \tag{Eq. 5-1}$$

$$V = \frac{I \cdot t \cdot R \cdot T}{z \cdot F \cdot p} \tag{Eq. 5-2}$$

with :

V Volume of the produced gas [l]

R Ideal gas constant = 8.314 [Jmol^{-1}K^{-1}]

T Absolute temperature of the produced gas [K]

z Valence of the produced gas [-]

F Faraday's constant = 96487 [Cmol^{-1}]

p Pressure of the produced gas [Pa]

Results

Full lines in Figure 42 represent the theoretical and the dotted lines experimentally measured values of gas during the EC experiment. As shown in Figure 42, every experiment resulted in a higher amount of produced gas than anticipated in Faraday's law and the ideal gas law. As soon as the electricity was turned off, measurements showed no further gas production. When calculating the theoretical values, the atmospheric pressure of 1.013 x 10^5 Pa was taken as the pressure of the produced gas, since the water level in the measuring cylinder was constantly balanced. Since the system was completely airtight, it was not possible to measure the temperature of the produced gas during EC. It was measured only after the

experiment. However, no shrinkage of the gas volume in the measuring cylinder was observed after the electricity was turned off (the measurements were running for an additional 5 minutes after turning EC off). Therefore, an assumption that the temperature during the experiment is the same as temperature after the experiment was taken and the measured temperature of 297.15 K (24 C) flowed into Eq 5-2.
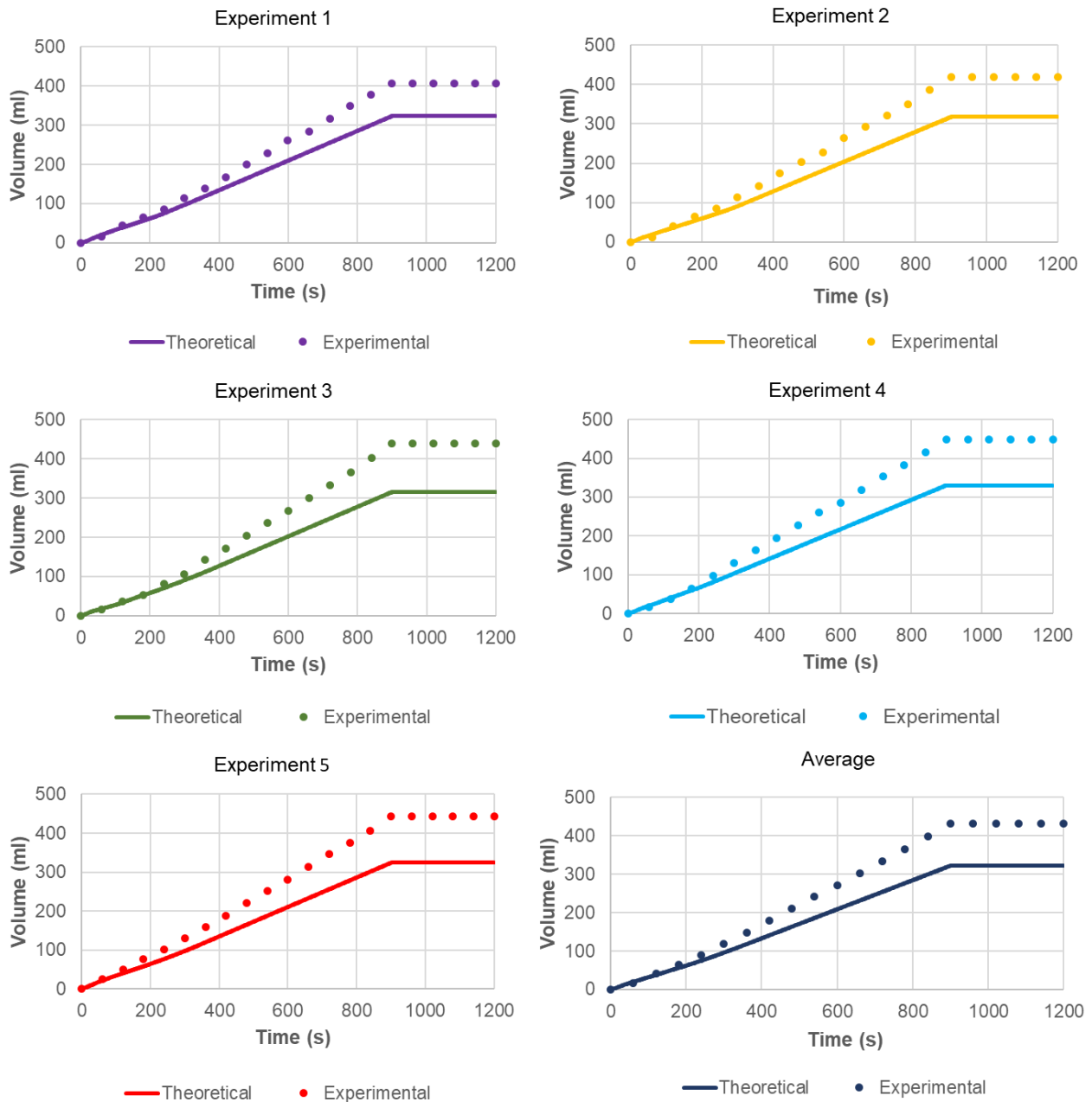
Figure 42:   Gas measurement experiments

Measured values and theoretical values of the produced gas for each experiment are listed in Table 13. It is apparent from Figure 42 and Table 13 that the experimentally measured

amounts of produced gas exceeded the theoretical amounts in all experiments. The additional amount of gas was in a range of 26 % – 37 % with an average of 34 %. Moreover, the cathodes lost on average 0.07 g per experiment.

Table 13:   Theoretical (theo) and experimental (exp) amount of produced gas

Experiment Nr.	H_2 theo (ml)	O_2 theo (ml)	Gas theo (ml)	Gas exp (ml)	Gas exp - gas theo (ml)	Gas exp – gas theo (%)
1	215.6	107.7	323.3	406.9	83.6	25.9
2	211.7	105.8	317.5	419.2	101.7	32.0
3	210.5	105.2	315.7	439.5	123.8	39.2
4	220.5	110.2	330.7	447.6	116.9	35.4
5	216.0	108.0	324.0	443.6	119.6	36.9
Average Ø	**214.8**	**197.4**	**322.2**	**431.4**	**109.1**	**33.9**

Discussion

This experimental series demonstrate that the amount of gas produced during EC was higher than the amount anticipated in Faraday's law and the ideal gas law. Moreover, the aluminium cathode was dissolving at every experiment. These results are consistent with the literature. However, no production of gas after the experiment was observed in this set of experiments.

Under the assumption that Eq 3-9 is correct and that there are no other unreported gas producing reactions during EC with aluminium electrodes, the complete measured additional amount of gas is only hydrogen. That means, for every 214.8 ml of hydrogen produced by electricity produces another 109.1 ml from the chemical dissolution of the aluminium cathode followed. This presents an increase of 51 % to the theoretical amount of hydrogen.

Moreover, the column O_2 theo was calculated under the assumption that all electrons coming to the anode are being "invested" in production of oxygen. This is correct for the electrolysis of water, in which the complete electrical current is being spent on reactions described in Eq 4-1 and 4-2, resulting in the evolution of hydrogen and oxygen at a ratio of 2:1. However, it is not correct for EC since the two reactions occur on anodes surface during EC: evolution of oxygen (Eq 4-2) and electrodissolution of the anode (Eq 3-3). An electron coming to the anode can react either to produce oxygen or to produce metal ions, but not both.

Electrodissolution is the basic concept behind EC and there is no doubt about this reaction occurring. However, gas bubbles were developing on the anode during the experiments,

which suggests that the evolution of oxygen on the anode also took place. That further suggests that a part of the electrons was involved in a reaction 4-2 and other part was in reaction 3-3. This means that the actual amount of produced oxygen was smaller than the amount written in Table 13 under O_2 theo, which further suggests that the additional amount of hydrogen could have been even higher than 51 %.

To stay on the safe side, the extreme case is taken into consideration, in which the whole amount of measured gas was only hydrogen. In this case, the complete difference between the experimentally measured amount of gas (Gas exp) and the theoretical amount of hydrogen (H_2 theo) would have been hydrogen that arose through chemical dissolution of the cathode (Eq 3-9). That means, every 214.8 ml of hydrogen produced by electricity would produce another 216.6 ml from chemical dissolution of the aluminium cathode. This shows an increase of 101 %

Scale-up recommendations

The ventilation system in the mid-scale prototype should be designed in a way that it can cope with the amount of hydrogen 51 % - 101 % higher than anticipated in Faraday's law.

5.3.7 LES7: Experiment retention time and mini scale up tests

The following experimental studies researched two aspects of EC treatment: retention time and scale up parameters. The retention time is the time after EC experiment, in which the suspension is still in the cell. The idea behind the retention time is to give metal ions more time to destabilise the suspension. According to some researchers, electrochemical reactions could continue for some time after turning off the electricity. This means that the results could be improved without investing further energy, only time. In order to test this idea, experiments with 15 minute EC duration and 15 minute retention time were performed. Retention time was implemented by not moving any part of the cell or the suspension for 15 minutes after the electricity was turned off. These experiments were compared with the experiments with an EC time duration of 15 and 30 minutes.

The goal of the mini scale-up experiments was to test if the increase of suspensions volume with proportional increase of electrode surface and electrical current results in a similar EC performance. Those experiments were performed in cell A. Due to its size, this cell makes the experiments with 4 l of suspension possible. Therefore, the experiments with 1 A and 2 l of suspension were compared with experiments with 2 A and 4 l of suspension. Due to the fact that the form of the electrodes follows the form of the cell, doubling the suspension volume also doubled the electrodes surface.

Results

The results of this set of experiments are shown in Figure 43.
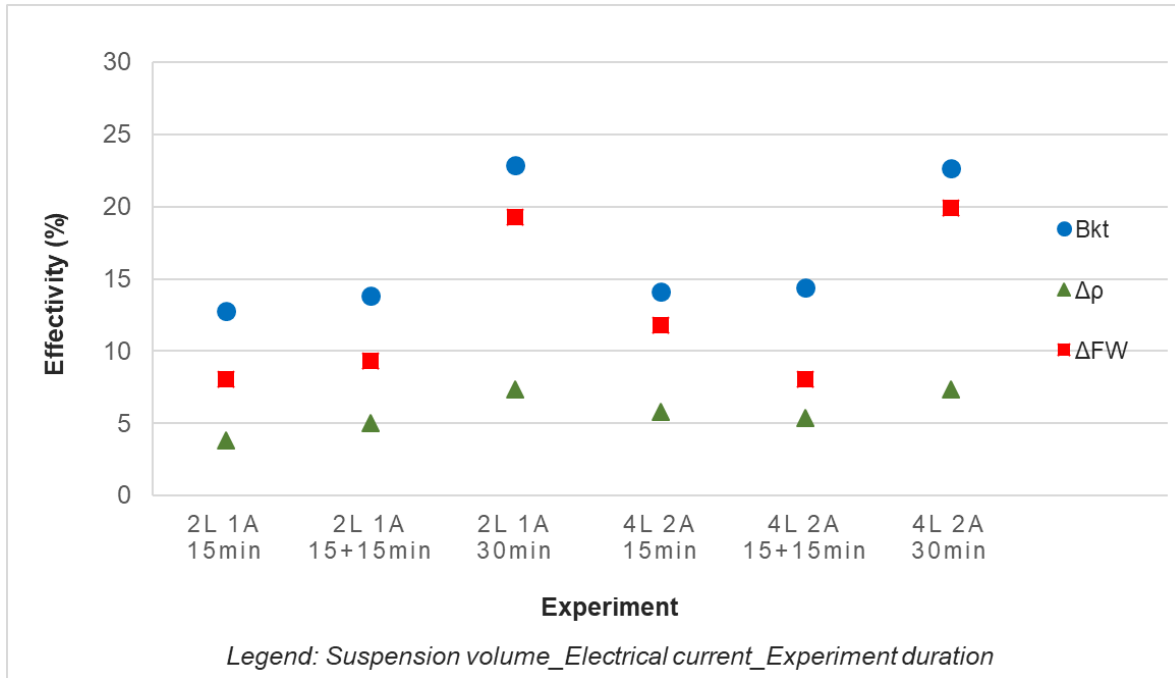
Figure 43:   Retention time and mini scale-up experiments

Retention time

The retention time was tested on experiments with 1 A - 2 l and 2 A - 4 l. The results with 1 A - 2 l did show a small improvement concerning all three effectivity parameters, but only 1 % in absolute values. In a case of 2 A - 4 l, there was no overall improvements. B_{kt} and $\Delta\rho$ changed less than 1 % and ΔFW sank from 12 to 8 %. When compared with the experiments with an EC time duration of 30 minutes, it is clear that the retention time brings no or small improvements.

Mini scale-up

What stands out in Figure 43 is the good correlation between the results of the 1 A - 2 l and 2 A - 4 l experiments. This is especially noticeable for the experiment time duration of 30 minutes. No difference greater than 1 % was observed. For 15 minutes and 15 + 15 minutes, B_{kt} and $\Delta\rho$ differed up to 2 % and ΔFW up to 4 %.

Discussion

Retention time does not bring any measurable improvements to the experiments. The reports from the literature could not be confirmed. This could be caused by the fact, that only the coagulated material from the anode and the material that stays on the sieve is considered as the coagulated material. If there is a residual collision of particles, the flocs produced on such a way are maybe not big enough to be filtered with the sieve. However, parameters B_k, $\Delta\rho$, and ΔFW did not show a clear improvement, which means that the suspension was not further destabilised after the electricity was turned off.

Mini scale-up experiments showed a good correlation. The results confirm the idea that the proportional increase of the increase of suspension volume while keeping the parameters electrode surface to suspension volume [cm²/m³], the surface current density [A/m²] and the volumetric current density [A/l] constant results in an identical EC performance.

Scale up recommendations

Retention time does not need to be planned in the new experimental series with the mid-scale prototype.

Current density (both surface as well as volumetric) and the ratio of electrode surface to suspension volume seem to be the right scale up parameters.

5.3.8 LES8: Electrodes passivation

Electrode passivation was described in chapter 3.3.5. It causes overvoltage and therefore higher energy consumption over time. The purpose of the following experimental series was to investigate in what extent this applies to EC of SUS and to test if the performance of the electrode concerning effectivity parameters decreases over time

In order to investigate the passivation, the coagulated material was completely removed from the anode's surface after every experiment and the electrodes were cleaned. However in contrast to all the other series, the electrodes were not polished between the experiments. Instead, the same surface layer was used for the complete set of experiments.

The experiments were performed in cell A, at 1 A, with a gap of 6.5 cm and an experiment time duration of 30 minutes.

Results

Electricity values of this experimental series are listed in Table 14 and effectivity parameters are presented in Figure 44.

Table 14:   Electrodes passivation experimental series – electricity and effectivity parameters

Experiment Nr.	1	2	3	4	5	6	7	8
Voltage (V)	47.16	44.22	40.83	42.95	43.28	43.75	44.55	44.61
Δ Voltage (V)	-	-2.94	-3.39	2.12	0.33	0.47	0.80	0.05
Current (A)	1.00	1.00	1.00	1.00	1.00	1.00	1.00	1.00

Figure 44:   **Electrodes passivation experimental series – effectivity parameters**

Regarding increase of voltage over time, the highest measured voltage was in the first experiment, as the electrode was still freshly polished. In the following two experiments, voltage was dropping. However, voltage reached a minimum at the third experiment and then rose each time in the following five experiments.

Regarding effectivity parameters, no decrease of B_k and $\Delta\rho$ over time was detected. Contrarily, these two parameters rose slightly. In the first experiment, B_k was 19 % and $\Delta\rho$ was 7 %. In the last experiment B_k was 23 % and $\Delta\rho$ was 10 %, which represents an increase of 4 % and 5 %, respectively. With the parameter ΔFW, it is hard to see any clear tendency. It was 16 % in the first experiment and 18 % in the last experiment. However, in the meantime it fluctuated from a maximum value of 28 % to minimum value of 14 %.

Discussion

Regarding overvoltage, no clear tendency to passivation was measured in this experimental series.

On average, over the last four experiments, voltage rose 0.4 V per experiment. With this tendency, the voltage of the first experiment with a clean polished electrode would be reached after 7 more experiments or rather after 3.5 more hours in discontinuous operation. After that, every next experiment would exhibit overvoltage. However, such assumption based only on last four experiments cannot be considered as a precise assumption.

Moreover, there was no sign that the multiple usage of electrodes without polishing their surface between the experiments negatively influence EC performance regarding effectivity parameters.

No in-depth analysis of this subject was found in the literature review. The data about the expected change of the voltage course over many experiments was missing. The information about the cell operation time after which the overvoltage problem in expected to occur was also not found.

Overall, the re-use of non-polished electrodes in experiments did not show any clear negative effects regarding energy consumption or effectivity parameters. However, only 9 experiments with 4.5 hours of EC operational time were performed.

Scale up recommendations

This experimental series did not explicitly confirm electrodes passivation effect. If it occurs by EC with the standard used suspensions, it does not occur that fast to be measured after 4.5 hours in operation. Therefore, there is no critical need to employ some kind of electrodes-polishing method by the bigger scale prototype. Nevertheless, it is generally a good idea to construct the mid-scale prototype in a way that the electrodes can be changed. After a sufficient amount of working hours, they will dissolute and start losing their form.

5.3.9 Further tests and calculations

Sedimentation tests

Sedimentation tests served as an additional evidence of the destabilising effect of EC on charged bentonite suspensions. However, sedimentation is not a convenient separation method in the praxis since it would require a lot of time and space. Therefore, the influence of EC on some aspects of sedimentation like sedimentation speed as well as the amount and quality of separated water at the surface was not further investigated in this dissertation.

The experiments were performed with the remaining suspension from the mechanical cleaning experimental series (chapter 5.3.4). After EC, the suspension was poured in the cylinders and left over the weekend. One cylinder was filled with reference suspension (non-electrocoagulated SUS). The photos from were taken 4 days later. The destabilisation effect of EC was clear.

Figure 45:   Sedimentation tests: a) no EC, b). R05, c) R10, d) R15, e) standard experiment

Methylene blue tests

Methylene blue tests are often performed as quality tests for bentonite. Methylene blue is a liquid colorant. It possesses cations that adhere very well to the negatively charged surface of montmorillonite. The more montmorillonite there is in bentonite powder, the more methylene blue will be adsorbed. Since the amount of montmorillonite in bentonite significantly influences its properties and basically differentiates bentonite from other clays, these test can be used to determine the quality of bentonite.

In this case, methylene blue tests were performed to compare the ratio of bentonite in the suspension before and after EC. First, a dried sample of the suspension was tested prior to the EC. Afterwards, coagulated material from the anode was dried and tested. The same was done with a sample of an used bentonite suspension from a construction site in Berlin. Methylene blue tests were performed as normed in DIN EN 933-9:2013-7. The results are presented in the Table 15.

Table 15:   The ratio of montmorillonite in a suspension and in a coagulated material

Experiment Nr.	Before EC (%)	After EC (%)	Density (g/cm³)
1	14	14	1.19
2	8	8	1.26

As seen from the table above, the results show that the montmorillonite amount in the coagulated material is the same as the amount in the suspension. This suggests that soil particles in the suspension originating from excavated material coagulate at the same rate as the bentonite particles. The difference between the montmorillonite amount in the used suspension from Berlin and SUS can be traced back to the difference in the density of those

suspensions. Due to a lower density of the suspension from Berlin, the ratio of bentonite particles to other soil particles in this suspension was higher than in SUS.

These findings are in good agreement with the zeta potential theory (chapter 2.2.6). Since all particles that do not possess electrical surface charge acquire it when in water, they are all attracted from electrodes. The particles from all tested suspensions in this dissertation coagulated on the anode, which means that all soil particles acquired negative zeta potential in water, as it was anticipated in theory. Methylene blue testes showed that non-bentonite soil particles coagulate at the same rate as bentonite particles.

5.4 Summary of the laboratory results

The purpose of the presented experimental study was to define a standard-used suspension and determine the best cell and operational parameters for EC of SUS. The results showed some similarities but also some significant differences to the experiments on pure bentonite suspension performed by Paya (2016).

The results of the experimental series indicate as following:

- aluminium should be used as electrode material for the mid-scale prototype.
- electrode gap should not be excessively large.
- Cell B should be used as a scale-up basis for a mid-scale prototype.
- MP-P electrode connection mode should be used in mid-scale prototype.
- Mechanical cleaning did not show clear positive influence by performed experiments. However, it is recommended to build some kid of cleaning system in the mid-scale prototype, in order to test it further in bigger scale.
- Optimal experiment duration is to be kept open to further research. No automatical safety shut-down system after 30 minutes of EC is to integrate in the prototype.
- Cleaning system should be built in the mid-scale prototype, in order to test it further in a bigger scale.
- Ventilation should be designed in a way to expect 51 % - 101 % more hydrogen that according to the Faraday's law.

Chronologically, the laboratory experiments were performed simultaneously to design of the mid-scale EC prototype. Some decisions have already been made based on the results of the first phase of the research. Therefore, not all of these findings were considered for the end design.

6   Experiments with mid-scale prototype

Upon investigating the optimal parameters for the EC of SUS, a larger EC cell was constructed. The cell with its complete equipment is called the mid-scale prototype. This prototype is planned as a transition step between laboratory cells and real-scale cells for construction sites. The design of the prototype as well as all experiments that were performed using it are described in this chapter.

Prior to constructing the mid-scale prototype, the scale-up parameters had to be determined. This was based on the parameters of the EC laboratory cell B.

6.1   Scale-up from laboratory cell to prototype cell

The EC prototype cell was constructed based on the cell and operational parameters of the EC laboratory cell B, listed in Table 16. The electrodes are connected in parallel circuit, as shown in Figure 46.

Table 16:   Scale-up parameters for the EC prototype cell (Popovic & Schößer, 2019)

Parameter	EC laboratory cell B		EC prototype cell	
Active electrode surface (cm²)	212		18600	
Cell volume (cm³)	2000 (2 l)		300 000 (300 l)	
Ratio of active electrode surface to cell volume (cm² /cm³)	0.106		0.106	
Electrical current (A)	1	2	150	300
Surface current density (mA/cm²)	4.7	9.4	4.7	9.4
Volumetric current density (mA/cm³) (A/l)	0.5	1.0	0.5	1.0
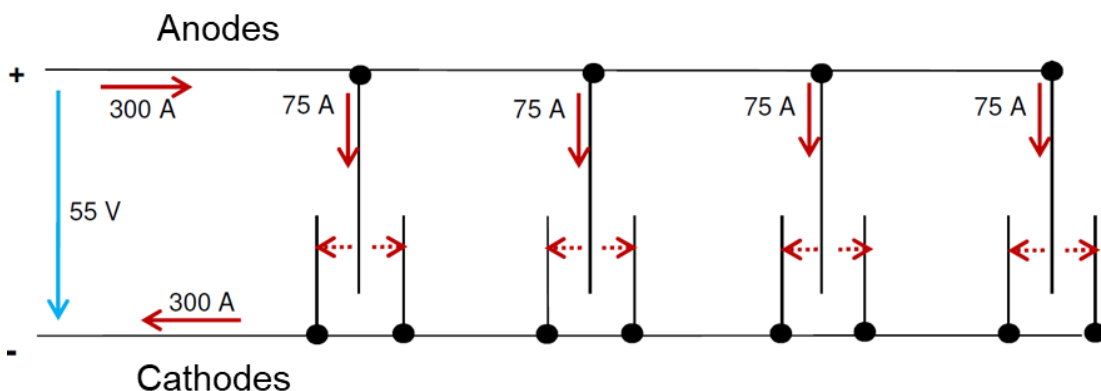
Figure 46:   Simplified electrical circuit schema of the EC mid-scale cell (Glück, 2015)

In addition to size, there are other differences between the laboratory and the mid-scale cell. Those differences arose as solutions to construction and safety challenges that emerged during the design phase. The biggest design differences are:

- Electrodes are completely submerged in suspension during EC
- Electrodes are round-shaped and anodes can rotate.
- On each side of an anode, there is one cathode (Figure 46). The polarisation of electrodes cannot be changed.
- The cell is equipped with an automatic anode cleaning system. These scrapers scratch the coagulated material from the anodes while they rotate. EC does not have to be turned off during rotation and cleaning.

The first difference resulted from required safety measures, since the production of hydrogen was sufficient to create an explosive atmosphere in the cell (chapter 3.5.1). Rather than altering the atmosphere to reduce explosive hazards, the system was designed to avoid all possible ignition sources. Among other measures, this was achieved through avoiding the contact of electrodes or any other live parts with potentially explosive atmosphere in the cell by "covering" the electrodes with suspension during the experiment.

The other differences resulted from the need to scratch the coagulated material from the electrodes' surface during or after the experiments. Anodes were designed round shaped with a well that can be rotated from outside the cell. Scrapers were placed on both sides of each anode. During rotation, they automatically scratch the coagulated material from the anodes' surface. Further design details are described in the following chapters.

6.2 Experimental setup

Experimental setup consists of one EC Container and laboratory chamber filter press (LCFP). The equipment was designed and built in cooperation with partners of this research project. The companies Herrenknecht AG from Schwanau and GeneSys Elektronik GmbH from Offenburg undertook the construction of EC Container and the company MSE-Filterpressen from Remchingen delivered the LCFP.

6.2.1 EC Container

The complete equipment needed for secure and functional EC process was integrated into one standard 20' container. It was placed at the laboratory at the Institute for Tunnelling and Construction Management at the Ruhr University Bochum, where all experiments presented in this thesis were performed.

Containers dimensions are 6.06 m length x 2.44 m width x 2.59 m height without the chimney or 4.30 m height including the chimney. The container is divided into two rooms by a

welded steel wall. The first room is a mixing and control room; here, the suspension is pre-pared and the complete process is controlled. The EC prototype cell with a total volume of 320 litres is placed in the second room, called the EC room. The construction drawing of the container is shown in the Figure 47. The ECC weighs around 5 t, from which 2 t are self-weight of the container and the rest are built-in devices required for the EC process.
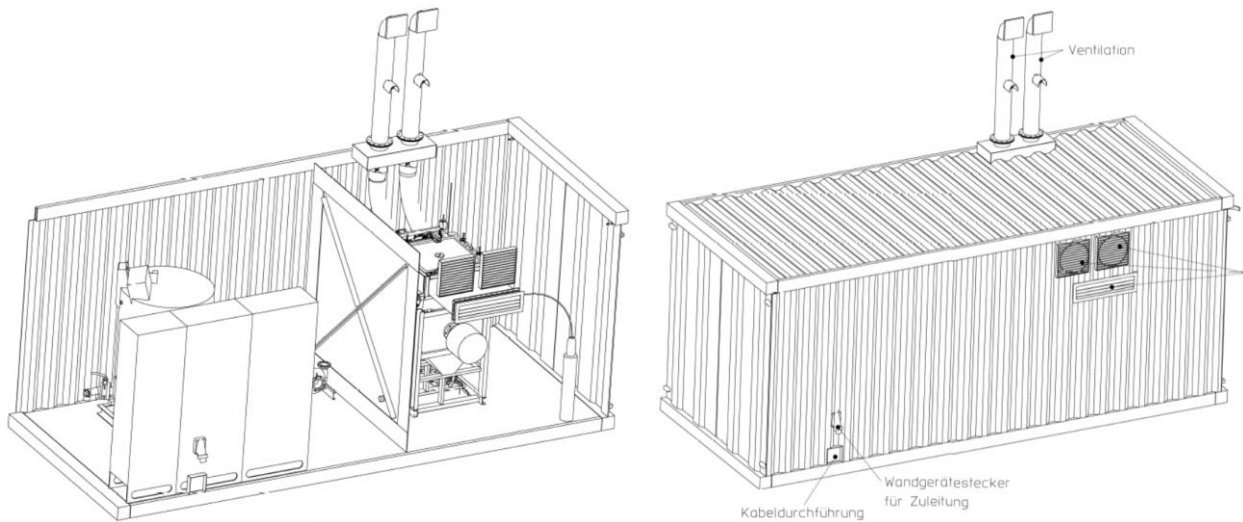
Figure 47:   Drawing of the EC Container: left: inside; right: outside (Meyer/Herrenknecht AG, 2017)

Control and mixing room

The control and mixing room (Figure 48 and Figure 49) consists of a stirrer with a volume of 800 l, a pump, a DC power source (300 A/55 V) with control screen for EC processes, and a cabinet with a control panel for general ECC functions. Besides this main equipment, there is also a control box for hydrogen sensors, air conditioning device for the cabinet, illumina-tion and pipes connecting the stirrer to the pump and EC cell in the EC room.

Figure 48: Control and mixing room: (1) stirrer, (5) control box for hydrogen sensors (6) air-conditioning device for cabinet, (7) illumination, (after Popovic et al., 2018)

Figure 49: Content of the control and mixing room: (1) stirrer, (2) pump (3), DC source with control screen, (4) control panel, (8) pipes (after Popovic & Schößer, 2019)

EC room

Figure 50 shows the EC room. The main device in this room is the EC prototype cell. Besides the cell, the room is equipped with two ventilation systems (one for the cell and one for the room), hydrogen sensors, door sensors, a control panel for the pump, one small gas cylinder, and regular and emergency lighting.
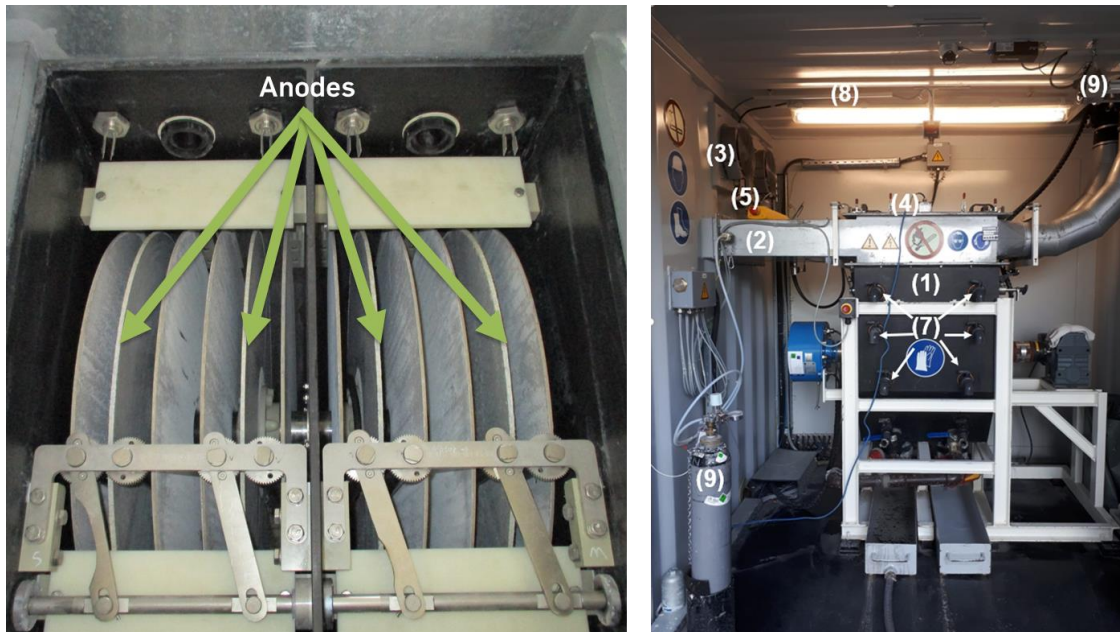
Figure 50:   EC room: (1) EC prototype cell, (2) cell ventilation system, (3) room ventilation system, (4) hydrogen sensors, door sensors, (5) control pad for the pump, (6) one small gas canister, (7), extraction points on the cell, (8) regular and (9) emergency illumination (after Popovic et al., 2018)

EC prototype cell

The components of the EC prototype cell are shown in Figure 51.
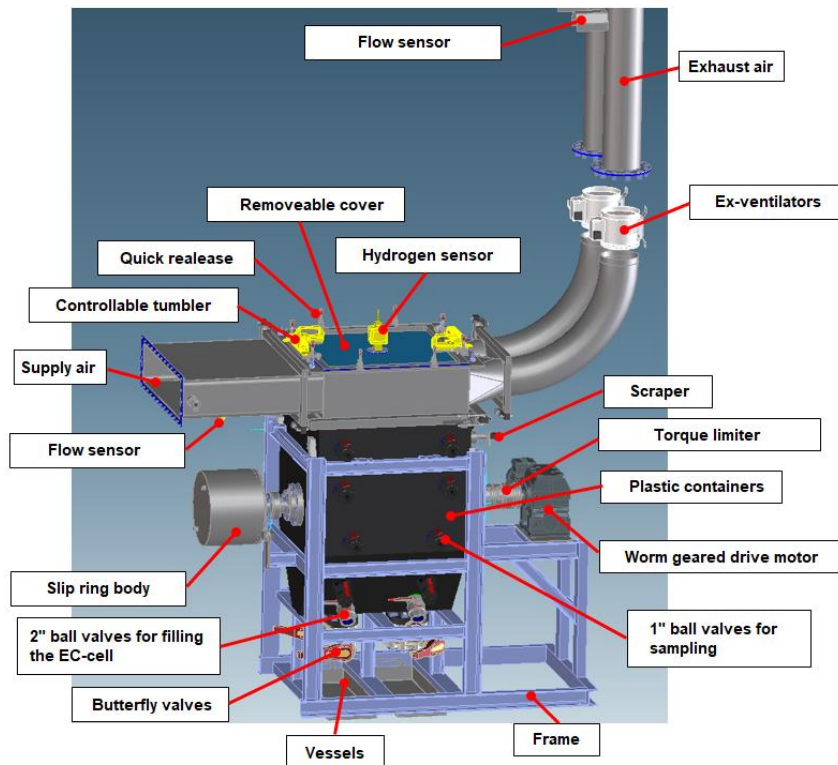
Figure 51:   Components of the EC mid-scale cell (Meyer/Herrenknecht AG, 2017)

The cell consists of two identically constructed chambers, each with a volume of 160 l. In each chamber there are 2 anodes and 4 cathodes, with the anodes arranged between two cathodes (Figure 50). The electrodes are circular with a diameter of 70 cm. Anodes have an area of 0.38 m² and cathodes slightly less, 0.35 m². This difference in area arose from the need to allow the variation of operational parameters during optimisation. Each chamber has five extraction points in form of ball valves (Figure 50). These extraction points allow the suspension to be analysed at different heights in the cell. The components of the EC mid-scale cell are shown in Figure 51.

A hollow shaft passes through the centre of the electrodes (Figure 52). It provides an attachment point for the anodes and also supplies them with electricity. The shaft is attached to a geared motor on the outside, which rotates the shaft and anodes. Scrapers installed in the lower part of the cell (Figure 53) clean the anodes by sweeping the coagulated material from the surface as anodes rotate.

Cathodes, on the other hand, are not attached to the shaft and cannot rotate. Instead, they are placed in the slots of the cell, which are built at distances of 4.5, 5.5 and 6.5 cm from the sides of each anode. The electrode gap is changed simply by lifting the cathode and placing it in another slot. In order to make this possible, cathodes have a recess in the part

directly under the shaft (Figure 54). Therefore, cathodes have a slightly smaller area than anodes.
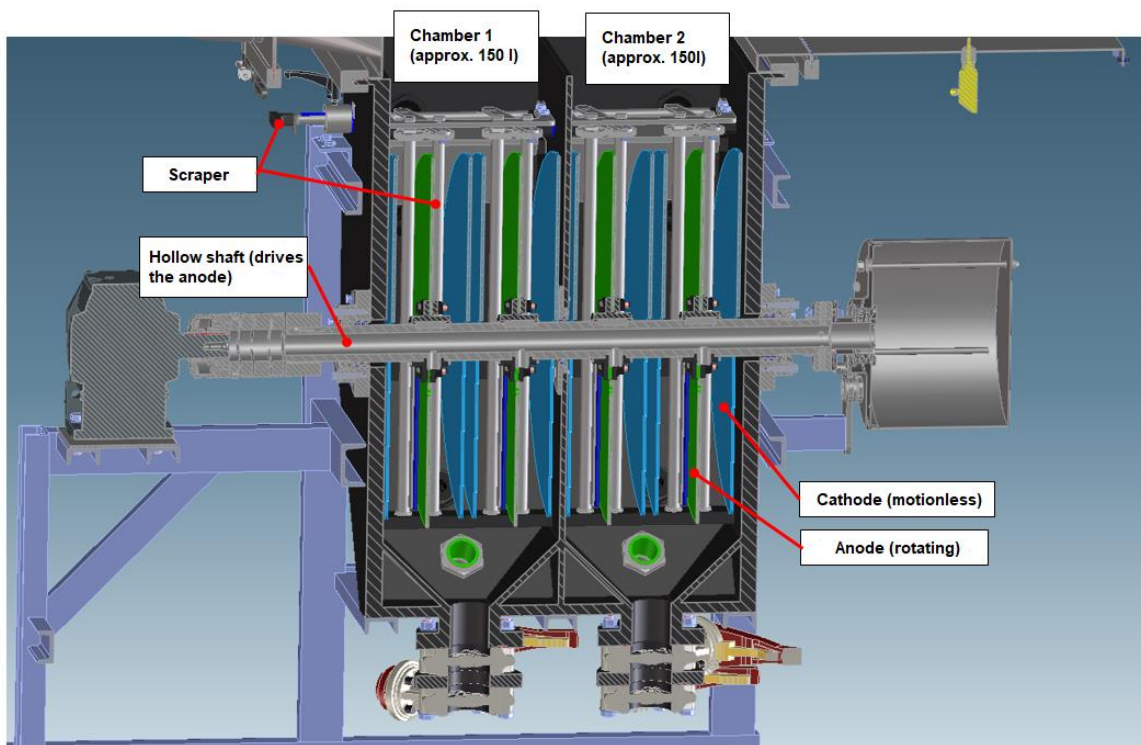
Figure 52: Cross section through the EC mid-scale cell (Meyer/Herrenknecht AG, 2017)
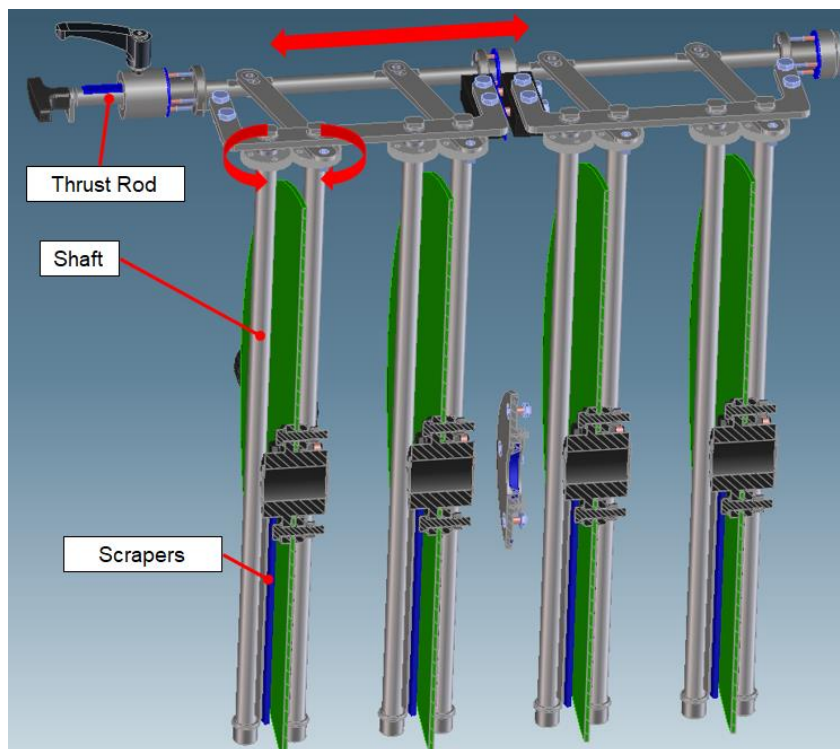
Figure 53: Scrapers system (Meyer/Herrenknecht AG, 2017)
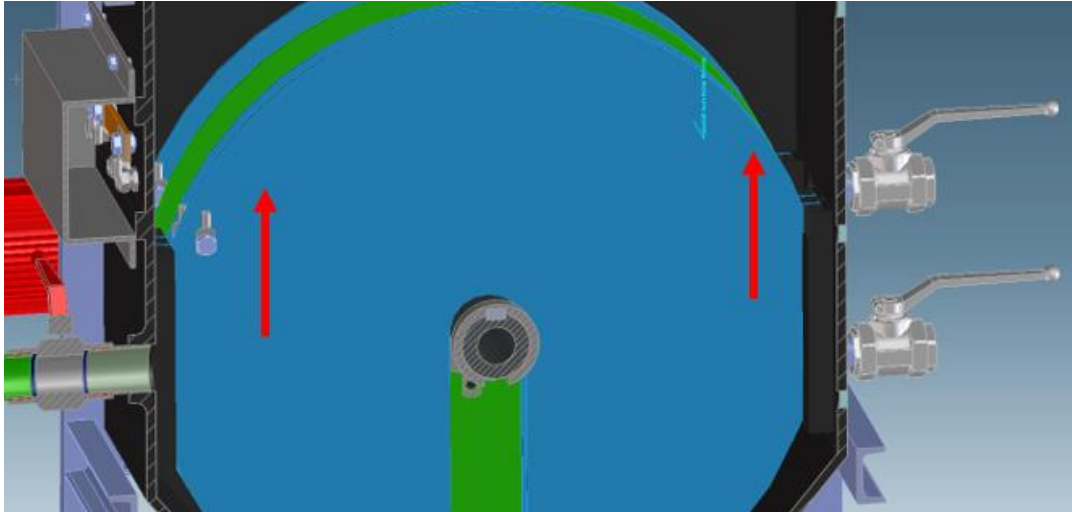
Figure 54:   Cathodes placing (Meyer/Herrenknecht AG, 2017)

Operational parameters

The design of the cell allows a comprehensive parametric study with following operation parameters:

- the amperage can be varied between 1 and 300 A
- the rotation speed, which dictates the cleaning period of the anodes, is between 0 and 0.45 min^{-1}
- the electrode gap can be set at 4.5, 5.5 or 6.5 cm
- there is no technical limit for the duration of the test.

Safety measures

By implementing the electrical current of 300 A in Eq 5-2 and considering the experimentally obtained additional amount of hydrogen (chapter 5.3.6), the hydrogen production of 210 - 280 l/h was calculated. In order to prevent hydrogen from creating an explosive atmosphere (> 4% H_2 concentration in the atmosphere, chapter 3.5.1), a strong ventilation system was integrated in the prototype. The system consists of two ventilators with a nominal volume of 310 m³/h each, which maintains an average hydrogen concentration in the cell of 1 to 2 % of the LEL, meaning 0.04 – 0.08% H_2 concentration in the atmosphere (Dekra, 2016).

Twenty six safety measures were put in place to ensure safe operation of the prototype, some of which are:

- The DC source cannot be turned on if the both cell chambers are not completely filled with fluid. This makes the contact of electrodes with potentially explosive atmosphere impossible. For this reason, fluid level sensors were integrated in the cell, placed just above the anodes.

- The DC source cannot be turned on if the ventilation is not running. This prevents development of an explosive atmosphere. The ventilation system is equipped with sensors that measure the air current in the chimney.
- The DC source cannot be turned on if the EC cell cover is not mechanically and magnetically sealed. This measure keeps hydrogen in the closed ventilation system of the cell and does not allow it to collect in the EC room of the container.
- The DC source cannot be turned on if the doors of the EC room are not completely opened. This prevents building up of an explosive atmosphere in the EC room if the cell leaks. For this reason, door sensors and an additional ventilation system were integrated into the EC room.
- If any of the above-mentioned requirements is no longer met during the experiment (fluid level in the cell drops, ventilation turns off, doors of the EC room close) the DC source is automatically turned off.
- The amount of hydrogen in the EC cell and in the EC room is constantly measured with hydrogen sensors. If the measured values are above allowed values, the sound alarm is activated and the DC source is automatically turned off.
- The ECC is equipped with a battery that keeps the vital security systems in operation in case of a power outage.
- If both the battery and electrical power supply simultaneously cease to function during an experiment, residual amounts of hydrogen can be ventilated manually using the gas cylinder placed in the EC room.

6.2.2 Laboratory chamber filter press (LCFP)

LCFP is basically a small scale chamber filter press, with official product designation LFP 250 Mobil. Its sketch is shown in Figure 55. The LCFP weights 80 kg with total dimensions of 0.8 x 0.6 x 0.45 m. It consists of ten chambers with a total volume of 8 litres and a filter surface of 0.92 m². Filter plates are square, with dimensions 0.25 m x 0.25 m. The LCFP is equipped with a pump which can double the incoming pressure.

The suspension is supplied to the chambers though an opening in the centre of each chamber, shown in the Figure 56. During filtration, the chambers are held together by means of a hydraulic system (up to 500 bar) such that the filtration pressure (up to 15 bar) cannot drive the chambers away from each other and the press remains sealed (Popovic et al., 2018).
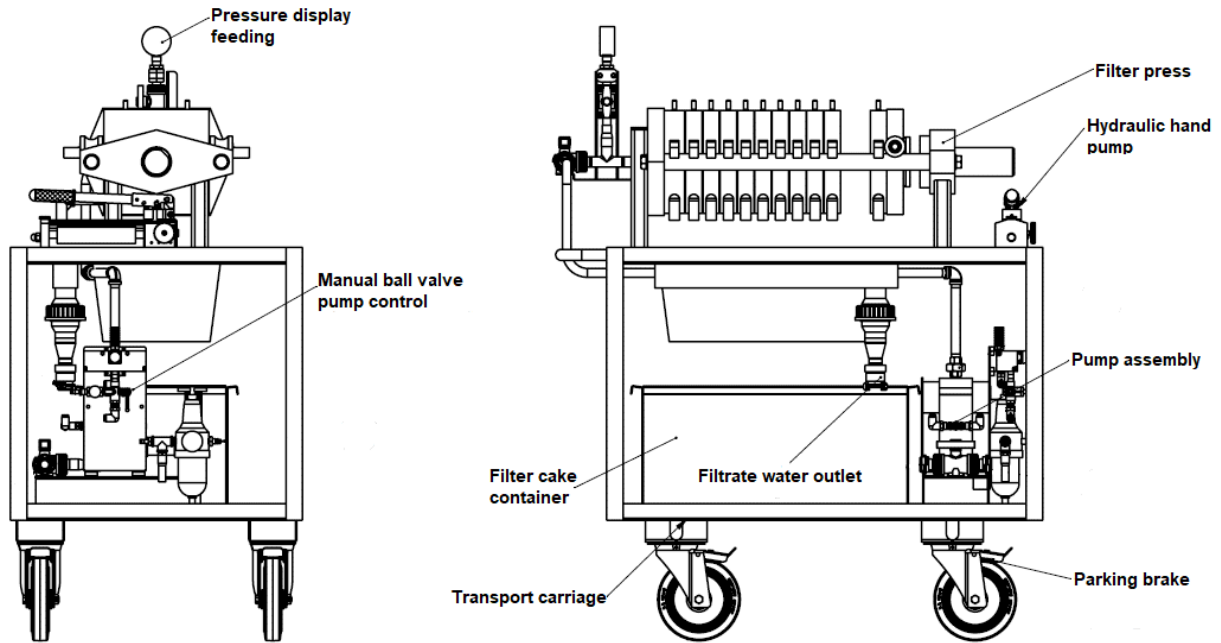
Figure 55:   Sketch of LCFP (MSE, 2016)

Figure 56:   Openings in the centre of the chambers (Popovic & Schößer, 2019)

LCFP allows the investigation of the influence of the EC treatment on the filtration of the suspension. A short pipe on the filtrate outlet drains the filtrate water to a bucket on a scale. The scale is connected to a laptop on which the values from the scale are recorded and stored (Figure 57).
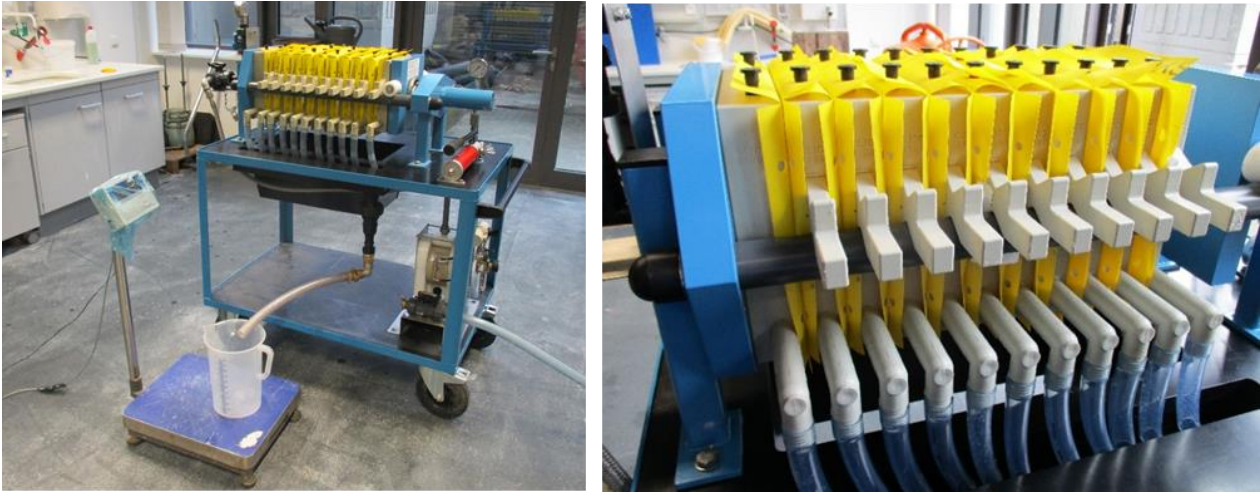
Figure 57: Laboratory chamber filter press (LCFP) with automatic filter water release measuring system (Popovic, 2019)

Since the reason for including the chamber filter press in experimental setup was to investigate the influence of EC on the following filtration, the operating parameters of LCFP were kept constant across experiments.

6.3 Experimental procedure

6.3.1 Mixing of the suspension

SUS was prepared at least one day before the EC experiment. First, the necessary amount of water, bentonite, kaolin, and silica flour was calculated depending on the number of experiments to be performed. Usually, 550 l of suspension were prepared – 3x160 l for three EC experiments and the rest as a backup or for a reference filtration experiment. Even though the stirrer in the ECC had a total volume of 800 l, mixing of the amounts bigger than 600 l had a negative influence on the suspension's quality.

The required amount of water was poured into the stirrer, followed by the step-wise addition of bentonite particles while simultaneously mixing. After mixing, the suspension was left to swell for at least four hours before the addition of kaolin and silica flour particles. These particles were added to the suspension in the same way that the bentonite was previously added to the water. Afterwards, the suspension was left to swell at least for one day before being employed in an EC experiment.

The mixing step does not apply to the experiments in chapter 6.6, since those experiments were performed with a used suspension from a tunnelling construction site.

6.3.2 **Preparation and execution of EC experiment**

Since both chambers in the EC mid-scale cell are identical in construction, the experiments were usually performed in one chamber at a time. The other chamber was filled with water prior to the experiment, because even the electrodes in the non-active chamber had to be covered with fluid during EC. Once the non-active chamber was filled with water or, the cover of the cell was sealed. This allowed activation of the pump.

To homogenize the SUS prior to pumping it into the chamber, it was mixed again for 10 minutes, in case partial sedimentation had occurred.

The EC experiment is operated from the control and mixing room of ECC, with the following main steps:

- The suspension was pumped into the EC cell.

- After clearance of all safety functions, the direct current source was switched on, the intended electrical current was set, and the test was started.

- During the experiment, electrical data was gathered. When necessary, electrical current was manually adjusted on control display of the DC source.

- After conclusion of the planned experiment time, the DC source was turned off. The suspension was left in the cell for about 15 minutes, to ensure complete venting of the residual hydrogen bubbles. In the meantime, samples of the remaining suspension were taken from five extraction points and were analysed for pH value, electrical conductivity, temperature and density.

- The remaining suspension was then pumped out of the cell and gathered in three 50 l buckets. Coagulated material remained on the anodes even after the suspension was completely removed from the cell.

- Samples of the coagulated material were taken from each anode to determine the residual moisture of the coagulated material.

- The complete coagulated material was scratched of the anode, accumulated, dried in the oven and weighed, to determine the total amount of coagulated material

- The EC cell was thoroughly cleaned.

Detailed descriptions of the procedure can be found in appendix B. Figure 58 shows the course of an EC experiment.

Figure 58:   a) Before the experiment: water in the left chamber, SUS in the right chamber, b) Gas developing during the experiment c) After the experiment: the remaining suspension is pumped out of the cell, coagulated material remains on the anodes, d) Thickness of the coagulated material e) Coagulated material with small holes originating from oxygen development on the anodes

6.3.3 Preparation and execution of filtration experiment

The LCFP was usually prepared during the EC experiment. Filter cloth on the filter plates was adjusted and the plates were pressed together. A short pipe was attached to the filtrate water outlet, conveying the filtrate water to a bucket placed on a scale. The scale was connected to a laptop, on which the measured data were stored. The LCFP was connected to the pressure source using pipes.

Detailed execution procedure of filtration experiments can be found in Appendix B. Here, only the main steps are described:

- One 50 l bucket with electrocoagulated suspension was connected to the LCFP using pipes.

- The experiment was started: the pressure supply was turned on and began pumping the suspension from the bucket into the chambers of the press.

- Starting filtration pressure was 7 bar. 3 minutes after the start, the pressure was doubled to 14 bar. The filtration pressure does not however immediately increases to 14 bar; instead, the LCFP regulates it automatically.

- The filtrate water was collected in the buckets on the scale. When the bucket was full during the experiment, it was replaced with a new one.

- After the designated filtration time was reached, the pressure was turned off. This represents the end of the filtration experiment.

- After the pressure inside the chambers had dropped, the hydraulic press holding the plates together was released. From that moment on, the filter plates could again be separated from each other.

- Two filter cakes were collected to measure their residual thickness

- Collected filtrate water was analysed.

- The LCFP was thoroughly cleaned.

Followings figures show the execution and the products of a filtration experiment.

Figure 59:   Execution of a filtration experiment

Figure 60:   Filtrate water (Bezhenov, 2019)

Figure 61:   Filter cakes in the LCFP (links), released from the chambers (right)

6.3.4 **Variations of LCFP experiments execution**

The most common procedure was to filter the remaining suspension directly after EC without further adjustment of the suspension parameters. By using a standardised suspension, a direct connection/correlation between the EC operational parameters and filtration performance could be drawn. This variation of LCFP experiments execution was labelled as "filtration variation 1" (FV1). It is sketched in Figure 62.
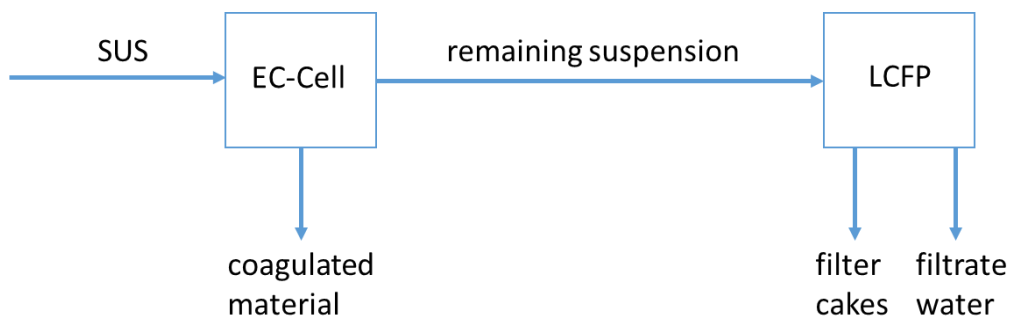
Figure 62:   Suspension flow chart – standard execution of the filtration experiment (filtration variation 1- FV1) (Popovic & Schößer, 2019)

However, in some LCFP experiments, the parameters of the remaining suspension were changed prior to filtration. For example, at one set of experiments, the coagulated material from the anodes was "returned" to the remaining suspension in order to filter all material in the LCFP. At other sets of experiments, conditioning agents (CA) in the form of coagulants and flocculants were added to the suspension and prior to filtration. Those variations of LCFP experiments execution were labelled as FV2a and FV2b, respectively (Figure 63).
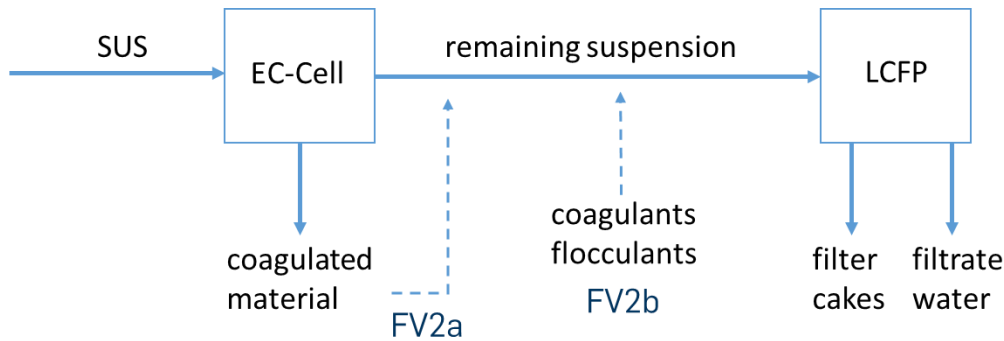
Figure 63:   Suspension flow chart – filtration variation 2a and 2b (Popovic & Schößer, 2019)

Besides two cases of direct (material-specific) influences, the suspension parameters were also indirectly influenced in certain sets of experiments. This was done with adjustments of the suspension's temperature or by ageing of the suspension (not filtering directly after EC but one or more days later). Those variations of LCFP experiments execution were labelled as FV3a and FV3b, respectively (Figure 63).
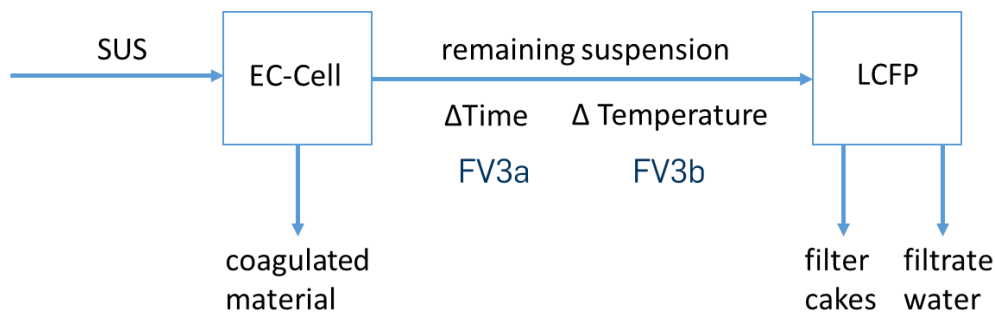
Figure 64:   Suspension flow chart – filtration variation (FV) 3a and 3b (Popovic & Schößer, 2019)

6.4 Evaluation and overview of the mid-scale experimental series

6.4.1 Evaluation parameters

The EC experiments with the mid-scale prototype were evaluated using the same parameters as the laboratory experiments, and in addition, selected new parameters.

The effectivity parameters from the laboratory scale allow a comparison between laboratory and mid-scale experiments. No adaptation of those parameters (percentage of coagulated

soil B_{kt}, the decrease of the remaining suspension density $\Delta\rho$ and the decrease of the remaining suspension stability ΔFW) for the larger scale was necessary.

However, some of those parameters were less well suited to larger scale experiments. The parameter ΔFW was used to evaluate the destabilization effect of EC treatment on the suspension through increase of the filter water release in the API-filter press. As the results from chapter 6.5 show, this parameter cannot accurately predict the effect of EC on the filtration. Therefore, the actual filtration performance in LCFP was much more significant when than the parameter ΔFW evaluating the experiments.

Besides three evaluation parameters from the previous research phase, several new parameters were defined. The first parameter is the residual moisture of the coagulated material on the anode, RM_{CM}. It is calculated as the difference of the wet and dry sample weight divided by the wet weight (Eq. 6-1). This parameter complements the parameter B_{kt}. By taking both paramters into consideration, not only the total amount but also the residual moisture of the coagulated material on the anodes is described.

$$RM_{CM} = \frac{m_{w,CM} - m_{d,CM}}{m_{w,CM}} \qquad \text{(Eq. 6-1)}$$

with:

RM_{CM} residual moisture of coagulated material [-]

$m_{w,CM}$ wet weight of coagulated material [kg]

$m_{d,CM}$ dry weight of coagulated material [kg]

Further parameters describe the filtration process in the LCFP. The first parameter is the residual moisture of the filter cakes, RM_{FC}. It is defined similar to the previous parameter.

$$RM_{FC} = \frac{m_{w,FC} - m_{d,FC}}{m_{w,FC}} \qquad \text{(Eq. 6-2)}$$

with:

RM_{FC} residual moisture of filter cakes [-]

$m_{w,FC}$ wet weight of filter cakes [kg]

$m_{d,FC}$ dry weight of filter cakes [kg]

The following two parameters evaluate the filtration performance of the suspension after EC in comparison to filtration performance of the same suspension conditioned with CA. The parameter ΔFV_{EC} (Eq. 6-3) describes the change of filtration volume with EC. It is defined as the increase of the volume of the dewatered suspension after EC compared to the volume of the dewatered suspension by the filtration with CA.

$$\Delta FV_{EC} = \frac{V_{FW,EC} + V_{cfp}}{V_{FW,CA} + V_{cfp}} - 1 \qquad \text{(Eq. 6-3)}$$

with:

ΔFV_{EC} change of the volume of the filtrated suspension after EC [-]

$V_{FW,EC}$ filtrate water discharge after EC [m³]

$V_{FW,CA}$ filtrate water discharge with CA [m³]

V_{cfp} volume of the chamber filter press [m³]

The parameter ΔFt_{EC} (Eq. 6-4) describes the change of filtration time with EC. Similar to the previous parameter, it is defined as the increase of the filtration time after EC compared with the filtration time with CA.

$$\Delta Ft_{EC} = \frac{t_{FW,EC}}{t_{FW,CA}} - 1 \qquad \text{(Eq. 6-4)}$$

ΔFt_{EC} change of the filtration time after EC [-]

$t_{FW,EC}$ filtration time after EC [h]

$t_{FW,CA}$ filtration time with CA [h]

The last parameter that describes filtration performance is the FW_{rel} (l), stating the filter water release at the end of the filtration experiment.

It should be noted that an increase in filtrate water release does not necessarily indicate that a filtration process is improved, i.e. that it will be completed more quickly. If two suspensions with different densities have the same filtrate water release after a certain filtration time, the filter cake from the suspension with a lower density will have a higher residual moisture. Since EC reduces the density of the used suspension, a higher filtrate water release is required to complete the filtration process and achieve acceptable residual moisture of filter cakes.

In practice, two criteria determine when the filtration process is considered complete:

- when approximately 80 % of the total amount of filtrate water is released
- when the maximum filtration pressure is reached.

The second criteria cannot be used for filtration with the LCFP because the maximum filtration pressure is reached very early (after approx. 5 minutes). Therefore, the first criteria is used in further analysis.

To explain how this affects the parameters ΔFV_{EC} and $\Delta Ft_{EC,}$ one example with two filtration experiments is shown in Figure 65. In the figure, the abscissa corresponds to the filtration

time and the ordinate to the filtrate water discharge. The second EC experiment from the fifth experimental series with the prototype (PES5_EC2) and the reference filtration experiment with CA were chosen for this example.
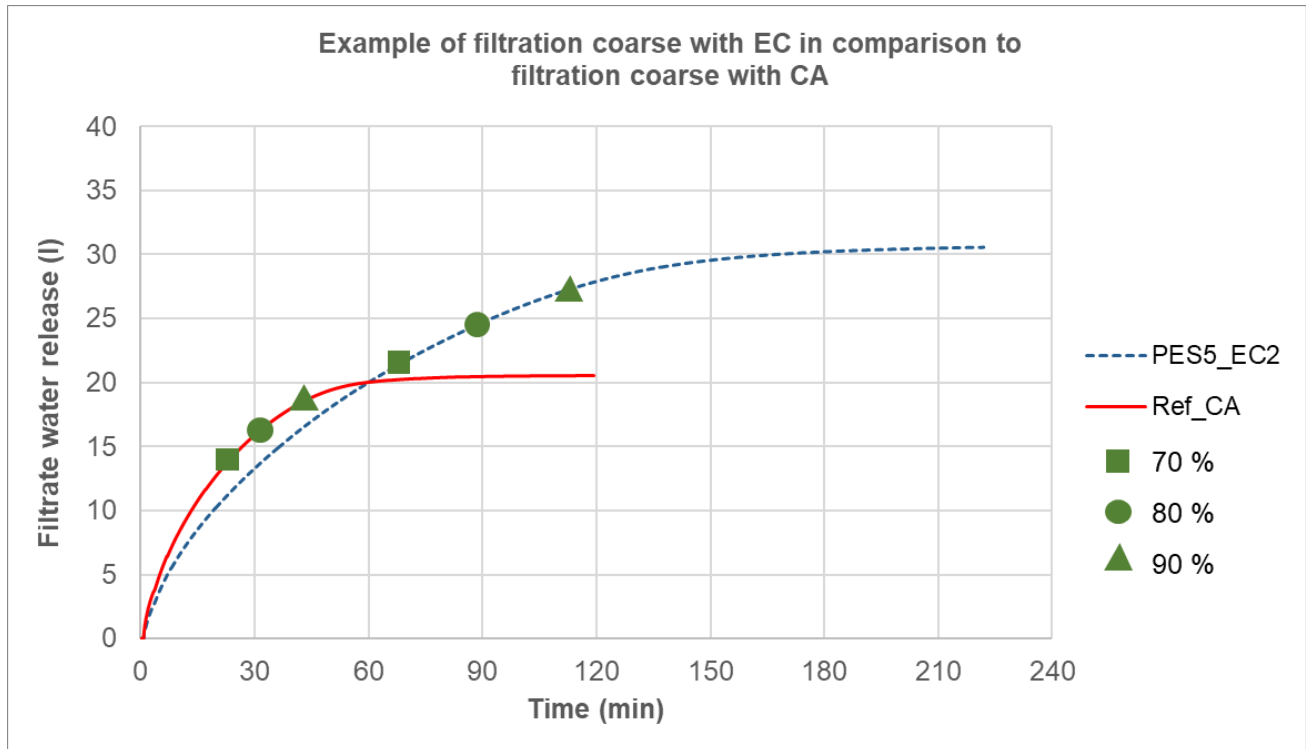
Figure 65:   Example of filtration experiments with SUS, with CA (Ref_CA) and with EC (PES5_EC2)

To determine how the criteria "approximately 80 % of total amount of filtrate water release" influences the evaluation parameters ΔFV_{EC} and ΔFt_{EC}, a sensitivity analysis was performed. The points on the filtration curve at which 70, 80 and 90 % of the total amount of filtrate water was released are marked in the figure. Those filtration times and the corresponding filtrate water volumes are listed in Table 17. Parameters ΔFV_{EC} and ΔFt_{EC} were calculated after Eq. 6-3 and Eq. 6-4. The variable V_{cfp} throughout this thesis is equal to 8 l, since the same amount of LCFP chambers (all ten of them) was used at every filtration experiment.

Table 17:   Calculation of parameters ΔFt_{EC} and ΔFV_{EC} at 70, 80 and 90 % of the filtration

Experiment	FW$_{rel}$	70 %		80 %		90 %	
		Time (min) $t_{FW,EC/CA}$	Volume (l) $V_{FW,EC/CA}$	Time (min) $t_{FW,EC/CA}$	Volume (l) $V_{FW,EC/CA}$	Time (min) $t_{FW,EC/CA}$	Volume (l) $V_{FW,EC/CA}$
PES5_EC2	30.6	67.9	21.4	88.5	24.6	115.3	27.5
Ref_CA	20.5	24.6	14.4	31.8	16.4	42.3	18.5
		$\Delta Ft_{EC}=1.76$	$\Delta FV_{EC}=0.31$	$\Delta Ft_{EC}=1.78$	$\Delta FV_{EC}=0.34$	$\Delta Ft_{EC}=1.73$	$\Delta FV_{EC}=0.34$

As shown in Table 17, the parameters ΔFV_{EC} and ΔFt_{EC} are only slightly affected by the point at which the filtration is evaluated. ΔFV_{EC} was in the range of $0.31 - 0.34$ and ΔFt_{EC} in the range of $1.73 - 1.78$. Considering the whole range of values for those to parameters and the difference between single EC experiments, this difference can be neglected. Therefore, the values for ΔFV_{EC} and ΔFt_{EC} in the further analysis are always calculated at the point of 80 % of total amount of the filtrate water release.

On this place, two main differences between the new evaluation system for filtration and the parameter ΔFW, used for the evaluation of the laboratory experiments, need to be highlighted:

- ΔFW compares the filtration after EC to the filtration prior to EC without CA. The new parameters always compare the filtration after EC to the filtration with CA. This is a huge difference. As the results of reference filtration experiments show (chapter 6.5.1), CA significantly improve the filtration. Moreover, it a more practice-relevant comparison, since CA are usually employed in fine separation process.

- ΔFW compares two filtrations at the same filtration time. The higher the filter water release at a fixed time (7.5 minutes after DIN 4127:2014-02), the more destabilised the suspension is. This is mostly correct; however, such evaluation cannot predict the filtration performance as it does not take into consideration the decrease of the suspensions density after EC. When looking at Figure 65, evaluation of the filtration at t = 30 min just by comparing the filtrate water volume would conclude that CA is more effective than EC. At t = 60 min the effectiveness is equal, and at t=90 min, EC performs better than CA. Therefore, it is necessary to compare filtrations at the same stage of completion, instead of at the fixed filtration time.

6.4.2 Prototype experimental series (PES)

EC and filtration experiments presented in this thesis are listed in Table 18. First, EC operating parameters were investigated in the experiments using SUS. Additionally, suspension parameters were investigated by performing EC experiments with different suspension mixes. In one case, an SUS with reduced density was mixed. The same bentonite concentration and the same soil particles were used, but with less load. In another case, a used suspension from a construction site (CUS) was tested. Moreover, in order to determine the effects of EC on the filtration performance, reference filtration experiments without EC were performed.

After every EC experiment there was enough remaining suspension to perform three filtration experiments. Therefore, the amount of filtration experiments was in some experimental studies higher that the amount of EC experiments.

Table 18:   Experimental series with mid-scale prototype and LCFP

Experimental series	Code	Suspension	Number of EC experiments	Number of LCFP experiments
Validation experiments	PES1	SUS	17	36
Influence of the current density	PES2	SUS	3	3
Influence of the electrodes gap	PES3	SUS	6	6
Influence of the anodes' cleaning interval	PES4	SUS	4	4
Influence of the EC experiment duration	PES5	SUS	4	4
Fine-tuning experiments	PES6	SUS	6	6
Influence of the suspension's density	PES7	SUS with reduced density	3	3
Experiments with the suspension from the construction site	PES8	CUS	7	34
Reference filtration experiments with LCFP	Ref	SUS, CUS, SUS with reduced density	-	13
		∑	**50**	**109**

The most important findings from PES1, PES5 and PES8 were presented in the final report of this research (Popovic & Schößer, 2019).

6.5 Experiments with SUS / standard used suspension

6.5.1 Reference experiments in LCFP

Reference experiments are the filtration experiments in which the suspension has not been electrocoagulated previously. They serve as a basis for comparison; the filtration curves after EC tests are compared to each other and to reference tests. In order to carry out a practice-relevant evaluation, the filtration after EC had to be compared to the filtration without conditioning agents (CA) as well as with CA.

The reference tests are shown in Figure 66 and Figure 67. Figure 66 presents reference filtration experiments without CA, where SUS was mixed with the following densities: 1.26, 1.22, 1.20 and t/m³. SUS with reduced density was always mixed the same way. The bentonite concentration in the suspension was not changed. Instead, the loading with kaolin, M300 and M500 was reduced, but the ratio between them was kept constant (kaolin W : M300 : M500 = 3 : 4 : 10). As can be seen from the figure, the reduction of suspensions density has an influence on the filtration. More filtrate water is released in the same time.
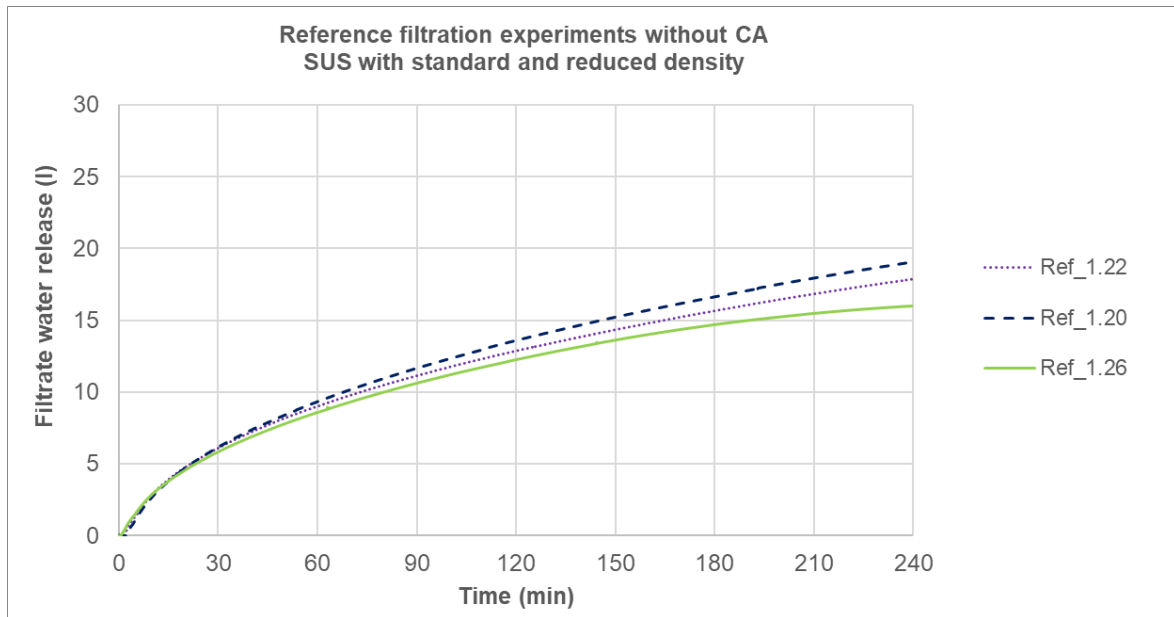
Figure 66: Reference filtration experiments without CA – SUS with standard and reduced density

Figure 67 presents the reference filtration experiments with CA. Ferric chloride ($FeCl_3$) was used as coagulant and anionic polyacrylamide was used as flocculant. The data sheet of conditioning agents can be found in appendix A. The density of the suspension before conditioning was 1.26 t/m³. However, due to the addition of CA, the density was reduced to 1.24 t/m³. The same occurs on the construction sites when CA are added prior to filtration.

For every filtration experiment, 40 l of suspension was prepared. In the experiments with CA, the suspension was conditioned with 40 ml FeCl3 and 8 g polymers (dissolved in 4 l tap water).
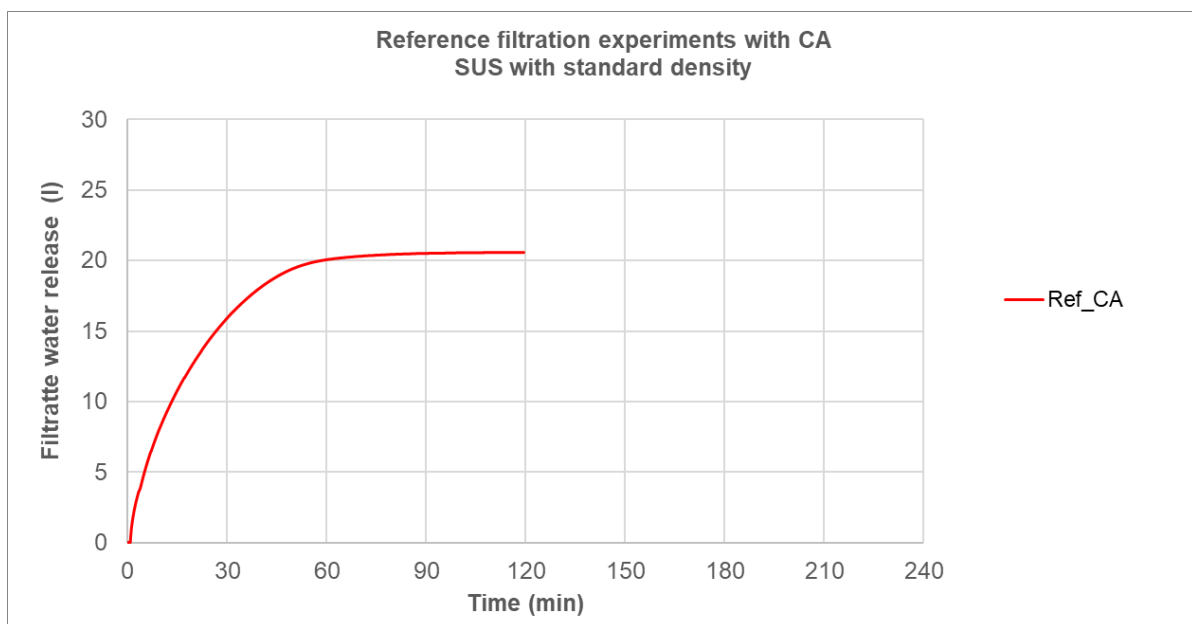
Figure 67: Reference filtration experiments with CA

Not all of the reference experiments are presented here. For example, the reference filtration experiment with SUS density of 1.26 t/m³ was performed 7 times. The filtration curve presented here is the average value over all those experiments. Since deviations in this case were proven insignificant, reference experiments with reduced densities were generally performed fewer times (i.e. once or twice). All reference filtration experiments can be found in appendix C.

6.5.2 PES1: Validation EC experiments

The aim of the first prototype experimental series (PES) was to determine whether the operating parameters in the EC prototype cell have a similar effect on the SUS as in the laboratory-scale experiments. The performed experiments and their operation parameters are listed in Table 19. The parameters electrical current and current density represent the average values since the electrical current fluctuates during EC.

Table 19:   Validation experimental series (PES1) – EC operational parameters

Code	Electrode gap (cm)	Duration (min)	Electrical current (A)	Current density (A/l)	Charge density (Ah/l)	Cleaning interval (min⁻¹)
PES1_EC1	4.5	30	142.4	0.89	0.45	0.45
PES1_EC2	4.5	30	120.0	0.75	0.38	0.2
PES1_EC3	4.5	30	128.0	0.80	0.40	0
PES1_EC4	4.5	30	120.0	0.75	0.38	0
PES1_EC5	4.5	30	80.8	0.51	0.26	0
PES1_EC6	4.5	30	20.6	0.13	0.07	0
PES1_EC7	4.5	60	86.4	0.54	0.27	0
PES1_EC8	4.5	30	124.8	0.78	0.39	0
PES1_EC9	6.5	30	62.4	0.39	0.20	0
PES1_EC10	6.5	30	70.4	0.44	0.22	0.45
PES1_EC11	6.5	30	52.8	0.33	0.17	0
PES1_EC12	4.5	30	42.8	0.27	0.14	0
PES1_EC13	4.5	60	100.8	0.63	0.63	0.45 until minute 35
PES1_EC14	4.5	30	120.0	0.75	0.38	0
PES1_EC15	4.5	30	113.6	0.71	0.35	0
PES1_EC16	4.5	30	104.0	0.65	0.33	0

As mentioned in chapter 6.3, the suspension is after EC treatment filtrated in LCFP, in order to evaluate the influence of EC on the dewatering of used suspensions. The figures in this

chapter present the results on those filtrations. The evaluation parameters (chapter 6.4.1) are always listed in the tables, they are not presented in figures. Since the filtration after EC in PES1 was conducted only for 2 hours and not fill the end (determined with horizontal or almost horizontal line at the end of filtration curve), it was not possible to calculate parameters ΔFV_{EC} and ΔFt_{EC}. The same goes for PES7 and PES8.

The first question in PES1 was: is the increase in filtrate water release caused only by a reduced density of the remaining suspension, or is the suspension after EC actually destabilised? The remaining suspension after EC experiments 2, 3 and 4 had a density of 1.19, 1.20 and 1.21 t/m³, respectively. The comparison of filtration curves EC2, EC3 and EC4 with the reference filtration experiments Ref_1.20 and Ref_1.22 shows that the remaining suspension could be filtered much faster than the non-electrocoagulated SUS with the same density (Figure 68). In this case, calculating the parameters ΔFV_{EC} and ΔFt_{EC} is unnecessary since the densities of the compared suspensions are identical. However, the EC experiments 2, 3 and 4 were not as effective as the addition of CA in destabilizing the SUS.
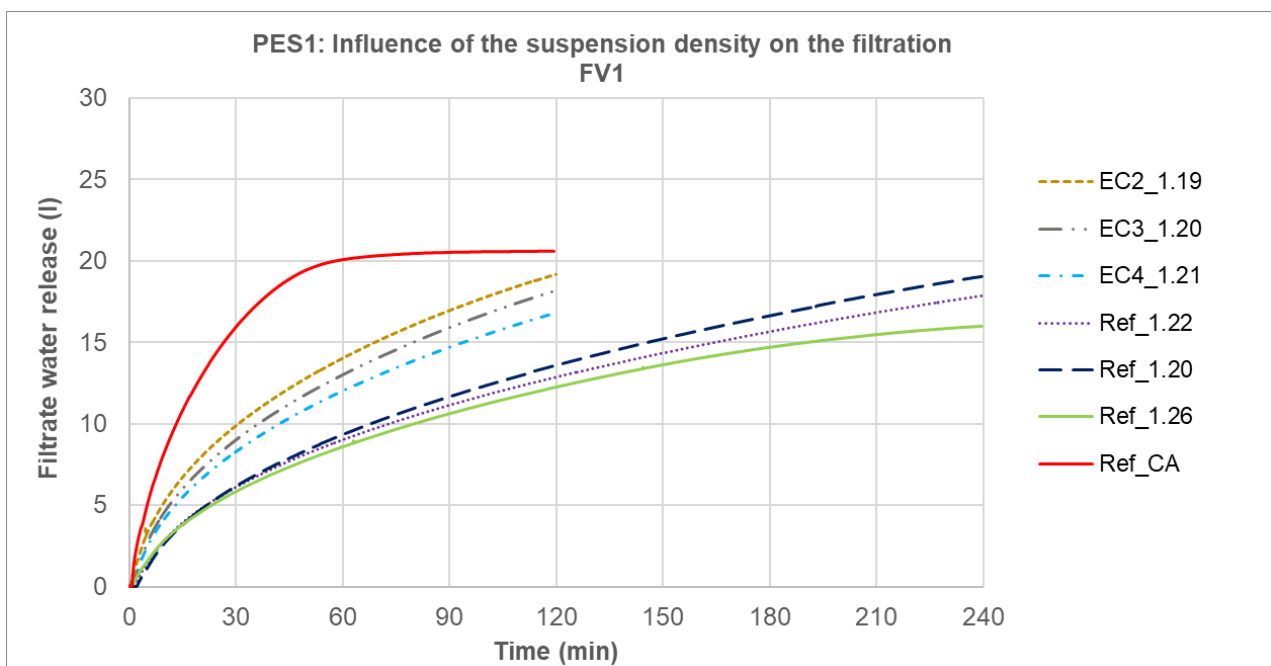
Figure 68: Influence of the remaining suspension density on the filtration

This led to the next research question: can the coagulated material from the anodes be returned to the remaining suspension in order to filter everything together? This could be beneficial due to the fact that the residual moisture of the coagulated material was higher than the residual moisture of the filter cakes. Filtrating everything together should produce output with overall lower residual moisture. This was tested in filtration variation FV2a. The results of this series of experiments are shown in Figure 69. Overall, it can be said that the return of the coagulated material to the remaining suspension had a negative effect on the

subsequent filtration. After 30-minute EC experiments (EC10 - EC12), the filtration improvement through EC was minimal. Only at a 60-minute EC test (EC13) the improvement of the filtration was noticeable. This means, if the FV2a is performed, more electrical consumption is required to improve the filtration after EC.

To further investigate the effects of the return of the coagulated material to the remaining suspension, the suspension from the EC13 experiment was filtered again, this time without the return of the coagulated material (EC13_1.11_FV1 in Figure 69). The remaining suspension without addition of the coagulated material showed a significantly higher increase in filtrate water release at any given time. In the first 30 minutes, the filtrate water release of this filtration was almost identical to the filtrate water release of the reference experiment with CA. The comparison between filtration curves EC13_1.25 and EC13_1.11_FV1 showed that the filtration performance reduces significantly if the coagulated material is returned to the remaining suspension.
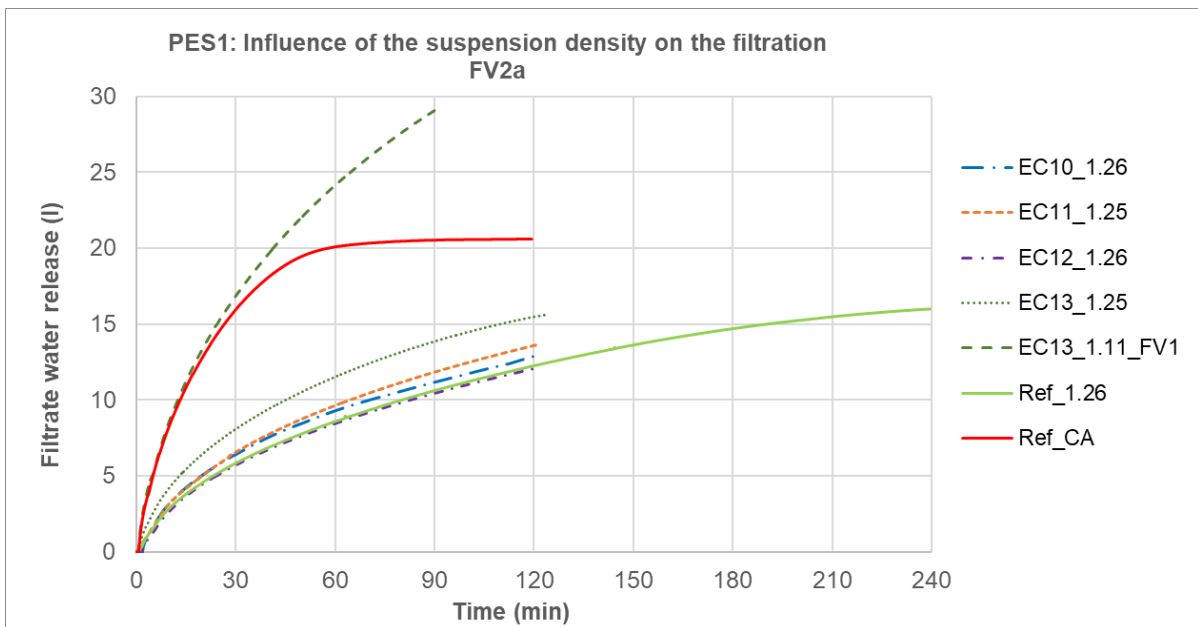
Figure 69:   Influence of the remaining suspension density on the filtration, with (FV2a) and without (FV1) return of the coagulated material to the suspension

The next focus was directed at the influence of volumetric current density (in further text: current density) on filtration. In Figure 70, the filtration curves are divided into two groups: 0.65 - 0.80 A/l (orange lines) and 0.39 - 0.51 A/l (blue lines). The duration of all EK experiments was 30 minutes. Therefore, the results present also the influence of charge density (Ah/l) on the filtration. The diagram shows that higher current densities are more effective than the lower current densities. At current densities lower than 0.5 A/l, or rather, the charge densities lower than 0.25 Ah/l, the destabilisation effect of EC was negligible. The filtration was similar to reference experiments without CA.
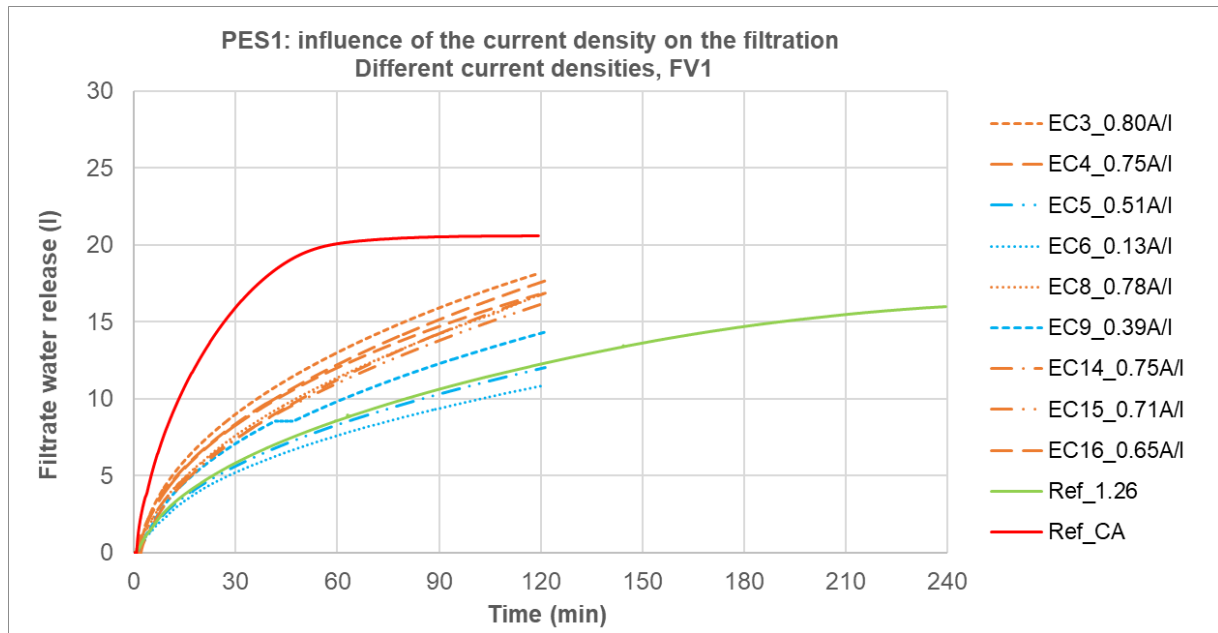
Figure 70:   Influence of the current density on the filtration

Figure 71 shows the filtration curves after three EC tests with the same current density and the same charge density. The filtration curves are almost identical. This highlights either current density or charge density as one of the most important operating parameters.
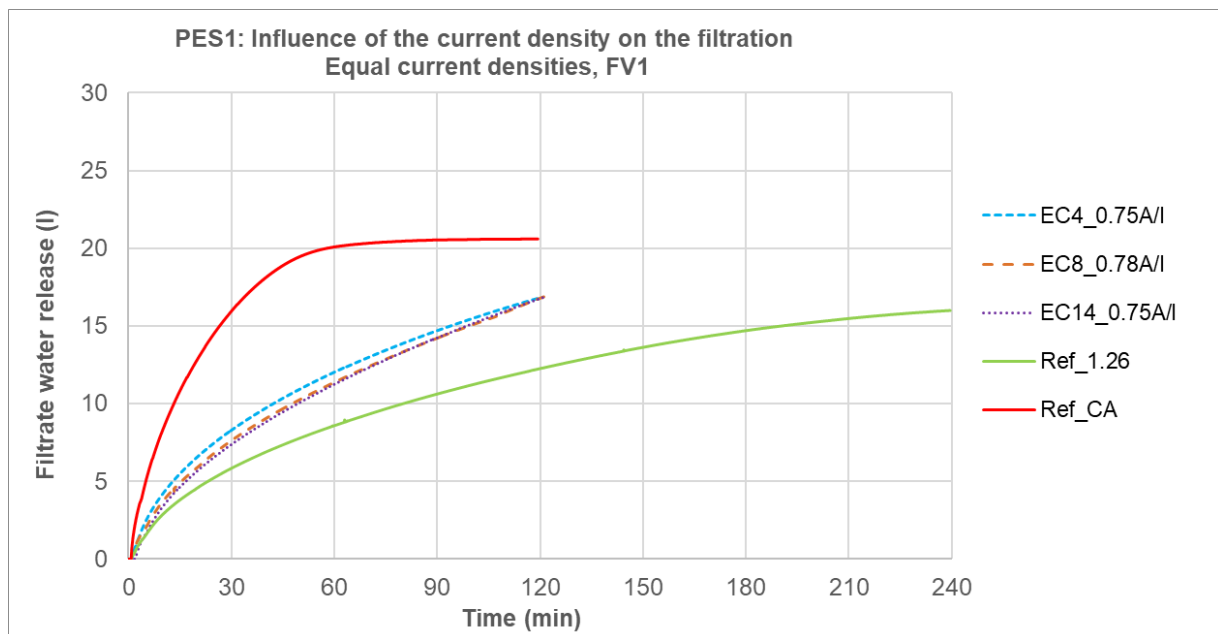
Figure 71:   Influence on the identical current density on the filtration

To investigate which one of those operating parameters is decisive, EC experiments with identical current densities (A/l) but different charge densities (Ah/l) were performed. Different charge densities were achieved through variation of EC duration. The results are shown in Figure 72. EC tests 5 and 7 (blue lines) as well as 15 and 17 (purple lines) were performed

with the same current density, with EC17 lasting 15 minutes longer than EC15 and EC7 lasting 30 minutes longer than EC5. The positive influence of the EC experiment duration or rather of charge density on filtration performance is clearly visible.
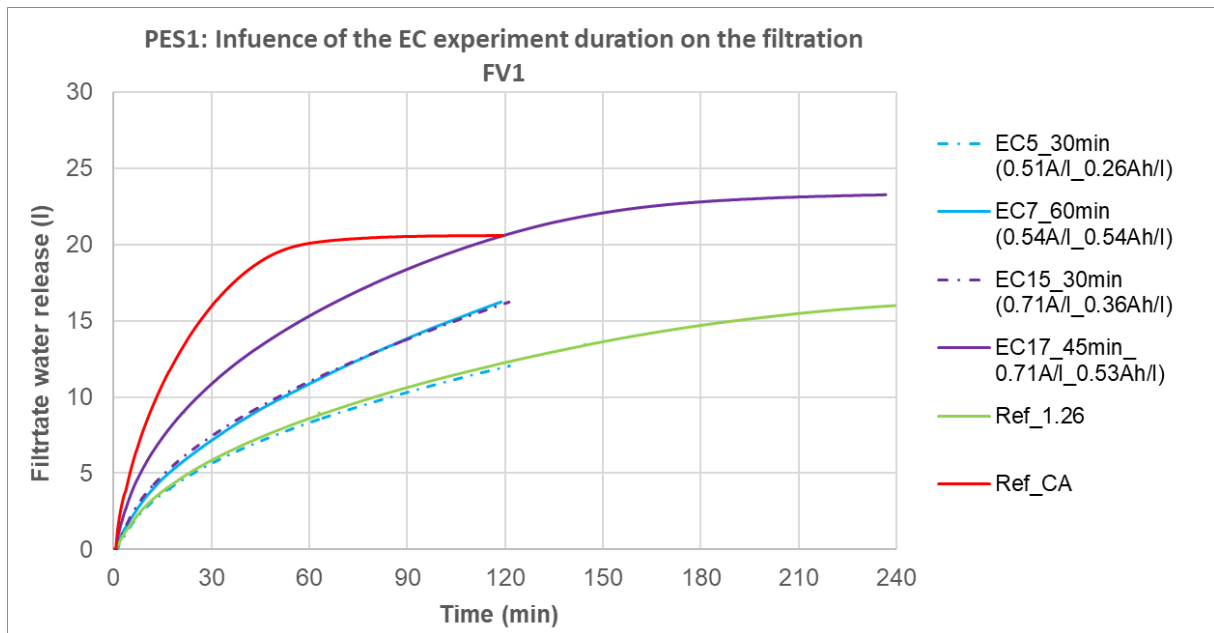
Figure 72:   Influence of the experiment duration and charge density on the filtration

The next part of the investigation was concerned with the effect of the waiting time on the filtration (FV3a). As mentioned previously, after every EC experiment there was sufficient remaining suspension to perform three filtration experiments. The remaining suspension from experiments EC1-EC4 was filtrated once directly after EC (FV1) and once on the next day. Suspension from the EC2 and EC3, was filtrated once more (third time), 4 days after EC. The results are presented in Figure 73.

Analysing the filtration after EC1 and EC4, it can be seen that the waiting time of one day did not influence the filtration performance. However, the waiting time after EC2 and EC3 showed a negative influence on the following filtration, reducing the positive effect of EC.

The waiting time issue was further researched in chapter 6.6.
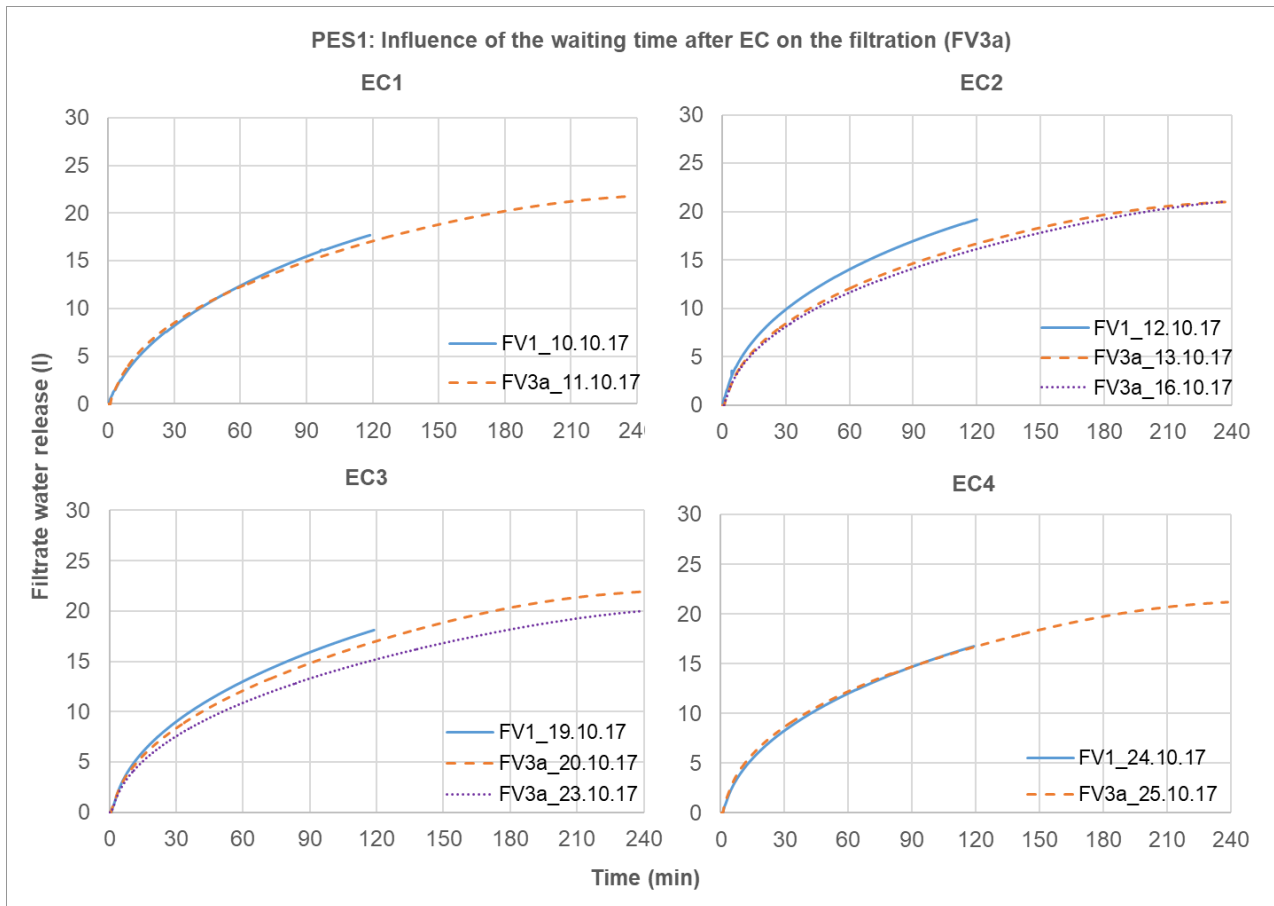
Figure 73: Influence of the waiting time after EC on the filtration (FV3a)

Discussion

This experimental series provided several interesting findings. One of them is the influence of electric current (A), or rather, current density (A/l), on the results – higher current improves EC performance. This is consistent with the laboratory results on electrical current (chapter 5.3.2). Presenting the results in terms of current density instead of electrical current is becoming a standard in EC literature, since it makes possible to compare the effectiveness of EC cells with different sizes. Therefore, the same was done in this thesis. The influence of the current density is further investigated in the following experimental series (PES2).

Another interesting finding is that the optimal duration for EC is not always 30 minutes. The EC experiments with 45-minute or 60-minute duration provided better results than EC experiments with the same current and 30-minute duration. This is in agreement with the laboratory results on experiment duration (section 5.3.4). In summary, the laboratory and prototype results showed that the optimal EC duration time for the SUS is not always 30 minutes, as it was for the not-loaded bentonite suspension researched by Paya (2016). This can be explained by higher density of SUS and the fact that all those fine soil particles need to be destabilised. Optimal EC duration is further researched in section 6.5.6.

Those two operational parameters, current density (A/l) and experiment duration (h), can be defined as one operational parameter - charge density (Ah/l). This parameter seems to have the highest influence on the results, which is consistent with the theory. According to the Faraday's law (Eq. 3-5), the electrodissolution of the anode is controlled by electrical charge (Ah) - electrical current (A) and current flow duration (h). Furthermore, the bigger the suspension volume is, the more particles need to be destabilised.

The third finding is that the return of the coagulated material back to the remaining suspension significantly reduces benefits of EC treatment. An initial objective of this idea was to investigate if the complete material from the EC cell could be transferred to the filter press and dewatered, rather than doing two-phase separation. However, the results suggest that two-phase separation is significantly more effective. Furthermore, the residual moisture of the coagulated material is not high enough to require further dewatering. This subject is further discussed in chapter 7.

6.5.3 PES2: Influence of the current density

The next experimental series focused on further investigation of the influence of the current density on filtration. Three experiments with different current densities were performed. Since this experimental series was performed at an outdoor temperature close to 0° C, only relatively small current densities were reached. Nevertheless, they delivered interesting results and supplemented the knowledge gained in the validation experiment series. The complete operational parameters are listed in Table 20 and the evaluation parameters in Table 21.

Table 20: Current density experimental series (PES2) – operational parameters

Code	Electrode gap (cm)	Duration (min)	Electrical current (A)	Current density (A/l)	Charge density (Ah/l)	Cleaning interval (min^{-1})
PES2_EC1	4.5	30	56	0.35	0.18	0
PES2_EC2	4.5	30	72	0.45	0.23	0
PES2_EC3	4.5	30	83	0.52	0.26	0

Results

Table 21: Current density experimental series (PES2) – evaluation parameters

Code	Δρ (%)	ΔFW API (%)	B$_{kt}$ (%)	RM$_{cm}$ (%)	Rm$_{fc}$ (%)	ΔFt$_{EC}$	ΔFV$_{EC}$	FW$_{rel}$
PES2_EC1	14.5	18.7	10.5	46.8	26.6	2.99	0.03	21.5
PES2_EC2	19.2	29.4	11.2	46.6	26.4	2.70	0.04	21.9
PES2_EC3	16.7	19.8	15.0	46.7	27.3	3.11	0.08	22.8

The filtration course from these three experiments and their respective reference experiments are shown in Figure 74. The results show a slight positive influence of increasing current density during EC on the filtration efficiency. Moreover, more soil particles coagulated at higher current densities (Table 21).

The filtration experiments, however, did not match the performance of filtration of SUS with added CA. The parameters ΔFV_{EC} and ΔFt_{EC} show how bad EC performed in comparison to CA: the increase of the volume of the filtrated suspension was 3 – 8 % ($\Delta FV_{EC} = 0.03 - 0.08$), while the filtration time was prolonged for 299 – 311 % ($\Delta Ft_{EC} = 2.99 - 3.11$).
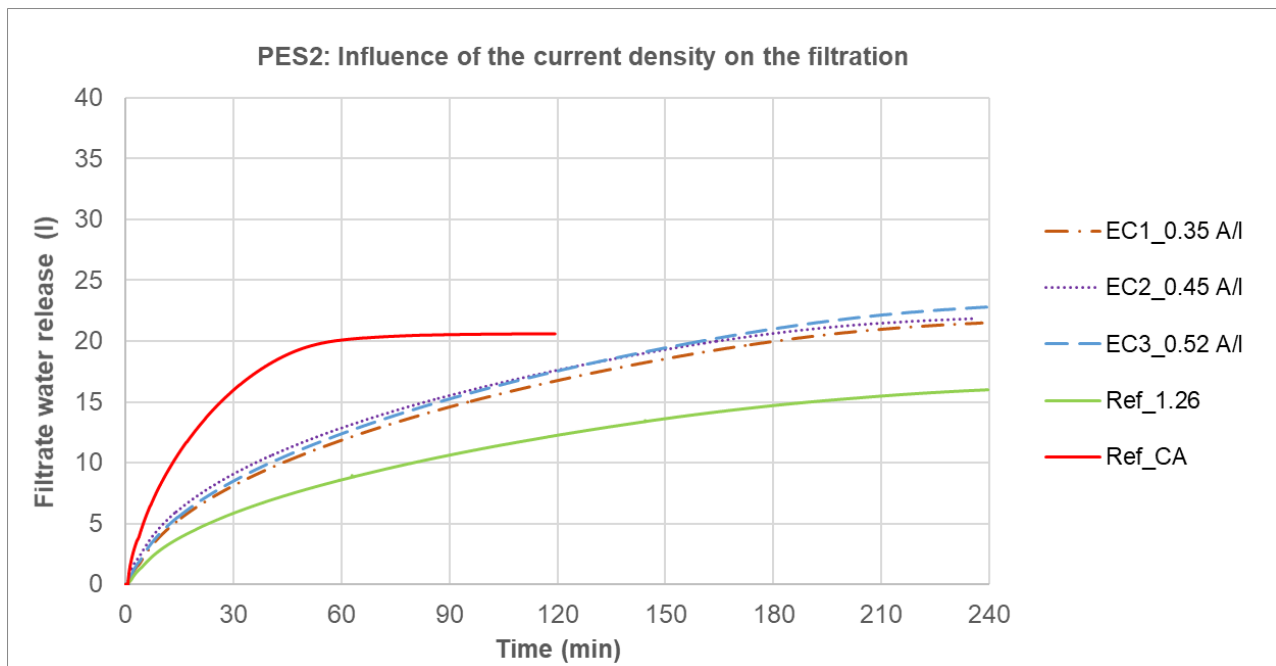
Figure 74: **Influence of the current density on the filtration**

Discussion

The objective of the experimental series was to further investigate the influence of current density on the EC results. Even though only relative small currents were achieved and the difference between them was insignificant, this experimental series showed clear influence of current density on the results. Higher current densities produced better results. These results are in agreement with the literature (chapter 3.3.2), laboratory results (chapter 5.3.2), and the results of the validation experimental series (chapter 6.5.2).

Concerning the optimal current density within the technical limits of the EC prototype, the results of this experimental series, together with the results from the validation EC experiments, suggest that this operational parameter should be as high as possible. The technical limit of the prototype is 0.94 A/l when both chambers are in use (300 A / 320 l) and 1.25 A/l for one chamber only (200 A / 160 l). However, only current densities up to 0.89 A/l were tested in PES1 and PES2. The economic impacts of the recommendation for the maximum

current density are at the moment not discussed: only the filtration performance is taken into consideration.

6.5.4 **PES3: Influence of the electrode gap**

The next experimental series was concerned with the influence of the electrode gap on the EC performance and subsequent filtration. Six EC experiments were conducted: EC1 - EC3 with the duration of 30 minutes and EC4 - EC6 with duration of 60 minutes. At each of those durations, all three possible electrode gaps were investigated.

Increasing the gap between electrodes increases the resistance (Eq 3-12), which means that at the same voltage, lower current can be reached. In order to exclude the influence of the current density and investigate only the influence of the electrode gap, the experiments EC1 - EC3 were performed with identical current densities. First, the experiment with the electrode gap of 6.5 cm was performed. Afterwards, the electrical current for the experiments with the electrode gaps of 5.5 and 4.5 cm was manually decreased in the last minutes of experiments, as shown in Figure 75. In this way, the same average current density was applied in all three experiments.
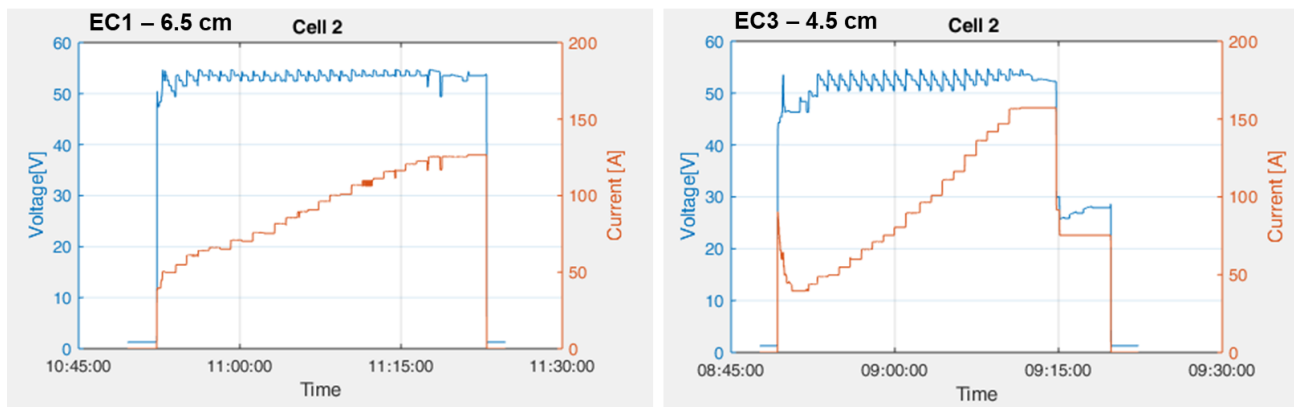
Figure 75:   Time lapse of voltage and electrical current during PES3_EC1 and PES3_EC3

In the second part of the parametric study (EC4 - EC6), the experiments were performed with the maximum voltage rather than with the same average current density. This means that the electrical current was at the maximum possible value for the given voltage and the gap (Figure 76), during the whole experiment. It is clear from these experiments that a larger electrode gap resulted in a lower electrical current with the same voltage. In addition, this set of experiments (EC4 - EC6) was performed with the EC duration of 60 minutes.

Complete list of operational parameters of this experimental series is presented in Table 22.
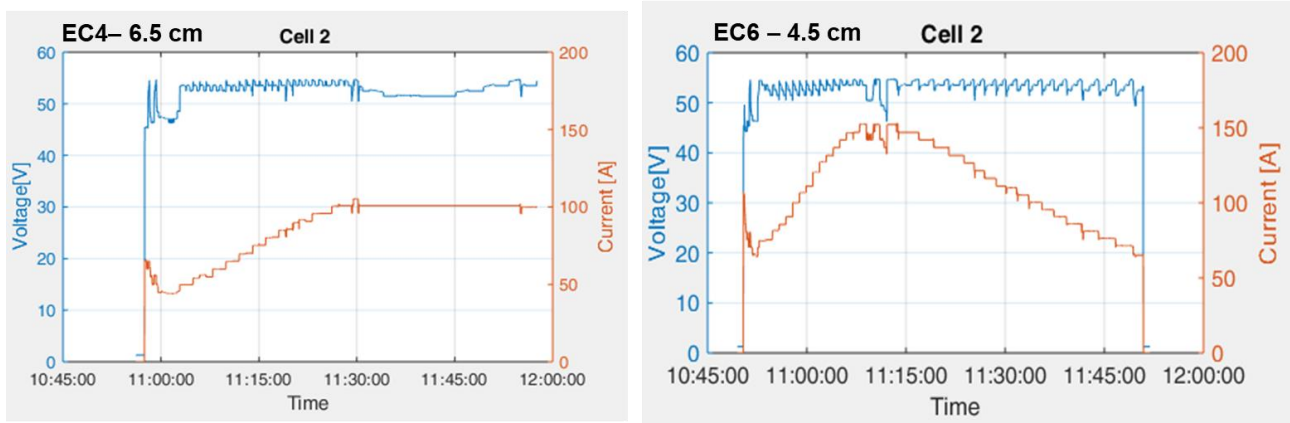
Figure 76: Course of voltage and electrical current during PES3_EC4 and PES3_EC6

Table 22: Electrodes gap experimental series (PES3) – operational parameters

Code	Electrode gap (cm)	Duration (min)	Electrical current (A)	Current density (A/l)	Charge density (Ah/l)	Cleaning interval (min⁻¹)
PES3_EC1	6.5	30	93	0.58	0.29	0
PES3_EC2	5.5	30	93	0.58	0.29	0
PES3_EC3	4.5	30	93	0.58	0.29	0
PES3_EC4	6.5	60	max. / 85	0.53	0.53	0
PES3_EC5	5.5	60	max. / 96	0.60	0.6	0
PES3_EC6	4.5	60	max. / 110	0.69	0.69	0

Results

The filtration results of EC1-EC3 are shown in Figure 77 and Table 23. None of those experiments filtrated more used suspension than Ref_CA, and the duration was up to 300 % longer. However, at the gap of 4.5, the filter water release was at its minimum and volume of the filtrated suspension was even smaller than with CA. It can be concluded that the results at this gap were worse than by other gaps.

In contrast to results from EC1 – EC3 with equal current densities, the results from EC4 – EC6 (Figure 78 and Table 23) showed a preference for a smaller gap. At the electrode gap of 6.5 cm, the volume of the filtrated suspension was increased for 49 %, while the duration of the filtration was increased for 155 %. At the gap of 4.5 cm, those values were 39 % and 183 %, respectively.

The electrode gap of 5.5 cm was optimal for the parameter B_{kt}.

Table 23:   Electrodes gap experimental series (PES3) – evaluation parameters

Code	Δρ (%)	ΔFW API (%)	B_{kt} (%)	RM_{cm} (%)	Rm_{fc} (%)	$ΔFt_{EC}$	$ΔFV_{EC}$	FW_{rel}
PES3_EC1	18.7	16.5	17.4	46.8	25.9	3.00	0.00	20.4
PES3_EC2	22.8	32.7	20.6	45.5	26.7	2.91	0.00	20.4
PES3_EC3	30.7	62.9	19	44.3	25.5	2.92	-0.06	18.6
PES3_EC4	41.3	89.6	27.4	50.1	27.1	1.83	0.39	32.5
PES3_EC5	31	100.0	30.7	47.9	27	1.28	0.32	30.1
PES3_EC6	38.1	105.7	27.9	49.6	24.7	1.55	0.49	35.3
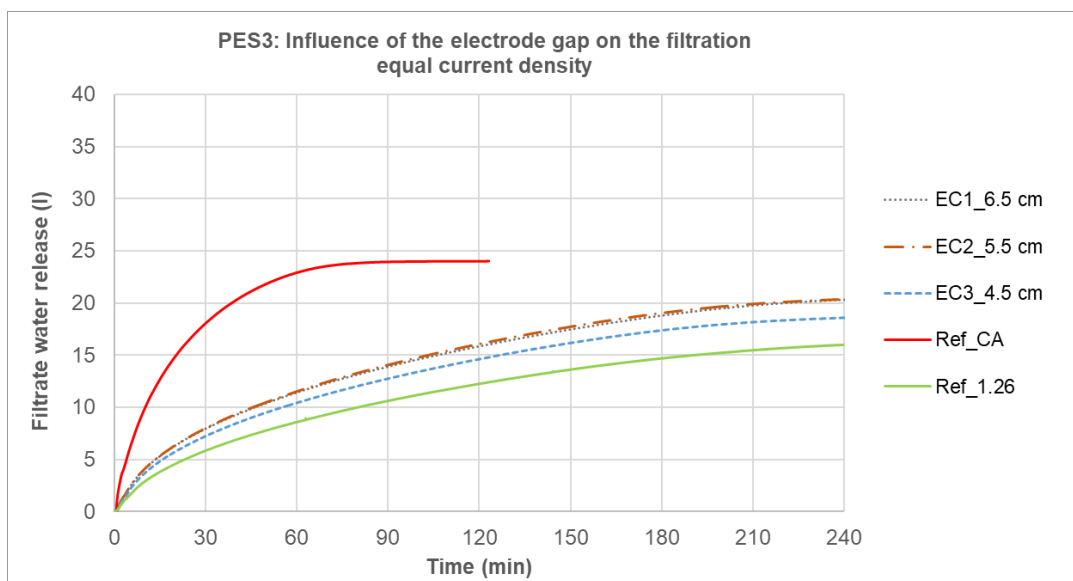
Figure 77:   Influence of the electrode gap on the filtration – equal current density, 30 minutes EC
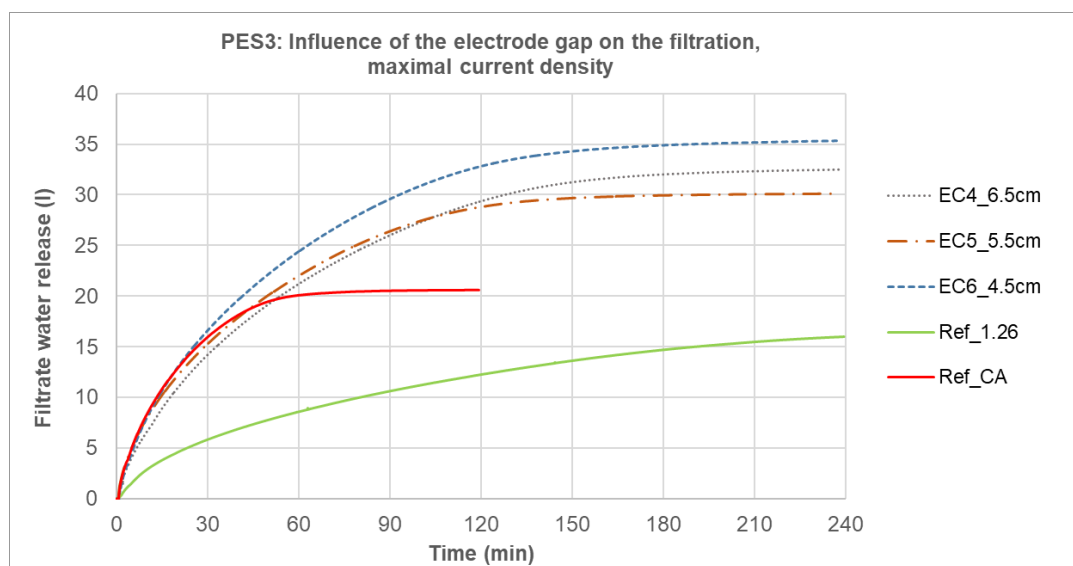
Figure 78:   Influence of the electrode gap on the filtration – maximal current density, 60 minutes EC

Discussion

From the results of experiments EC1 – EC3, bigger gap increased the volume of filtrated suspension. This can be explained through the decrease of the suspension volume between two cathodes or one cathode and the wall of the cell (red arrows in Figure 79). This space in the EC cell can be called "dead volume". In dead volume, no electrical current flows and therefore no electrochemical reactions take place. After an EC experiment, the remaining suspension was pumped away from the cell. At that point, the fraction of the suspension that was in dead volume mixes with the rest, reducing the effects of EC on destabilisation of the suspension. Therefore, at the same current density (EC1 – EC3), a larger gap provides better results due to a smaller dead volume.
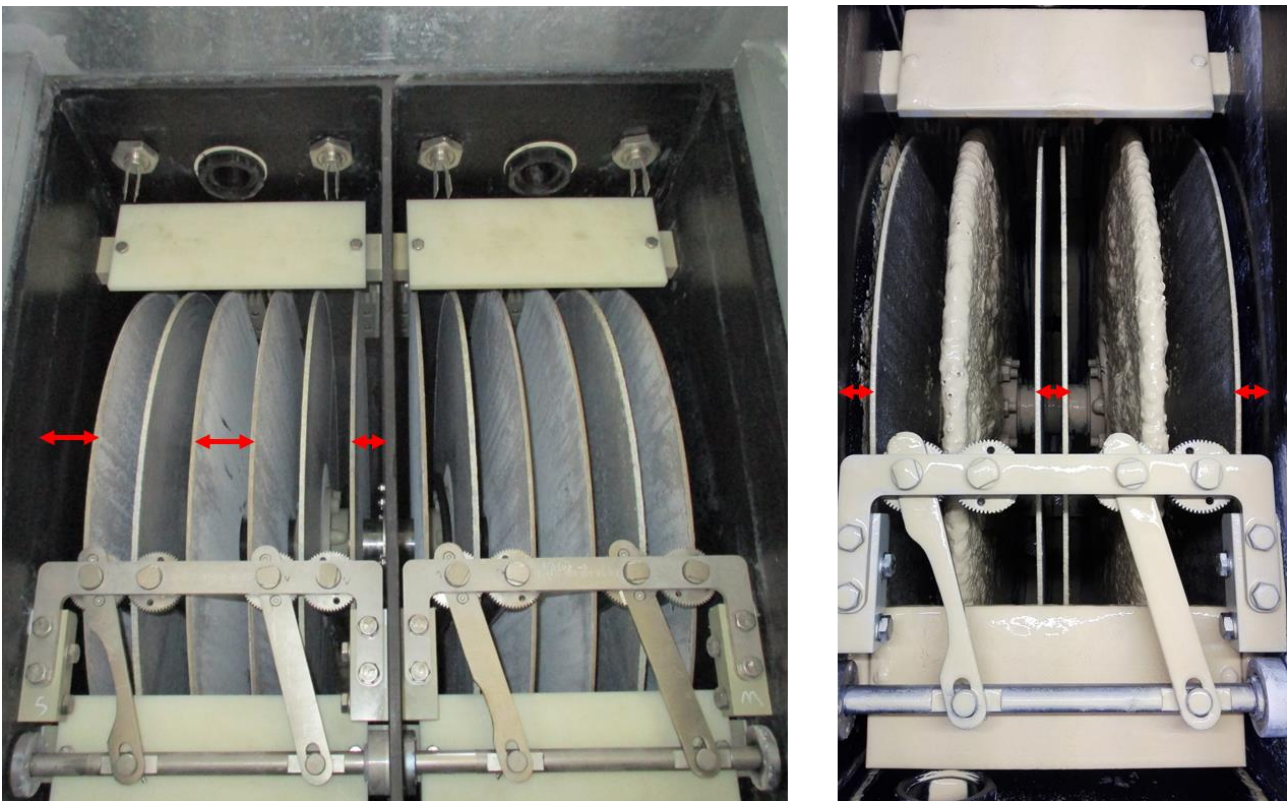
Figure 79:   Dead volume in the cell with an electrode gap of 4.5 cm (left) and 6.5 cm (right). The photo on the right side is from the experiment PES1_EC11 (0.17 Ah/)

However, the results of experiments E4 – E6 showed that a smaller electrode gap provided better filtration results. A smaller gap caused decreased resistance, which produced higher electrical currents. This is an important finding; it means that the positive effect of the in-creased current density caused by a smaller electrode gap overwhelms the negative effect of increased dead volume.

Considering the above reasoning, the gap of 4.5 cm provides the best results concerning filtration and can be proclaimed as the optimal operational parameter for the EC prototype cell.

However, at the gap of 5.5 cm, the amount of coagulated soil particles was higher. This could be a measurement mistake, since the parameter $\Delta\rho$ does not fit to measurements of B_{kt}.

This experimental series provided insights in the importance of the electrodes' arrangement in the cell. At the next scale-up phase, the arrangement of cathodes and anodes should be revised to decrease the dead volume. This is further discussed in chapter 8.

6.5.5 PES4: Influence of the anodes cleaning interval

The focus of the fourth experimental series was to determine the influence of the anode cleaning interval on the EC and subsequent filtration. Four experiments were performed. The first was performed at the maximal anodes rotation speed, the second one at half speed, the third one at the one-fourth rotation speed and the fourth experiment was performed without rotation and thus also without cleaning of the anodes. The electrical current was always maximized. However, with increasing rotational speed of the anodes, smaller electrical currents were reached (Figure 80). The complete list of operational parameters is presented in Table 24.
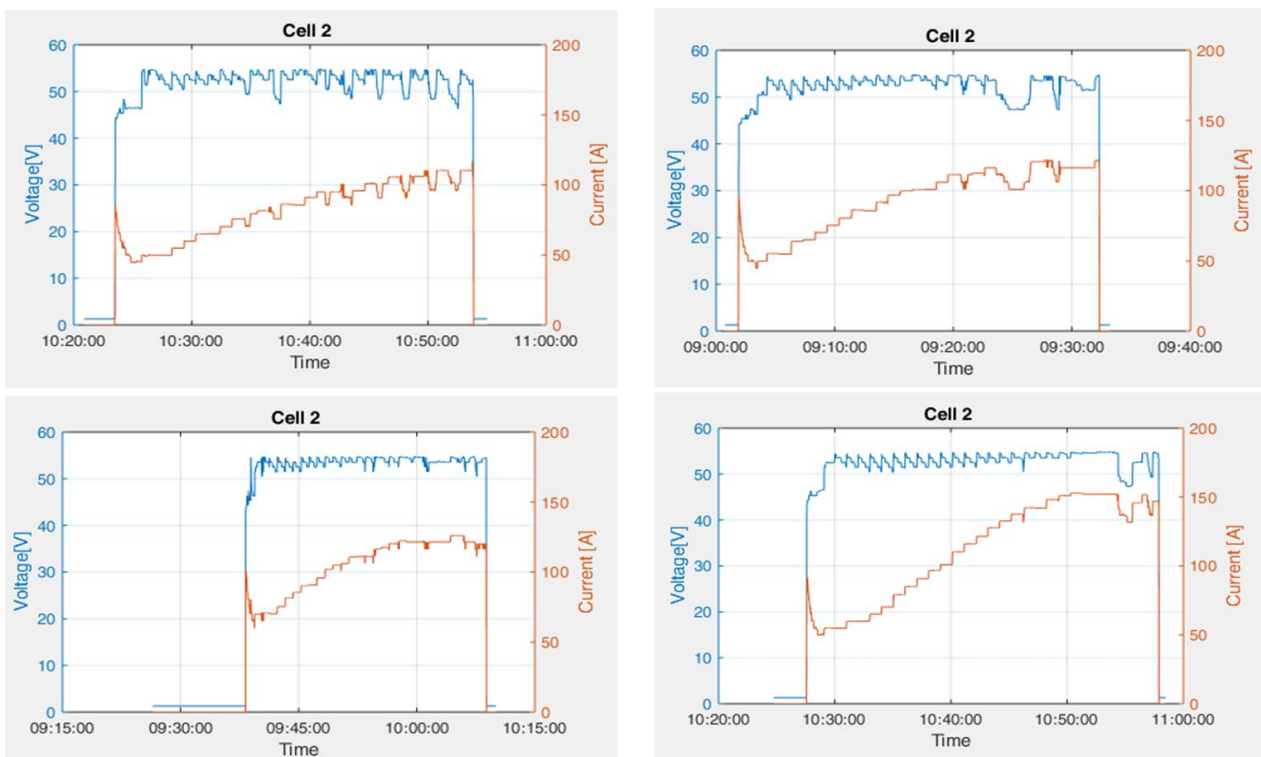
Figure 80:   Course of voltage and electrical current during ES4: influence of the cleaning interval and rotation speed of anodes on the development of electrical current

Table 24: Anodes cleaning interval experimental series (PES4) – operational parameters

Code	Electrode gap (cm)	Duration (min)	Electrical current (A)	Current density (A/l)	Charge density (Ah/l)	Cleaning interval (min^{-1})
PES4_EC1	4.5	30	max. / 81.8	0.51	0.26	0.46
PES4_EC2	4.5	30	max. / 92.6	0.58	0.29	0.23
PES4_EC3	4.5	30	max. /104.6	0.65	0.32	0.11
PES4_EC4	4.5	30	max. / 111.5	0.70	0.35	0.00

Results

The results of this experimental series were quite surprising. The faster the anodes rotated, the lower the electrical current was, causing less filtrate water to be released in filtration experiments (Figure 81).

The evaluation parameters are presented in Table 25. Since the rotation is turned off automatically and simultaneously with the shut down of the DC power supply, some coagulated material remained on the anodes. To remove it all, the rotation should make one more full circle after turning DC power off. Therefore, the parameters B_{kt} and $Δρ$, are not equal 0 %, as they theoretically should be in this experimental series.

Concerning the parameters $ΔFV_{EC}$ and $ΔFt_{EC}$, slower rotation increases the volume of the filtrated suspension and reduces the filtration duration (with exception of EC4). The values however show that the filtration performance was worse than with CA, as shown in Figure 81.

Table 25: Anodes cleaning interval experimental series (PES4) – evaluation parameters

Code	$Δρ$ (%)	$ΔFW$ API (%)	B_{ct} (%)	RM_{cm} (%)	Rm_{fc} (%)	$ΔFt_{EC}$	$ΔFV_{EC}$	FW_{rel}
PES4_EC1	17.4	20.6	5.3	46.5	26.1	2.87	0.07	22.5
PES4_EC2	21.6	29.7	9.2	48.5	26.2	2.70	0.11	23.7
PES4_EC3	22.5	37.7	11.2	45.7	26.1	2.41	0.12	24.3
PES4_EC4	25.1	34.1	18.8	48	25.1	2.61	0.17	25.7
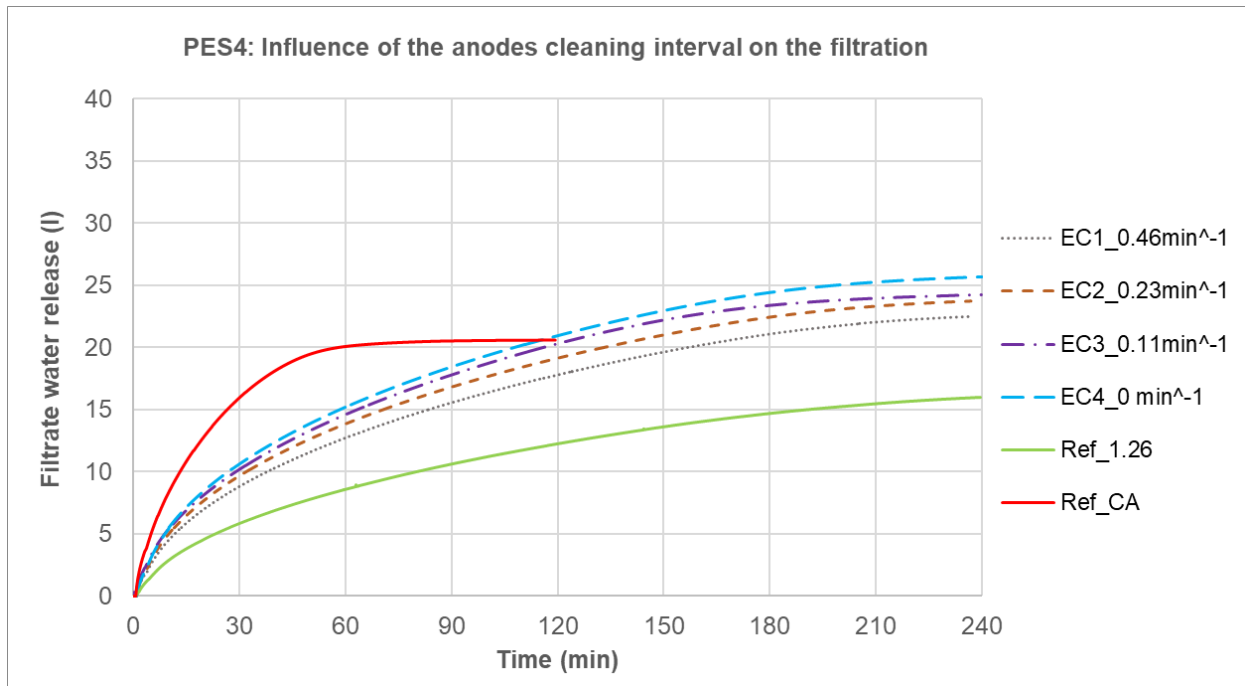
Figure 81:   **Influence of the anodes cleaning interval on the filtration**

Discussion

The findings in this experimental series were quite unexpected and suggest that the rotation of the anodes and removal of the coagulated material from their surface during the experiment actually has a negative influence on the development of electrical current and filter water release after EC. The results were consistent: the faster the anodes were rotated and cleaned, the lower the electrical currents were reached during EC, resulting in less filter water being released during filtration. These findings are, however, consistent with the laboratory results from chapter 5.3.4 for the experiments with a duration of 60 minutes. In both cases, the more often the anodes were cleaned, the worse the results became.

The reason for the negative effect of the rotation and cleaning on the development of electrical current during the experiment remains unclear. One possibility is that the unsynchronised movement of the electrodes (anodes rotate while cathodes stay still) might have had a negative influence on the development of the electrical current during EC. Otherwise, it could actually be caused by the scratching of the coagulated material from the anodes. To further investigate these options, an experiment with rotation of the anodes but without cleaning should be performed. However, with the current EC prototype cell, this is not possible. As soon as anodes rotate, they are being scraped clean. Further experiments concerning anode cleaning are described in chapter 6.5.5.

6.5.6 **PES5: Influence of the EC experiment duration**

The next experimental series focused on the influence of the EC experiment duration on the subsequent filtration. Four experiments with lengths of 30, 45, 60 and 90 minutes were conducted. Table 26 shows the full list of operational parameters. The course of voltage and electrical current during the experiments is shown in Figure 82. The figure shows a "standard" course of electrical current, observed in most of the experiments. First, it rises due increase of the electrical conductivity of the suspension caused by the release of the aluminium ions from the anode. Its reaches a peak in 20-25 minute. Afterwards, it declines, probably due to the coagulated material on the anode that increases the resistance on the path of electricity between two electrodes.

Table 26: **EC duration experimental series (PES5) – operational parameters**

Code	Electrode gap (cm)	Duration (min)	Electrical current (A)	Current density (A/l)	Charge density (Ah/l)	Cleaning interval (min^{-1})
PES5_EC1	4.5	30	Max / 111	0.69	0.35	0
PES5_EC2	4.5	45	Max / 128	0.80	0.60	0
PES5_EC3	4.5	60	Max / 110	0.69	0.69	0
PES5_EC4	4.5	90	Max / 94	0.59	0.88	0
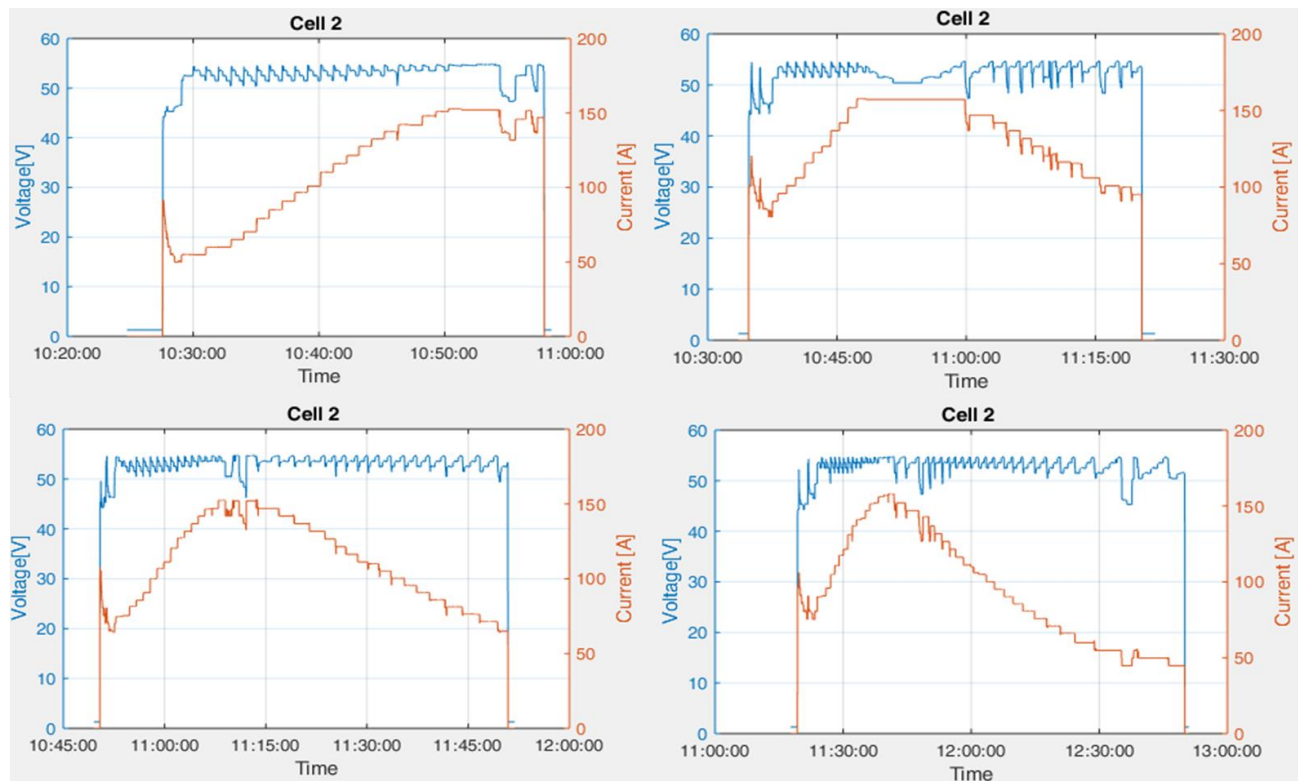
Figure 82: **Course of voltage and electrical current during PES5: influence of the EC duration on the development of electrical current**

Results

The extension of the EC experiment duration improved the results up to a certain time threshold. The amount of coagulated bentonite reached its maximum between 30 and 45 minutes (Table 27). Beyond minute 45, no statistically significant increase of this parameter was measured. However, the filtration results showed further destabilization of the suspension up to an experiment duration of 60 minutes. The filtration curves for 60 and 90 minutes were nearly identical, indicating that the suspension was not further destabilized between 60 and 90 minutes of the EC experiment. Only a small improvement in a parameter ΔFt_{EC} was measured, due to the fact, that the filtration after 90-minutes EC experiment reached 80% of the total filter water release 5 minutes before the filtration after 60 minutes EC. With increasing EC duration form 30 to 60 minutes, the parameters ΔFV_{EC} and ΔFt_{EC} showed a clear improvement (ΔFV_{EC} rose, ΔFt_{EC} fell).

Table 27:   EC duration experimental series (PES5) – evaluation parameters

Code	$\Delta\rho$ (%)	ΔFW API (%)	B_{kt} (%)	RM_{cm} (%)	Rm_{fc} (%)	ΔFt_{EC}	ΔFV_{EC}	FW_{rel}
PES5_EC1	25.1	34.1	18.8	48	25.1	2.61	0.17	25.1
PES5_EC2	41	111.2	26.2	51.8	26.9	1.77	0.33	26.9
PES5_EC3	41.3	105.7	27.9	50.1	27.4	1.55	0.49	27.4
PES5_EC4	48	160.1	24.6	52.7	27.6	1.39	0.48	27.6
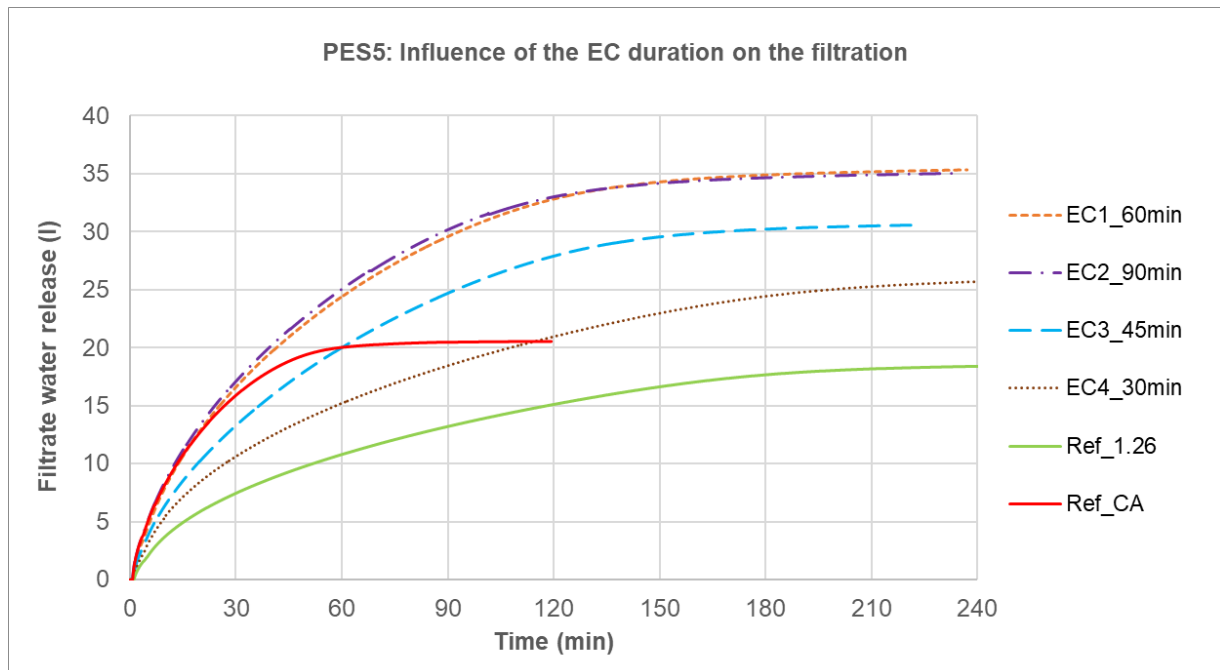
Figure 83:   Influence of the EC duration on the filtration

Discussion

An increase of the EC experiment duration generally improves the results, but only up to the certain duration. The amount of coagulated bentonite reached its maximum between 30 and 45 minutes of the experiment. A possible explanation for this might be that after a certain thickness, the voltage drop over the coagulated material on the anode consumes almost the complete voltage in the cell and the particles are no longer strongly attracted to the anodes' surface because it is "blocked" by coagulated material. Another possible explanation might be that the particles in the suspension after 45 minutes of EC get so destabilised that their zeta potential turns to almost 0 mV and they no longer act as negatively charged particles, reducing their attraction to the positively charged anodes. However, this would also mean that the particles cannot be further destabilised after 45th minute, which does not fit with the filtration results. Therefore, the first theory presented seems more plausible.

Filtration results show further destabilisation of the particles for up to 60 minutes, but not beyond that. It should be pointed out that the total amount of electrical charge at 90 minutes of EC is only 28% higher than for a 60 minute duration. This is because the electrical current between 60 and 90 minute was on average 50 A, as shown in Figure 82. This should anyway continue to cause further destabilisation of the suspension, but that was not observed. There are again two possible explanations for this occurrence. The first is that the aluminium ions after 60 minutes become stuck in the coagulated material and do not come into contact with the suspension. However, if this is the case, it could and should have happened previously and not only after 60 minutes. Moreover, the cathode also dissolves and creates aluminium ions that destabilise the particles in the suspension. Therefore, this explanation does not seem very probable. The second explanation is again related to zeta potential. Perhaps the particles after 60 minutes of EC treatment reach a zeta potential of close to 0 mV and the addition of 28% more electrolytes does not further destabilise the suspension. This seems more plausible. That would also mean that an even longer EC treatment, or rather, even more electrical charge, could actually have a negative effect on the filtration of SUS because the zeta potential of the particles could become positive, which would cause re-stabilisation of the suspension. Such cases were found in literature review (chapter 3.3.7).

Overall, the finding from this experimental series could be explained with a combination of voltage drop and zeta potential. After 45 minutes of the experiment, the voltage drop over the coagulated material was high and the zeta potential of the particles in the suspension was reduced, which resulted in significantly lower attraction of particles towards the anode. These attraction forces may not have been strong enough to keep the particles firmly bound to the rest of the coagulated material. Pumping of the remaining suspension out of the cell after the experiments might have caused those particles to be washed out from their position on or near the surface of the coagulated material, resulting in almost the same amount of

coagulated material on the anodes after the 45, 60, and 90 minute experiments. However, the zeta potential of the particles might have continued to drop until the duration reached 60 minutes. Therefore, further destabilisation of the suspension between 45 and 60 minutes was possible. After 60 minutes, the zeta potential might have been near 0 mV and continuation of the experiment beyond this point did therefore not further contribute to destabilisation of the suspension.

Even though this theory would fit the current knowledge about zeta potential and EC, it was impossible to provide experimental evidence for this explanation.

6.5.7 PES6: Fine-tuning experiments

The aim of this experimental series was to test several ideas that arose from the results of the previous experiments. Those included various ways to improve anode cleaning and one idea concerning the effectivity of EC at different heights of the cell. The operational parameters of this experimental series are listed in Table 28.

Table 28:   Fine-tuning experimental series (ES6) – operational parameters

Code	Electrode gap (cm)	Duration (min)	Electrical current (A)	Current density (A/l)	Charge density (Ah/l)	Cleaning interval
PES6_EC1	4.5	60	119.1	0.74	0.74	constant
PES6_EC2	4.5	60	118.9	0.74	0.74	abrupt
PES6_EC3	4.5	60	96.1	0.6	0.6	manual
PES6_EC4	4.5	60	95.0	0.59	0.59	manual
PES6_EC5	4.5	60	107.0	0.67	0.67	none

Since it was observed in the PES4 that anodes rotation and cleaning negatively influences the development of the electrical current, the first two experiments of this series tried to overcome this challenge. In the first experiment (EC1), cleaning was not turned on until 20 minutes had elapsed, after the electrical current had already reached its peak. The cleaning was then run continuously. However, the rotation had stopped after approximately 15 minutes (35th minute of experiment), because the scraper at the anodes was clogged due to too much coagulated material.

In the second experiment (EC2), the idea was to perform discontinuous cleaning. The rotation was turned on at the peak of the electrical current (after 15 minutes) and turned off after two full cleaning circles at maximal rotation speed, which lasted 4.5 minutes. The plan was to turn the cleaning on again after 15 minutes, at minute 35. However, this was not possible because there was too much coagulated material on the anodes. Due to clogging, the scrapers could not rotate.

In the next two experiments, cleaning was performed manually. This was performed with following procedure: EC was turned off after 30 minutes, the remaining suspension was pumped out, the anodes were cleaned manually and coagulated material was removed from the cell, the suspension was returned to the cell and EC was continued for another 30 minutes. The idea was to simulate the situation in which the scrapers would be able to remove the material from the anode and from the cell at the certain point of EC. However, because the coagulated material was removed from the cell, it was necessary to electro-coagulate more than 160 l of suspension in the first EC round in order to have enough for the second round.

In the experiment EC3, EC was first performed in both chambers simultaneously for 30 minutes. After manual cleaning of the anodes, the remaining suspension was combined and poured back in one chamber, then electrocoagulated for another 30 minutes. However, at the first round of EC, the amount of electrical current in chamber 1 was significantly lower than in chamber 2.

Therefore, one more similar experiment (ES4) was conducted, but everything was performed in chamber 2. This basically means that 3 EC experiments in a row were conducted: the first two with SUS and the last one with the combined remaining suspension from both experiments. The anodes were always cleaned after the experiment, and each experiment lasted 30 minutes. This time, the electrical current in both EC experiments with SUS was similar.

The last experiment (EC5) in this thesis was a standard experiment (duration 60 minutes, 4.5 cm electrode gap, without anodes cleaning) except that only the upper 2/3 of the remaining suspension in the cell was filtrated. This idea came as a results of the analysis of suspension probes from the 5 extraction points In previous experiments, this analysis typically showed that the electrical conductivity of the suspension in the upper 2/3 of the cell is significantly higher than in the lower third (Figure 84 right). Moreover, the temperature was often at its highest in the middle of the cell, and the density of the suspension in the lower part of the cell did not change at all or there was a small decrease compared to starting density (Figure 84 left).
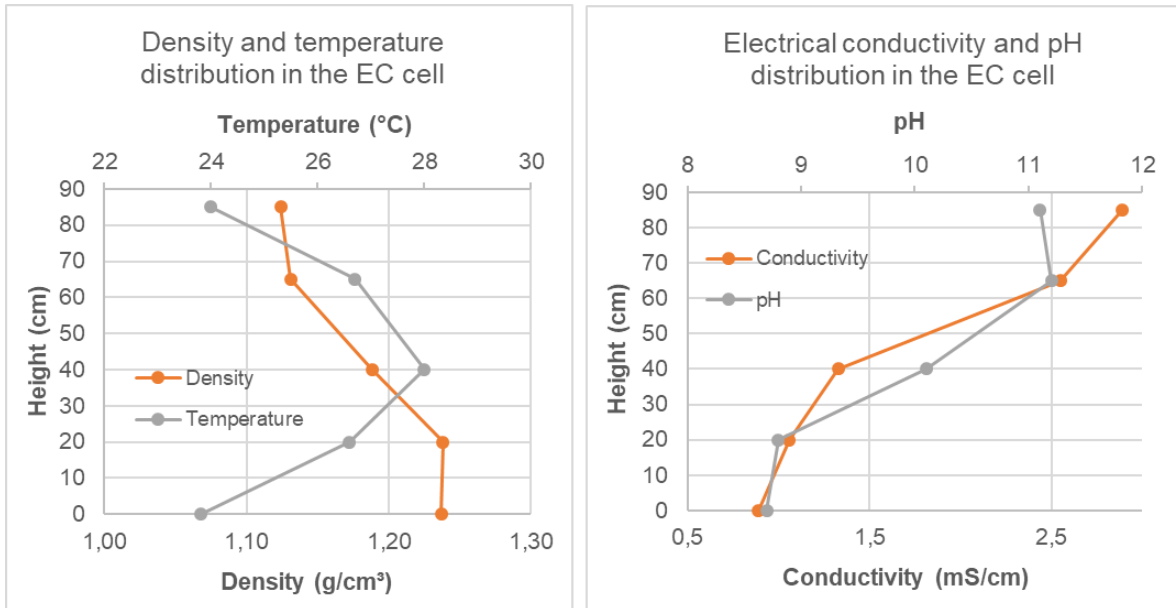
Figure 84:   Vertical distribution of the parameters in the cell: left) Temperature and density, right) pH and electrical conductivity (after Vishnyakov, 2019)

Those differences can be explained by the design of the cell. Since the electrodes do not reach into the lower part of the cell, there are fewer or no electrochemical reactions. There-fore, fewer electrolytes are produced in the lower third of the cell. This makes the suspension in the bottom of the cell less destabilised. Another possible explanation is that the most of the EC reactions occur in the middle of the cell, where the electrodes are as wide as the cell. Upon reducing the density of the suspension in the middle of the cell, this suspension goes up and switches places with the upper suspension with higher density, which than comes to the middle of the cell and gets electrocoagulated. However, the suspension from the lower part of the cell always remains heavier and stays at the bottom of the cell for the whole duration of the experiment.

Results

The results are presented in Table 29 and Figure 85.

In first two experiments, the cleaning mechanism was not able to cope with the amount of coagulated material that developed during the experiment. Due to a relatively short period of cleaning, the electrical current was not significantly affected and the filtration results were very similar to those with same EC operational parameters but without cleaning.

In the following two experiments, in which the cleaning was performed manually, the results were worsened. PES6_EC3 basically consists of two EC experiments and PES6_EC4 of three EC experiments, the parameters $\Delta\rho$, ΔFW, Bkt and RM_{CM} in Table 29 are listed for each one of them.

When the suspension from the upper 2/3 of the cell was pumped out separately without mixing with the suspension from the lower part, the filtration performance was better than when the entire remaining suspension was homogenised prior to filtration. Considering filtration performance, the experiment PES6_EC5 was the best experiment in this thesis. In further analysis in chapters 7 - 10, this experiment is called "Best Combo", since it represents the best combination of EC operational parameters. With Best Combo experiment, the duration of the filtration was prolonged for 120 %, and 58 % more suspension was filtrated.

Table 29:   Fine-tuning experimental series (PES6) – evaluation parameters

Code	$\Delta\rho$ (%)	ΔFW API (%)	B_{kt} (%)	RM_{cm} (%)	Rm_{fc} (%)	ΔFt_{EC}	ΔFV_{EC}	FW_{rel}
PES6_EC1	40	111	28.3	44.79	27.69	1.43	0.51	35.3
PES6_EC2	45	147	25.8	52.09	27.76	1.49	0.54	36.5
PES6_EC3	14.7 / 25.0	11.6 / 42	7.4 / 8.3	46.2 / 55.0	26.8	3.14	0.35	31.1
PES6_EC4	29/32/18	64/89/24	21/19/-	46/47/53	26.96	2.66	0.35	31.08
PES6_EC5	49.0	206.0	27.4	48.6	27.6	1.20	0.58	38.0
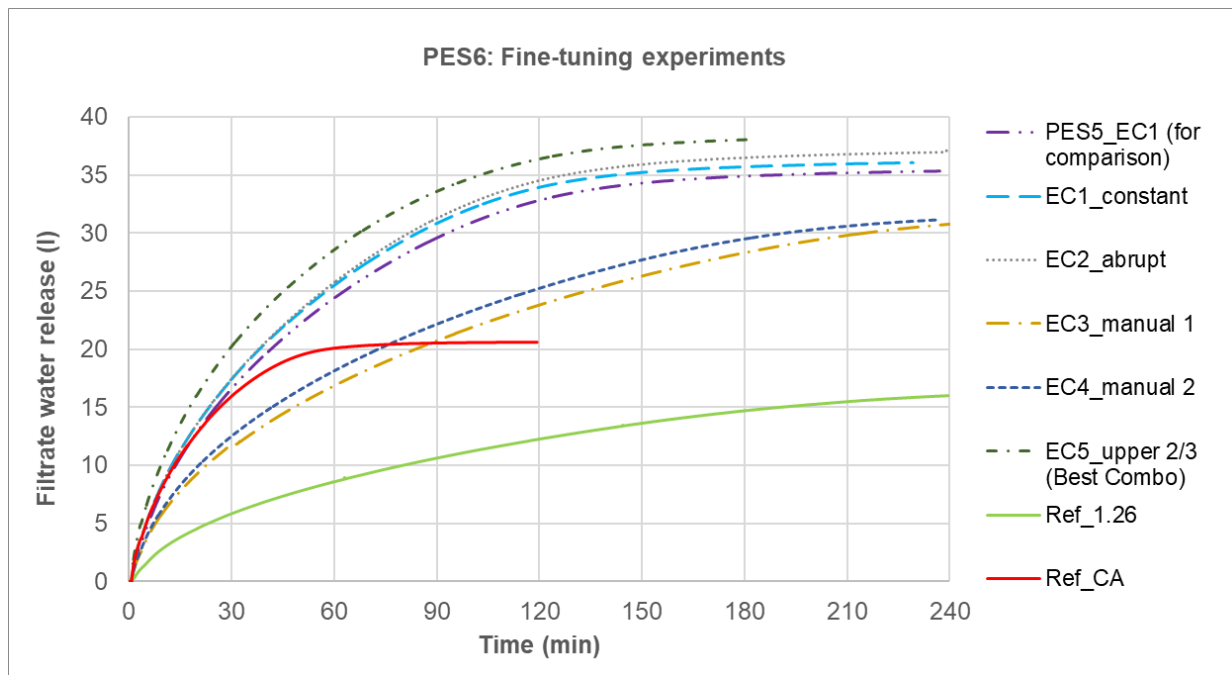
Figure 85:   Influence of the fine-tuning EC experiments on the filtration

Discussion

This experimental series was designed to test a few different ideas which could have improved the EC performance. One idea was to start cleaning anodes only after peak electrical current was reached. This idea came from analysis of previous results and literature, in

which it was not reported that cleaning the anodes could have a negative influence on EC performance.

Turning on the rotation only after electrical peak was reached did allow electrical current to develop to higher values, but the amount of coagulated material on the anodes was too large for scrapers to handle. In general, difficulties concerning scraping the material from the anodes arose in experiments that lasted more than 30 minutes.

The manual cleaning worsened the results. In comparison to the experiment with a 60-minute duration and no cleaning, there are two differences in experimental procedure: first, the suspension was electrocoagulated twice with 30 minutes per experiment and with a break of approx. 1 hour between the experiments; secondly, the anodes were completely cleaned before the start of the second 30 minutes. Therefore, the difference in the results depends on one or both of those procedural changes. Either the EC time cannot be simply added, meaning that two experiments with 30 minutes and pause of one hour between them do not have the same effect as one continuous experiment with 60-minute duration, or the cleaning of the anodes actually has negative influence on the results. The latter option has not been found in the literature, but when considering the results of all mechanical cleaning experiments in this thesis, this possibility should not be neglected.

Further experiments with the following operational parameters would offer deeper insights into the subject of mechanical cleaning: 2x30 minutes EC with one hour break between the experiments, but without cleaning of the anodes. The suspension can be pumped out from the cell between the experiments to exactly reproduce the operational procedure from experiments EC3 and EC4, but also an option in which the suspension stays in the cell during the break can be tested. If the results show that the break does not negatively influence the results, then the only remaining option is that the cleaning of the anodes during the experiment actually has a negative effect on the EC performance and should be considered anymore.

The last experiment (PES6_EC5 - Best Combo) showed the best results regarding filtration performance. This is due to the fact that the part with more electrolytes was taken for filtration, which simulates the decrease of the dead volume. The implications of this finding on the cell parameters for a real-scale prototype is discussed in chapter 8.

6.5.8 PES7: Influence of the suspension density

This experimental series focused on the influence of the suspension parameters, in this case density, on the EC and filtration performance. Three EC experiments with suspension densities of 1.20, 1.16 and 1.12 t/m³ were conducted. As previously mentioned, decreased SUS density was achieved by using the same amount of bentonite and water, but with less load.

To achieve densities of 1.20, 1.16 and 1.12 t/m³, the load dosage was reduced to 68%, 52% and 37%, respectively. The ratio of materials in the load stayed the same. The full list of operational parameters is shown in Table 30. Since this experimental series was performed with reduced density SUS, new reference filtration experiments both with and without CA were performed. The reference experiment with the suspension density of 1.12 t/m³, without CA, could not be successfully performed. Three attempts failed due to leakage of the suspension from the press upon applying the filtration pressure. Slower application of pressure was also tested but the result did not change. Possibly a suspension with such a low density needs to be destabilised in order to be filterable.

Table 30: **Suspension density experimental series (PES7) – operational parameters**

Code	Electrode gap (cm)	Duration (min)	Electrical current (A)	Current density (A/l)	Charge density (Ah/l)	Cleaning interval (min^{-1})
PES7_EC1	4.5	30	Max / 110.7	0.69	0.35	0
PES7_EC2	4.5	30	Max / 107.3	0.67	0.34	0
PES7_EC3	4.5	30	Max / 112.7	0.70	0.35	0

Results

First of all, it is interesting to mention that the suspensions density did not have any influence on the electrical current. This operational parameter was set to maximum for all three EC experiments and almost similar currents were produced as a result.

The evaluation parameters of PES7 are listed in Table 31. The results of new reference filtration experiments are presented in Table 32.

Table 31: **Suspension density experimental series (PES7) – evaluation parameters**

Code	$\Delta\rho$ (%)	ΔFW API (%)	B_{kt} (%)	RM_{CM} (%)	FW_{rel}	RM_{FC} (%)
PES7_EC1	27	-	11.7	49.77	27.7	30.77
PES7_EC2	22	41	14.2	55.39	28.6	38.74
PES7_EC3	25	66	15.6	63.6	28.7	47.55

Table 32: **Reference filtration experiments (PES7) – evaluation parameters**

Parameter	Ref_1.20	Ref_1.16	Ref_1.12	Ref_1.20_CA	Ref_1.16_CA	Ref_1.12_CA
FW release	19.1	19.6	-	25.4	23.7*	26.6
RM_{FC}(%)	30.9	34.8	-	26.0	29.1	43.9

Concerning the EC, it is important to mention that the decrease of the suspension's density increased the residual moisture of the coagulated material on the anode. This is important when considering the disposal of the coagulated material, which is discussed in chapter 7.2.1. It is worth mentioning that the decrease of the suspension's density increased the parameter B_{kt}. This is due to the fact that this parameter (Eq 4-4) represents the percentage of coagulated material in relation to total amount of soil particles in suspension, which is less at lower densities.

Figure 86 presents the filtration curves from all filtration experiments in PES7. It is quite revealing in several ways. When comparing the filtration curves in the same group of experiments (experiments with EC, reference experiments without CA and reference experiments with CA), the influence of the suspension's density over the course of the filtration is insignificant. Nevertheless, for every group of filtration experiments, a small but consistent increase of filtrate water release for lower density suspensions can be observed.
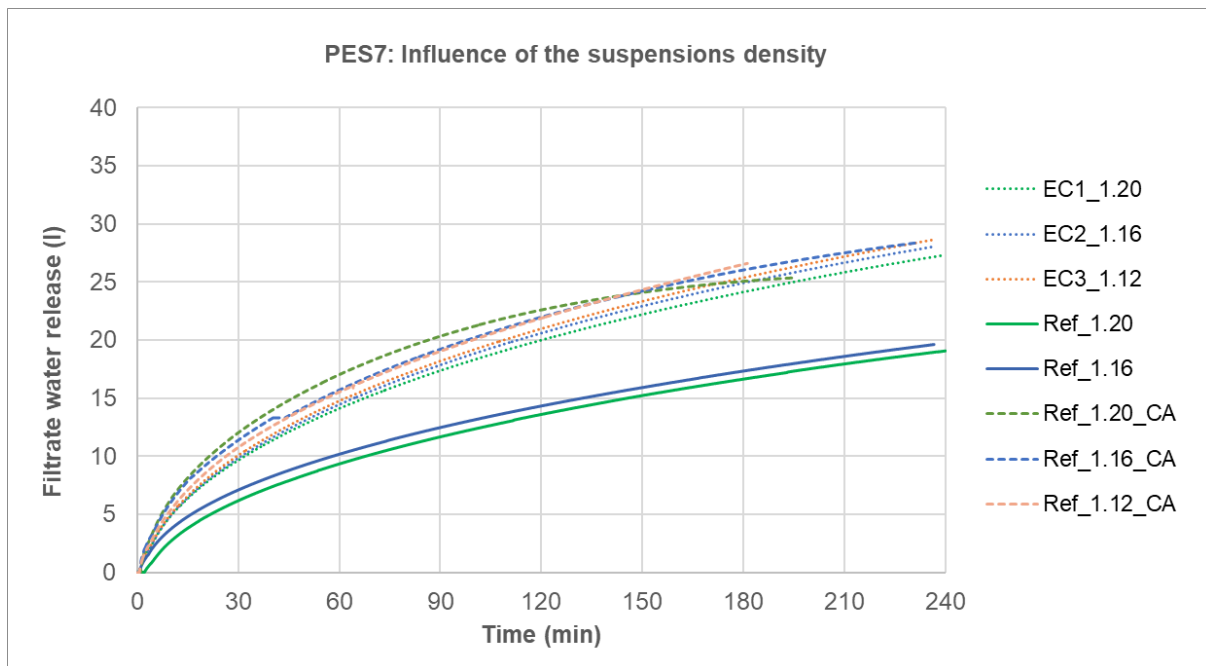
Figure 86:   **Influence of the suspension density on the EC and the filtration**

Observing only the course of the filtration can be deceiving. As can be seen from Table 31 and Table 32, residual moisture of filter cakes was significantly higher for low-density suspensions. For example, it increased from 30.8 % for EC1 to 38.7 % for EC2 and finally to 47.6 % by EC3. Similar results were produced in reference filtration experiments, in which the residual moisture rose from 26.0 to 29.1 and 43.9%. That means that even though the course of the filtration was very similar, decrease of the suspension density caused a significant prolongation of the filtration. For lower density suspensions, longer filtration times would be needed in order to reach equal filter cake moistures.

Another interesting finding is that the filtration after EC was very similar to the filtration with CA. This has previously happened only with EC experiments having a duration of 60 minutes, whereas in this experimental series, the EC duration was 30 minutes.

Discussion

One important finding in this experimental series is the effect of suspension density on the residual moisture of the coagulated material and filter cakes. Since the goal of the fine separation procedure is to separate fine particles from water, high residual moisture is not favourable. Moreover, it is detrimental when disposing the separated soil material. The low-density suspensions have shown a clear tendency to create high-moisture coagulated material and filter cakes. On construction sites, this problem can be solved with addition of lime prior to filtration.

The course of filtration after EC was very similar to reference experiments with CA. To discuss this further, the filtration experiments from this experimental series are compared to previous experiments which used standard-density SUS.

When comparing to filtration after EC experiments from ES1 with similar electrical current, but with standard density of SUS (1.26 t/m³), there is more filtrate water released in the experiments with lower density (Figure 87). One reason for that is lower density itself. Another reason is that the amount of fine soil particles in suspension was lower, but the same electrical charge was used. This means that those particles should be more destabilised. However, it remains unclear as to why the gap between standard density of 1.26 t/m³ and those of 1.20 t/m³ is much bigger than the gap between 1.20 t/m³ and 1.12 t/m³.

When comparing only reference filtration experiments with CA (Figure 88), filtration performance with lower-density suspension was much worse. The reason could lie in the conditioning, since the same amount of CA was used as for standard-density SUS. This dosage may not have been optimal. However, this highlights the challenges regarding the proper conditioning of suspensions on the construction sites.

Due to worse performance of reference filtration with CA and higher filtrate water release after EC with lower density suspensions, the filtration after EC was similar to the filtration with CA.
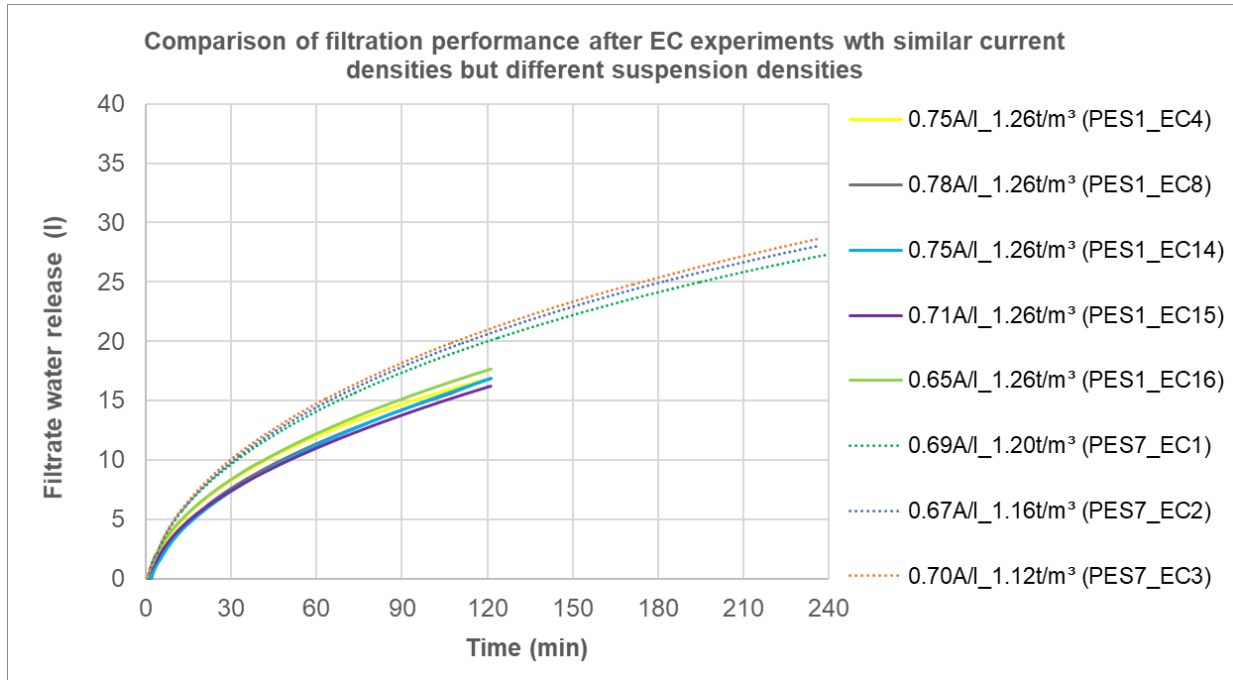
Figure 87:   Filtration curves from PES7 compared to those from PES1 with similar current densities
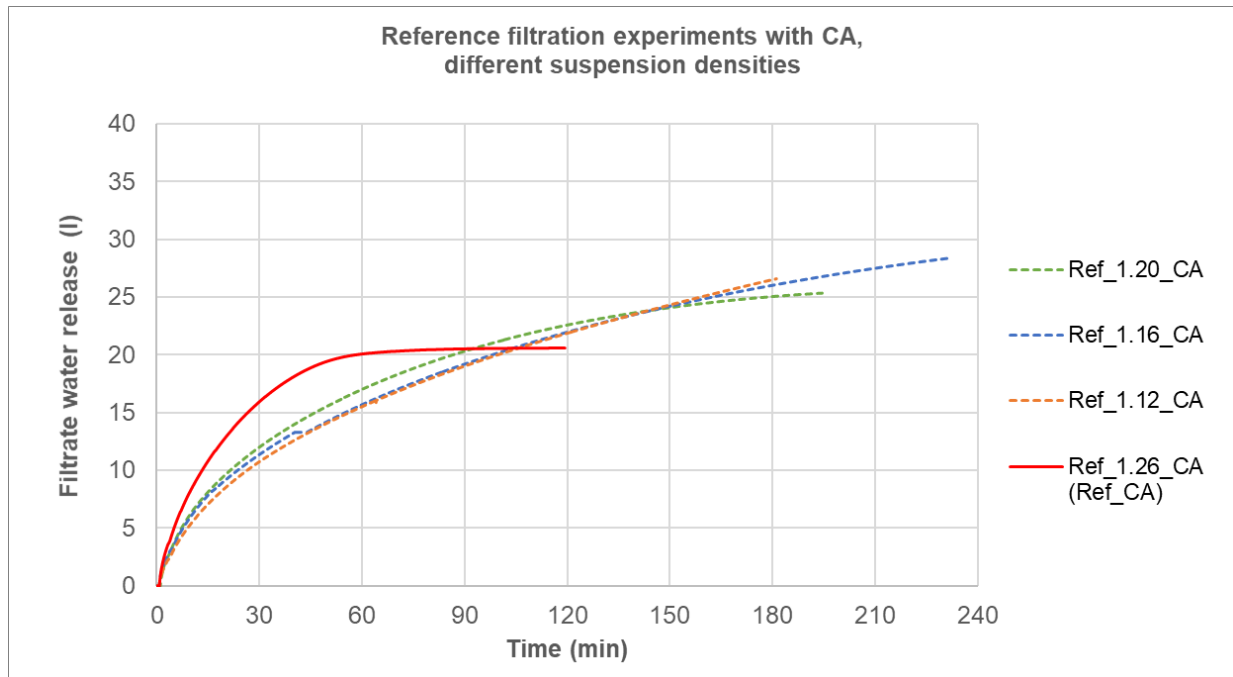
Figure 88:   Reference filtration experiments with CA, all tested densities of SUS

Overall, low-density suspensions did not show a significant influence on EC process. Similar electrical currents as with standard-density SUS were achieved. The lower the density was, the more particles coagulated (in percentage) but the residual moisture of the coagulated material was also higher. However, as the reference filtration experiments showed, this is a general challenge with low-density suspensions in the separation process.

Concerning the filtration process, filtration after EC seems to be beneficial for lower-density suspensions when compared to filtration with CA. For filtration after EC, lower density suspensions performed better than standard-density SUS, while filtration with CA was less effective for low density suspensions than for standard-density SUS. However, this subject needs to be further investigated, i.e. with a different amount of CA.

6.6 Experiments with suspension from construction site (PES8)

In order to validate the EC experiments with SUS, a used suspension from a tunnelling construction site was tested. The company operating the construction site has requested that the origin of the suspension remains anonymous. Therefore, this suspension is titled only as construction site used suspension (CUS) throughout this thesis.

According to the geological profile, the tunnelling machine was going through soil consisting of clay in the upper quarter of the working face and sand underneath at the time when the suspension was collected. In some areas, there were intermediate deposits of peat. According to the information from the construction site, the data in the geological profile matched the actual soil very well. The EC-relevant properties of CUS are listed in Table 33. All the experiments were performed within eight weeks from the beginning of June to the end of July 2018. This mentioned, there were no significant outside temperature differences that would eventually influence the EC performance. CUS was kept in the laboratory on the constant temperature of approx. 21°C between the experiments.

Table 33:   Properties of the construction site suspension (CUS)

Suspension	Density (g/cm³)	API Filtrate water (mg)	Conductivity (µS/cm)	pH-value	Temperature
CUS	1.17	12.4	1.5	7.6	21.4°C

In addition to the used suspension, the CA with which the suspension was conditioned on the construction site were also provided. Information about the way the suspension was conditioned and about the amount of coagulants and flocculants was acquired. For the experiments with LCFP, the conditioning ratio was kept the same as on the construction site.

The CA from the construction site were the same CA which were used in the reference filtration experiments with SAS. The conditioning ratio was also the same: 40 ml $FeCl_3$ and 8 g polymers (dissolved in 4 l tap water) per 40 l used suspension. That was no coincidence: this experimental series was chronologically second series, performed right after validation experiments with SUS. However, since it is the only series with a used suspension from a construction site, it is categorised as PES8 in this thesis, after all experimental series with SUS.

A total of 7 EC tests and 34 filtration tests were carried out in this experimental series. After every EC experiment, three filtration experiments (on average) with the remaining suspension were performed. The remaining 13 filtration experiments were reference experiments. All filtration experiments in this experimental series are chronologically numbered. As already mentioned, due to the fact that the filtration in this experimental series was performed only for 2 hours and not fill the end (determined with horizontal or almost horizontal line at the end of filtration curve), it was not possible to calculate parameters ΔFV_{EC} and ΔFt_{EC}.

6.6.1 **Reference filtration experiments in LCFP**

As with SUS, the first step of the parametric studies with CUS was to perform reference filtration experiments. In this experimental series, the possibility of reducing the amount of CA in combination with the EC was also investigated. Therefore, three different conditioning options were tested:

- Filtration without coagulating agents, marked with *0CA* in the experiment codes.

- Filtration with coagulating agents, but with only half of the ratio used on the construction site. This means, that 40 l of suspension were treated with 20 ml of $FeCl_3$ and 4g polymers dissolved in 4 l tap water. These experiments are marked with *0.5CA*.

- Filtration with coagulating agents, with full ratio applied, marked with *1CA*.

The reference experiments are shown in Figure 89. Each combination (*0CA*, *0.5CA* and *1CA*) was performed at least two times. As presented in Figure 89, the more CA were used, the bigger was the filtrate water release.

Moreover, the reference experiments with diluted suspension (1.1 t/m³ and 1.15 t/m³) were performed. In Figure 89 they are marked as Ref_1.12_0CA and Ref_1.15_0CA.
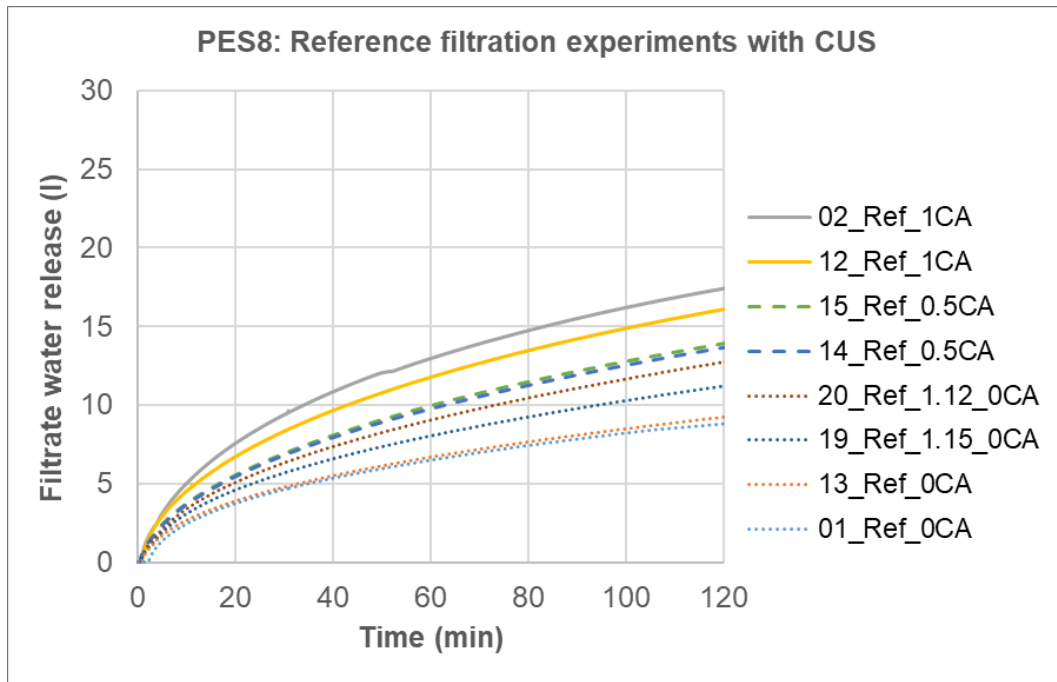
Figure 89: **Reference experiments with construction site suspension**

6.6.2 **EC and filtration experiments**

The operational parameters of the EC experiments are presented in Table 34. The first three experiments were performed with the same electrode gap and EC duration, but different electrical currents. The electrode gap was varied in EC4 and EC duration in EC5 and EC6. In the last EC experiment, the operational parameters were the same as in EC2, but the filtration experiments were performed for 4 hours instead for 2 hours as in EC1-EC6. The filtration operational parameters is this experimental series were variated between FV1, FV2b, FV3a and FV3b. Only the variation FV2a with the return of the coagulated material to the remaining suspension was not investigated.

Table 34: **Experimental series with CUS (PES8) – operational parameters**

Code	Electrode gap (cm)	Duration (min)	Electrical current (A)	Current density (A/l)	Charge density (Ah/l)	Cleaning interval (min^{-1})
PES8_EC1	4.5	30	137.1	0.86	0.43	0
PES8_EC2	4.5	30	157.5	0.98	0.49	0
PES8_EC3	4.5	30	126.4	0.79	0.40	0
PES8_EC4	6.5	30	121.5	0.76	0.38	0
PES8_EC5	4.5	45	150.3	0.94	0.70	0
PES8_EC6	4.5	20	156.5	0.98	0.33	0
PES8_EC7	4.5	30	156.6	0.98	0.49	0

Figure 90 and Figure 91 show the EC and the filtration experiments with CUS.

Figure 90:   EC experiments with CUS: left) Gas bubbles during EC, right) coagulated material on the anodes

Figure 91:   Filtration experiments with CUS: left) filter cakes, right) filtrate water

EC1 – EC3

Three filtrations, 0CA, 0.5CA and 1CA, were performed after each of the experiments EC1 - EC3. To test the aging effect of the remaining suspension on filtration performance, different filtrations were performed each time directly after EC: after EC1 the first filtration was 0CA, after EC2 it was 1CA, and after EC3 it was 0.5CA. The remaining filtrations were performed on the following day.

As seen in Figure 92, Figure 93 and Figure 94, the filtrations that were performed directly after EC (03_EC1_0CA in Figure 92, 06_EC2_1CA in Figure 93 and 09_EC3_0.5CA in Figure 94) had a clear increase of the filtrate water release measured in the first two hours when compared with the reference experiments with the same amount of CA. The filtrations performed on the following day had slight to no increase. This is clear to observe in Figure 95, Figure 96 and Figure 97, where all the filtrations from the same "day after EC" are put together. The increase of the filter water release directly after EC is clear in all three cases: without CA, with half the amount and with the full amount. One day after EC, the increase is visible only in the case of 0CA.

One more interesting finding is that the filtration 09_EC3_0.5CA performed almost as well as the reference experiment with full amount of CA (Ref_1CA) and that the experiment 06_EC2_1CA performed significantly better than reference experiment with full amount of CA. This means that EC and CA can be combined to reduce the amount of CA or to improve the filtration performance even further than CA only.
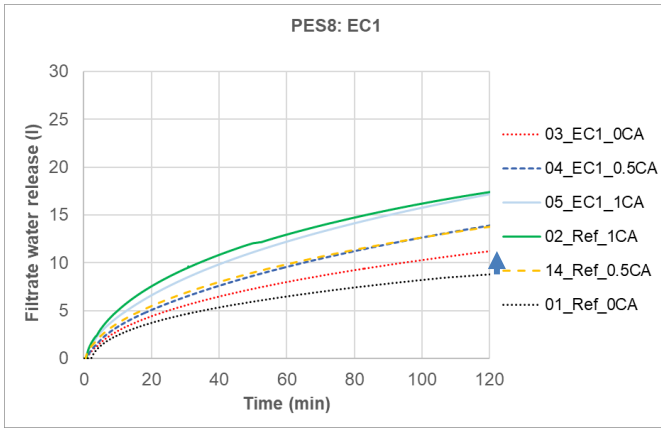
Figure 92:   Filtration after PES8_EC1
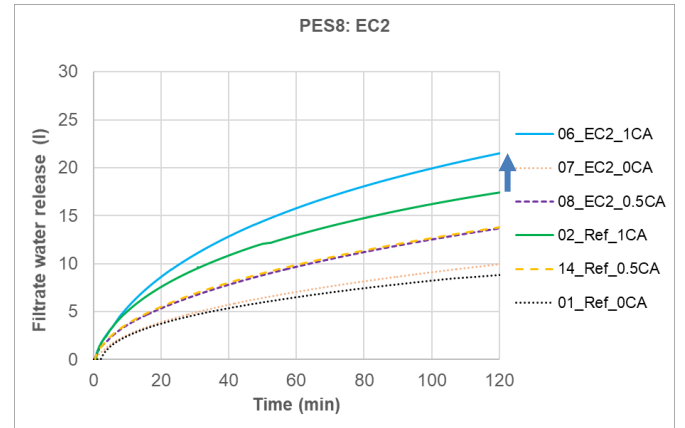
Figure 93:   Filtration after PES8_EC2
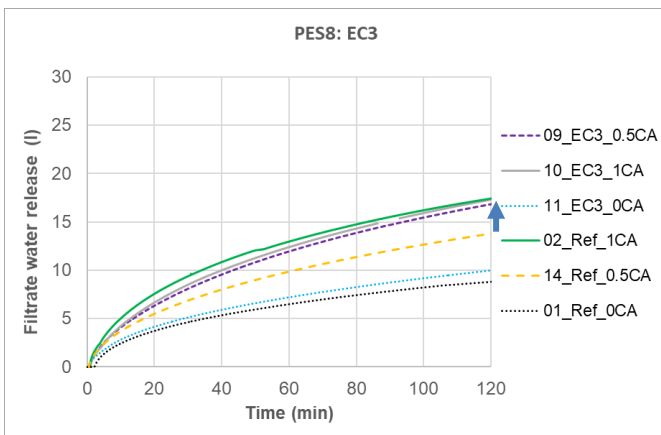
Figure 94:   Filtration after PES8_EC1
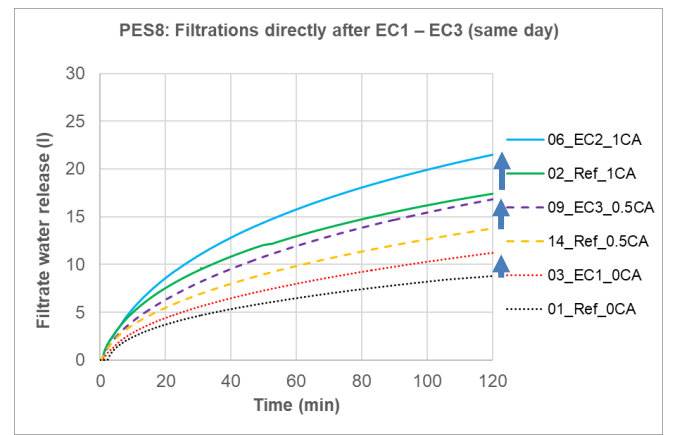
Figure 95:   Filtrations directly after EC1 – EC3, (1st filtration)
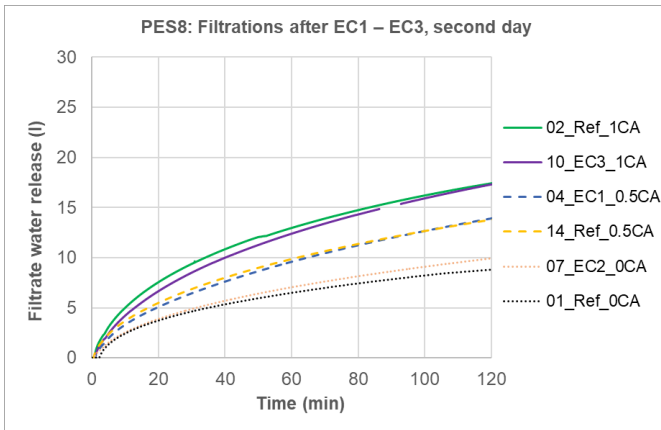
Figure 96:   Filtrations after EC1 – EC3, 1 day after EC (2nd filtration)
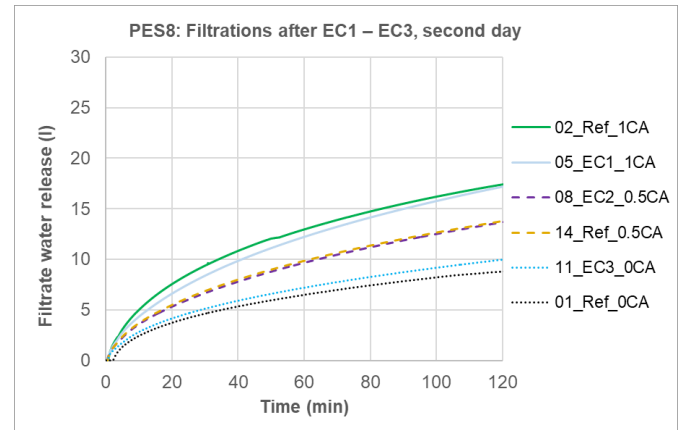
Figure 97:   Filtrations after EC1 – EC3, 1 day after EC (3rd filtration)

EC4

In EC4, the electrode gap was increased to 6.5 cm. The same effect as in EC1 – EC3 happened also here: the first filtration was 0CA and it showed an increase in filter water release in comparison to the reference experiment. Filtrations 0.5CA and 1CA, which were performed on the day following EC, did not show any improvement in comparison to their reference experiments.
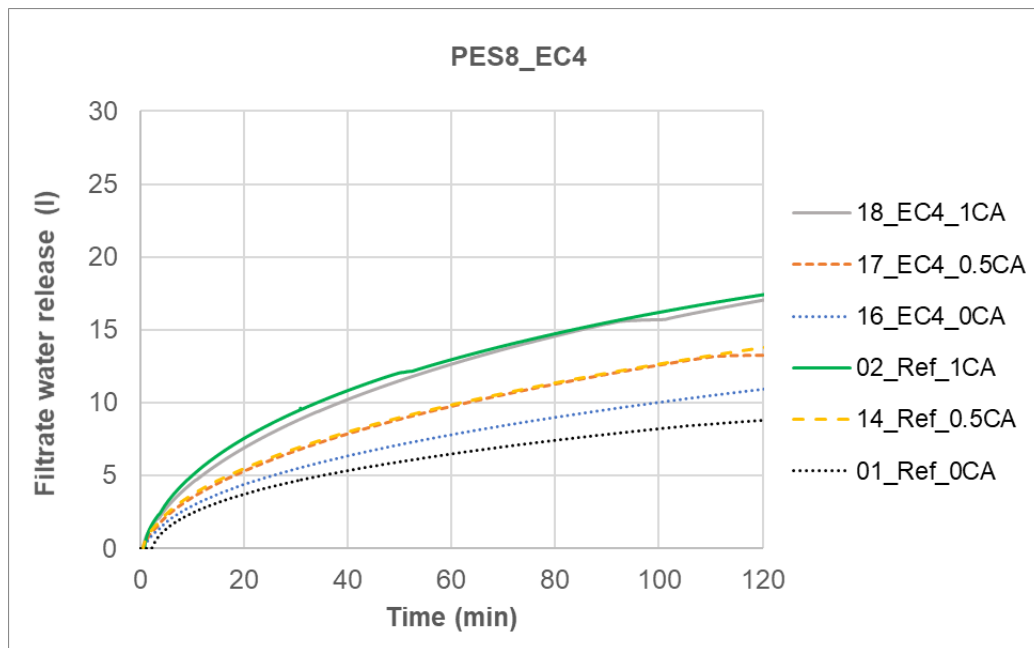
Figure 98:   Filtrations after EC4

EC5

The EC experimental duration was varied in EC5 – it was set to 45 minutes. In EC5, for the first time in PES8, at least two filtrations with the same amount of CA were performed. In Figure 99, the filtration curve 21_EK5_0CA, which was performed directly after EC, had a bigger increase of filtrate water release than the curves 22_EK5_0CA and 23_EK5_0CA, performed on the second day. This confirms the previous conclusion that waiting time has a negative effect on the filtration, reducing the positive effects of EC.

From EC5 on, all filtration experiments were performed as 0CA
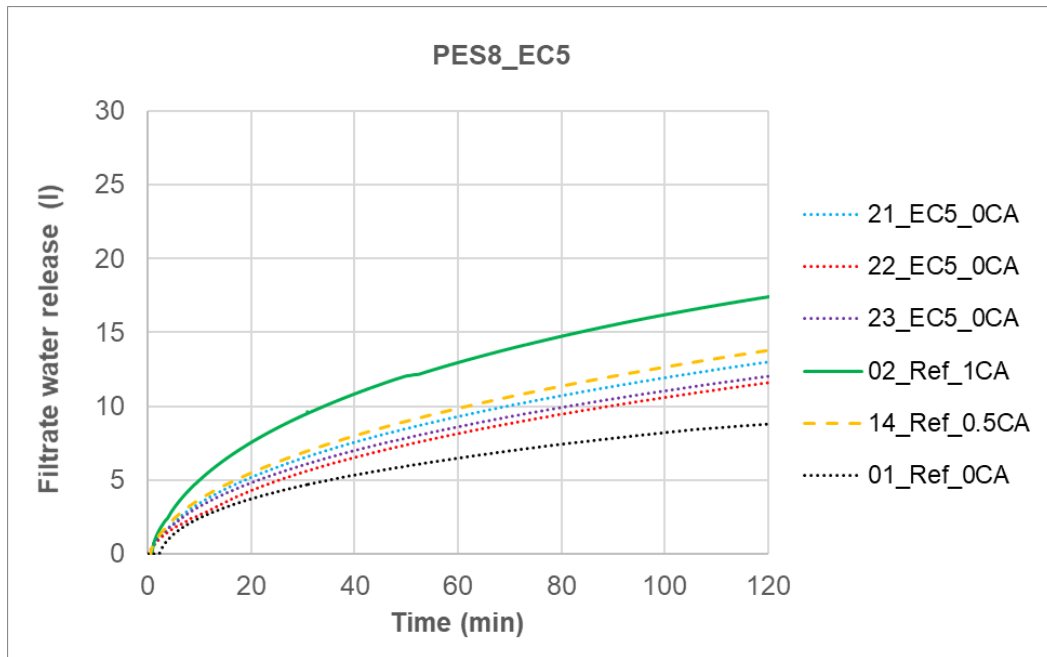
Figure 99:   Filtrations after EC5

EC6

In the next experiment (EC6), the effects of the temperature on filtration were investigated. For the filtration series after this round of EC, four probes were prepared. As the suspension was filtrated directly after EC, its temperature was 30°C. On the next day, three further filtrations were performed. Suspension probes were prepared on a following way: one probe was left at the laboratory temperature and two were put in oven and warmed up to 70°C. Prior to filtration, one of the two warmed probes was taken out of the oven and left to cool to 30°C. Did filtration did however not work out, there was a leakage in LCFP. The last probe was filtrated directly from the oven, having a temperature of 70°C at the start of the filtration. By comparing those filtrations curves with respect to their filtrate water release and temperature, conclusions about the influence of temperature on the filtration performance were drawn. The increased temperature did improve the filtration one day after EC. The filtration one day after EC (line 27) was even slightly better than those directly after EC (line 25). However, the temperature by the line 27 was 70 C, and by the line 25 was 30°C. Better comparison would be with the filtration experiment 26 (one day after EC, 30 C) but this experiment did not work out.

However, an influence of the temperature on the filtration performance has been established. Increase of the temperature improves the filtration performance.
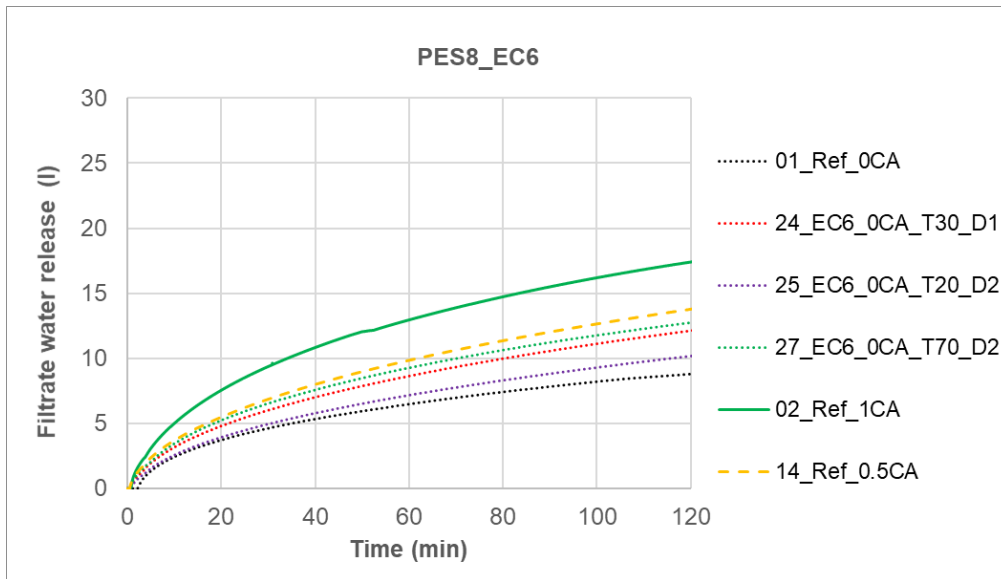
Figure 100: Filtrations after EC6

EC7

The experiment EC7 was a "standard" experiment, but the following filtration was performed for 4 hours instead of 2. The goal was to see if the filtration would be finished after 4 hours, so that parameters ΔFV_{EC} and ΔFt_{EC} can be calculated. Due to the fact that longer filtration requires more suspension volume, only two 4-hour filtrations were performed. One filtration experiment was performed as OCA and other as 1CA. The results are shown in Figure 101.
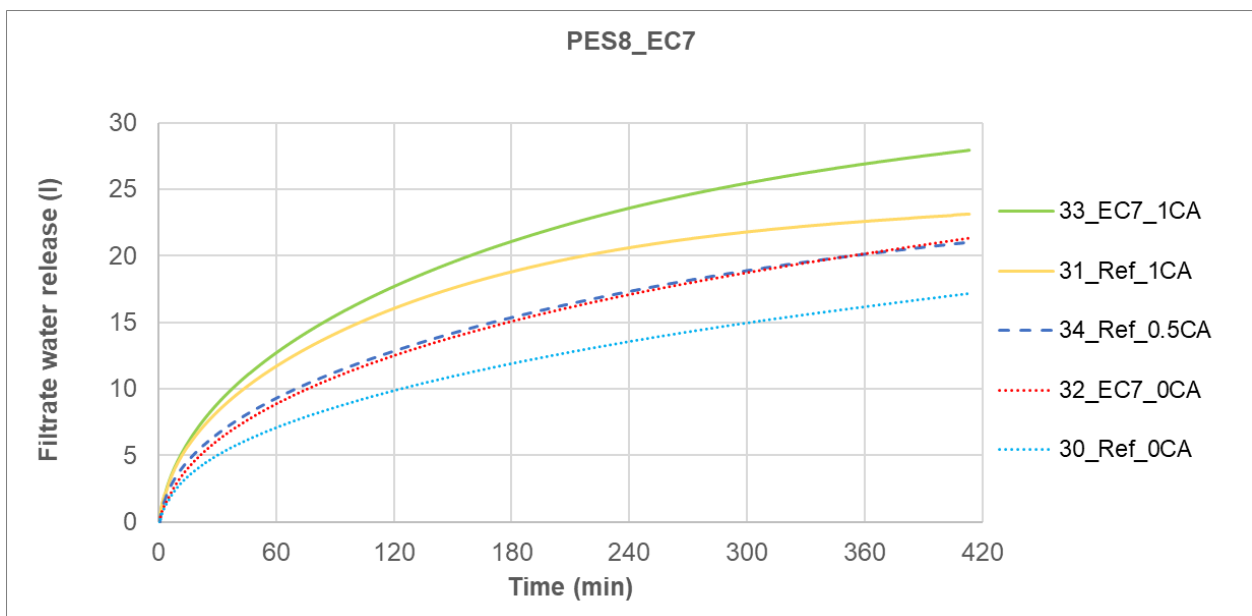
Figure 101: Filtrations after EC7

Even after 4 hours, the filtration did not seem to end. The parameters could not be calculated. However, the experiment did show some interesting results. Once again, filtration after

EC, without CA, was the same as filtration with half of CA amount (0.5CA). In addition, the combination of EC and full amount of CA was better than filtration only with CA.

Evaluation Parameter

Table 35 presents the evaluation parameters for all experiments in this experimental series. Additionally, charge density is also listed the table.

Table 35:   Construction site suspension experimental series (ES4) – evaluation parameters

Code	Charge density (Ah/l)	$\Delta\rho$ (%)	ΔFW API (%)	B_{kt} (%)	RM_{CM} (%)	FW_{rel}	RM_{FC} (%)
PES8_EC1	0.43	25.6	6.8	20.4	57.6	11.2	51.1
PES8_EC2	0.49	35.6	88.6	22.1	56.0	21.5	47.0
PES8_EC3	0.40	32.1	51.1	16.0	63.3	16.8	53.7
PES8_EC4	0.38	23.8	14.1	11.7	64.1	10.9	54.9
PES8_EC5	0.70	49.6	15.3	21.5	42.7	13.0	71.6
PES8_EC6	0.33	19.3	8.1	7.5	65.2	12.1	54.4
PES8_EC7	0.49	33.5	18.8	-	58.1	12.5	265.8

In Table 35, two information deserve special attention:

- B_{kt} was at minimum at the experiment EC6. This was the only experiment with 20 minutes duration. Accordingly, it has the lowest charge density. The higher the charge density was, the more soil coagulated on the anodes. After the charge of 0.49 Ah/l, there was no more increase of the amount of coagulated bentonite. However, something else occurred:

- B_{kt} in experiments EC1, EC2 and EC5 was approximately the same, but the residual moisture on the coagulated material on the anode (RM_{CM}) is significantly lower by the experiment EC5. This was the only experiment with the duration of 45 minutes. That could mean, it was possible to dry the coagulated material by letting the experiment run after the maximum B_{kt} was reached. This is an important finding for the disposal concept. High residual moisture could increase the disposal costs of the separated soil material. This experiment showed that it was possible to dry the coagulated material by letting the experiment run longer.

   However, this drying method consumes electricity and therefore produces costs. Moreover, such result was not observed by the experiments with SUS. Therefore, this subject needs to be further investigated.

6.7 Summary of the results with the mid-scale prototype

The results with the mid-scale prototype can be summarised as follows:

- Coagulated material remained on the anodes upon the suspension was pumped out of the cell. This makes the two-phase separation possible. One part of the fines could be separated from the suspension directly in the cell by performing EC, and the other part would be separated by filtration.
- Return of the coagulated material to the suspension had a negative influence on the subsequent filtration. Preferably, only the remaining suspension should be filtrated.
- Optimal duration of the EC experiment was 60 minutes.
- The higher the current densities (A/l) were, the better the results were.
- Influence of the higher current density overwhelmed the influence of the increased dead volume at smaller electrode gaps.
- Charge density (Ah/l) seemed to be the crucial operating parameter, uniting the influence of the current density and the experiment duration.
- None of the investigated anodes cleaning methods produced better results regarding the destabilisation of the suspension than the standard experiment without cleaning.
- EC could be beneficial for suspensions with lower densities. This needs further investigation.
- Waiting time between EC and the filtration decreased the positive effects of EC.
- EC was successfully performed also with used suspension from a construction site.
- EC could be combined with CA to reduce the required CA amount or to improve the filtration even more than CA or EC alone.
- Temperature played a role by filtration: higher temperature improved the filtration.
- It was possible to reduce the residual moisture of coagulated material by continuing with EC even after the maximal amount of the coagulated material on the anode was reached. However, this was observed only once and needs further investigation.
- The experiment that produced the best results was performed by filtrating the upper 2/3 of the suspension in the cell separately. This simulated a reduction of the dead volume of the cell.

In this chapter, the influence of EC on the filtration process in the LCFP was analysed. In the next chapter, the analysis is extended. The influence of EC on a total filtration cycle and on the complete separation and disposal concept is evaluated.

7 Impact of the new method on separation and disposal concept

7.1 Implementation of the electrocoagulation prototype in conventional separation plant

There are two ways that EC can be implemented in the separation process of fines: either as a support for a conventional separation technology or as a stand-alone technology. Both options are sketched in Figure 102.
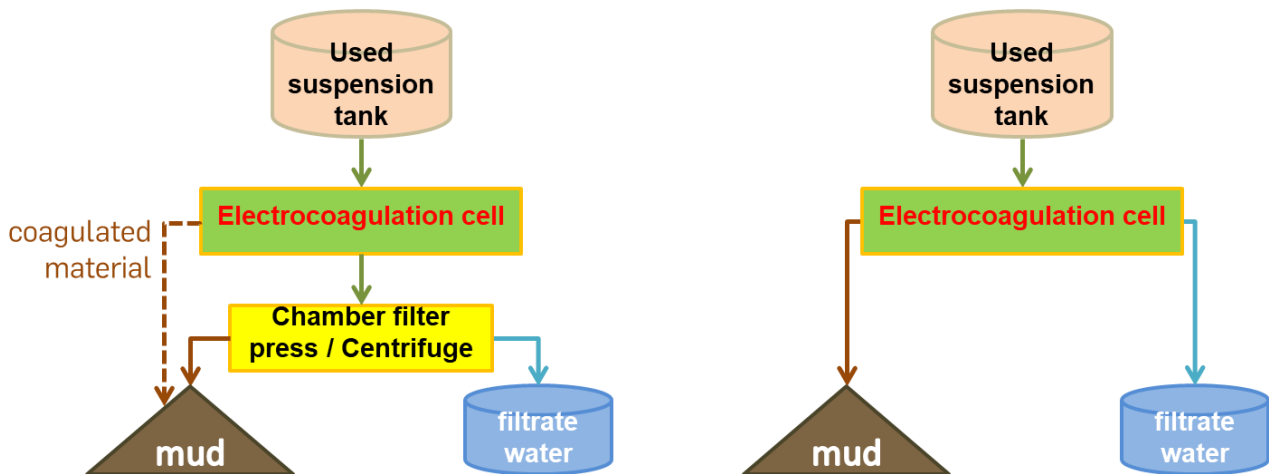
Figure 102: EC as a support technology (left) or a stand-alone technology (right)

7.1.1 EC as a support technology

A shorter version of the following analysis (up to the page 156 - Table 40) was presented in the final report of this research (Popovic & Schößer, 2019)

The results of this study have showed that EC could be used to support the conventional separation process. An EC cell could be placed directly before chamber filter presses or centrifuges (Figure 102 left), to begin separation of the soil material from the suspension and help destabilise the remaining suspension. The coagulated material from the EC cell could be disposed of in conjunction with filter cakes from the chamber press or mud from the centrifuge. The disposal of the coagulated material is further discussed in chapter 7.2.

When implementing EC as a support for a conventional separation technology, three options concerning the usage of CA are possible:

1) Replacement of CA usage by EC

2) Reduction of CA usage by support with EC

3) Standard usage of CA supplemented with EC to achieve higher separation efficiency in chamber filter presses and centrifuges

The third case could provide economic, but no ecological advantages. The eco-friendly effects of EC would be eliminated because the amount of CA used in the separation process would not be reduced.

One of the motivating ideas of this research was to eliminate the usage of CA through the implementation of EC. Therefore, further analysis in this section concentrates only on the first case.

Filtration time

The results of the majority of the filtration experiments showed an increase of the filtrate water release after EC, as compared to the reference filtration without CA. Through use of a certain combination of EC operating parameters, greater filtrate water release was also possible in comparison to reference filtration experiments with CA.

Greater filtrate water release does not necessarily mean that the filtration was improved. This is why the parameters ΔFV_{EC} and ΔFt_{EC} were introduced in the analysis of the experiments. However, these parameters consider only the filtration itself and not the whole process preceding and following filtration. One complete filtration cycle, together with the average duration of specific operations, is shown in Table 36. The presented data originates from a construction site.

Table 36: Filtration cycle of a filter press

Action	Closure cylinder	First filling	Filtration process	Press filter cake together	Pressure drop compensation	Filter cake discharge	Total cycle
Duration (min)	2	4	32	9	2	5	54

As shown in Table 36, in addition to the filtration time of 32 minutes another total of 22 minutes was spent on various required operations before and after filtration itself. This needs to be taken into account when calculating the influence of EC on filtration performance.

In the following example, the test series PES5 which varied experiment duration is analysed. Additionally, the experiment with the best EC parameters (PES6_EC5, referred to as Best Combo) and the corresponding reference filtration experiments are included. The points in Figure 103 represent the time at which 80% of the total amount of filtrate water were reached.
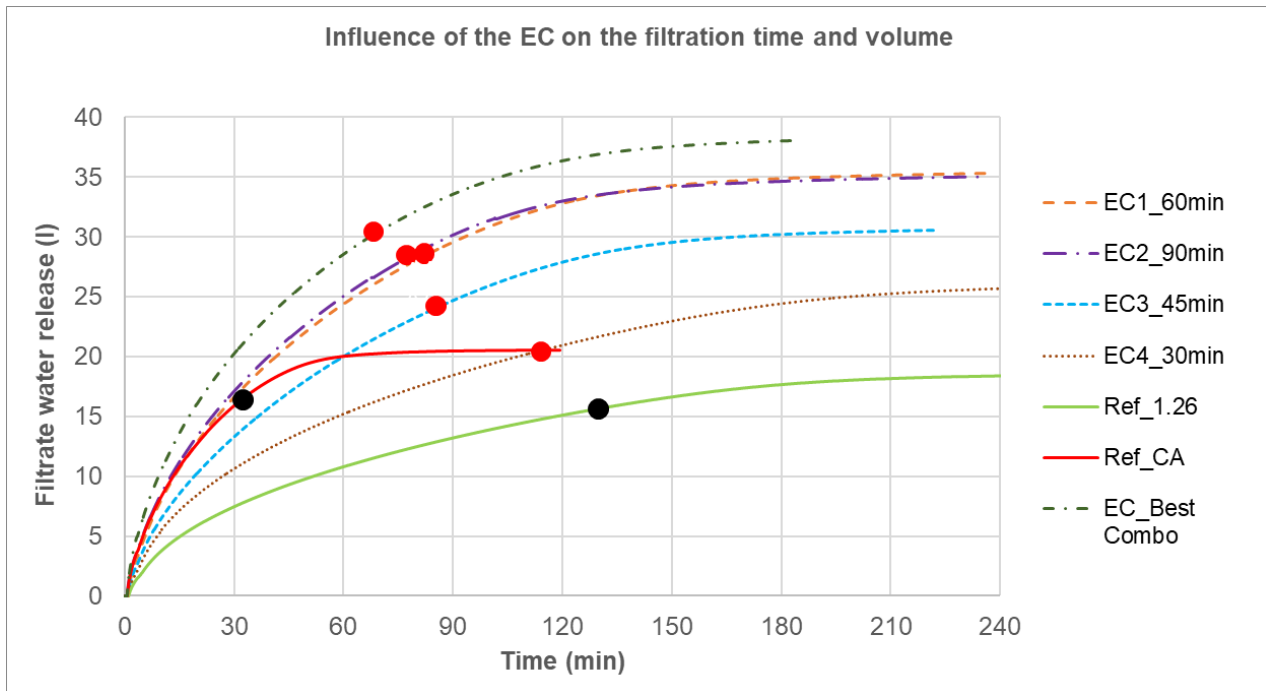
Figure 103: Filtration times from PES5 & PES6_EC5 (Best Combo)

Compared to the reference experiment without CA (Ref_1.26), the filtration performance was significantly improved after EC: the filtration time is shortened, and also more filtrate water is recovered per filtration cycle. Compared to the reference experiment with CA (Ref_CA), more filtrate water is released per cycle, but the duration of filtration is extended. The amount of filtrate water and the filtration time, calculated using the 80% criterion, are listed in Table 37.

Table 37:   Filtration time and filtrate water release after EC

Experi-ment	Ref_1.26	Ref_CA	30 min	45 min	60 min	90 min	Best Combo
Duration (min)	130	**31.4**	114.8	84.9	79.5	75.9	**69.3**
Filtrate water release (l)	15.2	**16.4**	20.6	24.0	28.0	28.0	**30.4**

Two cases from Table 37 have been further analysed: reference filtration with the CA (Ref_CA), which reflects the construction site practice most accurately and filtration with the best combination of EC operating parameters (Best Combo). Table 38 compares these two cases in terms of volume of filtrate water and filtration time. As shown in the table, Ref_CA resulted in 16.4 l of filtrate water in 31.4 minutes, while Best Combo delivered 14 additional litres but took 37.9 minutes longer. This shows an 85% increase of the volume of filtrate water for a 120% prolongation of the filtration process.

Table 38:   Filtration time and filtrate water release: comparison between Ref_CA and Best Combo

	Ref_CA	Best Combo	Δ (Best Combo - Ref_CA)	Δ (Best Combo to Ref_CA) (%)
Duration (min)	31.4	69.3	37.9	120.7
Filtrate water release (l)	16.4	30.4	14	85.4

The productivity of the chamber filter press, however, should not be measured only as a ratio of filtrate water release over time. Instead, the complete volume of the suspension treated in one filtration process should be considered. This volume includes both the volume of filtrate water and the volume of filter cake in the filter press. For LCFP, the latter is equal to the volume of the chambers, which is 8 l.

Table 39 again compares the cases from Table 38, but with respect to the total volume of filtered suspension. After EC, one filtration cycle still treats 14 l more used suspension than one filtration cycle with CA. However, in terms of complete volume of the treated suspension, it is only 57% more suspension than with the filtration process with CA.

Table 39:   Filtration time and volume of treated suspension: comparison between Ref_CA and Best Combo

	Ref_CA	Best Combo	Δ (Best Combo - Ref_CA)	Δ (Best Combo to Ref_CA) (%)
Duration (min)	31.4	69.3	37.9	120.7
Filtrated suspension (l)	24.4	38.4	14	**57.4**

Overall, treatment of the SUS with EC instead of CA resulted in an increase of the volume of treated suspension by 57 % and an increase of the filtration time by 120 %.

Duration of one complete filtration cycle with EC was calculated in Table 40. A reasonable assumption was made that EC prolongs only the filtration process and has no influence on the duration of other actions in a filtration cycle. In that case, EC prolonged the filtration process from 32 to 70 minutes, which increased filtration cycle time from 54 minutes to 92 minutes. As shown in Table 40, EC would prolong one complete filtration cycle by a comparatively small 70 %.

Table 40:   Duration of complete filtration cycle with CA and with EC

Action	Closure cylinder	First filling	Filtration process	Press filter cake together	Pressure drop compensation	Filter cake discharge	Total cycle
Duration with CA (min)	2	4	32	9	2	5	54
Duration with EC (min)	2	4	70	9	2	5	92
Δ (EC to CA) (%)	0	0	120	0	0	0	**70**

Overall, the calculations in this section showed that EC would prolong the duration of one filtration cycle by 70 % while increasing the volume of treated suspension by 57 %. As shown in Table 41, this means that a filtration with EC would actually only need 8 % more time to filtrate a given amount of suspension as compared to filtration with CA. For example, if a chamber filter presses on a construction site would treat 60 m³ of used suspension per hour, after implementation of EC they would be able to treat 55 m³ per hour.

Table 41:   Overview: Influence of EC on duration of one filtration cycle and on the volume of treated suspension in one filtration cycle

	Filtration with CA	Filtration with EC
Time (%)	100	170
Volume (%)	100	157
Δ (EC to CA) (%)	0	**- 8**

Instead of going step by step, the above analysis can be summed up in the following equations:

$$P_{cfp} = \frac{1+\Delta FV_{EC}}{1+\Delta Ft_{EC} \cdot F\%} \tag{Eq. 7-1}$$

$$P_{cfp} = \frac{\frac{V_{FW,EC}+V_{cfp}}{V_{FW,CA}+V_{cfp}}}{1+(\frac{t_{FW,EC}}{t_{FW,CA}}-1) \cdot F\%} \tag{Eq. 7-2}$$

whereby:

P_{cfp} factor for change of productivity of chamber filter press with EC [-]

ΔFV_{EC} change of the volume of the filtrated suspension after EC [-]

ΔFt_{EC} change of the filtration time after EC [-]

$V_{FW,EC}$ filtrate water discharge after EC [m³]

$V_{FW,CA}$ filtrate water discharge with CA [m³]

V_{cfp} volume of the chamber filter press [m³]

$t_{FW,EC}$ filtration time after EC [h]

$t_{FW,CA}$ filtration time with CA [h]

$F\%$ time ratio of a filtration process within a full filtration cycle [-]

The result of Eq. 7-2 is a factor P_{cfp} that, when multiplied by filter press capacity [m³/h used suspension], gives the capacity in a case of replacing CA with EC. The variables $V_{FW,EC}$, $V_{FW,CA}$, $t_{FW,EC}$ and $t_{FW,CA}$ (defined in chapter 6.4.1) are acquired through filtration experiments, while $F\%$ is the data from construction site. For the data used in the above analysis, the factor P_{cfp} is equal to 0.92. The exact calculation can be found in appendix D. This means that the filter press capacity without EC multiplied with 0.92 gives the filter press capacity after EC, which is an 8 % decrease.

Filtration volume

Besides filtration time, EC also influences the total filtration volume. Since flocculants have to be added to the suspension in the form of a water-based solution prior to the filtration, the usage of CA increases the total filtration volume. For the conditioning of the used suspensions investigated in this thesis, 0.1 m³ of water for flocculants solution was required per 1 m³ of suspension. The usual amount of water required for flocculants solution is 0.2 m³ per 1 m³ used suspension (MSE-Filterpressen, 2019). This depends on the in-situ soil, the density of the used suspension and the concentration of the flocculant solution. The increase of total filtration volume due to addition of coagulants is negligible, since coagulants are added in volume percentages smaller than 0.5 %.

This means that conventional conditioning with CA increases total filtration volume by 20%. For every 1 m³ of used suspension, 1.2 m³ of fluid have to be filtrated.

On the other hand, EC decreases total filtration volume. In the Best Combo experiment, 27.4 % of soil particles from the suspension coagulated on the anode, retaining a residual moisture of 48.4 %. This reduces the suspension volume by 24 l, which is a 15 % of the cell volume. Therefore, for every 1 m³ of used suspension, only 0.85 m³ would have to be filtrated. Overall, filtration volume after EC in comparison to conventional conditioning with CA would decrease for 29 %. An overview of filtration volume is shown in Table 42.

Table 42:   Filtration volume with CA and with EC

	Used suspension volume	Filtration volume with CA	Filtration volume with EC	Difference CA-EC	Difference (%)
Volume (m³)	1	1.2	0.85	0.35	**29**

The influence of EC on the total filtration volume can be described with parameter *FV* in Eq. 7-8. The path to this equation is shown in equations 7-3 – 7-7.

$$FV = \frac{1-V_{CM}}{1+V_{CA}} \qquad\qquad\qquad\qquad \text{(Eq. 7-3)}$$

$$V_{CM} = V_{S,CM} + V_{W,CM} \qquad\qquad\qquad\qquad \text{(Eq. 7-4)}$$

$$V_{S,CM} = (\delta_{SUS} - 1)/(\delta_S - 1) \cdot B_{kt} \qquad\qquad\qquad\qquad \text{(Eq. 7-5)}$$

$$V_{W,CM} = (\delta_{SUS} - 1)/(\delta_S - 1) \cdot B_{kt} \cdot \delta_S \cdot \frac{RM_{CM}}{1-RM_{CM}} \qquad\qquad \text{(Eq. 7-6)}$$

$$V_{CM} = (\delta_{SUS} - 1)/(\delta_S - 1) \cdot B_{kt} \cdot (1 + \delta_S \cdot \frac{RM_{CM}}{1-RM_{CM}}) \qquad\qquad \text{(Eq. 7-7)}$$

$$FV = \frac{1-(\delta_{SUS}-1)/(\delta_S-1)\cdot B_{kt}\cdot(1+\delta_S\cdot\frac{RM_{CM}}{1-RM_{CM}})}{1+V_{CA}} \qquad\qquad \text{(Eq. 7-8)}$$

whereby:

FV factor for decrease of filtration volume due to EC [-]

V_{CA} volume of CA added to suspension per m³ suspension [m³]

V_{CM} volume of coagulated material per m³ suspension [m³]

$V_{S,CM}$ volume of soil in coagulated material per m³ suspension [m³]

$V_{W,CM}$ volume of water in coagulated material per m³ suspension [m³]

δ_{SUS} suspension density [t/m³]

δ_S grain density EC [t/m³]

B_{kt} ratio of coagulated material after EC [-]

RM_{CM} ratio of residual moisture in coagulated material [-]

In Eq. 7-8, the variables B_{kt} and RM_{CM} are acquired through EC experiments, while V_{CA} is based on data from a construction site. For the data used in above analysis, the factor FV would be equal to 0.71, meaning that the total filtration volume by filtration with CA multiplied with 0.71 results in the volume after replacement of CA with EC. The calculation of this factor can be found in appendix D.

An overview of mass and volume balance by the filtration with CA and with EC is presented in Figure 104. This is a spreadsheet application which calculates mass and volume in the filtration process according to the given assumptions in yellow boxes. The same spreadsheet is also used for the analysis of the disposal concept in chapter 7.2.

Assumptions & Variables

Used suspenson volume	Used suspenson density	Grain density	Water for flocculants solution	Filter cake residual moisture	Coagulated material amount	Coagulated material moisture	Filtrate water re-use (only EC)
[m³]	[t/m³]	[t/m³]	[m³/m³ US]	[%]	[%]	[%]	[%]
1	1,25	2,65	0,2	40%	27%	48%	50%

Coagulating agents

CA vol. [m³] 0,2
US vol. [m³] 1
Total filtration vol. [m³] 1,2

Used suspension tank → chamber filter presses

	Suspension before CA	Suspension after CA			Filtration products	
					Filtercake	Filtrate water
Soil vol. [m³]	0,152	0,152		Soil vol. [m³]	0,152	0
Soil w. [t]	0,402	0,402		Soil w. [t]	0,402	0
Water Vol.	0,848	1,048		Water Vol.	0,268	0,781
Water w. [t]	0,848	1,048		Water w. [t]	0,268	0,781

Disposal   Sewage

US vol. [m³] 1
Total filtration vol. [m³] 0,855

Used suspension tank → EC cell → chamber filter presses

	Suspension before EC	Coagulated material	Suspension after EC			Filtration products	
						Filtercake	Filtrate water
Soil vol. [m³]	0,152	0,042	0,110		Soil vol. [m³]	0,110	0
Soil w. [t]	0,402	0,110	0,292		Soil w. [t]	0,292	0
Water Vol.	0,848	0,103	0,745		Water Vol.	0,194	0,551
Water w. [t]	0,848	0,103	0,745		Water w. [t]	0,194	0,551

Disposal   Sewage / Re-use

Disposal of soil material	CA	EC	comparison
Soil vol. [m³]	0,152	0,152	+0,0%
Soil w. [t]	0,402	0,402	+0,0%
Water Vol.	0,268	0,298	+11,2%
Water w. [t]	0,268	0,298	+11,2%
Total volume [m³]	0,419	0,449	+7,1%
Total weight [t]	0,669	0,699	+4,5%
Moisture (%)	40,0%	42,6%	

Total filtration volume	CA	EC	comparison
Volume	1,2	0,855	-28,7%

Filtrate water	CA	EC	comparison
total	0,781	0,551	-29,4%
sewage	0,781	0,275	-64,7%

Figure 104: Mass and volume balance of the filtration process with CA and with EC

Summary – filtration performance with EC

The result of this analysis suggests that implementation of EC as a replacement for CA would decrease the filter press efficiency by 8 %, but would also lower the total filtration volume by 29 %. Therefore, EC would have an overall positive impact on the filtration. An example is shown in Table 43.

Table 43:   Example of filtration with EC and and CA

	Used suspension volume (m³)	Total filtration volume (m³)	Chamber filter press productivity (m³/h)	Filtration time (h)
With CA	1000	1200	60	20
With EC	1000	855	55	15.5
Δ (%)	0	- 29	- 8	- 22

Assuming a chamber filter press is designed to operate a certain number of hours per day, introduction of EC to the separation process would allow a decrease of the filter press capacity. This means that EC would make it possible to use smaller or fewer chamber filter presses. The results of this calculation (Table 43) show that the required capacity of chamber filter presses on a construction site could be reduced for around 20 % when replacing CA with EC.

The complete analysis of influence of EC on the filtration time and the filtration volume can be summed up in the following equations:

$$P_{sep} = \frac{P_{cfp}}{FV} = \cfrac{\cfrac{\cfrac{V_{FW,EC}+V_{cfp}}{V_{FW,CA}+V_{cfp}}}{1+(\frac{t_{FW,EC}}{t_{FW,CA}}-1)\cdot F\%}}{\cfrac{1-(\delta_{SUS}-1)/(\delta_S-1)\cdot B_{kt}\cdot(1+\delta_S\cdot\frac{R_{M,CM}}{1-R_{M,CM}})}{1+V_{CA}}} \qquad \text{(Eq. 7-9)}$$

$$P_{sep} = \frac{P_{cfp}}{FV} = \cfrac{\frac{V_{FW,EC}+V_{cfp}}{V_{FW,CA}+V_{cfp}}\cdot(1+V_{CA})}{\left[1+(\frac{t_{FW,EC}}{t_{FW,CA}}-1)\cdot F\%\right]\cdot\left[1-\frac{\delta_{SUS}-1}{\delta_S-1}\cdot B_{kt}\cdot(1+\delta_S\cdot\frac{R_{M,CM}}{1-R_{M,CM}})\right]} \qquad \text{(Eq. 7-10)}$$

or:

$$R_{cfp} = \frac{FV}{P_{cfp}} = \cfrac{\left[1+(\frac{t_{FW,EC}}{t_{FW,CA}}-1)\cdot F\%\right]\cdot\left[1-\frac{\delta_{SUS}-1}{\delta_S-1}\cdot B_{kt}\cdot(1+\delta_S\cdot\frac{R_{M,CM}}{1-R_{M,CM}})\right]}{\frac{V_{FW,EC}+V_{cfp}}{V_{FW,CA}+V_{cfp}}\cdot(1+V_{CA})} \qquad \text{(Eq. 7-11)}$$

whereby:

P_{sep} factor for productivity of separation process when replacing CA with EC [-]

R_{cfp} factor for calculation of required chamber filter press capacity when replacing CA with EC [-]

The factor P_{sep} is the coefficient that, multiplied with the installed filter press capacity on a construction site, gives the fine separation capacity that would be available after implementation of EC. The variables required to calculate P_{sep} are filtration results regarding the filtration volume and the filtration time ($V_{FW,EC}$, $V_{FW,CA}$, $t_{FW,EC}$ and $t_{FW,CA}$), EC experiment results concerning coagulated material (B_{kt} and RM_{CM}) and the data from construction site concerning the usage of CA (V_{CA}) and the filtration process ($F\%$). For the data used in the analysis above, the factor P_{sep} would be equal to 1.29. That means that the separation capacity after installation of EC would be 29 % higher than with CA.

The reversed factor R_{cfp} could be used in the planning phase to reduce the required filter press capacity on the construction site before beginning. In this case, the variables in the equation Eq. 7-11 would not be the actual used suspension from the construction site but rather the planned data or empirical values for the given presses and soil. For the data used in the analysis above, the factor R_{cfp} would be equal to 0.78. The planned capacity of the chamber filter press could be multiplied with this factor in the planning phase, which would result in 22 % lower required capacity when CA is replaced with EC (as in Table 43). The calculations of both factors can be found in appendix D.

Calculation model

The influence of EC on separation and disposal concept is suspension-specific. With the current experimental setup, any suspension can be tested. The results can be analysed with the calculation model (Eq 7-1 – Eq- 7-11) and spreadsheet application from Figure 104. There are no constants in the equations; the calculations are valid for any given suspension and even any design of experimental setup, as long as there is one EC cell and one chamber filter press.

This opens further research possibilities, which are presented in the outlook.

7.1.2 EC as stand-alone technology

In order to implement EC as a stand-alone technology, i.e. a complete replacement for filter presses or centrifuges, EC would have to completely separate the soil material from the suspension. This was not realized in the experiments described in this thesis. The highest value of B_{kt} was 30.7% in experiments with SUS (PES3_EC5) and 22.1 % in experiments with CUS (PES8_EC2).

Still, this option could be feasible. By designing the process in a way that the coagulated material could be removed from the cell during EC while automatically replacing the removed volume with new used suspension, a continuous process could be possible. In theory, the only output would be the coagulated material from the anodes. This, however, is easier said than done. In addition to safety issues of removing the material from the cell during EC, challenges also include the influence on zeta potential of the particles and the energy consumption of such a continuous EC process.

As mentioned in the discussion of the results and in the literature review, it is possible to decrease the zeta potential of the particles to zero, which would completely destabilise them. If the particles stay in the cell for a sufficient amount of time, this is likely to occur. The question is this: if the particles do not coagulate on the anode up to the point of decreasing their zeta potential to 0 mV, what happens next? In theory, further EC could even re-stabilise the particles by turning their zeta potential to positive values (>0 mV). However, further addition of coagulant through electrodissolution of the anode could also promotes other coagulation mechanisms, such as sweep coagulation. These additional research questions would have to be investigated. More importantly, the technical requirements of this process would have to be fulfilled: developing a safe way to completely remove the coagulated material on the anode during EC.

The experiments PES6_EC3 and PES6_EC4, which were intended to manually simulate a continuous process with the prototype, did not work as planned. This could be explained by the fact that removing the material from the cell and replacing it with a new suspension lasted for more than one hour, due to the security measures and experimental procedure required. The suspension had to be pumped out of the cell, anodes had to be cleaned and the coagulated material had to be removed, which was followed by pumping the suspension back into the cell and continuing with EC. The pause of 1 hour between the two parts of EC process, with pumping the suspension out of the cell and back in, does not truly represent a continuous process.

However, the idea of a continuous EC separation process could be tested under laboratory conditions, where the security requirements can be relaxed due to lower electrical currents and therefore smaller hydrogen production. The experimental procedure would be similar to the mechanical cleaning experiments, except the removed coagulated material would be replaced with new suspension. In laboratory conditions, this action would take up to 10 seconds, during which direct current would have to be turned off. Several cycles would have to be performed. For example, the coagulated material could be removed and replaced every 15 minutes and the experiment would go on for few hours. The development of the parameters B_{kt} and $\Delta\rho$ over time should be analysed. If the removal efficiency does not decrease over subsequent cycles, that would be a sign that a continuous process could be possible.

Still, it needs to be emphasised that not a single EC experiment in this thesis nor in the first phase of this research project (Paya, 2016) came close to removal efficiency of centrifuges of chamber filter presses regarding the removal of fines from used suspensions. While centrifuges and chamber filter presses remove most of the particles from the suspension, EC did not separate even a half of them. Even if it would be technically feasible to significantly increase the removal efficiency of EC (for example with much higher electrical current), the question remains if it is economically viable to separate every soil particle from the suspension by only using EC, rather than using EC as a support for conventional separation technology.

7.2 Impact of the electrocoagulation on disposal concept

Regardless of the support or stand-alone implementation of EC in the separation technology, EC creates one disposal product that until now did not exist on construction sites: coagulated material. This opens a question of how this material should be disposed of. Coagulated material is made of the same soil material as the filter cake from chamber filter presses or mud from centrifuges. Therefore, it needs to meet the same disposal requirements as the current disposal material on the construction site. Figure 105 presents an overview of the disposal possibilities for products of fine separation and according regulations.
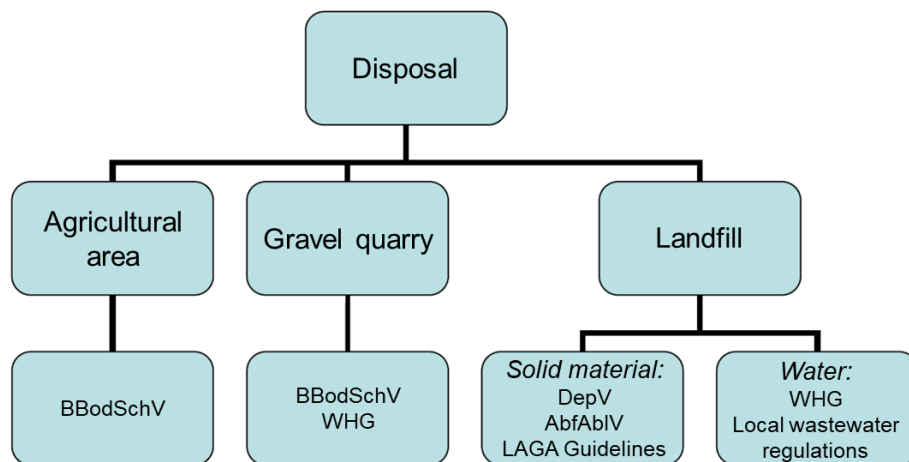
Figure 105: Disposal options for products of fine separation (second row) and the corresponding regulations (third row) (after Biermann, 2010)

Nowadays, due to stricter environmental criteria, disposal in agricultural areas or gravel quarries is rarely, if ever, allowed (Förster, 2016). Instead, the soil is brought to the landfill and water is disposed in the sewage system. Therefore, the requirements from the according regulations need to be fulfilled, as already mentioned in 2.5.4. For the disposal of fine soil material from construction sites, corresponding regulations in Germany are The Landfill Ordinance (Verordnung über Deponien und Langzeitlager – Deponieverordnung (DepV)),

The Directive on the Dumping of Waste (Verordnung über die umweltverträgliche Ablagerung von Siedlungsabfälle – Abfallablagerungsverordnung (AbfAblV)) and LAGA Guidelines (LAGA-Richtlinien).

For the separated water, requirements from Water Resources Act (Wasserhaushaltsgesetz (WHG)) and local wastewater regulations must be fulfilled.

By replacing CA with EC, there will no longer be remains of coagulants (aluminium or iron ions and chloride, sulphate or nitrate groups, depending on the coagulant type) and flocculants in the products of fine separation. However, there will be remains of electrode material, since it dissolves during EC. The aluminium alloy EN AW-5754 (chemical designation AlMg3) was used as raw material for electrodes in EC prototype cell. The chemical composition of this alloy is shown in Table 44.

Table 44:   Chemical composition of electrode material as mass percentage

Si	Fe	Cu	Mn	Mg	Cr	Ni	Zn	Ti	other	Al
0.40	0.40	0.10	0.50	2.6 – 7.7	0.30	-	0.20	0.15	0.10 - 0.60 Mn+Cr	rest (89,7 - 95,3)

Disposal regulations prescribe maximal allowed concentrations for some of the stated metals. Moreover, EC influences the pH and the electrical conductivity of a suspension and also of the products of fine separation (soil material and filtrate/centrate water). Those parameters are analysed more deeply in the following sections.

7.2.1 **Disposal of soil material (coagulated material, filter cake, mud)**

Depending on the concentrations of certain elements in the soil and the eluate (the discharged mixture of solvents and dissolved substances, Figure 106), DepV classifies materials into different deposition classes (DK). From all the metals in aluminium alloy, only Cu, Ni, Zn and Cr are listed in DepV (Table 45 and Table 46). In addition to restrictions on metal concentrations, requirements for eluate include limits for electrical conductivity and an acceptable range for pH-value. However, chloride and sulphate in the eluate, which can originate from conventional coagulants, are also restricted. The requirements for deposition classes I and II are further defined in AbfAblV. Here, the stiffness of the deposited material is defined (Table 47).
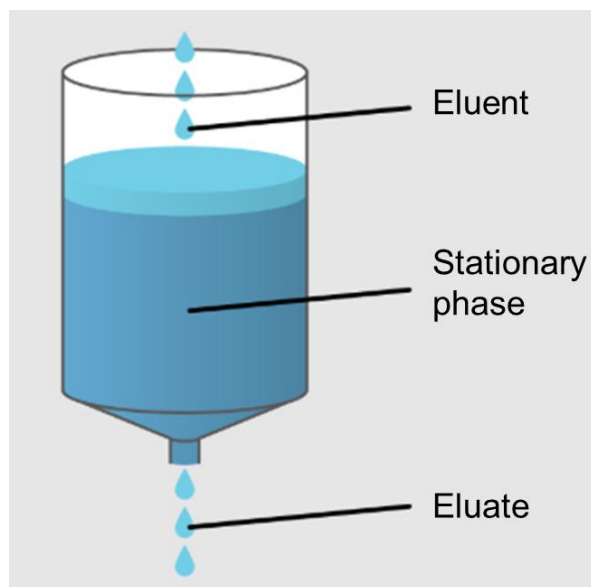
Figure 106: Creation of an eluate (Uphoff Lab, 2019)

Table 45:   DepV criteria for soil (DepV, 2009)

Parameter	Unit	Geological barrier	DK 0	DK 1	DK 2	DK 3	Re-cultiva-tion layer
Cr	mg/kg dry weight	-	-	-	-	-	≤120
Cu	mg/kg dry weight	-	-	-	-	-	≤80
Ni	mg/kg dry weight	-	-	-	-	-	≤100
Zn	mg/kg dry weight	-	-	-	-	-	≤300

Table 46:   DepV criteria for eluate (DepV, 2009)

Parameter	Unit	Geological barrier	DK 0	DK 1	DK 2	DK 3	Re-cultiva-tion layer
Cr	mg/l		≤ 0.05	≤ 0.3	≤ 1	≤ 7	≤ 0.03
Cu	mg/l	≤ 0.05	≤ 0.2	≤ 1	≤ 5	≤ 10	≤ 0.05
Ni	mg/l	≤ 0.04	≤ 0.04	≤ 0.2	≤ 1	≤ 4	≤ 0.05
Zn	mg/l	≤ 0.1	≤ 0.4	≤ 2	≤ 5	≤ 20	≤ 0.1
Chloride	mg/l	≤ 10	≤ 80	≤ 1500	≤ 1500	≤ 2500	≤ 10
Sulphate	mg/l	≤ 50	≤ 100	≤ 2000	≤ 2000	≤ 2500	≤ 50
pH	-	6.5 - 9	5.5 - 13	5.5 - 13	5.5 - 13	4 - 13	6.5 - 9
Electrical conductivity	µS/cm	≤400	≤400	≤3000	≤6000	≤10000	≤500

Table 47:   AbfAblV criteria for soil stiffness (AbfAblV, 2001)

Parameter	Unit	DK 1 & 2
Shear strength	kN/m²	≥ 25
Axial deformation	%	≤ 20
Unconfined compressive strength	kN/m²	≥ 50

Besides disposing, the excavated soil material can also be used as construction material. The requirements for this are listed in LAGA Guidelines. LAGA Guidelines restrict the same metals as DepV, but with different concentrations. The range for the pH value and limits for the electrical conductivity are also defined. The requirements are listed in Table 48 and Table 49. Z in the tables stands for "Zuordnungswerte ", meaning "assignment criteria".

Table 48:   LAGA Guidelines criteria for soil material (Laga-Richtlinie, 1998)

Parameter	Unit	Z 0	Z 1.1	Z 1.2	Z 2
Cr	mg/kg	≤ 50	≤ 100	≤ 200	≤ 600
Cu	mg/kg	≤ 40	≤ 100	≤ 200	≤ 500
Ni	mg/kg	≤ 40	≤ 100	≤ 200	≤ 500
Zn	mg/kg	≤ 120	≤ 300	≤ 500	≤ 1500

Table 49:   LAGA Guidelines criteria for eluate (Laga-Richtlinie, 1998)

Parameter	Unit	Z 0	Z 1.1	Z 1.2	Z 2
Cr	µg/l	≤ 15	≤ 30	≤ 75	≤ 150
Cu	µg/l	≤ 50	≤ 50	≤ 150	≤ 300
Ni	µg/l	≤ 40	≤ 40	≤ 150	≤ 200
Zn	µg/l	≤ 100	≤ 100	≤ 300	≤ 600
pH	-	6.5 - 9	6.5 - 9	6 – 12	5.5 - 12
Electrical conductivity	µS/cm	≤ 500	≤ 500	≤ 300	≤ 1500

To determine the influence of EC on disposal of separated soil material, an analysis of metallic and Cl remains in the filter cakes and coagulated material was performed. The results are presented in Table 50. The samples of coagulated material were taken from experiment

PES6_EC1 and filter cake after EC from PES5_EC2. The remaining samples were taken from reference experiments.

Table 50: **Analysis of soil material / Concentration of metals in coagulated material and filter cake (mg/kg)**

Elements in soil material (mg/kg)	Coagulated material	Filter cake after EC	Filter cake with CA	Filter cake without EC and CA	Re-cultivation layer (DepV)	Construction material Z0 (LAGA-Regulations)
Cu	4	5	4	4	120	50
Ni	7	8	5	5	80	40
Zn	25	26	25	25	100	40
Cr	20	23	18	18	300	120
Al$_2$O$_3$	69300	71200	68800	67600	Not listed	Not listed
Fe$_2$O$_3$	12600	13000	13100	12100	Not listed	Not listed
Cl	65	72	104	70	only for eluate	Not listed

The analysis showed that the concentration of Ni and Cr in coagulated material and filter cakes after EC was slightly higher than in filter cakes without EC. In order to determine the significance of the increased concentration, the limit values from DepV and Laga Regulations (class Z0) are listed in the table. The direct comparison of those values shows that the slightly increased concentration of Ni and Cr is negligible.

The concentrations of Al, Fe, and Cl were also analysed. Those three elements were chosen as they represent the coagulants: FeCl$_3$ in the conventional conditioning and Al in EC process.

The concentration of Al and Fe is not limited in the current regulations and therefore they do not influence the disposal concept at this time. Nevertheless, the analysis was performed because the regulations could change in the future. The concentration of Cl is not restricted in soil, but it is restricted in eluate based on that soil.

The results were not surprising. The smallest concentration of Al, Fe and Cl was measured in a filter cake from a reference experiments without EC and CA. The highest concentration of Fe and Cl was measured in filter cake with CA. The highest concentration of Al was measured in coagulated material and filter cakes after EC. Those samples also had increased concentration of Fe since it is a part of the aluminium alloy (Table 44).

Looking at the relative increase of concentrations, the concentration of Al and Fe do not differ significantly. What stands out in the table is the concentration of Cl, which increased by 50 % in comparison to separated soil material without CA. However, it is more precise to compare the measured concentrations in absolute values, not as relative increase or decrease. The usage of the coagulant FeCl$_3$ has increased the Cl concentration in soil by 34

mg/kg. Even if the initial concentration of Cl had been higher, the increase of the Cl concentration due to the usage of the coagulant should still be 34 mg/kg and not 50% of the initial value. The change of concentrations of all tested materials is listed in Table 51.

The last column in Table 51 describes an estimated influence of CA and EC on the disposal class of the soil material. The change of concentration of elements Cu, Ni, Zn and Cr is negligible and does not influence the disposal class. Al and Fe have no influence since their concentration is not limited in the regulations. Only Cl could have a certain influence on the disposal class, depending on which class the soil would be without usage of CA. However, the allowed concentration of Cl in DepV is quite high in comparison to metals.

Table 51:   Change of the concentrations of materials in absolute values, with the concentration from the filter cake without EC and CA as initial value

Elements in soil material (mg/kg)	Coagulated material	Filter cake after EC	Filter cake with CA	Filter cake without EC and CA	Estimated influence on the disposal class
Cu	0	1	0	0	none
Ni	2	3	0	0	none
Zn	0	1	0	0	none
Cr	2	5	0	0	none
Al_2O_3	+ 1700	+ 3600	+ 1200	0	none
Fe_2O_3	+ 500	+ 900	+ 1000	0	none
Cl	- 5	+ 2	+ 34	0	very small

With the results of soil analysis, the analysis of eluate has become superfluous. Due to the process of eluate extraction and only a small difference in the concentration of metals and Cl in the tested samples, the concentration of the same elements in the eluate made from the same soil samples would not differ significantly. Moreover, the goal of the analysis was not to determine the deposition class of SUS, but to determine the influence of EC on the deposition of separated fine soil material. SUS is mixed in the laboratory and has no external pollution of any kind. Therefore, SUS is not representative for determination of a deposition class of a used bentonite suspension from a construction site, but can be used to investigate the influence of EC on deposition classes.

Since eluate has not been analysed, the influence of replacing CA with EC on the pH and the electrical conductivity of the eluate has not been tested.

Another important criterion that is not listed in the regulations is the residual moisture of coagulated material. This is not only important because it influences stiffness requirements from AbfAblV (Table 47), but also because it influences the mass and volume of the material to be deposited, directly influencing the cost of disposal. Lower residual moisture results in lower costs. As shown in the spreadsheet calculation example in Figure 104, EC caused an

increase of the total deposition volume by 7.1 % and total deposition weight by 4.5 %. This results from the difference in residual moisture of coagulated material (48 %) and assumed residual moisture of filter cake (40 %). However, if a construction site utilizes centrifuges for fine separation, there would likely be no additional weight nor volume to deposit, since the mud from centrifuges usually possesses a residual moisture of around 50 %.

If it would be required to reduce the residual moisture of coagulated material on a construction site that uses chamber filter presses for fine separation, the coagulated material could be returned to the remaining suspension in order to filtrate everything together. However, the results in 6.5.2 showed that the return of the coagulated material back to the suspension reduces the positive effect of EC before filtration. A more promising idea would be to dispose of the coagulated material and filter cakes together. If approximately a quarter of the soil material in the suspension can be separated with EC and the rest using the chamber filter presses, the composition of the combined soil material from both separation steps would have a residual moisture closer to that of filter cakes.

Overall, the analysis of the separated soil material showed that replacement of CA with EC would not worsen the deposition class of soil material. There is even a small chance of improving the class due to decreased concentration of Cl in the soil. However, depending on the residual moistures of filter cakes or mud, and the residual moisture of coagulated material, the weight to be deposited could increase.

7.2.2 Disposal of filtrate / centrate water

One of the benefits of EC is that CA are not required for filtration. This eliminates the possibility that CA contaminate the filtrate water through suboptimal dosing. However, filtrate water after EC could have a certain level of pollution through remains of metal ions originating form electrode dissolution. Depending on the concentration of those ions in filtrate water, this water could be re-used on construction sites for mixing of a new bentonite suspension, which is not the case with the filtrate water with CA.

Reuse of filtrate water

In the case of replacing the usage of CA through EC, flocculants would be completely removed from the separation process. This eliminates the risk of contaminating filtrate water with flocculants through under-dose or overdose, which brings ecological advantages for the disposal of filtrate water. Moreover, it brings up an interesting possibility: reuse of filtrate water on a construction site as technological water for mixing of the new bentonite suspension.

In order to test the potential reuse of filtrate water after EC, the filtrate water released from filtration experiments after the EC experiment PES1_EC2 was gathered (Figure 107). Even

though the water looks turbid due to some residual particles, it had a density of 1.00 g/cm³. The buckets are chronologically positioned; the filtrate water at the beginning of the filtration experiment was gathered in the first bucket from the left, which was then replaced with second bucket and so on.

Two filtration experiments were performed and from each of them, two filtrate water samples were created: one made of filtrate water from every bucket and one without the water from the first two buckets. With those samples, 4 % bentonite suspensions of type B1 were mixed. As a reference, the same suspension was mixed with a tap water. Afterwards, the suspensions' properties were tested. The marsh time was tested with a marsh funnel and yield point with ball harp. The results are presented in Table 52.

Figure 107: Filtrate water after PES1_EC2_FD1

Table 52:   Properties of the B1 4 % bentonite suspension mixed with filtrate and tap water

Sample	Water	Density (g/cm³)	Marsh time (s)	API Filtrate water (mg)	Yield point (N/m²)
1	Filtrate*	1.025	$t_{1000}=38$ $t_{1500}=71$	10.1	16
2	Filtrate	1.025	$t_{1000}=38$ $t_{1500}=72$	10.1	16
3	Filtrate*	1.026	$t_{1000}=38$ $t_{1500}=71$	10.1	16
4	Filtrate	1.025	$t_{1000}=38$ $t_{1500}=72$	9.7	16
5	Tap	1.025	$t_{1000}=38$ $t_{1500}=71$	9.6	16

*without the water from first two buckets

As can be seen from the table (above), the only measured differences in comparison with suspension from tap water was slightly increased filtrate water release. This is an indication that a certain amount of the aluminium ions landed in filtrate water. According to the specifications of B1 suspension provided by the manufacturer (Appendix A), a 4 % suspension should have a filter water release of 11 ml +/- 35 %. Even though the suspension made of filtrate water had an increased filtrate water release after EC, it still met the stated requirements by far. The other properties of the suspension that are relevant for its use in civil engineering (i.e. density, marsh time and yield point) were the same as for the suspension mixed with tap water.

This is an important finding: it suggests that the filtrate water produced when replacing CA with EC can be re-used to mix a new bentonite suspension on a construction site. This way, huge amounts of water on construction sites could be conserved. The increased filtrate water release, however, suggests that the water will not be infinitely reusable; at some point in time, it will have to be disposed. Since a part of the water from the used suspension remains in the coagulated material and in the filter cakes as residual moisture, the filtrate water itself is not sufficient the replace the whole volume of the used suspension that is discharged from the slurry circuit. The missing volume would have to compensated using fresh water. This would reduce the effects of filtrate water on the filter water release of the suspension.

In Figure 104, an assumption was made that 50 % of filtrate water after EC could be reused for new suspension. This way, on average 275 l of filtrate water per 1 m³ suspension could be reused. This would not only further decrease the demand for fresh water, but also reduce the water disposal amount.

In another set of experiments, a fresh bentonite suspension was mixed with the filtrate water gained from the reference filtration experiment with CA. This suspension was obviously instable, as shown in the .the suspension segregated and a layer of water accumulated on the suspensions surface.

Figure 108: left) Fresh suspension mixed with tap water, right) Fresh suspension mixed with filtrate water after filtration with CA

Further research is required on this matter. Additional cycles of EC, filtration, and mixing of new suspension using filtrate water could be performed; this would allow the investigation of the maximum number of cycles before the requirements are no longer met. After a curtain number of cycles, filtrate water after EC will have too much aluminium ions and will not be able to create a stable suspension. Moreover, these tests were performed with filtrate water from SUS. They should be repeated with a used suspension from a construction site.

Disposal

The filtrate water that is not going to be reused must be disposed. After WHG, there are three possibilities for water disposal:

- discharge in groundwater

- discharge in sewage water

- discharge in bodies of water (rivers, lakes,…)

For all three disposal options, the local wastewater regulations of the cities and regions apply. As for the disposal of soil material, only those parameters that could be changed through replacement of CA with EC were considered in the analysis. In the place where this research was conducted (Bochum), those requirements are as follows (Table 53):

Table 53:   Parameter limitations in wastewater regulations of city Bochum (Abwassersatzung der Stadt Bochum, 2011)

Cu (mg/l)	Ni (mg/l)	Zn (mg/l)	Cr (mg/l)	Cr VI (mg/l)	Sulphate (mg/l)	pH (-)	Al / Fe
1	1	3	1	0.2	600	6.5 - 10	*Not lim-ited**

*„*without limitation, if there is no interference with discharge and purification*"*

To investigate to which degree the filtrate water fulfils the requirements from Table 53, filtrate water samples were subjected to chemical analysis. Sulphates are listed in Table 53 because they come with standard coagulants like $Al_2(SO_4)_3$. Since the coagulant used in this thesis was $FeCl_3$, the concentration of Cl was measured to serve as an approximation for the case when a coagulant with sulphates would be used. The results of the chemical analysis are presented in Table 54.

Table 54:   Filtrate water quality

Elements in filtrate water	Filtrate water after EC	Filtrate water with CA	Filtrate water without EC and CA
Cu (mg/l)	0.017	0.016	0.012
Ni (mg/l)	< 0.005	0.0083	< 0.005
Zn (mg/l)	0.012	< 0.01	0.013
Cr (mg/l)	0.039	0.012	0.0075
Cl (mg/l)	0.05	0.05	0.09
pH (-)	9.4	9.0	9.0
Al (mg/l)	98	0.06	0.28
Fe (mg/l)	0.049	0.1	0.038

Compared with the filtrate water without EC and CA, the biggest rise in the concentration of metals was measured for Fe in the case of filtration with CA and for Al for filtration after EC. While the concentration of Fe rose from 0.038 mg/l to 0.1 mg/l (+0.06 mg/l), the concentration of Al rose from 0.28 mg/l to 98 mg/l (+97.7 mg/l). When comparing those results with the filter cake analysis from Table 50 and Table 51, it is clear that the use of CA and EC has a much higher influence on the metal remains in the filtrate water than in the filter cakes.

The concentration of Cl in tested specimens is not credible, since it was only possible to measure bonded Cl. Not-bonded (free) Cl promptly discharges from the water. The real Cl concentration could have only been measured during or directly after the filtration. Therefore, the measurement of Cl could not serve as an approximation for the case when a coagulant with sulphates would be used.

Regarding the limitations from Table 53, all three probes passed the required regulations. However, it should be proved if the measured Al concentration of almost 0.1 g/l would interfere with the discharge and purification of disposed water. Moreover, the remains of flocculants in the filtrate water with CA were not tested. Since no stable suspension could be mixed with filtrate water after EC (Figure 108), a reasonable assumption can be made that there were remains of flocculants in the filtrate water. Even though they are not listed in the local wastewater regulations of city Bochum, they are regarded as obviously to highly hazardous to water (chapter 2.5.5).

Furthermore, Figure 104 shows additional advantages of EC in comparison to CA, concerning the disposal volume of filtrate water. Since CA solution increase the total filtration volume and the amount of filtrate water, replacing the CA with EC would decrease the filtrate water amount. Under the assumptions in Figure 104, filtration of 1 m³ used suspension with CA would produce 781 l of filtrate water, in comparison to 551 l with EC. Even if the complete filtrate water after EC would be disposed, there would still be 230 l less to dispose per 1 m³ used suspension, since no water needs to be added to the suspension prior to the filtration. That is a decrease of 29% in comparison to conventional conditioning. With an assumption of 50 % filtrate water reuse, the disposal volume of filtrate water would decrease for 65 %. For clarification, the 50 % reuse of filtrate water is not meant as taking 50 % of filtrate water from every filtration cycle to mix a new suspension. Rather, it would mean taking the whole amount of filtrate water for a few cycles (until the filtrate water release of the suspension reaches the allowed limit – effects from Table 52) and afterwards taking only fresh water for a few cycles (to reduce the filtrate water release and stabilise the suspension).

8 Recommendations for scale-up to a real-scale prototype for construction sites

A short summary of recommendations from chapters 8.1 - 8.3 was presented the final report of this research (Popovic & Schößer, 2019)

Based on the knowledge and experience gained from the experimental phase with the EC prototype cell, several ideas developed that would improve the design of the current or the next stage prototype.

The main ideas are the following:

- Decrease of the "dead" volume of the EC cell

- Increase of the volumetric current density either by increasing of the total surface of the electrodes or allowing a higher maximal voltage

- Improvement of the cleaning mechanism

- Electrode polarity switch for balanced utilization of the electrodes or as an alternative cleaning method

8.1 Dead volume decrease

8.1.1 Problem

As shown in 6.5.4, the increase of the electrode gap by identical electric current improved the results. This was already observable in the laboratory experiments of Paya (2016). However, in the literature is usually recommended to keep the gap as small as possible in order to reduce costs. At a smaller gap, lower voltage is required to reach intended electric current.

The reason why the laboratory and prototype experiments showed better results at larger electrode gaps is because the increase of the electrode gap caused a decrease in the dead volume. As already defined in 6.5.4, the dead volume is the space in the cell minus the space between an anode and a cathode. For example, the space between two cathodes or a cathode and the wall of the cell are considered the dead volume. This is shown with red arrows in Figure 109 left, at the electrode gap of 4.5 cm.

The volume between two cathodes and the cathode to the wall of the cell is not the only dead volume. The part of the suspension that is not directly between two electrodes but rather on a side should also be considered as dead volume. By measuring the properties of the remaining suspension in five sampling points of the cell, it was found that most electrochemical processes take place in the middle of the cell (Figure 84).This is because the EC prototype cell is rectangular but the electrodes are circular. Electrodes are as wide as the

cell itself only in the middle of the cell. (Figure 109 right). Therefore, the dead volume is at its smallest in the middle of the cell, which explains the measured data.
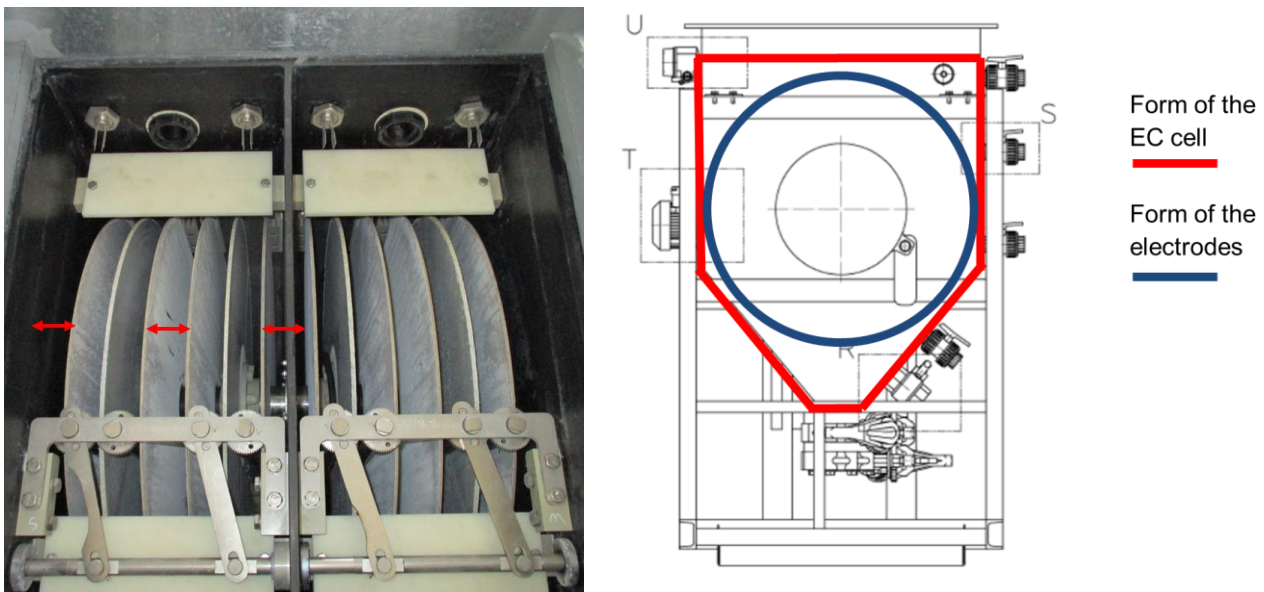
Figure 109: left: Dead volume in the EC cell (Popovic & Schößer, 2019), right: Comparison of the cell and electrodes form

Since the experiments were conducted in rest state, the movement of the particles in the suspension was caused only by diffusion. Therefore, the suspension that was inside the dead volume during EC presumably received little to no electrocoagulation.

Table 55 presents the ratio of the dead volume to the total cell volume at different electrode gaps. When the electrode gaps are increased from 4.5 cm to 5.5 cm or 6.5 cm, the space between two cathodes or a cathode and the cell wall decreases, decreasing the dead volume.

Table 55:   Dead volume at different electrode gaps

	Gap 4.5 cm	Gap 5.5 cm	Gap 6.5 cm
Dead volume (l)	87	70	54
Dead volume (%)	54	44	34

As shown in Table 55, the percentage of the dead volume in the cell was quite high. When considered that even a Best Combo experiment was performed with the electrode gap of 4.5 cm, there is still a room for improvement of the EC cell and the therefore the effectiveness of the process.

8.1.2 **Solution**

The dead volume should be decreased as much as possible in the next development stage of the prototype in order to enable the EC process to reach its full potential. This can be done through changes in the electrodes form and arrangement. First of all, the electrodes should follow the shape of the cell. In the current prototype, this means that the electrodes should have a shape like the red line in Figure 109.

Furthermore, the arrangement of the electrodes should be changed. The dead volume between the cathodes and between a cathode and the wall of the cell can be avoided by changing the electrode arrangement from **c**athode-**a**node-**c**athode-**c**athode-**a**node-**c**athode to **c**athode-**a**node-**c**athode-**a**node-**c**athode-… and by mounting the outermost electrodes as close as possible to the cell wall.

These changes should allow electrocoagulation of the complete suspension in the cell.

8.2   Increase of the volumetric current density

8.2.1 **Problem**

Most of the EC prototype experiments described in this thesis were performed with the "maximal electrical current" operational parameter. This means that the maximal pre-set for electrical current was chosen (200 A for EC experiments with one chamber, 300 A for those with both) but the actual electrical current was automatically regulated by DC source software whenever maximal voltage was reached. Therefore, the actual electrical current during the experiment resulted from a combination of the remaining operational parameters and suspension parameters. For example, shorter gaps between the electrodes made higher electrical currents possible. In an additional example, higher current densities were reached with CUS than with SUS, because the CUS possessed higher electrical conductivity.

All experiments showed that the electrical current capacity of the DC source could not be fully used due to instant reach of maximal voltage at the beginning of the experiment. This resulted in software automatically lowering the electrical current. Since most of the experiments were performed in one chamber, maximal possible current density was 1.25 A/l (200 A / 160 l). However, the highest average current density by EC experiments with SUS was 0.89 A/l and with CUS it was 0.98 A/l. Out of 50 EC experiments presented in this thesis, only two experiments with CUS reached the maximal electrical current of 200 A at some moment during the experiment. It is not obligatory to use the DC source to its fullest capacity, but higher electrical currents would increase current density and likely speed up the destabilisation process.

Two methods to increase electrical currents are as follows:

- Increase of the total surface of the electrodes
- Increase of the maximal allowed voltage

8.2.2 Solution 1: Increase of the total surface of the electrodes

The suspension between the electrodes can be considered as a regular conductor, such as an electrical cable. Increasing the electrodes' surface without increasing their gap is analogous to increasing the cross-section of a conductor without increasing its length. The resistance of the conductor decreases, even though its electrical conductivity does not change (Eq 3-12). Through reduced resistance, higher electrical current are achievable without increase of the voltage.

Therefore, increasing the total electrodes' surface would decrease the surface electrical density (A/m²), which would allow higher electrical currents (A) and thus higher volumetric current densities (A/l) to be reached. A good example of this effect were the laboratory experiments with cells A and B (chapter 5.3.2). Due to the larger electrode surface of cell B, the pre-set electrical current of 2 A was reachable at larger electrode gaps and lower voltage than by the experiments with cell A. In order to reach 2 A in cell A, an average surface current density of 16.13 mA/cm² was required, but the highest reached average current density was 14.72 mA/cm² at the gap of 3.5 cm, resulting in an electrical current of 1.83 A and volumetric current density of 0.91 A/l (Table 11). At the gap of 6.5 cm, only 11.09 mA/cm² was reached, resulting in an electrical current equal to 1.37 A and volumetric current density of 0.69 A/l. In contrast to that, the average surface current density required to reach 2 A in cell B was 9.40 mA/cm². This was reached at the gaps of 3.5 - 5.5 cm. At the gap of 6.5 cm, the surface current density was equal to 9.25 mA/cm², resulting in an electrical current of 1.96 A and volumetric current density of 0.98 A/l (Table 12). This is a 0.29 A/l more than in a cell A at the same gap. This is a proof that the increase of the electrodes surface allows higher electrical currents by the same voltage.

Even if the experiments would show that further increase of electrical current does not improve the results, which is unlikely, the increase of the electrode surface would still bring some positive effects. The experiments could be purposely performed at "lower than maximum available" electrical currents. Since those electrical currents would be reachable with lower voltages, the operating costs of the EC would be reduced.

8.2.3 Solution 2: Increase of the maximal allowed voltage

The voltage in the prototype was restricted to 55 V due to electrical security reasons; more precisely to prevent the damage on the human body when in contact with live electrodes. However, this decision was made before all aspects of hydrogen issue (chapter 3.5.1) were

known and before the extensive hydrogen safety measures were installed in the prototype. One of those measures, namely the condition that the electrical current can only flow if the EC cell cover is closed, makes it impossible to come into contact with live electrodes.

Since the hydrogen safety measures are unlikely going to be decreased for the next scale-up phase, the voltage restriction becomes unnecessary. Therefore, the maximum allowed voltage could be increased without influencing the security of the EC process. This would most probably speed up the process, because higher electrical currents could be reached and the intended amount of Ah would be reached faster.

However, the cost aspect needs to be considered here. In terms of EC, voltage is costly. Electrical current creates coagulants/metal cations which destabilise the suspension, whereby voltage is only necessary to overcome the resistance between the electrodes. Higher maximal voltage would allow higher electrical currents, but also result in higher costs. In contrast, the increase of the electrodes surface allows higher electrical currents without increasing the voltage. The additional cost for aluminium material is negligible in comparison to constantly higher operational costs caused by higher voltage.

8.3 Automatic cleaning mechanism

8.3.1 Problem

One research idea was to remove the coagulated material from the anode surface during the experiment in order to allow new deposits to form. However, the results of the "anodes cleaning interval" experimental series (chapter 6.5.5) showed that the current cleaning mechanism did not improve overall EC performance. In contrary, it had negative effects on development of electrical current. Moreover, when the coagulated material was stripped of the anode's surface during the experiment, it remained in the residual suspension and had to be filtered afterwards. This made the two-phase separation impossible.

The cleaning mechanism was however not required only to remove the coagulated material from the anodes during the experiments, but also to remove the material after them (in the experimental series without cleaning). Since this did not work out as planned, the removal of the coagulated material was performed semi-manually. This, together with thorough cleaning of the anodes surface, took approximately one hour after each EC experiment.

The importance of the cleanness of the electrodes can be seen from Figure 110. When the electrodes are thoroughly cleaned, higher electrical currents can be reached in the next experiment. Quick cleaning represents the scraping with the installed cleaning mechanism, and thorough cleaning is manual scraping of all the rest from the electrodes surface.
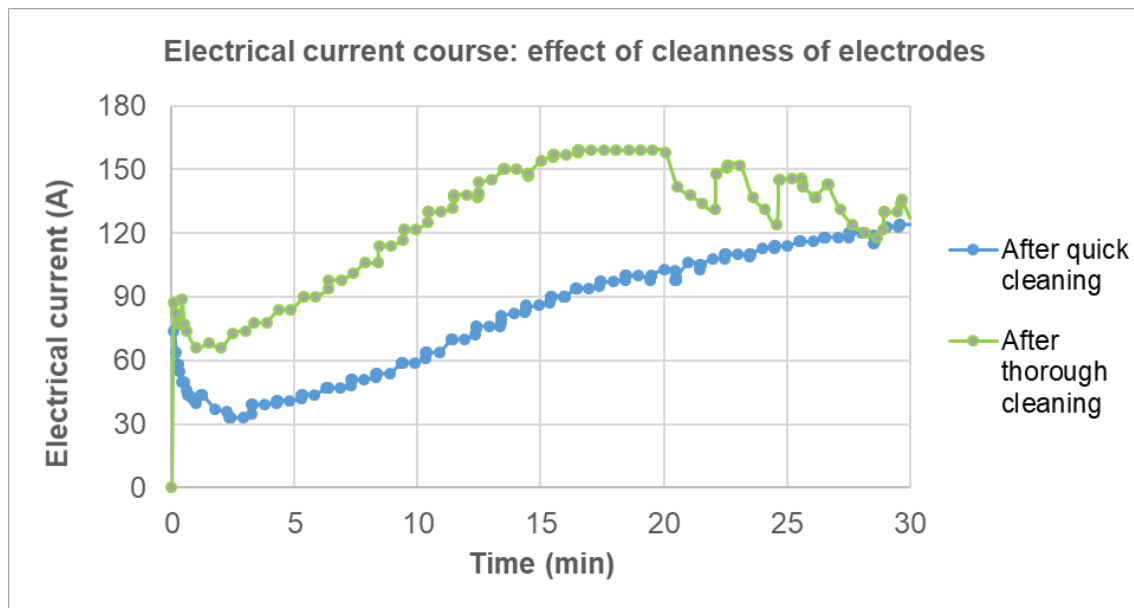
Figure 110: Effect of the cleanness of the electrodes on the electrical current course in the next experiment

However, it is not practical to employ someone at the construction site to remove the coagulated material form the anodes after each experiment. This causes delays since a new EC cycle cannot begin before the remains of the previous one are removed from the EC cell. The process must be performed automatically and quickly. Therefore, a cleaning mechanism is an obligatory part of the next stage design.

8.3.2 Solution

First, the idea of rotating anodes and using fixed-in-place cleaning mechanism should be abandoned in the next design phase. This way of cleaning had a negative effect on the results and was sensitive to clogging. Moreover, it complicates the design of the cell. It requires circular anodes, which are connected to the EC source through a rotating well going through the middle of the electrodes. This well also reduces the electrode's surface. In contrast to anodes, cathodes are connected to the DC source through simple cable connections near their slots in the cell. That is also how anodes should be connected on electricity in the next design phase.

The cleaning mechanism should be modified in such a way that it enables scratching all of the coagulated material from the anodes during or after the test. This could be done in the following ways:

- For cleaning during the experiment, with small modifications of the current prototype: The rotation direction of the electrodes could be changed. In the current rotation direction, the coagulated material reaches the holders of the scrapers before it reaches

the scrapers itself. Therefore, a part of the materials is "scraped" before intended. This contributes to the clogging. The scrapers were deliberately installed at the lower part of the electrodes so that the scraped material falls directly in trapezoidal-prism-formed bottom of the cell and does not clog the movable parts in the surrounding.

- For cleaning after the experiment: This is a simple process. The cell could be designed with an openable bottom. After pumping the remaining suspension out, the bottom would open. The scrapers could scrape the coagulated material downward. Material can be accumulated in a reservoir or conveyor belt installed under the cell that brings the material to the same location where mud from the centrifuge or filter cakes from filter presses are accumulated.

However, the cleaning does not have to be performed mechanically, but rather electrically. This would be enabled through the electrode polarity switch.

8.4 Electrodes polarity switch

Electrode polarity switching could bring several advantages to the EC process.

Both types of electrodes dissolve during EC – anodes due to electrical (Eq 3-3) dissolution and cathodes due to chemical (Eq 3-9) dissolution. Anodes dissolve more than cathodes. Switching the polarity of the electrodes could balance both dissolutions so that all electrodes have to be changed at the same time. This would reduce the maintenance time on the EC cell.

Moreover, according to the literature, switching the electrodes polarity should help prevent the passivation of electrodes. It should be pointed out that no certain evidence of passivation was found in the experiments presented in this thesis.

The polarity switch was not integrated into the current prototype because Payá's (2016) results showed that the switch of the electrodes polarity during EC worsens the results. After every switch, a certain time was required for electrical current to reach its pre-switch values. However, the polarity change does not to be performed during EC but rather between the experiments.

Enabling the electrodes polarity switch would also mean that the cleaning mechanism would needs to be installed in a way in which it can clean every electrode, since each one of them could be an anode. This could be resolved with the possibility to electrically clean electrodes.

The experiments showed that the switch of the anodes polarity caused the coagulated material to fall off the anode, thus making this switch to the electrical cleaning method. The problem with the electrical cleaning is that the coagulated material stays in the suspension. This has a negative result on the following filtration, as shown in the experiments with the mid-scale prototype. However, the suspension could be screened after EC.

When the coagulated material falls off the electrode due to switch of electrode polarity, it would not disintegrate into small flocs and disperse in the suspension, but rather remain in the form of bigger blocks. Those blocks could be screened like the soil in the separation plant. The cell could be designed with an openable bottom and a screen could be installed for separation of coagulated material from remaining suspension. The coagulated material would stay on the screen and the remaining suspension would flow through. Afterwards, coagulated material could be carried to the waste disposal site and the remaining suspension could be pumped to chamber filter presses or centrifuges.

This would be practical in terms of EC cell design since it would make mechanical cleaning parts unnecessary. The electrodes' polarity could be switched after the end of planned experimental duration. However, an iteration process would be required to find the optimal EC duration after switching. As soon as the cathode turns to the anode, the soil particles from the remaining suspension could start to coagulate on its surface. The duration should be long enough to release the material from the anodes but not long enough for the new layer of coagulated material to accumulate on the cathode.

It is hard to recommend one of the two above-mentioned cleaning methods at the current stage of research since the electrical cleaning was tested neither in the mid-scale prototype nor in the laboratory experiments presented in this thesis. On the other hand, the mechanical cleaning did not perform as well as expected. Since the next development phase of the prototype is still going to be a research phase, it would be great to install polarity switch and test this possibility.

8.5 Recommendations summary

8.5.1 Improvements for the current EC prototype

In this section, the ideas presented in 8.1 - 8.4 that could be implemented without changing the dimensions of the EC cell or security and control systems in the prototype are discussed. Under the assumption that presented changes could be implemented without excessive re-designing of the prototype, they serve as recommendations to increase EC performance.

First, the number of the electrodes should be increased for one electrode per chamber and the arrangement of electrodes should be changed. Instead of six electrodes in arrangement **c**athode-**a**node-**c**athode-**c**athode-**a**node-**c**athode the seven electrode should be arranged as **c**athode-**a**node-**c**athode-**a**node-**c**athode-**a**node-**c**athode. Outermost cathodes should be mounted as close as possible to the EC cell wall. This measure would simultaneously decrease the dead volume (8.1) and increase the total electrodes surfaces, which would allow higher current densities in the experiments (8.2.2).

The future form of the electrodes depends on the installed cleaning mechanism. If it would be possible to install an electrode polarity switch (8.4), which is only a change of direction of DC and as such should not be a difficult challenge, the electrodes could be designed to follow the form of the EC cell (red line in Figure 109). The new arrangement of the electrodes described in the previous passage and their new form would almost completely eliminate the dead volume in the cell. It would also make the equipment installed for rotation of the electrode superfluous.

If the electrodes polarity switch cannot be installed, new ideas for mechanical cleaning need to be tested, e.g. change of the rotation direction of the anodes. However, an option of abandoning the idea of electrodes rotation and mechanical cleaning could be taken in consideration. This would allow fitting the shape of the electrodes to the shape of the cell and eliminating the dead volume. The cleaning could be performed manually after the experiment. This would be a short-term solution with a goal to perform the EC tests without dead volume. Mechanical cleaning could be installed in another form by the next stage scale-up.

8.5.2 **Real-scale prototype design**

The results of EC with SUS showed that the optimal EC duration was 60 minutes. One filtration cycle after EC would last around 90 minutes (Table 40). In order to perform EC and filtration simultaneously, the real-scale EC cell would need to have a volume of approximately 70 % the volume of the chamber filter presses. Since the number of presses varies from one construction site to another, the end-product EC cell should be designed with several units that can be connected together.

One unit can be tested as a next real-scale prototype.

To keep the operational costs of the new real-scale prototype low, the surface current densities should be as low as possible, meaning that the ratio of electrodes surface to the volume of the cell should be as high as possible. Simply stated, there should be as much electrodes as possible in the cell. This will not increase the costs for the electrodes over longer period, since the electrodissolution is controlled only by the electrical charge (Ah). If the number of the electrode is increased but the electrical charge remains the same, each of the electrodes will dissolve less and therefore will need to be replaced less frequently. However, the voltage would be lower than with smaller number of electrodes and therefore the electrical consumption of the cell would decrease, reducing the operating costs of the process.

The electrode gap should however not be smaller than 4.5 cm. As the experiments showed, the amount of coagulated material on the anodes can be so thick that, by smaller gaps, it would completely fill the void between the electrodes.

Furthermore, the idea of fix scrapers and rotating electrodes should be abandoned. The cell should be simple rectangular cell with rectangular electrodes. The scrapers should either be moveable or the electrical cleaning method should be installed. For the purpose of collecting the coagulated material, the cell should be designed with an openable bottom and a conveyor belt underneath.

The cleaning process would proceed as follows:

- With scrapers:
    - Pumping the suspension out of the cell
    - Opening the bottom of the cell
    - Scraping the coagulated material away
    - Material falls down on the conveyor belt and is taken away
- With electrical cleaning.
    - Switching the polarity of the electrodes upon reaching the desired treatment duration.
    - After few minutes (the actual time needs to be tested and optimised) turning the electricity off and opening the bottom of the cell
    - The content of the cell falls on a screen: coagulated material stay on the screen and the remaining suspension flows through
    - Coagulated material is taken away with a conveyor belt.

Both of those methods can be tested also as a cleaning method "during" the experiment. After the cleaning, the suspension would be pumped back to the cell and the treatment would continue. The removed volume would need to be replaced with a new suspension.

The cell could be designed vertical so that it consumes less space on a construction site.

A sketch of a design is shown in Figure 111 and the EC procedure in Figure 112. Only the option with scrapers is shown in the figures. The option with electrical cleaning would have no scrapers and no outlet channel. The screen would be installed underneath the cell and a basin under the screen, to collect the suspension.
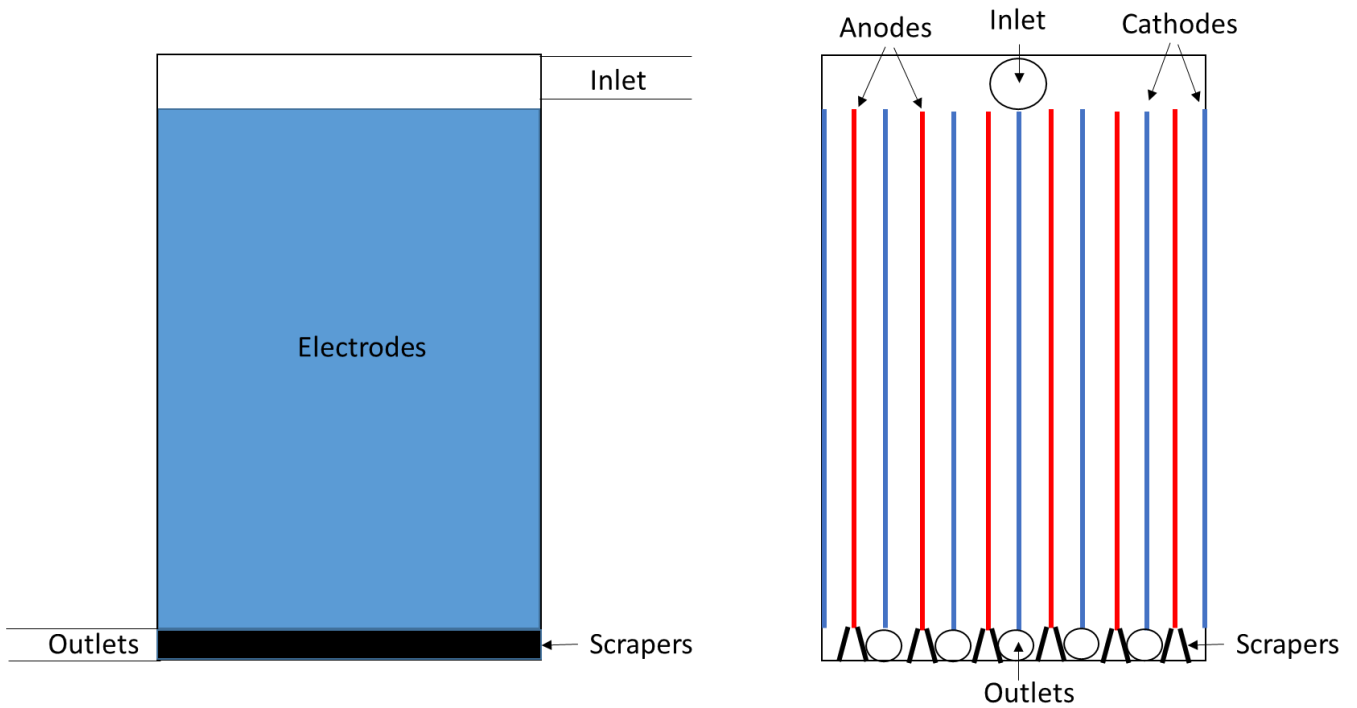
Figure 111: Design of a real-scale prototype
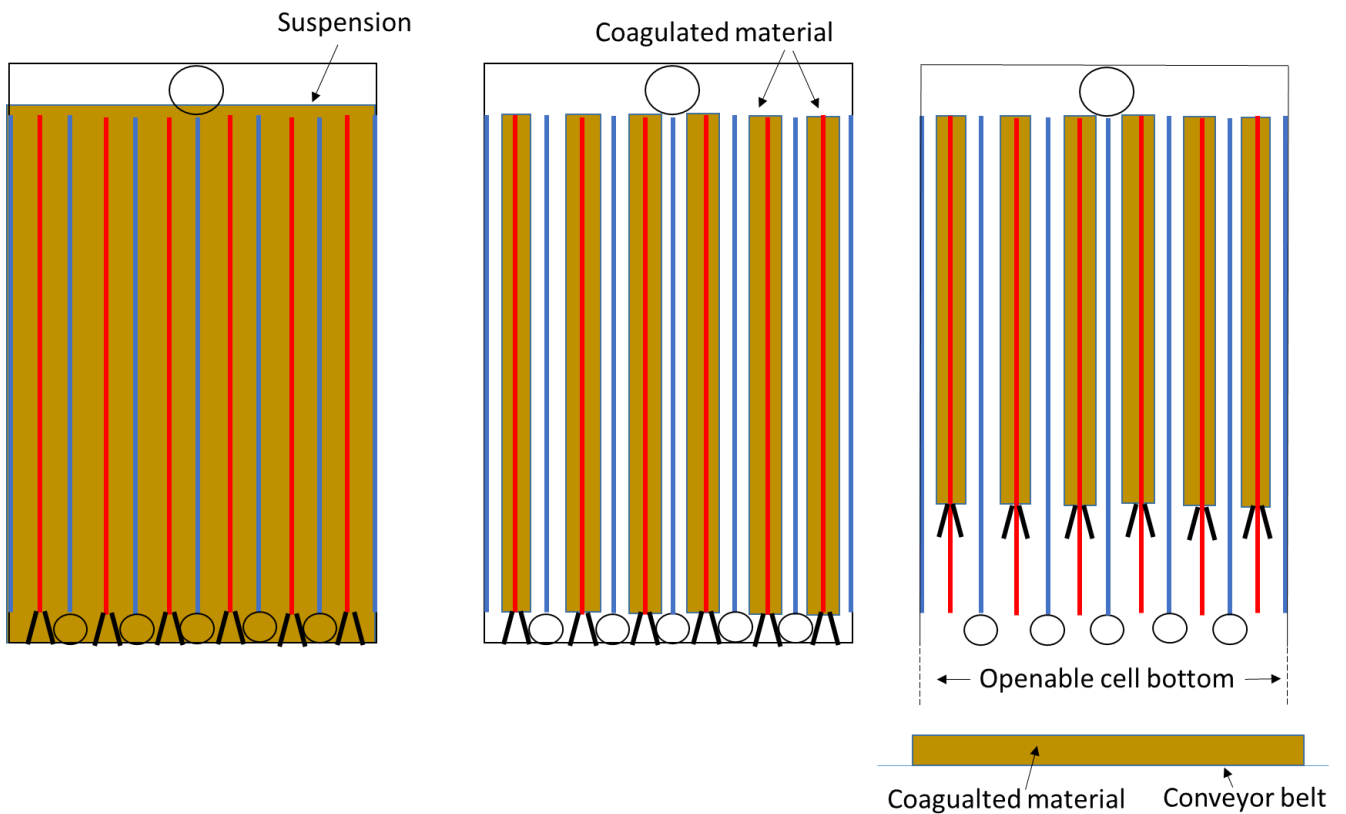
Figure 112: EC treatment procedure in a real-scale prototype: left) during EC; middle) remaining suspension is pumped out of the cell, coagulated material remains on the anodes, right) the bottom of the cell opens, the coagulated material is scraped off and falls down to the conveyor belt

9 **Ecological considerations**

From theoretical and regulations point of view, this subject was already discussed in chapter 2.5.5 and 3.4. The results of the chemical analysis of the fine separation products and the influence of EC on water consumption and disposal concept was presented and discussed in chapter 7.2.1 and 7.2.2. In this chapter, a summary of most important ecological advantages of EC is presented.

9.1 **Coagulants**

According to VwVwS (Administrative Regulation on Water-Polluting Substances, 1999), conventional coagulants like aluminium chloride ($AlCl_3$), aluminium chlorohydrate ($Al_2Cl(OH)_5$), aluminium nitrate ($Al(NO_3)_3$), aluminium sulphate ($Al_2(SO_4)_3$), iron(III) chloride ($FeCl_3$), ferric chloride sulphate ($FeClSO_4$), iron(III) nitrate ($Fe(NO_3)_3$), and iron(III) sulphate ($Fe_2(SO_4)_3$) are categorised in water hazard class 1, meaning that they are slightly hazardous to water sources. Therefore, coagulants represent a relatively small problem in ecological terms. Nevertheless, after dissolution of conventional coagulants in water, metal cations as well as other chemical groups (nitrates, sulphates, chlorides, etc.) inevitably end up disposed in the water or into the environment (Eq 9-1 & Eq 9-2). It is important to mention that the concentration of sulphates and chlorides is limited in disposal regulations; sulphates in water disposal regulations and chlorides in soil disposal regulations.

$$FeCl_3 \rightarrow Fe^{3+} + 3Cl^- \qquad \qquad \text{(Eq 9-1)}$$

$$Al_2(SO_4)_3 \rightarrow 2Al^{3+} + 3(SO_4)^{2-} \qquad \qquad \text{(Eq 9-2)}$$

This was proven through a soil chemical analysis (Table 50), which found an increased concentration of Fe and Cl in filter cakes by the filtration with CA.

In contrast to conventional coagulants, those produced by EC through electrodissolution of the anode come as aluminium or iron cations in pure form, without other substances (Eq 9-3).

$$Al \rightarrow Al^{3+} + 3 e^- \qquad \qquad \text{(Eq 9-3)}$$
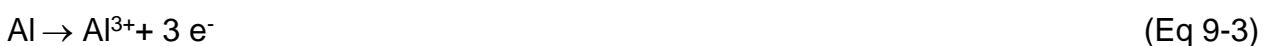
This means that only metal cations end up in environment, without other groups like nitrates, sulphates, chlorides. Aluminium and iron cations in pure form are not listed in VwVwS. Even if they technically could be considered hazardous, their water hazard class would not be higher than those of conventional coagulants.

9.2 Flocculants

The main ecological improvement that EC would bring to the fine separation process is due to the elimination of the flocculants usage. This would conserve water on a construction site and decrease water pollution. The improvements can be summarized as following:

- Flocculants like non-ionic, anionic and cationic polyacrylamides are classified as obviously to highly water hazardous substances. As such, they are not allowed to end up in the environment.
- Abandoning the usage of flocculants conserves on average 0.2 m³ water per 1 m³ used suspension.
- Abandoning the usage of flocculants opens the possibility to reuse the filtrate water, reducing the requirements for fresh water even further.
- Water saving from the previous two points also reduces the amount of water disposed. By calculations in Figure 104, the amount of disposed water was reduced by 65 %.

The results of this thesis show that the EC can have a similar influence as the use of CA on the destabilization and coagulation of the suspension. The implementation of EC on the construction site could therefore make the usage of CA obsolete. This would completely eliminate flocculants from the dewatering process, while coagulants would be produced in-site in a pure form.

10 Evaluation of construction management aspects

In order for EC as a new technology to be attractive from a construction management point of view, it should be reliable and provide some clear benefits as compared with conventional fine separation process. The most important aspect is cost. Furthermore, it would be beneficial if EC would provide technological and ecological improvements, while also being practical to handle. Those aspects are discussed in this chapter.

According to the results from this thesis, there are two possibilities for EC implementation on construction site.

- EC as replacement for coagulating agents (CA) (Figure 113a)
- EC combined with CA (Figure 113b)

In both ways, EC would serve as separation and destabilisation method for used suspensions prior to further fine separation in chamber filter presses or centrifuges.
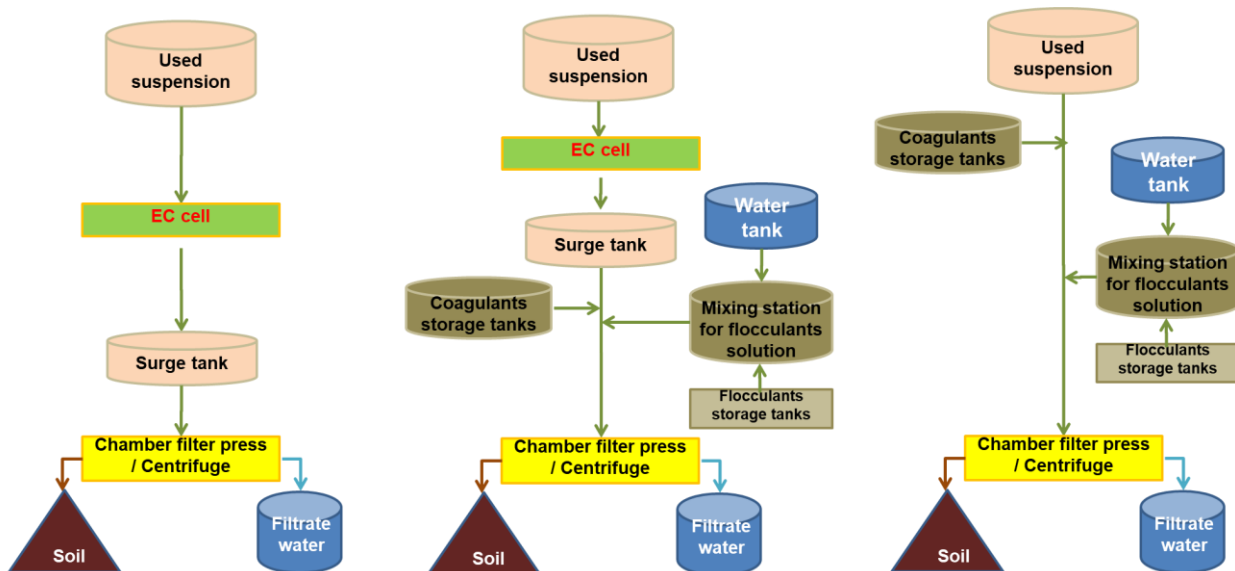
Figure 113: Fine separation process including EC and the conventional separation process: a) EC as replacement for CA, b) EC in combination with CA, c) conventional conditioning

Prior to further analysis it is important to mention the findings from section 7.1.1. Used suspension treated with EC at the best combination of operating parameters showed higher filter water release but also longer filtration times in the chamber filter press. Moreover, EC reduced total filtration volume since it does not require the addition of coagulants and flocculants in solution prior to filtration. Overall, the productivity of separation process could be increased when replacing CA with EC. Therefore, following sections analyse and compare operational costs of EC (Figure 113a) with those of conventional conditioning (Figure 113c). The costs of combining EC with CA (Figure 113b) are not explicitly discussed, but they can be inferred from the single costs for EC and CA.

10.1 Cost aspect - estimation of operational costs

In this section, operational costs of EC are compared with conventional conditioning costs. EC operational costs could be calculated entirely and very precisely, since detailed measurements were performed during the experiments with the EC prototype. On the other hand, conditioning costs are the exact costs from three tunnelling projects, but due to some missing information, a few assumptions were made to compare those costs to EC costs.

10.1.1 EC operational costs

Electricity

Operational costs of the EC include costs for electricity and costs for new aluminium electrodes. The electricity costs from the PEC5 (experimental series "EC experiment duration") and from the experiment PES6-EC5 (Best Combo experiment) are shown in Table 56. The series PES5 was chosen as example because this series covers the widest range of electricity consumption - EC experiments with duration from 30 minutes to 90 minutes.

The EC electricity consumption per 1 m³ suspension was calculated by scaling the required consumption for 160 l in a 1:1 ratio with the increase in volume, meaning that the consumption for the 160 l was multiplied by a coefficient of 6.25 (1000/160). This is a plausible assumption that fits the scale up experiments (chapter 5.3.7). While converting the electricity consumption to costs, electricity price of 0.17 €/kWh was taken, which was the average industrial electricity price in Germany for 2018.

Table 56:   Electricity costs: PES5 and PES6_EC5 (after Popovic & Schößer, 2019)

Experiment	Experiment duration (min)	EC Electrical consumption (kWh/0.16 m³)	EC Electrical consumption (kWh/m³)	EC Process costs (€/m³)	Peripheral consumption (kWh/0.16 m³)	Peripheral costs (€/m³)
PES5_EC1	30	3.0	18.5	**3.1**	0.9	0.2
PES5_EC2	45	5.1	31.9	5.4	1.4	0.4
PES5_EC3	60	5.8	36.5	6.2	1.9	0.5
PES5_EC4	90	7.5	47.6	**7.9**	2.7	0.7
PES6_EC5	60	5.7	35.4	6.0	1.9	0.5

As shown in Table 56, the operational costs of EC process were in the range of 3.1 – 7.9 €/m³ suspension. The EC experiment that resulted in the best filtration performance costed 6.0 €/m³ suspension.

However, the EC peripheral costs are not included in this price. Those are the costs generated from all other electrical appliances besides the EC cell, including ventilation, sensors,

illumination, consumption from control devices and energy loss by the conversion from alternating current to direct current in the DC source. As it turned out, peripheral costs during the experiment are independent of electrical current in the cell, and only depend on experiment duration. While the electrical consumption of the EC process varied throughout the experiment, the peripheral consumption was constant at 1.9 kW.

Those costs cannot be scaled with the same coefficient as the EC process costs, since larger suspension volume does not necessarily cause a linear increase in amount of illumination, sensors or control devices required. Most likely, only the energy consumption from ventilation and the DC source would rise linearly with increase of the suspension's volume, but not in a 1:1 ratio as the EC process costs. Moreover, peripheral consumption is dependent on the current design of the ECC, which can change in the next scale-up phase.

This being said, an assumption was made in Table 56 that the peripheral consumption increases in a ratio of 1:4 with the increase of the suspension volume, meaning that the consumption for 160 l of used suspension was multiplied with 1.56 (1000/160/4) in order to approximate the consumption for 1 m³ of used suspension.

Including peripheral consumption, the operational costs of EC process would be in the range of 3.3 – 8.6 €/m³ suspension, with the Best Combo experiment having a cost of 6.5 €/m³ suspension.

Aluminium

According to the Faraday's law (Eq. 3-5), aluminium in worth of 0.06 € would be dissolved from the anode in the Best Combo experiment. The calculation is shown in Table 57. In order to achieve similar results for 1 m³, charge density (Ah/l) needs to remain constant, meaning that the electrical current needs to increase in a ratio 1:1 with the increase of the volume. When scaled to 1 m³, this would cause additional costs of 0.4 €/m³ used suspension in the Best Combo experiment, which would than cost 6.9 €/m³ used suspension.

Table 57:   Electrodissolution of aluminium in the Best Combo experiment

M (g/mol)	z (-)	F (As/mol)	I (A)	t (s)	Dissolved aluminium (g)	Aluminium price (€/kg)	Aluminium costs (€)
26.98	3	96485	107	3600	36	1.6	0.06

However, the actual electrodissolution of aluminium is lower than in Faraday's law, since one part of the electricity going through the anode reacts to produce oxygen. On the other side, the cathodes dissolve too, in a chemical reaction that does not directly depend on a current. Therefore, the values from the Faraday's law were taken in a calculation. For other experiments from Table 56, the costs for aluminium are calculated in Table 58.

Table 58:   Aluminium costs for experiments from PES5 and the Best Combo experiment (PES6_EC5)

Experiment	Electrical charge (Ah)	Aluminium dissolved in experiment (g)	Aluminium dissolved for 1 m³ suspension (g)	Aluminium costs (€/m³ suspension)	Costs for EC Process + periphery + aluminium (€/m³ suspension)
PES5_EC1	56	19	117	0.2	3.5
PES5_EC2	96	32	201	0.3	6.1
PES5_EC3	110	37	231	0.4	7.1
PES5_EC4	141	47	296	0.5	9.1
PES6_EC5	107	36	224	0.4	6.9

The operational costs of EC are now in a range of 3.5 – 9.1 €/m³, including costs for aluminium electrodes and electricity costs for the EC process and the peripheral devices.

Due to electrodissolution, the aluminium electrodes have to be changed after a certain amount of operating hours. According to the Faraday's law, the anodes in the current prototype would completely dissolve after 289 h of experiments with the electrical current from the Best Combo experiment (107 A) This is an important information from construction management aspect. This subject needs to be further researched, as discussed in Outlook.

10.1.2 Conventional conditioning operational costs

The costs of the conventional conditioning were obtained from three tunnelling projects. The consumption of CA was provided in form of kg CA/m³ excavated soil. The costs for 1 kg of CA used on the site was also obtained. Therefore, it was possible to calculate the conditioning costs per m³ excavated soil, as presented in Table 59.

Table 59:   Costs of conventional conditioning from three tunnelling projects (Popovic & Schößer, 2019)

Project	Soil	Consumption (kg CA/m³ soil)	CA costs (€/kg)	Conditioning costs (€/m³ soil)
Project 1	clay	4	2	8.0
Project 2	gravel / sand	0.3	3.1	0.9
Project 3	clay	2.6	3.25	8.5

However, there was no data about the total amount of discharged used suspension in the projects. This made a direct cost comparison from Table 58 and Table 59 impossible. In order to compare the costs, the units had to be standardised, or rather, the amount of used suspension in above-mentioned projects had to be estimated.

A sensitivity analysis was performed to get an approximation of the amount of used suspension and calculate the costs for conventional conditioning in unit €/m³ suspension. The variables in the calculations were the density of used suspension at time of discharge from the slurry circuit and dispersion degree of the soil. Dispersion degree was defined by Weiner (2018) as the percentage of soil particles that disperse in the suspension to the size that cannot be separated in the separation plant, but only with the fine separation device (chamber filter presses and centrifuges). These are the particles that remain in the suspension and cause an increase of its density.

Two assumptions were made in the analysis. The first assumption was that the density of fresh suspension was 1.03 t/m³. This suits to the usual densities of fresh suspensions. Moreover, since the variables are covering a broad range, the accuracy of this assumption has almost no influence on the results. The second assumption was that the increase of the density was the only reason to discharge the suspension from the slurry circuit. Other reasons may include low yield points or high filtrate water discharges, which could cause a discharge of the suspension prior to reaching a borderline density.

As the result of the calculation, the amount of discharged used suspension per 1 m³ excavation in dependence of two above mentioned variables was obtained (Table 60). Due to the second assumption, the actual amounts of discharged used suspension could be higher.

Table 60: **Amount of discharged used suspension per 1 m³ excavation in dependence of the density of the used suspension at the time of discharge and dispersion degree of the soil (Popovic & Schößer, 2019)**

Density (t/m³)/ α_{dis} (-)	1.3	1.25	1.2	1.15
0.1	0.60	0.74	0.95	1.35
0.2	1.20	1.47	1.91	2.70
0.3	1.80	2.21	2.86	4.05
0.4	2.40	2.95	3.81	5.40

Following, the conditioning costs from the Project 1 were taken (8 €/m³ excavated soil). When combining those costs with the amount of discharged used suspension per 1 m³ excavation from Table 60, the conditioning costs in form €/m³ used suspension were obtained (Table 61). Overall, the costs for CA were in the range of 1.5 – 13.3 €/m³ used suspension. However, when considering the most probable dispersion degree and discharge density, the costs could be limited to 2.8 – 6.7 €/m³.

Table 61:   Approximation of costs for CA from the Project 1 (€/m³ suspension)

Density (t/m³)/ α_{dis} (-)	1.3	1.25	1.2	1.15
0.1	13.3	10.9	8.4	5.9
0.2	6.7	5.4	4.2	3.0
0.3	4.4	3.6	2.8	2.0
0.4	3.3	2.7	2.1	1.5

These are the costs for the CA excluding water costs and other peripheral costs like electrical consumption of pumps by conditioning. However, the cost specifically for the water needed to mix flocculants solution is an important factor and should be considered when calculating the operating costs of conventional conditioning. As previously mentioned, 0.2 m³ of water is usually used to mix a flocculants solution for 1 m³ of used suspension. The water price for industry in Germany for 2018 was 2 €/m³ (Berger, 2018). This increases the costs for 0.4 €/m³ used suspension, which sums up the conditioning costs to 3.2 – 7.1 €/m³, excluding peripheral costs due to missing data.

It is important not to wrongly interpret Table 61. It does not mean that the conditioning costs rise at higher densities and lower dispersion degree. The CA costs from Project 1 are already known – 8 €/m³ excavated soil. The total amount of the conditioned used suspension is not known. If the amount was quite low (0.6 m³ suspension per 1 m³ excavation, for density 1.3 t/m³ and dispersion degree 0.1), the costs for conditioning per m³ used suspension were quite high and vice versa.

10.1.3 Operational costs comparison

After standardisation of the units, a cost comparison between EC and CA costs was possible.

The analysis of the EC electricity consumption data resulted in operational costs of EC in the range of **3.5 – 9.1** €/m³ used suspension, including peripheral consumption. The Best Combo experiment costed 6.5 €/m³ used suspension. Further cost savings would be possible by recycling flocculants-free filtrate water as a technical water to mix the new bentonite suspension (chapter 7.2.2). According to the assumptions in Figure 104, this could provide 275 l water per m³ used suspension. Recycled filtrate water would save on deposition costs (0.5 €/m³ water, Berger, 2018) and fresh water costs (2 €/m³ water), thus making further cost savings of 0.7 €/m³ used suspension possible.

Since EC operational costs consist for the most part of electricity costs, they are highly dependent on the location of the construction site. This is further discussed in chapter 10.1.4.

The range of operational costs for conventional conditioning with CA could be narrowed down to **3.2 – 7.1** €/m³, excluding peripheral costs due to missing data. For more accurate cost calculations, the following data from the construction sites is required: the total amount of CA and discharged used suspension, the water consumption for flocculants solution, and the electrical consumption of peripheral devices like mixing tanks for flocculant solutions and pumps.

Overall, the analysis showed that the operational costs of EC and CA are in the same order of magnitude.

An additional interesting aspect of EC is the production of hydrogen. In this thesis, hydrogen was only considered as a safety issue, but it could be also considered as a source of clean energy. Water electrolysis is not considered as one of the most effective ways to produce hydrogen, but in the case of EC, the electrolysis is a side reaction and not the purposely-performed reaction with a goal to acquire hydrogen. Therefore, if the hydrogen is being produced anyway during EC, it could be economically feasible to re-use it. Fuel cell technology already exists that supports this.

Initial research shows that 1m³ of hydrogen equals to 3 kWh of energy (Linde Gas, 2019) Considering the measured values in the LES6 (chapter 5.3.6) and the electrical current values in the prototype experiments, 3 kWh of DC during EC can produce up to 40 l of hydrogen. If the hydrogen would be reused to produce electrical energy, this would sink operational costs by approx. 4 %. Otherwise, hydrogen could be collected and sold as a raw material or used to fuel the machines on the construction site.

10.1.4 Dependence of the operational costs on the location of the construction site

The most intriguing aspect of the operational costs comparison is the dependence of the costs on a location of a construction site. The operational costs of the EC are highly dependent on a location, which is not the case with the operational costs of CA.

Electricity costs

The operational costs of EC in Table 56 are calculated with the electricity price for industry in Germany in 2018 (0.17 €/kWh). However, compared to other countries, electricity in Germany is very expensive. A comparison of prices in Europe from the year 2016 can be found in Figure 114. As shown in the figure, the electricity in Germany was approximately 25 % more expensive than the European average price. When compared to some of the neighbouring countries, the industrial electricity price in Germany is approx. 35 % higher than in Belgium, 45% higher than in Austria, 50 % higher than in France, 75 % higher than in Netherlands and 85 % higher than in Poland and 100% higher than in Czech Republic. On the

other side, costs for acquiring CA for a construction site in those countries are most likely the same as in Germany, since the European Union is an open market. This has huge influence on comparison of operation costs of EC and CA. An estimation of EC costs in those countries is shown in Table 62.
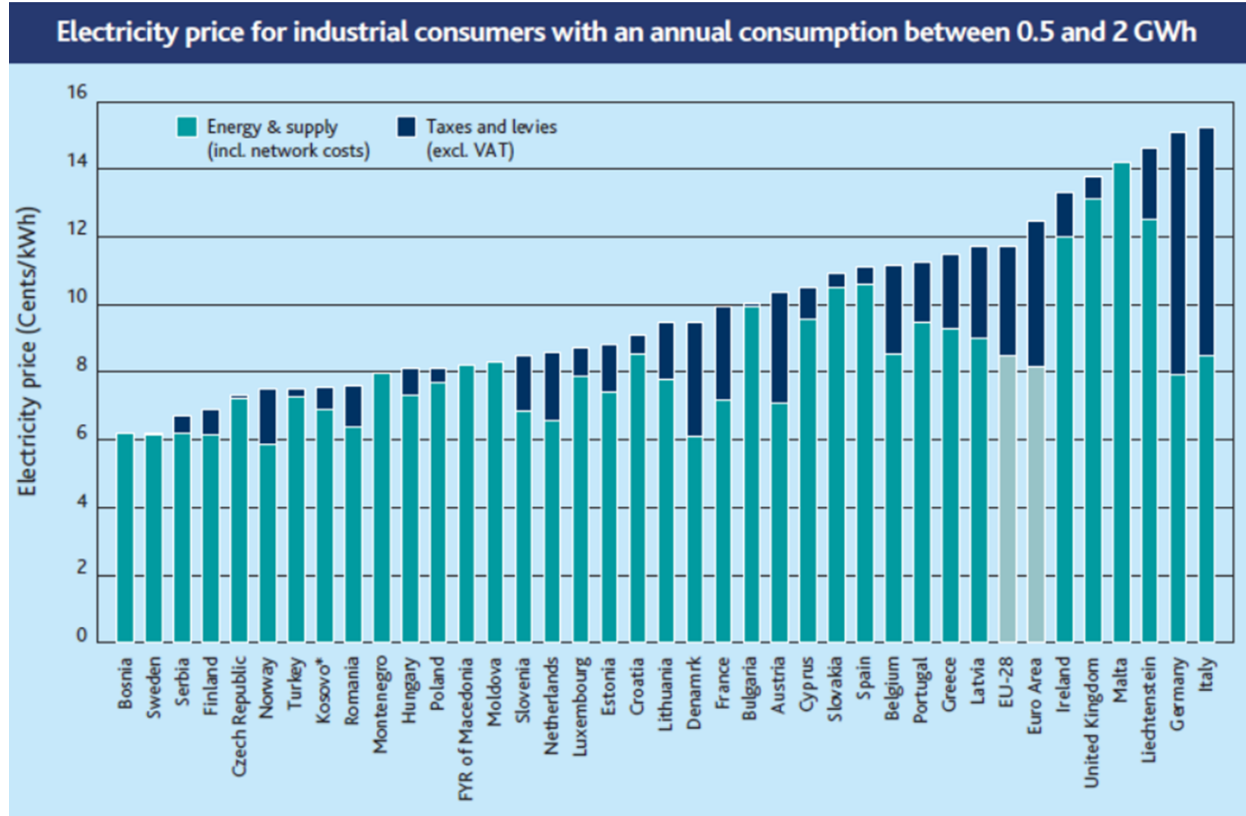
Figure 114: Industrial electricity prices in Europe in 2016, for annual consumption 0.5 – 2 GWh (Reuter et al., 2017; Eurostat, 2016)

Table 62:   Operational cost of EC in different countries [€/m³ used suspension]

Germany	Belgium	Austria	France	Nether-lands	Poland	Czech Re-public	Estimated CA opera-tional costs
3.5 – 9.1	2.6 – 6.7	2.5 – 6.4	2.3 – 6.1	2.0 – 5.2	1.9 – 4.9	1.8 – 4.6	3.2 – 7-1

Moreover, the electricity price also depends on the overall annual electrical consumption of an industrial user. The more electricity the user annually consumes, the lower the price. For an annual consumption of 100 GWh, the industrial electricity price in 2016 in Germany was only 0.06 €/kWh (Reuter et al., 2017). With this price, EC would cost only 1.2 – 3-2 €/m³ used suspension.

All mentioned EC operational costs in this section were calculated excluding the eventual re-use of filtrate water. The re-use of filtrate water would sink the prices even further.

Water costs

As previously mentioned CA operational costs of 3.2 – 7.1 €7m³ used suspension were calculated as the sum of costs for CA (2.8 – 6.7 €/m³ used suspension) and water for the flocculant solutions (0.5 €/m³ used suspension). Fresh water costs were estimated as 2 €/m³ water and disposal costs as 0.5 €/m³ water. However, as with electricity, the water costs are also location-dependent. Water costs can fluctuate significantly even inside the same country. Fresh water costs in 2013 for several European cities is shown in Table 63.

Table 63: Fresh water costs in several European cities in 2013 ($/m³) (Rahaman & Ahmed, 2016)

Paris	Bordeaux	Esbjerg	Copenha-gen	Amster-dam	Den Haag	Brussels	Liege
1.66	2.33	2.80	3.83	2.10	2.07	2.11	3.40

The water saving factor of EC could play even bigger role in the future. The global fresh water demand is expected to increase by 55 % until 2050 (UN, 2015). As the water demand and price grow, EC will become more attractive option than conventional conditioning.

All things considered, the question of which method is more beneficial in terms of operational costs is highly dependent on a location of the construction site. There is no unique answer.

Following, the investment costs are discussed.

10.2 Cost aspect - estimation of investment costs

10.2.1 New investment costs

As shown in Figure 113, the implementation of EC would require an EC cell and a surge tank to store the suspension between EC and filtration in chamber filter presses. Since the results showed that the positive effects of EC could decline when the suspension waits for filtration, the tank should ideally store just enough suspension for one filtration cycle. However, should an EC cell have a malfunction or require maintenance, it would be wise to have a surge tank with a volume for eight filtration cycles. Since the results showed that one filtration cycle after EC would last approximately 90 minutes, this would allow 12 hours of EC cell standby time without stopping the filtration.

The cost estimation for a real-scale EC cell is hard to estimate at this point of research. The costs of the current EC cell cannot be simply scaled up to required volume. Firstly, personnel costs in a research phase are significantly higher than in a production phase of the final product. Secondly, the recommendations for a new real-scale cell (8.5.2) suggest a much different (simpler) cell design, which makes it impossible to scale the material costs of a current cell. Moreover, it was suggested in chapter 8.5.2 that a cell should be divided in units

that can be put together depending on the required volume on the construction site. This suggests that even when it comes to a final product, the price will depend on the capacity. Therefore, estimating a price at this point of research would be a pure speculation. Maybe only the upper limit could be roughly estimated: it should not cost more than a few hundred thousand €.

10.2.2 Reduction of the costs of the conventional conditioning equipment

Replacing CA with EC would mean that the storage tanks for coagulants and flocculants and mixing station for the flocculants solution become unnecessary.

Moreover, the analysis in chapter 7.1.1 showed that EC could decrease the required chamber filter press capacity by 22 %. The cost for a chamber filter press depends on its volume, and can be roughly estimated to a range of few hundred thousand €.

The space on a construction site is also important. EC would require space for an EC cell and surge tank, but a new space would be acquired by removing storage tanks for coagulants and flocculants and mixing station for the flocculants solution.

10.3 Costs summary

The overview of cost categories when replacing CA with EC can be summed up as follows:

- New investment costs: EC cell and surge tank
- New operating costs: electricity for EC cell, aluminium anodes
- Saved investments costs: storage tanks for coagulants and flocculants, mixing station for the flocculants solution, smaller chamber filter press
- Saved operation costs: coagulants, flocculants, water for mixing of the flocculants solution, eventually re-use of filtrate water after filtration with EC

The analysis in chapter 10.1 showed that operational costs of EC and CA are in the same range, whereby EC shows potential to be economically beneficious in countries with low electricity prices or high water prices. The investment costs require further research in order to be precisely compared, especially concerning the costs for a real-scale EC cell.

10.4 Practicability & improvement aspect

Completely automatic EC cells could be designed that would require no additional workforce to operate the cell. The same workforce operating fine separations procedure could also overlook the EC cells. The technology itself is not complicated. During the EC process, no actions from personnel are required.

EC definitely presents an ecological improvement for the current separation process: it requires no water hazardous substances and reduces water consumption (chapter 9). Being eco-friendly, EC could provide decisive points in the bidding process.

11 Summary and outlook

11.1 Summary

The separation of fines and the disposal of used bentonite suspensions are one of the biggest challenges in hydroshield tunnelling and the construction of diaphragm walls, with significant economic and ecological impacts. Conditioning agents (coagulants and flocculants) are applied to support the separation process by reducing the treatment time in chamber filter presses and centrifuges and thereby increase overall separation capacity. However, those agents are classified as water hazardous substances. If they are not correctly dosed, they end up not only in dewatered soil material but also in separated water that needs to be disposed of. Furthermore, flocculants need to be mixed with water and added to the suspension prior to the filtration. This increases the water consumption on the construction site and ads up to the total volume of the suspension that needs to be separated.

The purpose of this thesis was to investigate electrocoagulation as an alternative support method for the fine separation of used bentonite suspensions. This technology is already implemented in the wastewater treatment and it is considered to be eco-friendly and cost-effective. When applied to bentonite suspensions, it destabilises the suspension and causes coagulation of the soil particles on the anode.

At the beginning of the thesis, a literature overview about bentonite suspensions, electrocoagulation, and previously performed research in this field was given. In the first part, the focus was on the stability of bentonite suspensions. The mechanisms behind stability and the ways in which the suspension can be destabilised are explained. Furthermore, the electrokinetic behaviour of non-bentonite fine soil particles in a suspension and their effect on overall stability was explained.

In the second part, the focus was on electrochemical reactions behind electrocoagulation and the parameters effecting its performance. The special focus involved parameters that were afterwards empirically researched in the experimental series. In the third part, an overview of the previously performed research about electrocoagulation of bentonite suspensions at the Institute for Tunnelling and Construction Management in Bochum was presented.

The literature research was followed by an experimental part. First stage of experiments was performed in the laboratory scale. Prior to performing electrocoagulation experiments, a standard used suspension was defined. This suspension was used in all laboratory parametric studies. The influence of the electrode material and the gap, the cell design, the electrical current, the electrodes connection mode, the experiment duration, and the electrodes cleaning interval and passivation was investigated. Moreover, gas measurements and mini

scale-up test were performed. The experiments were evaluated based on three parameters: the percentage of coagulated soil, the decrease of the suspensions density and the increase of the filtrate water release with the API-filter press. The latter was applied as a measurement of the suspension stability. Based on the results and knowledge gained by laboratory experiments, a mid-scale electrocoagulation prototype was built. The scaling factor was 160, starting from 2 l laboratory cells and resulting in the 320 l prototype cell.

Besides the prototype, a laboratory chamber filter press was provided. Those two devices were used in the experimental setup for the second stage of experiments. The suspension was first electrocoagulated in the prototype cell and afterwards filtrated in the laboratory chamber filter press. Additional evaluation parameters were defined, describing the influence of electrocoagulation treatment on the filtration cycle time and volume of the filtrated suspension. Those parameters were comparing the filtration after electrocoagulation with the filtration supported with conditioning agents This is done in order to have a practice-relevant comparison. The influence of the electrical current, electrode gap, anode cleaning intervals, experiment duration, and suspension density was investigated. It was found that electrocoagulation could cause similar filtration effects as conditioning agents. The experiments with standard used suspension were validated with a suspension from one tunnelling construction site.

Furthermore, experimental results were used to evaluate the impact that electrocoagulation would have on the disposal and separation concept, in situations where it would replace the usage of conditioning agents. It was found that electrocoagulation could decrease the required chamber filter press capacity and reduce the water consumption on the construction site. Calculations showed a 22 % reduction of required capacity and a reduction of water consumption with a range of 0.2 – 0.48 m³ water per m³ used suspension. However, the numbers are dependent on the operational parameters of electrocoagulation, conditioning agents, and most of all, the suspension itself. Therefore, a mathematical calculation model of the analysis was developed. With this calculation model, the influence of the electrocoagulation on the fine separation process can be calculated for any given operational parameters, conditioning agents and any suspension. Moreover, the model is not dependent on the design of the experimental setup, meaning that it can be used in subsequent research phases or any similar research; as long as the setup contains one electrocoagulation cell and one chamber filter press.

Concerning the disposal concept, the chemical analysis showed that the conditioning agents increase the concentration of chlorides in separated soil, which did not occur with electrocoagulation. The other parameters did not differ enough that they would change the deposition class of the soil. However, if the residual moisture of the coagulated material would be

higher than that of a filter cake, the electrocoagulation would cause a slight increase of the weight of the soil material to be disposed.

Following, the recommendations for the improvement of the current prototype and the design of a new, real-scale prototype were made.

In conclusion, the ecological aspect was discussed and the economic aspect was evaluated. In ecological terms, electrocoagulation is advantageous because it can destabilise a suspension without the substances that are classified as water hazardous. Moreover, it reduces water consumption on the construction site.

Concerning the costs, there is no unique answer to which method is favourable. The cost comparison depends to a great extent on electricity price and to a smaller extent on water prices on site. The electricity price differs significantly between countries and water price differs even between towns and regions in the same country. When calculating using the average industrial electricity and water prices in Germany, the methods are in the same cost range. However, electrocoagulation could be economically advantageous in countries with lower electricity prices or high water prices.

Overall, this technology shows a lot of potential for a further research and an implementation on a construction site. Electrocoagulation cells can be designed to be simple and automatic. They do not require much more than a waterproof barrel, electrodes, direct current source, and security mechanisms like ventilation. Since the ecological standards are on a constant rise, the conventional conditioning agents could become less attractive or even forbidden in the future. However, even without ecological implications, electrocoagulation has a potential to be economically advantageous. This is one of the subjects that should be further researched.

11.2 Outlook

The ideas for the future research can be summed up in following points:

- Further experiments with used suspensions from construction sites
- Creation of an databank as a basis for a prognosis model for future projects
- Further research concerning the potential re-use of filtrate water
- Electrocoagulation experiment supported with addition of sodium chloride (NaCl)
- Electrocoagulation in combination with a centrifuge

11.2.1 Further experiments with used suspensions from construction sites

Further experiments with used suspension from construction sites could be performed with the procedure and analysis methods developed in this thesis. If the experimental setup is to

be improved with ideas from chapter 8, this will have no influence on the analysis with the calculation model.

The experimental plan can be designed as following:

- Acquiring 2 m³ used suspension from a construction site.
- Performing 10 electrocoagulation experiments with subsequent filtration, each time using only one chamber of the cell. This requires 1600 l of suspension and ten working days of test programme. The main focus in the experiments should be in finding the optimal experiment duration, or rather, the optimal charge density (Ah/l).
- Performing reference filtration experiments with conditioning agents, with the exact ratio as on the construction site. Three experiments would require 120 l and two working days.
- With the remaining 280 l of suspension: Optionally, performing reference filtration experiments without conditioning agents or with a reduced ratio. This input is not required for the calculation model, but it could provide some interesting insights. Otherwise, one additional electrocoagulation experiment can be performed. This would take one to two working days.

The analysis runs as follows:

- Acquiring data from the construction site concerning the volume of flocculants solution added to the suspension prior to the filtration (V_{CA}) and time ratio of a filtration process in one filtration cycle *(F%)*.
- Input of this data and experimental data - ratio of coagulated material after EC (B_{kt}), residual moisture of coagulated material (RM_{CM}) filtrate water discharge after EC ($V_{FW,EC}$), filtrate water discharge with CA ($V_{FW,CA}$), filtration time after EC ($t_{FW,EC}$), filtration time with CA ($t_{FW,CA}$) - in the calculation model for separation capacity (Eq 7-10 & Eq. 7-11).
- Additionally, input of further experimental data – residual moisture of filter cakes and reuse of filtrate water – in spreadsheet application (Figure 104) the analyse the disposal concept.

The results of the analysis show how a certain combination of electrocoagulation operational parameters influences the separation capacity and the disposal concept, and which combination produced the best results.

The above-mentioned experiments and the complete analysis can be performed within three weeks.

11.2.2 **Creation of a databank as a basis for a prognosis model for future projects**

The results of the analysis should be stored in a databank, together with electrical consumption of electrocoagulation experiments, information about used suspension (density and geological profile) and information about conventional conditioning on a construction site.

This databank can be used to estimate if it would be economically advantageous to employ electrocoagulation in an upcoming project. For a given geological profile, the following data could be taken from a databank:

- Electric power consumption for electrocoagulation experiments per m³ used suspension
- Consumption of water and conditioning agents for the conventional conditioning per m³ used suspension
- Influence of electrocoagulation on the required fine separation capacity (reduction of required chamber filter press capacity when replacing conventional conditioning with electrocoagulation)
- Influence of electrocoagulation on disposal concept (change of the soil disposal weight if there is a difference between the residual moisture of filter cakes and the residual moisture of coagulated material, reduction of water disposal due to elimination of polymers solution, reuse/no reuse of filtrate water)

Following, the costs could be calculated as follows:

- Operational costs: Electricity and water consumption need to be multiplied with electricity and fresh water price on location. Costs for coagulating agents need to be estimated based on their expected consumption and prices of available products on the market.
- Investment costs: First, an estimation of required fine separation capacity (number and size of chamber filter presses) needs to be made. Based on that, the reduction of investment costs for a chamber filter presses due to electrocoagulation and the investment costs for an electrocoagulation cell can be calculated.
- Disposal costs: If an increase of soil disposal weight caused by electrocoagulation is expected, this increase needs to be multiplied with soil disposal costs on the location. Furthermore, the decrease of water disposal due to reduced water consumption (elimination of polymers solution and potential reuse of filtrate water) needs to be multiplied with water disposal costs on location.
  Furthermore, the local disposal regulations should be checked regarding elements that can be found in typical conditioning agents. If the concentration of e.g. chlorides,

sulphates, or polyacrylamides in water and soil is limited in the regulations, the usage of electrocoagulation could lower the disposal class and thus lower the costs.

The last step would be summarising the costs in two groups (electrocoagulation and conventional conditioning) and comparing them.

11.2.3 Further research concerning the potential re-use of filtrate water

In future research, especially with used suspensions from construction sites, it should become standard procedure to mix a fresh bentonite suspension with filtrate water after every filtration experiment. It the suspension would turn out to be stable, its properties should be tested. This way, more data can be gathered about the extent to which filtrate water can be re-used to mix fresh bentonite suspensions.

Moreover, this subject could be further researched with standard used suspension. Electrocoagulation experiments with different durations or different electrical currents could be performed and a fresh bentonite suspension could be mixed using filtrate water after each experiment. The concentration of aluminium ions in filtrate water would increase with the increase of experiment duration and electrical current. The goal of those experiments would be to investigate how charge density (Ah/l used suspension) during electrocoagulation experiments influences the properties of fresh bentonite suspensions mixed with filtrate water, and to determine the maximum amount of charge after which it is still possible to mix a stable suspension. If necessary, the stable suspensions mixed with filtrate water could be electrocoagulated again and the filtrate water of those experiments could be used to mix a new suspension. This can be repeated until the suspension mixed with filtrate water is no longer stable or the properties are significantly worsened.

The tests performed in 7.2.2 showed that there is a potential to reuse the filtrate water. However, since the reuse of filtrate water could bring important ecological and economic advantages, it is necessary to investigate this subject more deeply.

11.2.4 Precise calculation of dissolution of electrodes

As already mentioned in 10.1.1, Faraday's law cannot give a precise estimation of electrodissolution of the anodes. Moreover, there is no law that would enable to calculate the chemical dissolution of the cathode based on the operational parameters of the experiment.

In the current prototype, the anodes are fixed on the well. However, cathodes are not fixed and can therefore be lifted. If the experimental setup is to be improved with ideas from chapter 8, the anodes are not going to be fixed on a well anymore. In this case, all electrodes can be lifted.

It should therefore become a standard experimental procedure to weight all electrodes after every experiment. A device similar to that of handheld luggage scale (for weighting the baggage before the flight by lifting it) could be acquired. It needs to have a resolution in gram. This would allow precise measurements of electrodes dissolution after every experiment.

11.2.5 Electrocoagulation experiment supported with addition of sodium chloride (NaCl)

As already mentioned in 3.3.9, there is a significant number of researchers that use NaCl (salt) to improve the electrocoagulation process. They claim that addition of NaCl prior to electrocoagulation has following impacts on the process:

- Increases electrical conductivity of treated solution, which decreases voltage and therefore decreases electric power consumption of the process
- Increases electrodissolution, meaning that more aluminium ions would be created with the same amount of electrical current
- Decreases electrodes passivation, meaning that the overvoltage at the beginning of the experiment would be decreased, which decreases power consumption

Overall, power consumption would be decreased and more aluminium ions would be produced, meaning that the suspension would be further destabilised for a lower cost.

However, the cells used in electrochemistry literature are usually very small, not even near the volume of prototype cell or even laboratory cells used in this thesis. Prior to performing the experiments with NaCl, it should be investigated if chloride ions (Cl^-) that remain in the suspension after dissolution of NaCl oxidise on anodes to create chlorine in gas form ($Cl_{2(g)}$), which is very toxic. With the volumes used in this research, it could cause some difficulties.

Moreover, chlorides are one of the substances limited in disposal regulations. Increased Cl concentration in soil could increase the deposition class of the soil, which would increase disposal costs for soil. Therefore, the optimal concentration should be found, that would not cause an increase of the deposition class.

11.2.6 Electrocoagulation in combination with a centrifuge

In this research, the influence of the electrocoagulation on fine separation was investigated using a chamber filter press. However, electrocoagulation should also be able to improve the separation process in centrifuges. As mentioned in 2.5.3 , a centrifuge essentially works as accelerated sedimentation. The results from 5.3.9 showed that electrocoagulation improves sedimentation process because it destabilises the suspension. Therefore, the combination of electrocoagulation and centrifuge should work as well as the combination with chamber filter press.

12 **Literature**

Abdel-Gawad, S. A.; Baraka, A.M.; Omran, K.A.; Mokhtar, M.M. (2012): Removal of Some Pesticides from the Simulated Waste Water by Electrocoagulation Method Using Iron Electrodes. In: International Journal of Electrochemical Science (7), S. 6654–6665.

Abwassersatzung der Stadt Bochum: Satzung über die Entwässerung der Grundstücke und den Anschluss an die öffentliche Abwasseranlage in der Stadt Bochum (Abwassersatzung) vom 3. Juni 2011.

American Society for Testing and Materials (1985): Annual book of ASTM standards. University of California: ASTM.

Anger, I. (2004): Flockung: Kapitel 5. In: K. Luckert (Hg.): Handbuch der mechanischen Fest-Flüssig-Trennung. Essen: Vulkan-Verlag, S. 71–102.

Arbeitsgemeinschaft der Leiter der Beurfsfeuerwehren (AGBF -Bund) (2008): Wasserstoff und dessen Gefahren - Ein Leitfaden für Feuerwehren. Arbeitsgemeinschaft der Leiter der Berufsfeuerwehren in der Bundesrepublik Deutschland - Arbeitskreis Grundsatzfragen (AK-G).

Aswathy, P.; Gandhimathi, R.; Ramesh, S. T.; Nidheesh, P. V. (2016): Removal of organics from bilge water by batch electrocoagulation process. In: Separation and Purification Technology 159, S. 108–115.

Au, P-I.; Leong, Y-K. (2013): Rheological and zeta potential behavior of kaolin and bentonite composite slurries. In: Colloids and Surfaces A: Physicochemical and Engineering Aspects (Volume 436), S. 530–541.

Baik, M. H.; Lee, S. Y. (2010): Colloidal stability of bentonite clay considering surface charge properties as a function of pH and ionic strength. In: Journal of Industrial and Engineering Chemistry (16), S. 837–841.

Bebeselea, A.; Pop, A.; Orha, C.; Danielescu, C.; Manea, F.; Burtica, G. (2006): Electrocoagulation application on organic load and suspended solids removal from wastewater. In: The 13th Symposium on Analytical and Environmental Problems, S. 101–105.

Berger, S. H. (2018): Untersuchung der energetischen Effizienz einer Elektrokoagulationszelle sowie Abschätzung der Betriebskosten der Elektrokoagulation im Vergleich zu den klassischen Verfahren der Separationstechnologie im maschinellen Tunnelbau". Masterarbeit. Beuth Hochschule für Technik, Berlin. Master-Fernstudiengang Energie- und Ressourceneffizienz.

Berufsgenossenschaft (2009): Sicherheit bei Arbeiten an elektrischen Anlagen unterwiesenen Mitarbeiter (BGI 519): Eine Broschüre für die Elektrofachkraft und den elektrotechnisch unterwiesen Mitarbeiter.

Bezhenov, S. (2019): Untersuchung des Einflusses der Stromstärke, des Abstands zwischen Elektroden und des Reinigungsintervalls der Anoden auf die Elektrokoagulation und die Entwässerung der Bentonitsuspensionen. Master Thesis. Ruhr-Universität Bochum, Bochum. Fakultät für Bau- und Umweltingenieurwissenschaften.

Bharath, M.; Kristhna, B. M.; Manoj Kumar, B. (2018): Electrocoagulation Process for Wastewater Treatment. In: International Journal of Environmental Health & Technology (1(2)), S. 44–48.

Bidder, H. (1997): Quantifizierung des Eintrags von Spurenelementen aus Fällungs- und Flockungsmitteln. In: KA - Korrespondenz Abwasser, Abfall (44 (7)).

Biermann, N. (2010): Untersuchung zur Trennung von gebrauchten Bentonitsuspensionen in die Bestandteile Bentonit und Wasser für eine kostengünstige Entsorgung auf der Baustelle. Diplomarbeit. Ruhr-Universität Bochum, Bochum. Fakultät für Bau- und Umweltingenieurwissenschaften.

Brillas, E.; Boye, B.; Baños, M. Á.; Calpe, J. C.; Garrido, J. A. (2003): Electrochemical degradation of chlorophenoxy and chlorobenzoic herbicides in acidic aqueous medium by the peroxi-coagulation method. In: Chemosphere 51 (4), S. 227–235.

Brillas, E.; Martínez-Huitle, C. A. (2015): Decontamination of wastewaters containing synthetic organic dyes by electrochemical methods. An updated review. In: Applied Catalysis B: Environmental 166-167, S. 603–643.

Bund / Länder-Arbeitsgemeinschaft Abfall (LAGA) (2001): Richtlinie für das Vorgehen bei physikalischen, chemischen und biologischen Untersuchungen im Zusammenhang mit der Verwertung/Beseitigung von Abfällen (LAGA-Richtlinien).

Bundesministeriums der Justiz in Zusammenarbeit mit der juris GmbH (2001): Verordnung über die umweltverträgliche Ablagerung von Siedlungsabfällen - AbfAbIV.

Bundesministerium der Justiz (1999): Verwaltungsvorschrift wassergefährdende Stoffe - VwVwS.

Bundesministeriums der Justiz und für Verbraucherschutz / Bundesamt für Justiz (2009): Gesetze zur Ordnung des Wasserhaushalts - WHG.

Bundesministeriums der Justiz und für Verbraucherschutz / Bundesamt für Justiz (2009): Verordnung über Deponien und Langzeitlager - DepV.

Bundesministeriums der Justiz und für Verbraucherschutz / Bundesamt für Justiz (2017): Verordnung über Anlagen zum Umgang mit wassergefährdenden Stoffen – AwSV.

Büttner, G. (1993): Bohrspülungen und Spülungstechnologie: Kapitel 8. In: W. Arnold (Hg.): Flachbohrtechnik. Leipzig: Dt. Verl. für Grundstoffindustrie, S. 296–403.

Can, O.T.; Byramoglu, M.; Kobya, M. (2003): Decolourization of reactive dye solutions by electrocoagulation using aluminum electrodes, Ind. E. In: Ind. Eng. Chem. Res., (42 (14)), S. 3391–3396.

Cañizares, P.; Jiménez, C.; Martínez, F.; Sáez, C.; Rodrigo, M. A. (2007): Study of the Electrocoagulation Process Using Aluminum and Iron Electrodes. In: Ind. Eng. Chem. Res. 46 (19), S. 6189–6195.

Cañizares, P.; Martínez, F.; Carmona, M.; Lobato, J.; Rodrigo, M. A. (2005): Continuous Electrocoagulation of Synthetic Colloid-Polluted Wastes. In: Ind. Eng. Chem. Res. 44 (22), S. 8171–8177.

Chen, G. (2004): Electrochemical technologies in wastewater treatment. In: Separation and Purification Technology 38 (1), S. 11–41.

Chen, G.; Hung, Y-T (2007): Electrochemical Wastewater Treatment Processes. In: L. K. Wang, Y-T Hung und N. K. Shammas (Hg.): Advanced Physicochemical Treatment Technologies, Bd. 5. Totowa, NJ: Humana Press (Handbook of Environmental Engineering), S. 57–106.

Chen, X.; Chen, G.; Yue, P. L. (2000): Separation of pollutants from restaurant wastewater by electrocoagulation. In: Separation and Purification Technology 19 (1-2), S. 65–76.

Conrad, E.U. (1984): Der Einsatz kontinuierlich arbeitender Abraumtransportssysteme in hydraulischen Rohrvortrieben. In: Deutsche Gesellschaft für Erd- und Grundbau e.V. (Hg.): Taschenbuch für den Tunnelbau. Essen: Glückauf, S. 357–382.

DEKRA 2016 Gutachtliche Stellungnahme zum sicheren Betrieb einer Anlage zur Elektro-koagulation am Standort Bochum. DEKRA. Bochum.

Delgado, Á. V. (Hg.) (2002): Interfacial electrokinetics and electrophoresis. New York, NY: Dekker (Surfactant science series, 106). Latest opened 11.03.2019, accessible online under: http://www.loc.gov/catdir/enhancements/fy0648/2001055552-d.html

Deryaguin, B. V.; Landau, L. D. (1941): A theory of the stability of strongly charged lyophobic sols and so the adhesion of strongly charged particles in solutions of electrolytes. In: Acta Physicochim URSS (14), S. 633–662.

Deutsche Gesellschaft für Erd- und Grundbau e.V. (Hg.) (1984): Taschenbuch für den Tun-nelbau. Essen: Glückauf.

DIN EN 15198:2007-11: Methodik zur Risikobewertung für nicht-elektrische Geräte und Komponenten zur Verwendung in explosionsgefährdeten Bereichen; Deutsche Fassung EN 15198:2007.

DIN EN ISO 12100:2011-03: Sicherheit von Maschinen - Allgemeine Gestaltungsleitsätze - Risikobeurteilung und Risikominderung (ISO 12100:210) Deutsche Fassung EN ISO 12100:2010.

DIN EN 1127-1:2011-10: Explosionsfähige Atmosphären - Explosionsschutz - Teil 1: Grundlage und Methodik. Deutsche und Englische Fassung EN 1127-1:2011.

DIN 4126:2013-09: Nachweis der Standsicherheit von Schlitzwänden.

DIN 4127:2014-02: Erd- und Grundbau - Prüfverfahren für Stützflüssigkeiten im Schlitz-wandbau und für deren Ausgangsstoffe.

DIN EN 1127-1:2017-12 - Entwurf: Explosionsfähige Atmosphären - Explosionsschutz - Teil 1: Grundlagen und Methodik; Deutsche und Englische Fassung prEN 1127-1:2017.

DIN VDE 0100-200, 2006-06: Errichten von Niederspannungsanlagen - Teil 2: Begriffe (IEC 60050-826:2004, modifiziert).

Donini, J. C.; Kan, J.; Szynkarczuk, J.; Hassan, T. A.; Kar, K. L. (1994): The operating cost of electrocoagulation. In: Can. J. Chem. Eng. 72 (6), S. 1007–1012.

Duc, M.; Gaboriaud, F.; Thomas, F. (2005): Sensitivity of the acid–base properties of clays to the methods of preparation and measurement. In: Journal of Colloid and Interface Science (289), S. 139–147.

Dzenitis, J. M. (1997): Soil chemistry effects and flow prediction in electroremediation of soil. In: Enviro. Sci. Technol. (37), S. 1191–1197.

Einstein, A. (1905): Über die von der molekularkinetischen Theorie der Wärme geforderte Bewegung von in ruhenden Flüssigkeiten suspendierten Teilchen. In: Ann. Phys. 322 (8), S. 549–560.

Elnenay, A. M. H.; Nassef, E.; Malash, G. F.; Magid, M. H. A. (2016): Treatment of drilling fluids wastewater by electrocoagulation. In: Egyptian Journal of Petroleum 26 (1), S. 203–208.

Ersoy, B.; Evcin, A.; Uygunoglu, T.; Akdemir, Z. B.; Brostow, W.; Wahrmund, J. (2014): Zeta Potential–Viscosity Relationship in Kaolinite Slurry in the Presence of Dispersants. In: Arab J Sci Eng 39 (7), S. 5451–5457.

Eyvaz, M.; Kirlaroglu, M.; Aktas, T. S.; Yuksel, E. (2009): The effects of alternating current electrocoagulation on dye removal from aqueous solutions. In: Chemical Engineering Journal 153 (1-3), S. 16–22.

Feifel, F.; Oechsle, D. (2000): Fliterpressen: Kapitel 3.9. In: Horst Gasper: Handbuch der industriellen Fest/Flüssig-Filtration. 2., vollst. überarb. und stark erw. Aufl. Weinheim: Wiley-VCH, S. 119–129.

Fischer, M. L.; Colic, M.; Rao, M. P.; Lange, F. F. (2001): Effect of Silica Nanoparticle Size on the Stability of Alumina/Silica Suspensions. In: Journal of the American Ceramic Society (Volume 84, Issue 4), S. 713–718.

Förster GmbH, (2016): Intern project documents

Garciagarcia, S.; Wold, S.; Jonsson, M. (2009): Effects of temperature on the stability of colloidal montmorillonite particles at different pH and ionic strength. In: Applied Clay Science 43 (1), S. 21–26.

Garcia-Segura, S.; Eiband, M. M.; Vieira de Melo, J.; Martinez-Huitle, C. A. (2017): Electrocoagulation and advanced electrocoagulation processes: A general review about the fundamentals, emerging applications and its association with other technologies. In: Journal of Electroanalytical Chemistry (Volume 801), S. 267–299.

Ghernaout, D.; Ghernaout, B.; Boucherit, A. (2008): Effect of pH on Electrocoagulation of Bentonite Suspensions in Batch Using Iron Electrodes. In: Journal of dispersion science and technology (29), S. 1272–1275.

Ghernaout, D.; Ibraheem Al-Ghonamy, A.; Boucherit, A.; Ghernaout, B.; Naceur, M. W.; Messaoudene, N. A.; Aichouni, M. (2015): Brownian Motion and Coagulation Process. In: AJEP 4 (5), S. 1.

Ghernaout, D.; Naceur, M. W.; Aouabed, A. (2011): On the dependence of chlorine by-products generated species formation of the electrode material and applied charge during electrochemical water treatment. In: Desalination 270 (1-3), S. 9–22.

Global Advantech Limited (2012): Remediation of Water-Based Drilling Fluids and Cleaning of Cuttings. Technology Data Sheet TDS831. United Kingdom. Latest opened 16.01.2019, accessible online under: http://www.globaladvantech.com/Oil-andgas/TDS831%20Remediation%20of%20Water-Based%20Drilling%20Fluids%20and%20Cuttings%20EN%2002.pdf

Glück, J. (2015): Konstruktive Entwicklung eines kleinmaßstäblichen Prototypen im Rahmen eines DBU- geförderten Forschungsprojektes zur Aufbereitung von Bentonit- Suspensionen mit dem Elektrokoagulationsverfahren. Hochschule Offenburg.

Greenwood, R.; Lapčíková, B.; Waters K.; LapčíkJr, L. (2006): The Zeta Potential of Kaolin Suspensions Measured by Electrophoresis and Electroacoustics. In: Chemical Papers - Slovak Academy of Sciences (61 (2)), S. 83–92.

Gregory, J. (2006): Particles in water. Properties and processes. Boca Raton, FL, London: Taylor & Francis; IWA.

Gupta, A.; Yan, D. (2016): Solid Liquid Separation – Filtration. In: Mineral Processing Design and Operations: Elsevier, S. 507–561

Hakizimana, J. N.; Gourich, B.; Chafi, M.; Stiriba, Y.; Vial, C.; Drogui, P.; Naja, J. (2017): Electrocoagulation process in water treatment. A review of electrocoagulation modeling approaches. In: Desalination 404, S. 1–21.

Halliburton (2010): Clean Wave SM Water Treatment Service. Halliburton. Latest opened 21.02.2019, accessible online under: https://2jc18v1irh0441xjkl3blrt4-wpengine.netdna-ssl.com/wp-content/uploads/2014/08/CleanWave_Service.pdf.

Hamaker, H. C. (1937): The London - van der Waals attraction between spherical particles. In: Physicia (Volume 4, Issue 10), S. 1058–1072.

Heffernan, T.; Rea, B. (2013) EcoFloc advanced electro-coagulation liquid waste treatment system and process. Patent, publicationnr: US20130180857.

Hering, E.; Martin, R.; Stohrer, M.; Käß, Hanno (2012): Physik für Ingenieure. 11., bearb. Aufl. Berlin: Springer (Springer-Lehrbuch).

Hiegemann, H.; Herzer, D.; Nettmann, E.; Lübken, M.; Schulte, P.; Schmelz, K.G.; Gredigk-Hoffmann, S.; Wichern, M. (2016): An integrated 45 L pilot microbial fuel cell system at a full-scale wastewater treatment plant. In: Bioresource Technology 218, S.115-122.

Hollmann, F. S.; Thewes, M. (2013): Assessment method for clay clogging and disintegration of fines in mechanised tunnelling. In: Tunnelling and Underground Space Technology 37, S. 96–106.

Holt, P. (2002): Electrocoagulation: unravelling and synthesizing the mechanisms behind a water treatment process. PhD. University of Sydney, Sydney. Department of Chemical Engineering.

Holt, P.; Barton, G. W.; Mitchell, C. (1999): Electrocoagulation as a wastewater treatment. In: The Third Annual Australian Environmental Engineering.

Holt, P. K.; Barton, G. W.; Mitchell, C. A. (2005): The future for electrocoagulation as a localized water treatment technology. In: Chemosphere 59 (3), S. 355–367.

Hosterman, J. W.; Patterson, S. H. (1992): Bentonite and Fuller´s Earth Resources of the United States. U.S. Department of the Interior Manuel Lujan. Denver.

Hotta, Y.; Banno, T.; Nomura, Y.; Sano, S.; Oda, K. (1999): Factors affecting the plasticity of Georgia Kaolin Green Body. In: J. Ceramic Soc. of Japan (107), S. 868.

Hu, C. Y.; Lo, S. L.; Kuan, W. H. (2003): Effects of co-existing anions on fluoride removal in electrocoagulation (EC) process using aluminum electrodes. In: Water Research 37 (18), S. 4513–4523.

Huang, W.; Leong, Y-K.; Chen, T.; Au, P-I.; Liu, X.; Qiu, Z. (2016): Surface chemistry and rheological properties of API bentonite drilling fluid. PH effect, yield stress, zeta potential and ageing behavior. In: Journal of Petroleum Science and Engineering 146, S. 561–569.

Hubbard, A. T. (2002): Encyclopedia of surface and colloid science. New York: Marcel Dekker (Volume 4).

Imerys (2019): Bentonite. Latest opened 11.06.2019, accessible online under: http://www.imerys-additivesformetallurgy.com/our-resources/bentonite/.

Jasmund, K.; Lagaly, G. (1993): Tonminerale und Tone. Struktur, Eigenschaften, Anwendungen und Einsatz in Industrie und Umwelt. Darmstadt: Steinkopff Verlag.

Jian, W. (2018): Untersuchung des Einflusses der Elektrokoagulation auf die Entwässerung der Altbentonitsuspension. Master Thesis. Ruhr-Universität Bochum, Bochum. Fakultät für Bau- und Umweltingenieurwissenschaften.

Jiang, J-Q.; Graham, N.; André, C.; Kelsall, G H.; Brandon, N. (2002): Laboratory study of electro-coagulation–flotation for water treatment. In: Water Research 36 (16), S. 4064–4078.

Júnior, J. A. A.; Baldo, J. B. (2014): The Behavior of Zeta Potential of Silica Suspensions. In: NJGC 04 (02), S. 29–37.

Kiefer, G.; Schmolke, H. (2017): VDE 0100 und die Praxis. Wegweiser für Anfänger und Profis. 16., neu bearbeitete und erweiterte Auflage. Berlin, Offenbach: VDE Verlag GmbH.

Kim, J.; F. Lawler, D. (2005): Characteristics of zeta potential distribution in silica particles. In: Bulletin of the Korean Chemical Society (Vol. 26 Issue 7), S. 1083–1089.

Kirmaier, N.; Hose, G.H; Reis, A. (1984): Theory, process engineering and practical results of anodic oxidation. In: Neue Deliwa (Z.35), S. 260–266.

Kobayashi, M.; Juillerat, F.; Galletto, P.; Bowen, P.; Borkovec, M. (2005): Aggregation and Charging of Colloidal Silica Particles Effect of Particle Size. In: Langmuir (21), S. 5761–5769.

Kobya, M.; Bayramoglu, M.; Eyvaz, M. (2007): Techno-economical evaluation of electro-coagulation for the textile wastewater using different electrode connections. In: Journal of hazardous materials 148 (1-2), S. 311–318.

Kobya, M.; Ulu, F.; Gebologlu, U.; Demirbas, E.; Oncel, M. S. (2011): Treatment of potable water containing low concentration of arsenic with electrocoagulation. Different connection modes and Fe–Al electrodes. In: Separation and Purification Technology 77 (3), S. 283–293.

Kobya, M.; Can, O. T.; Bayramoglu, M. (2003): Treatment of textile wastewaters by electro-coagulation using iron and aluminum electrodes. In: Journal of hazardous materials 100 (1-3), S. 163–178.

Leroy, P.; Tournassat, C.; Bernard, O.; Devau, N.; Azaroual, M. (2015): The electrophoretic mobility of montmorillonite. Zeta potential and surface conductivity effects. In: Journal of Colloid and Interface Science (Volume 451), S. 21–39.

Letterman, R. D. (1999): Water quality and treatment: a handbook of community water supplies. 5th edition. New York: McGraw-Hill.

Lin, B.; Hu, R.; Ye, C.; Li, Y.; Lin, C. (2010): A study on the initiation of pitting corrosion in carbon steel in chloride-containing media using scanning electrochemical probes. In: Electrochimica Acta 55 (22), S. 6542–6545.

Lin, S. H.; Peng, C. F. (1994): Treatment of textile wastewater by electrochemical method. In: Water Research 28 (2), S. 277–282.

Linde Gas Gmbh (2019): Datasheet: Rechnen sie mit Wasserstoff. Last opened 18.07.2019. Available online under: https://www.linde-gas.at/de/images/1007_rechnen_sie_mit_wasserstoff_v110_tcm550-169419.pdf

Lipka, K. (2009): Untersuchung zur Dimensionierung von Separieranlagen im Tunnelbau. Diplomarbeit. Ruhr-Universität Bochum, Bochum. Fakultät für Bau- und Umweltingenieurwissenschaften.

Loll, U.; Melse, A. (1992): Auswahl und Einsatz von organischen Flockungshilfsmitteln - Polyelektrolyten - bei der Klärschlammentwässerung. ATV Arbeitsbericht: Stabilisation, Entseuchung, Eindickung, Entwässerung und Konditionierung von Schlämmen, einschließlich der Kompositierung von Schlämmen und festen Abfällen. In: KA: Korrespondenz Abwasser, Abfall (39 (4)), S. 569–580.

Lorenz, P. B. (1969): Surface conductance and electrokinetic properties of kaolinite beds. In: Clays Clay Mineral (17), S. 299–340.

Luckham, P. F.; Rossi S (1999): The colloidal and rheological properties of bentonite suspensions. In: Advances in Colloid and Interface Science (82), S. 43–92.

Maidl, B.; Herrenknecht, M.; Maidl, U.; Wehrmeyer, G. (2012): Mechanised Shield Tunnelling. 2. Aufl. Berlin: Ernst & Sohn.

Malakootian, M.; Yousefi, N. (2009): The Efficiency of Eletrocoagulation Process using Aluminum Electrodes in Removal of hardness from Water. In: Iran. J. Environ Health Sci. (Volume 6), S. 131–136.

Mamelkina, M. A.; Cotillas, S.; Lacasa, E.; Sáez, C.; Tuunila, R.; Sillanpää, M. (2017): Removal of sulfate from mining waters by electrocoagulation. In: Separation and Purification Technology 182, S. 87–93.

Mameri, N.; Yeddou, A. R.; Lounici, H.; Belhocine, D.; Grib, H.; Bariou, B. (1998): Defluoridation of septentrional Sahara water of north Africa by electrocoagulation process using bipolar aluminium electrodes. In: Water Research 32 (5), S. 1604–1612.

Marriage-Cabrales, N.; Machuca-Martinez, F. (2014): Fundamentals of electrocoagulation. In: Evaluation of Electrochemical Reactors as a New Way to Environmental Protection, S. 1–16.

Martínez-Huitle, C. A.; Brillas, E. (2009): Decontamination of wastewaters containing synthetic organic dyes by electrochemical methods. A general review. In: Applied Catalysis B: Environmental 87 (3-4), S. 105–145.

Mechelhoff, M.; Kelsall, G. H.; Graham, N. J.D (2013): Electrochemical behavior of aluminium in electrocoagulation processes. In: Chemical Engineering Science 95, S. 301–312.

Metin, C. O.; Lake, L. W.; Miranda, C. R.; Nguyen, Q. P. (2011): Stability of aqueous silica nanoparticle dispersions. In: J Nanopart Res 13 (2), S. 839–850.

Meunier, N.; Drogui, P.; Montané, C.; Hausler, R.; Mercier, G.; Blais, J-F (2006): Comparison between electrocoagulation and chemical precipitation for metals removal from acidic soil leachate. In: Journal of hazardous materials 137 (1), S. 581–590.

Meyer, A.; Herrenknecht AG (2017): Intern project documents

Mickley, M. (2009): Treatment of concentrate. Denver Federal Center May.

Mollah, M. Y. A.; Morkovsky, P.; Gomes, J. A. G.; Kesmez, M.; Parga, J.; Cocke, D. L. (2004): Fundamentals, present and future perspectives of electrocoagulation. In: Journal of hazardous materials 114 (1-3), S. 199–210.

Mollah, M. Y. A.; Schennach, R.; Parga, J. R.; Cocke, D. L. (2001): Electrocoagulation (EC)--science and applications. In: Journal of hazardous materials 84 (1), S. 29–41.

Morbidelli, M.; Arosio, P. (2016): Polymer Reaction & Colloid Engineering. Institute for Chemical and Bioengineering Department of Chemistry and Applied Biosciences ETH. Zürich.

Mouedhen, G.; Feki, M.; Wery, M. De Petris; Ayedi, H. F. (2008): Behavior of aluminum electrodes in electrocoagulation process. In: Journal of hazardous materials 150 (1), S. 124–135.

MSE-Filterpressen (2017, 2019): Intern project documents

Murray, H. H. (1991): Overview - clay mineral applications. In: Applied Clay Science 5 (5-6), S. 379–395.

Nariyan, E.; Sillanpää, M.; Wolkersdorfer, C. (2017): Electrocoagulation treatment of mine water from the deepest working European metal mine – Performance, isotherm and kinetic studies. In: Separation and Purification Technology 177, S. 363–373.

Nikolaev, V. G.; Strelko, V. K, Korovin, Yu. F (1982). Treating natural waters in small water systems by filtration with electrocoagulation. In: Soviet Journal of Water Chemistry and Technology, 4; 3: 244- 247.

Nouri, J.; Mahvi, A. H.; Bazrafshan, E. (2010): Application of Electrocoagulation Process in Removal of Zinc and Copper From Aqueous Solutions by Aluminum Electrodes. In: International Journal of Environmental Research (4(2)), S. 201–208.

Ostermann, F. (2007): Anwendungstechnologie Aluminium. 2., neu bearbeitete und aktualisierte Auflage. Berlin, Heidelberg: Springer-Verlag Berlin Heidelberg (VDI-Buch).

Particles Sciences (2012): An Overview of the Zeta Potential. Hg. v. Particles Sciences.

Patermarakis, G.; Fountoukidis, E. (1990): Disinfection of water by electrochemical treatment. In: Water Research 24 (12), S. 1491–1496.

Payá Silvestre, S. (2016): Elektrokoagulation zur Trennung von gebrauchten Bentonitsuspensionen im Tunnelbau. Dissertation. Ruhr-Universität Bochum, Bochum. Lehrstuhl für Tunnelbau, Leitungsbau und Baubetrieb.

Picard, T.; Cathalifaud-Feuillade, G.; Mazet, M.; Vandensteendam, C. (2000): Cathodic dissolution in the electrocoagulation process using aluminium electrodes. In: Journal of environmental monitoring: JEM 2 (1), S. 77–80.

Popovic, I. (2019): Neue Trennmethode für gebrauchte Bentonitsuspensionen: Feinkornabtrennung mittels Elektrokoagulation – Laborversuche, Prototyp, Baustellenimplementierung. Proceedings of the STUVA Conference, 2019.

Popovic, I.; Schößer, B. (2019): Entwicklung einer innovativen Trennmethode für gebrauchte Bentonitsuspensionen zur ökonomisch vorteilhaften, ressourcenschonenden und umweltgerechten Entsorgung. Phase 2 - Research report. Lehrstuhl für Tunnelbau, Leitungsbau und Baubetrieb - Ruhr-Universität Bochum. Bochum.

Popovic, I.; Schößer, B.; Thewes, M.; Edelmann, T. (2018): Neue Trennmethode für gebrauchte Bentonitsuspensionen auf Basis der Elektrokoagulation. Proceedings of the RuhrGeo-Tag Conference, 2018.

Popovic, I.; Schößer, B.; Payá Silvestre, S.; Thewes, M.; Edelmann, T. (2017): Separation of used bentonite suspensions in slurry shield tunnelling: improvement of depositing costs by introduction of a new method. Proceedings of the ITA World Tunnel Congres, 2017.

Praetorius, S.; Schößer, B. (2016): Bentonithandbuch. Ringspaltschmierung für den Rohrvortrieb. Berlin: Wilhelm Ernst & Sohn.

Rahaman, M. M.; Ahmed T.S. (2016): Affordable Water Pricing for Slums Dwellers in Dhaka Metropolitan Area. The Case of Three Slums. In: Journal of Water Resoure Engineering and Managment (Volume 3, Issue 1), S. 15–33.

Reuter, B.; Faltenbacher, M.; Schuller, O.; Whitehouse, N.; Whitehouse, S. (2017): New Bus Re-Fuelling For European hydrogen Bus Depots. Guidance Document on Large Scale hydrogen Bus Refuelling. Hg. v. Dr. Benjamin Reuter. thinkstep AG. Leinfelden-Echterdingen, Germany.

Sahu, O.; Mazumdar, B.; Chaudhari, P. K. (2014): Treatment of wastewater by electrocoagulation. A review. In: Environmental science and pollution research international 21 (4), S. 2397–2413.

Santo, Carlos E.; Vilar, Vítor J.P.; Botelho, C. M.S.; Bhatnagar, A.; Kumar, E.; Boaventura, R. A.R. (2012): Optimization of coagulation–flocculation and flotation parameters for the treatment of a petroleum refinery effluent from a Portuguese plant. In: Chemical Engineering Journal 183, S. 117–123.

Schröder, V. (2002): Explosionsgrenzen von Wasserstoff und Wasserstoff/Methan-Gemischen. Research report from BAM.

Seidenfuß, T. (2007): Separationsanlagen für Microtunnelling, Rohrvortrieb und verwandte Verfahren. In: Tiefbau (49 (112)), S. 749–751.

Shang, J. Q. (1997): Zeta potential and electroosmotic permeability of clay soils. In: Can. Geotech. J. 34 (4), S. 627–631.

Sincero, A. P.; Sincero, G. A. (2003): Physical-chemical treatment of water and wastewater. London, Boca Raton, Fla: CRC Press.

Smith, R. W.; Narimatsu, Y. (1993): Electrokinetic behaviour of kaolinite in surfactant solutions as measured by both the microelectrophoriesis and streaming potential methods. In: Minerals Engineer (6), S. 753–763.

Song, P.; Yang, Z.; Zeng, G.; Yang, X.; Xu, H.; Wang, L. (2017): Electrocoagulation treatment of arsenic in wastewaters. A comprehensive review. In: Chemical Engineering Journal 317, S. 707–725.

Stein, D.; Schößer, B.; Statetzini, C. (2007): Entwicklung und Erprobung von optimierten Injektionsmitteln und -verfahren zur kontinuierlichen Ringspaltunterstützung beim Rohrvortrieb im heterogenen Baugrund. Ruhr-Universität Bochum, Fakultät für Bauingenieurwesen. Bochum.

Stein, Dietrich (2003): Grabenloser Leitungsbau. Berlin: Ernst.

Stowa (1995): Untersuchung der Umweltgefährdung von Polyelektrolyten in Kläranlagen.

Stumm, W.; Morgan, J. J. (1996): Aquatic chemistry. Chemical equilibria and rates in natural waters. Third edition. New York, Chichester, Brisbane, Toronto, Singapore: John Wiley & Sons Inc (A Wiley-Interscience publication).

Szynkarczuk, J.; Kan, J.; Hassan, T. A.; Donini Canmet, J. C. (1994): Electrochemical Coagulation of Clay Suspensions. In: Clays and Clay Minerals (Vol. 42), S. 667–673.

Thomas, D. N.; Jud, S.J; Fawcett, N. (1999): Flocculation Modelling: A Review. In: Water Res. (Volume 33), S. 1579–1592.

Tombácz, E.; Ábrahám, I.; Gilde, M.; Szántó, F. (1990): The pH-dependent colloidal stability of aqueous montmorillonite suspensions. In: Colloids and Surfaces 49, S. 71–80.

Tombácz, E.; Szekeres, M. (2004): Colloidal behavior of aqueous montmorillonite suspensions: the specific role of pH in the presence of indifferent electrolytes. In: Applied Clay Science (27 (1-2)), S. 75–94.

Tournassat, C.; Appelo, C. A. J. (2011): Modelling approaches for anion-exclusion in compacted Na-bentonite. In: Geochimica et Cosmochimica Acta 75 (13), S. 3698–3710.

Tunc, S.; Duman, O.; Uysal, R. (2007): The effect of different molecular weight of poly (ethylene gylcol) on the electrokinetic and rheological properties of Na-bentonite suspensions. In: Colloids and Surfaces A: Physicochem.Eng. Aspects (317), S. 93–99.

Tunc, S.; Duman, O.; Uysal, R. (2008): Electrokinetic and Rheological Behaviors of Sepiolite Suspensions in the Presence of Poly(acrylic acid sodium salt)s, Polyacrylamides, and Poly(ethylene glycol)s of Different Molecular Weights. Hg. v. Wiley Interscience. Department of Chemistry, Faculty of Arts and Sciences, Akeniz University, Antalya, Turkey; Faculty of Education, Akedeniz University, Antalya, Turkey.

Ulke, B. Bentonitentwässerung mit Hilfe der Elektroosmose. RWTH Aachen. Latest opened 16.07.2019, accessible online under http://www.geotechnik.rwth-aachen.de/forschung/Elektroosmose.pdf

Umweltbundesamt (2018): Wassergefährdende Stoffe. Hg. v. UBA. Latest opened 02.04.2019, accessible online under: https://webrigoletto.uba.de/rigoletto/public/language.do;jsessionid=10DCF2FE635F4F8AABEA49BFA1C82DCE?language=native.

UNESCO (2015): Water for a sustainable world. Paris: UNESCO (The United Nations world water development report, 6.2015). Latest opened 16.07.2019, accessible online under: http://www.unesco.org/ulis/cgi-bin/ulis.pl?catno=231823.

Uphoff Lab (2019): Eluate. Latest opened 19.07.2019, accessible online under: https://labor-uphoff.mwk-bionik.de/en/biogasanalytik-und-beratung/einzelanalytik/eluat.html

Valero, D.; Oritz, J.; Exposito, E.; Montiel, V.; Aldaz, A. (2008): Electrocoagulation of a synthetic textile effluent powered by photovoltaic energy without batteries. Direct connection behaviour. In: Solar Energy Materials and Solar Cells 92 (3), S. 291–297.

Van Olphen, H. (1963): An Introduction to Clay Colloid Chemistry: For Clay Technologists, Geologists, and Soil Scientists. Second Edition. New York: John Wiley & Sons.

Vane, L. M.; Zang, G. M. (1997): Effect of aqueous phase properties on clay particle zeta potential and electroosmotic permeability: Implications for electro-kinetic soil remediation process. In: J. Hazard. Matter (55), S. 1–22.

Vasudevan, S.; Lakshmi, J. (2011): Effects of alternating and direct current in electrocoagulation process on the removal of cadmium from water – A novel approach. In: Separation and Purification Technology 80 (3), S. 643–651.

Vasudevan, S.; Lakshmi, J.; Jayaraj, J.; Sozhan, G. (2009): Remediation of phosphate-contaminated water by electrocoagulation with aluminium, aluminium alloy and mild steel anodes. In: Journal of hazardous materials 164 (2-3), S. 1480–1486.

Verma, A. K. (2017): Treatment of textile wastewaters by electrocoagulation employing Fe-Al composite electrode. In: Journal of Water Process Engineering 20, S. 168–172.

Verma, A. K.; Dash, R. R.; Bhunia, P. (2012): A review on chemical coagulation/flocculation technologies for removal of colour from textile wastewaters. In: Journal of environmental management 93 (1), S. 154–168.

Verwey, E. J. W.; Overbeek, J. T .G. (1948): Theory of the stability of lyophobic colloids. In: Journal of Colloid Science 10 (2), S. 224–225.

Vik, E. A.; Carlson, D. A.; Eikum, A. S.; Gjessing, E. T. (1984): Electrocoagulation of potable water. In: Water Research 18 (11), S. 1355–1360.

Vishnyakov, S. (2019): Untersuchung des Einflusses der Dichte der Suspension, der Versuchsdauer und der Kombination der "best-fitting" Parameter auf die Elektrokoagulation und die Entwässerung der Bentonitsuspensionen. Master Thesis. Ruhr-Universität Bochum, Bochum. Fakultät für Bau- und Umweltingenieurwissenschaften.

Walsh, F. C. (1993): A first course in electrochemical engineering. Romsey: Electrochemical Consultancy.

Weiner, T. (2018): Prognose, Separation, Erfassung und Abrechnung des Bodenaushubs beim flüssigkeitsgestützten Schildvortrieb. Dissertation. Ruhr-Universität Bochum, Bochum. Fakultät für Bau-und Umweltingenieurwissenschaften.

West, L. J.; Stewart, D. L. (2001): Effect of Zeta Potential on Soil Electrokinesis. In: The Proc. of Geoenvironment, ASCE , S. 535–1549.

Wichern, M., Lübken, M., Kletke, T. (2012). MBZ NRW "Optimierung der Brennstoffzellentechnik für den Kläranlagenbetrieb" - Phase 1. Research report. Aachen & Bochum.

Williams, D. J.; Williams K. P (1978): Electrophoresis and zeta potential of kaolinite. In: J. Colloid Interface Sci (65), S. 79–87.

Wong, H.; Shang, C.; Cheung, Y.; Chen, G. (Hg.) (2002): Chloride assisted electrochemical disinfection. Proceedings of the Eighth Mainland-Taiwan Environmental Protection Conference, 2002.

Yilmaz, A. E.; Boncukcuoğlu, R.; Kocakerim, M. M.; Yilmaz, M. T.; Paluluoğlu, C. (2008): Boron removal from geothermal waters by electrocoagulation. In: Journal of hazardous materials 153 (1-2), S. 146–151.

Yukselen, Y.; Kaya, A. (2003): Zeta Potential of Kaolinite in the Presence of Alkali, Alkaline Earth and Hydrolyzable Metal Ions. In: Water, Air and Soil Pollution (Vol 154.), S. 155–168.

Żbik, M. S.; Williams, D. J.; Song, Y-F; Wang, C-C (2014): The formation of a structural framework in gelled Wyoming bentonite. Direct observation in aqueous solutions. In: Journal of Colloid and Interface Science 435, S. 119–127.

Zizka, Zdenek (2019): Stability of a slurry supported tunnel face considering the transient support mechanism during excavation in non-cohesive soil. Dissertation. Ruhr-Universität Bochum, Bochum. Fakultät für Bau-und Umweltingenieurwissenschaften.

13 **Appendix**

Appendix A: Materials used in experiments

Appendix A.1 Soil material

IMERYS
Civil Engineering

Aktiv-Bentonit IBECO B1

Beschreibung / Anwendung	Description / Application	Description / Application
IBECO B1 ist ein aktivierter Natrium-Bentonit für den Baubereich. Aufgrund seiner sehr guten rheologischen Eigenschaften und Robustheit ist IBECO B1 universell einsetzbar, insbesondere für Stützflüssigkeiten bei Schlitzwänden, Schildvortrieben, Bohrarbeiten und Rohrvortrieben.	IBECO B1 is an activated sodium bentonite for civil engineering. Due to its excellent rheological properties and robustness, IBECO B1 is universally applicable, especially as slurry for diaphragm walls, shield tunneling, drilling operations and pipe jacking.	IBECO B1 est une bentonite de sodium activé pour le secteur de la construction. Grâce à ses excellentes propriétés rhéologiques et robustesse IBECO B1 est universellement applicable, en particulier comme boue pour les parois moulées, les tunneliers, les forages et les fonçages.

Technische Durchschnittswerte	Technical average values	Valeurs techniques moyennes		
Wassergehalt	Water content	Teneur en eau	11 ± 3	%
Korndichte	Specific density	Poids spécifique	2,65	g/cm³
Schüttdichte	Bulk density	Densité apparente tassée	800 ± 100	g/l
Siebrückstand auf 0,063 mm	Screen residue on 0,063 mm	Refus au tamis 0,063 mm	20 ± 5	%
Suspension bei 50 kg/m³, nach 24 Stunden	**Slurry at 50 kg/m³, after 24 hours**	**Boue à 50 kg/m³, après 24 heures**		
Suspensionsdichte	Slurry density	Densité de Gel	1,028	t/m³
Marsh-Viskosität	Marsh viscosity	Viscosité Marsh	40	s/l
Fließgrenze (Kugel)	Liquid limit (ball)	Rigidité (billes)	30 (6)	N/m²
Filtratwasserabgabe	Filtrate volume	Volume de Filtrat	12	ml

Anmerkungen	Remarks	Remarques
Die oben genannten Werte verstehen sich als typische Durchschnittswerte und wurden unter Laborbedingungen ermittelt. Da es sich bei diesem Produkt um einen natürlichen Rohstoff handelt, sind die Messwerte als Richtwerte zu betrachten, die gewissen Schwankungen unterliegen. Jegliche Verwendung des Produktes liegt vollständig in der Verantwortung des Anwenders.	The values listed above were determined under laboratory conditions. Since this product is a natural raw material, the measured values are indicative and subject to variations. Any use of this product is entirely in the responsibility of the user.	Les valeurs ci-dessus ont été déterminées dans des conditions de laboratoire. Ce produit étant une matière première naturelle, les valeurs mesurées doivent être considérées comme indicatives car soumises à certaines fluctuations. Toute utilisation de ce produit est entièrement à la charge de l'utilisateur.

IMERYS Metalcasting Germany GmbH – Ruhrorter Straße 72 – D – 68219 Mannheim
Tel.+49 621 / 8 04 27-0 – Fax +49 621 / 8 04 27-50

JLEO/HSPE 2016-07-28

Figure A-1: Properties of B1 bentonite

ERBSLÖH Kaolin W

ERBSLÖH Kaolin W ist ein puderfeines Kaolin. Durch die gründliche Reinigung und anschließende Mahltrocknung können Sie sich auf die Qualität verlassen. Verwenden Sie Kaolin W dort, wo es Ihnen auf Feinheit, Trockenheit und schnelle Verfügbarkeit Ihres Füllstoffes ankommt.

ERBSLÖH Kaolin W ist das Kaolin, das von unseren Kunden am häufigsten verwendet wird. Die cremefarbene Tönung von *ERBSLÖH* Kaolin W ist ideal für viele technische Anwendungen. Für Ihre neuen Ideen hier einige „alte" Anwendungen:

Reifen und Gummierzeugnisse

Papier und Kartonagen

Tapeten

Klebstoffe

Kunststoffe

Farben und Lacke

Pflanzenpflege- und -schutzmittel

Kosmetika

Chemische Analyse

SiO_2	51,0 - 59,0	%
Al_2O_3	30,0 - 36,0	%
Fe_2O_3	1,50 – 5,00	%
K_2O	4,00 – 7,00	%
TiO_2	0,05 – 0,15	%
CaO	0,02 – 3,50	%
MgO	0,40 – 1,20	%
Na_2O	0,05 – 0,15	%
P_2O_5	0,05 – 0,25	%
BaO	0,05 – 0,20	%
Glühverlust	6,0 – 9,50	%

Figure A-2: Properties of kaolin W

EUROQUARZ

Mineralische Rohstoffe: Klassiert ● Getrocknet ● Gemahlen

Product Data Sheet
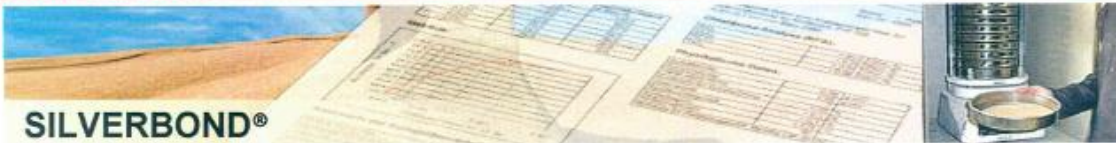
SILVERBOND®

Features and benefits

SILVERBOND® crystalline silica is produced from high purity quartz feed stock for manufacturing and formulation of applications which require structurally sound, chemically pure or non-reactive fine mineral fillers.

Completely inert and pH neutral, SILVERBOND® will not alter or initiate when incorporated in catalysed or multi-component chemicals systems, and will not degrade when employed in extreme temperatures or harsh environments. SILVERBOND® offers formulators a low surface area, minimal oil absorption option to achieve high loading in coatings and cementitious systems and stiffening in elastomeric and high performance epoxy. Chemically pure SILVERBOND® also serves as an excellent non-conductor in electrical assemblies and potting compounds, and non-combustible filler in thermal insulating.

All SILVERBOND® grades are processed with adherence to ISO and internal quality assurance programs. The result is chemical purity and consistently uniform particle size distributions for predictable results supported by reliable services.

		M300	M400	M500		Method
control sieve	>100 µm				%	Alpine
	> 63 µm				%	Alpine
	> 40 µm	1,8	0,1	0,012	%	Alpine
D_{10}		3	3	2	µm	Malvern MS2000
D_{50}		17	12	4	µm	Malvern MS2000
D_{90}		40	26	10	µm	Malvern MS2000
density		2,65	2,65	2,65	kg/dm³	
bulk density		0,85	0,7	0,65	kg/dm³	
specific surface		4000	6500	12000	cm²/g	Blaine
oil absorption		19	20	23	g/100 g	
hardness		7	7	7	Mohs	
pH		7	7	7		
loss on ignition		0,12	0,12	0,3	%	
colour	L*	92	93	94		Minolta CM-3610d
	a*	0,58	0,58	0,46		$D_{65}/10°$
	b*	2,73	3,0	2,78		
refractive index		1,55	1,55	1,55		
SiO_2		99,4	99,4	99,2		
Fe_2O_3		0,03	0,03	0,05		
Al_2O_3		0,3	0,3	0,4		
TiO_2		0,07	0,07	0,03		

9.7.15

Figure A-3: Properties of silica flour

Appendix A.2   Coagulation agents

Datenblatt FeCl3 füssig

technische Information   Seite 1 / 1

Beschreibung:

Das Material liegt in Form einer konzentrierten, dunkelbraunen, klaren Eisen-III-Chloridlö-sung vor. Es wird in der Brauchwasseraufbereitung, in der Abwasserbehandlung und zur Reinigung industrieller Abwässer als Fällungs- und Flockungshilfsmittel eingesetzt und als Ätzmittel bei der Platinen- oder Formätzteilherstellung. EISEN(III)CHLORID-Lösung 40% enthält rezepturgemäß keine organischen Chlorverbindungen und liefert insofern keinen Beitrag zu entsprechenden Parametern in mit Eisen(III)chlorid aufbereitetem Wasser.Das o.g. Produkt erfüllt die Anforderungen gemäß Anhang 40 Punkt 2.7.3 der Abwasserver-waltungsvorschrift. Darüber hinaus erfüllt EISEN(III)CHLORID-Lösung 40% die Anforde-rungen der DIN EN 888 Eisen(III)chlorid zur Aufbereitung von Wasser für den menschli-chen Gebrauch einschließlich der lebensmittelrechtlichen Vorschriften,insbesondere des Lebensmittel- und Bedarfsgegenständegesetzes (LMBG) und der Trinkwasserverordnung (TrinkwV).

Chem. Formel	$FeCl3(+H_2O)$

Chemische Zusammensetzung:

Wirksubstanz	ca. 2,5 mol Fe/k
Fe_{ges}	13,8 ± 0,2 %
	138 g Eisen pro kg
	200 g Eisen pro l
Dichte	1,43 ± 0,02 g/cm³
Viskosität (20°C)	10 mPas
Viskosität (0°C)	24 mPas
pH	<1
Beginn der Kristallisation	- 13°C

Lieferform
flüssig in Gefahrgutkanistern/-flaschen

Transport und Lagerung
Das Sicherheitsdatenblatt informiert über weitere Produkteigenschaften, enthält Hinweise zur Gefahreneinstufung sowie den zu beachtenden Vorschriften und beschreibt die erfor-derlichen Maßnahmen beim Umgang mit dem Produkt zum Schutz des Menschen und der Umwelt.

Bungard Elektronik GmbH & Co. KG, Rilkestraße 1, 51570 Windeck – Germany
Tel.: +49 (0) 2292/5036, Fax: +49 (0) 2292/6175, E-mail: support@bungard.de

BUNGARD
BEL

Figure A-4: Properties of FeCl₃ (coagulant)

kemira

Where water
meets chemistry ™

SUPERFLOC® PWG series Dry PAMs

Dry Anionic Polyelectrolyte

The Kemira Superfloc PWG series are highly effective flocculants which meet CEN 1407:2008 & CEN 1410:2008 regulation requirements. They are designed for rapid settling & clarification in the drinking water industry. They show exceptional performance in liquid-solid separations in a wide range of conditions.

Applications

These products may be beneficial in any liquid-solid separation process.

They are especially recommended for:

- Dissolved air flotation
- Filtration
- Gravity settling
- Mechanical dewatering
- Phosphorus removal.

Benefits

- Dry product minimizes storage requirements
- Economical to use - effective at very low
- dosage levels, resulting in reduced handling and storage costs
- Works over a wide range of conditions – the range of charges deal effectively with differing conditions of water
- Fast settling rates - achieve high solids removal efficiencies
- Easily soluble in water.
- Effective over a wide range of pH; does not alter the system pH.

- Eliminates or reduces use of inorganic salts

Health and Safety

Before handling these materials read the corresponding Kemira Material Safety Data Sheets (SDS) for safety and health data.

For chemical inventory regulatory control listing information, see the SDS.

Handling and Storage

Solutions are no more corrosive than water and recommended materials of construction include stainless steel, fibreglass, plastic, and glass or epoxy-lined vessels. Do not use iron, copper or aluminium.

The shelf life of these products is 24 months when stored in unopened packages in a dry atmosphere at temperatures no higher than 40°C/104°F.

Spilled polymer is very slippery and should be absorbed onto an inert material and collected prior to thoroughly flushing with water.

Product Addition

Stock solutions can be prepared up to 0.5 % concentration via an automated make-up unit or on a batch basis. Solutions should be aged 30-60 minutes for maximum effectiveness. High quality make up water should be used.
Secondary dilution water should be added to the stock solution prior to the addition point at a ratio up to 10:1. Centrifugal pumps should be avoided for polymer transfer.

Figure A-4: Properties of flocculants - 1

Kemira

Where water
meets chemistry ™

Delivery

The Superfloc PWG series products are typically available in 25 kg & 750 kg moisture-resistant bags. Other pack sizes may be available on request.

Regulatory Approvals

These products may conform to certain regulatory requirements. Please contact your Kemira sales representative for more details, or refer to the appropriate regulatory information sheet.

Product Properties – Anionic

	A-100PWG	A-110PWG	A-120PWG	A-130PWG	A-150PWG
Chemical Type	Anionic Polyacrylamide				
Appearance	Off-white, Granular Powder				
Relative Charge	Low	Low	Medium	Medium	High
Molecular weight	High	High	High	High	High
Bulk Density (kg/litre)	0.78	0.80	0.82	0.83	0.87
pH of 0.5% solution (25°C)	7 - 9	7 - 9	7 - 9	7 - 9	7 - 9
Viscosity @ 25°C (cp / mPa.sec)					
0.10%	100	150	180	200	240
0.25%	250	350	400	450	500
0.50%	500	700	800	900	1000

Product Properties – Cationic

	C-492PWG
Chemical Type	Cationic Polyacrylamide
Appearance	Off-white, Granular Powder
Relative Charge	Very Low
Molecular weight	High
Bulk Density (kg/litre)	0.75
pH of 0.5% solution (25°C)	3 - 5
Viscosity @ 25°C (cp / mPa.sec)	
0.10%	80
0.25%	200
0.50%	450
1.00%	1000

Product Properties – Nonionic

	N-100PWG	N-300PWG
Chemical Type	Polyacrylamide	
Appearance	Off-white, Granular Powder	
Relative Charge	V Low Anionic	None
Molecular weight	High	High
Bulk Density (kg/litre)	0.72	0.72
pH of 0.5% solution (25°C)	4 - 7	4 - 7
Viscosity @ 25°C (cp / mPa.sec)		
0.10%	25	10
0.25%	70	30
0.50%	150	100
1.00%	400	300

Figure A-5: Properties of flocculants - 2

Appendix B – Detailed description of working procedures

Appendix B.1   Working procedure for EC mid-scale cell

Experiment preparation:

- Weighting the required soil material and water

- Pouring the water in the stirrer in the EC container

- Addition of the bentonite in the stirrer while simultaneously mixing

- Pumping the suspension in circle (stirrer-pump-stirrer) for 10 minutes

- Leaving the suspension to quell for at least 4 hours

- Loading the suspension with soil materials (silica flour, kaolin)

- Letting the suspension quell until next day (16 – 24 hours)

- Pumping the loaded suspension in circle (stirrer-pump-stirrer) for 10 minutes

- SUS in ready

Experiment execution:

- If one 1 chamber is used: pouring water in the other chamber

- Closing the EC cell cover

- Pumping the suspension in the empty cell(s)

- Starting the automatic electricity measurement hardware and software

- Choosing the amount of the electrical current

- Starting the EC experiment (direct current flows in the cell)

- Adjusting the electrical current during the experiment, if necessary

- After conclusion of the planned experiment time, turning the DC source off

- Waiting for about 15 minutes, to ensure that the residuals of hydrogen are away

    o In the meantime, taking the samples of the remaining suspension from five extraction points in the EC cell

    o Analysing pH value, electrical conductivity, temperature and density of the samples

- Pumping the remaining suspension out of the EC cell into

- LCFP experiment can start (Appendix B.2)

- Gathering the coagulated material from the anodes

- Drying the samples of the coagulated material in the oven to determine the residual moisture of the coagulated material.

- The complete coagulated material was scratched of the anode, accumulated, dried in the oven and weighed, to determine the total amount of coagulated material

- Cleaning of the EC cell

- Measuring the properties of the remaining suspension (besides filtrate water release with LCFP)

   o pH, elec. conductivity and temperature

   o density

   o filtrate water release with API filter press

Appendix B.2 Working procedure for LCFP

Instructions for filtration experiment (from Jian, 2018)

- Scale set up, computer set up, connect the scale with the computer by USB port 1. Prepare 5 buckets for filtrated water and 1 black bucket under the LCFP.

- Start computer, find Software "Procell" on the desktop and open it. Change the data name. Give it a try with the data received, to make it sure that the software works well with the scale and the USB port. See Figure 3.11

- Close the valve.

- Screw the metal ring in 1. Chamber.

- Sort the Chamber with the number on it and press together.

- Drag the yellow membrane from the bottom until they aligned. See Figure 3.12

- Put on the black caps and water tubes on every chamber.

- Pay attention not to clamp the edge of the yellow membrane when the hydronic pressed together.

- Adjust the hydraulic pressure about 420-430 bar.

- Set up the Bentonite suspension input tube.

- Connect laboratory air pressure with the air tube on the LCFP air pump.

- Immerse the bentonite suspension input tube deep into the bentonite suspension.

- Switch the valve of LCFP to "stop", the rotary knob to minimal.

- Open the air pressure. Turn the air pump towards the downside, regulate it until it shows "7 bar". See Figure 3.18

- Double-check if everything is fine.

- Press the "Automatisches lesen (record automatic)" on the computer by "Procell"

- Air pump valve adjust to the "Umpumpen (transfer)"

- Turn on the rotary knob slowly carefully, so that the bentonite suspension won't splatter. If the bentonite suspension spritzes out from the chamber area, then this experiment should be considered as a mistrial.

- About 3 minutes later, change the air pump valve to "Stop", close the rotary knob fast.

- Change the air pump to the "Press", turn on rotary knob slowly and carefully.

- When the water in the bucket accumulated about 5 litres, change for a new bucket.

- Check the water in the bucket, change for a new bucket if needed so that the water won't overflow.

Finishing the experiment:

- Prepare 2 aluminium bowls, the weights should be recorded already.

- Cancel the check mark (in software "Procell") on computer, where the "automatisches lesen" is.

- Change the air pump valve to "Stop", close the rotary knob.

- Put the last water bucket with other buckets on a table.

- Wait until the pressure scale shows under 3 bars, it can last 5 to 15 minutes.

- Loose the hydraulic pressure, open the last chamber (Nr.10) with a aluminium bowel below, and get all the material that comes out. Sometimes it happens, that the filter cake falls directly when the chamber being opened, so it is better that the aluminium bowel is already there below before it opened.

- Take out the filter cake from chamber Nr.10 and chamber Nr.5 with the blue shovel, separately into 2 aluminium bowels that were prepared. The rest filter cake can be junked into the black bucket under LCFP.

- Make photos for the filter cake.

- Weigh the filter cake with the aluminium bowel together, record it and put them into the oven.

- Loose the air pressure tube both sides.

- Take LCFP outside.

- Open the valve, and remove the bentonite input tube, clean it with water.

- Unscrew the metal ring in the Nr.1 chamber and clean the chamber.

- Clean all the yellow membrane with water.

- Take LKFP back into the laboratory.

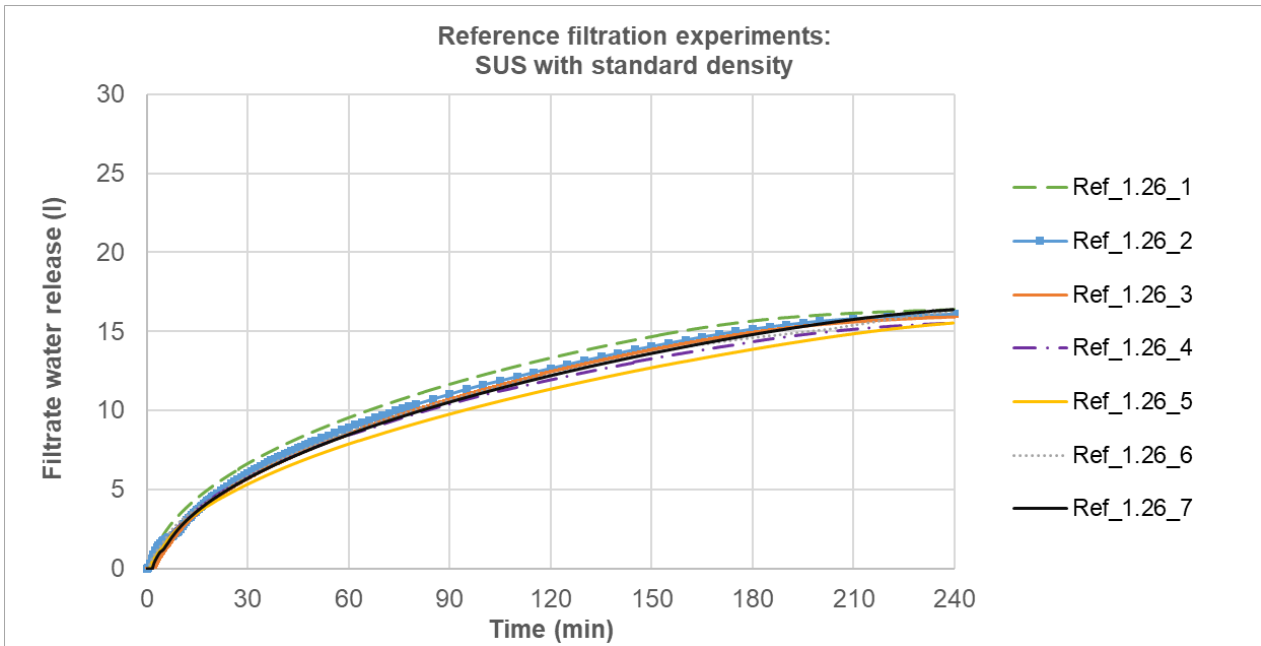## Appendix C – Reference filtration experiments with SUS

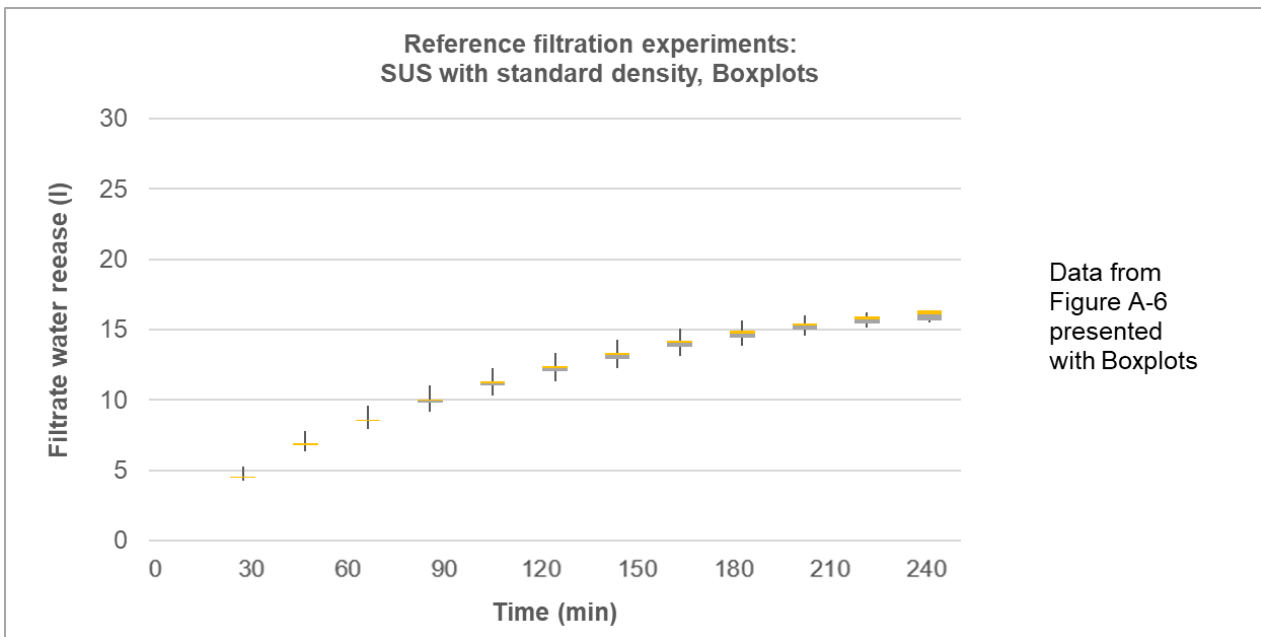**Figure A-6: Reference filtration experiments**

Figure A-7: Reference filtration experiments

Appendix D – Calculation model

Filtration time

$$P_{cfp} = \frac{\frac{V_{FW,EC}+V_{cfp}}{V_{FW,CA}+V_{cfp}}}{1+(\frac{t_{FW,EC}}{t_{FW,CA}}-1)\cdot F\%}$$ (Eq. 7-2)

P_{cfp} factor for change of productivity of chamber filter press with EC [-]

ΔFV_{EC} change of the volume of the filtrated suspension after EC [-]

ΔFt_{EC} change of the filtration time after EC [-]

$V_{FW,EC}$ filtrate water discharge after EC [m³]

$V_{FW,CA}$ filtrate water discharge with CA [m³]

V_{cfp} volume of the chamber filter press [m³]

$t_{FW,EC}$ filtration time after EC [h]

$t_{FW,CA}$ filtration time with CA [h]

$F\%$ time ratio of a filtration process within a full filtration cycle [-]

Table A-1:   Calculation example for Best Combo experiment

Parameter	$V_{FW,EC}$	$V_{FW,CA}$	V_{cfp}	$t_{FW,EC}$	$t_{FW,CA}$	F%	P_{cfp}
Unit	l	l	l	min	min	-	-
Value	30.4	16.4	8	69.3	31.4	32/54= 0.59	0.92

Filtration volume

$$FV = \frac{1-(\delta_{SUS}-1)/(\delta_S-1)\cdot B_{kt}\cdot(1+\delta_S\cdot\frac{RM_{CM}}{1-RM_{CM}})}{1+V_{CA}}$$ (Eq. 7-8)

whereby:

FV factor for decrease of filtration volume due to EC [-]

V_{CA} volume of CA added to suspension per m³ suspension [m³]

V_{CM} volume of coagulated material per m³ suspension [m³]

$V_{S,CM}$ volume of soil in coagulated material per m³ suspension [m³]

$V_{W,CM}$ volume of water in coagulated material per m³ suspension [m³]

δ_{SUS} suspension density [t/m³]

δ_S grain density EC [t/m³]

B_{kt} ratio of coagulated material after EC [-]

RM_{CM} ratio of residual moisture in coagulated material [-]

Table A-2:   Calculation example for Best Combo experiment, under assumptions from Figure 104

Parameter	δ_{SUS}	δ_S	B_{kt}	RM_{CM}	V_{CA}	FV
Unit	t/m³	t/m³³	-	-	m³	-
Value	1.25	2.65	0.27	0.48	0.2	0.71

$$P_{sep} = \frac{P_{cfp}}{FV} = \frac{\frac{V_{FW,EC} + V_{cfp}}{V_{FW,CA} + V_{cfp}} \cdot (1 + V_{CA})}{\left[1 + (\frac{t_{FW,EC}}{t_{FW,CA}} - 1) \cdot F\%\right] \cdot \left[1 - \frac{\delta_{SUS} - 1}{\delta_S - 1} \cdot B_{kt} \cdot (1 + \delta_S \cdot \frac{R_{M,CM}}{1 - R_{M,CM}})\right]} \qquad \text{(Eq. 7-10)}$$

P_{sep} factor for productivity of separation process when replacing CA with EC [-]

$P_{sep} = 1.29$ (see input in Table A-1 and Table A-2)

$$R_{cfp} = \frac{FV}{P_{cfp}} = \frac{\left[1 + (\frac{t_{FW,EC}}{t_{FW,CA}} - 1) \cdot F\%\right] \cdot \left[1 - \frac{\delta_{SUS} - 1}{\delta_S - 1} \cdot B_{kt} \cdot (1 + \delta_S \cdot \frac{R_{M,CM}}{1 - R_{M,CM}})\right]}{\frac{V_{FW,EC} + V_{cfp}}{V_{FW,CA} + V_{cfp}} \cdot (1 + V_{CA})} \qquad \text{(Eq. 7-11)}$$

R_{cfp} factor for calculation of required chamber filter press capacity when replacing CA with EC [-]

$R_{cfp} = 0.78$ (see input in Table A-1 and Table A-2)

14 **Curriculum Vitae**

Personal Information

Name:	Ivan Popovic
Title:	M. Sc.
Date and Place of Birth:	04. October 1989, Split, Croatia
Nationality:	Croatian
Contact:	ivan.popovic@rub.de

Professional Experience:

September 2019 –	Project Engineer ZPP Ingenieure AG
March 2014 – June 2019 August 2013 – January 2014	Research Assistant Intern Institute for Tunnelling and Construction Management Faculty of Civil and Environmental Engineering Ruhr University Bochum
August 2012 – September 2012	Intern Civil Engineering Department Faculty of Engineering University of Sao Paulo State

Education

October 2011 – February 2014	Civil Engineering - Master Studies Faculty of Civil Engineering, Architecture and Geodesy University of Split
October 2008 – July 2011	Civil Engineering - Bachelor Studies Faculty of Civil Engineering, Architecture and Geodesy University of Split
September 2004 – June 2008	Gymnasium of Natural Sciences and Mathematics, Split
September 1996 – June 2004	Primary School „Josip Pupacic", Omis